DOCTORAT BIOLOGIE BRETAGNE SANTE LOIRE

UNIVERSITÉ DE NANTES

THESE DE DOCTORAT DE

L'UNIVERSITE DE NANTES

ECOLE DOCTORALE N° 605
Biologie Santé
Spécialité : Bio-informatique et Physiologie

Par

Johanna ZOPPI

Impact of psychological stress on the remodeling of the host-microbiota interactome.

Thèse présentée et soutenue à Nantes, le 20/12/2021

Unité de recherche : INSERM TENS U1235

Rapporteurs avant soutenance :

Eric Pelletier Chercheur Senior, Genoscope/CEA
Hervé Blottière DR, Micalis UMR1315

Composition du Jury :

Président :	Jeroen Raes	DR, KU Leuven REGA Institute
Examinateurs :	Siobhain O'Mahony	DR, University College Cork
	Nathalie Vergnolle	DR, INSERM U1220 Institut de recherche en Santé Digestive
Dir. de thèse :	Michel Neunlist	DR, Université de Nantes, INSERM U1235 TENS
Co-dir. de thèse :	Patricia Parnet	DR, Université de Nantes, INRAE UMR1280 PhAN
Co-enc. de thèse:	Samuel Chaffron	CR, CNRS, LS2N UMR6004, Combi

True stability results when presumed order and presumed disorder are in balance. A truly stable system expects the unexpected, is prepared to be disrupted, waits to be transformed.

Tom Robbins, 1936

Remerciement

Après trois belles années de travail partagées entre l'équipe Combi du LS2N et le laboratoire TENS de l'INSERM, nous arrivons au terme d'une étude passionnante à cheval entre l'univers de la Biologie et de la Bioinformatique et qui par son caractère transversal m'a conduite à de nombreux échanges, d'incroyables rencontres et un apprentissage continu. Pour tous ces moments je tiens à remercier l'ensemble des deux équipes qui m'ont épaulée pour l'ensemble de ces tâches et m'ont apportée courage et réconfort.

Merci tout d'abord à Michel Neunlist pour m'avoir accueilli dans votre unité. C'était un défi pour nous deux de composer cette thèse entre physiologie et bioinformatique. Vous m'avez fait confiance mais aussi beaucoup appris, tant sur la pratique expérimentale que sur la rédaction. Je vous remercie pour tous ces échanges (et pour le vin chaud de Noël). Vous avez constitué une unité pleine d'entrain et accueillante et m'avez apporté une vision de la science très humaine qui j'espère me suivra jusqu'à la fin de ma carrière.

Je remercie aussi Samuel Chaffron. Après ce stage de M2, tu m'as offert cette très belle opportunité de continuer en thèse. Je suis contente d'avoir été ta première thésarde et je pense qu'on a construit ensemble un bel outil pour la communauté.

Merci aussi à Patricia Parnet pour ton accueil et nos discussions. J'aurais aimé pouvoir plus échanger et je pense que nous aurons de nouvelles occasions dans le futur.

Maxime Mahe et Justine Marchix, vous m'avez accompagné dans mes premiers pas dans le monde de la culture cellulaire et eu la patience de m'apprendre les ressorts de l'extraction d'organoïdes et l'art d'éviter les contaminations. Merci pour ce temps précieux et vos conseils qui m'ont aiguillé tout le long de cette thèse.

Merci aussi à Damien Eveillard qui a toujours été présent pour des échanges scientifiques passionnants. Ces discussions m'ont vraiment permis de prendre du recul sur notre travail du quotidien et la science en général. Ces moments-là sont essentiels.

A Marie Burel, ma première étudiante en stage, merci pour nos échanges. J'ai eu avec toi une très belle expérience d'encadrement pleine de questions fulgurantes.

Merci à Nils, Marko, Misbha, Julien, Matthieu, Charlery, Sophie, Albane, Anna, Marina, Ina pour les pauses café, les bières au Berthom, les bières au Berlin, les parties de Smash Bros, les courses à pied.

Merci à Adrien, Morgane, Marine, Killian, Julie, Jacques, Amélie, pour les soirées au bar d'à côté, les bons conseils quand les manips me paraissaient insurmontables et cette constante bonne ambiance que vous apportez tous les jours au laboratoire.

Merci à Katy et Karelle pour leur soutien et leur bonne humeur. Carine je te remercie aussi pour tout ton accompagnement à travers MiBiogate et ton aide constante pour ma thèse.

Merci à Philippe Aubert, Anne Bessard, Philippe Bordron de m'avoir aidé pour mes protocoles expérimentaux et mes pipelines d'analyses.

Benjamin Churcheward, fin joueur de Mario Smash Bros, merci pour les currys, les jeux de mots, le génépi maison. Merci aussi d'avoir été un si bon adversaire dans les jeux de sociétés, de m'avoir écouté raconter ma vie de si nombreuses fois et surtout d'avoir été présent pendant ces trois années qu'on a débutées ensemble.

Je remercie aussi Antoine Regimbaud, ses tomates et ses capsules de café. Je crois que même avec tes conseils je n'arriverai pas de sitôt à marcher sur les mains. Mais je continue de m'entraîner, ne t'en fais pas.

Merci Elise Loffet pour tous ces merveilleux moments partagés ensemble. Il y en a tellement : voyages, déménagements, pauses ensoleillés et pluvieuses, escalade, soirées post-boulot. J'ai hâte de fêter notre doctorat ensemble autour d'une bouteille de champagne.

Cette thèse a vu la naissance de plusieurs amitiés incroyables. Damien A, Marie H, Marie A, on a partagé des soirées incroyables pleines de rebondissement, organisé des anniversaires rebondissants, des week ends et voyages pleins d'aventures. Peu importe où la suite me mènera vous serez toujours avec moi.

Thibaut, merci d'avoir échanger des livres, et ce qui a suivi : l'escalade, le tennis, la clarinette, les randonnées qui mènent partout et nulle part, Valdeblore et le hérisson, la Martinique, le vélo, St Véran, le mariage basque, la forêt d'Achères, les repas gourmands, le canyoning, le rafting, la voile, les moments de bonheurs et les moments plus compliqués. Je te préviens, ce n'est que le début et j'ai prévu une via ferrata pour 2022.

Merci enfin à ma famille extraordinaire. J'ai la chance d'être accompagné par des parents géniaux qui décrochent au moindre soucis leur téléphone, qui m'ont soutenu dans chaque décision. Maman, Papa, Steph, vous avez une force et une bienveillance incroyables et je suis fière de notre complicité, de notre bonheur, de ces belles valeurs que l'on partage ensemble.

Enfin je dédie ma thèse à mes grands-parents.

Paul Zoppi, mon grand-père tellement curieux qui a partagé avec moi l'épicurisme et l'histoire. Des centaines d'histoires pleines de noms et de dates maintenant un peu floues qui m'ont donné l'envie de découvrir tous les jours un peu plus.

Jacqueline Zoppi, ma grand-mère forte et pleine de tendresse, qui n'oubliait jamais de m'appeler le soir après mes grosses journées de travail pour partager avec moi cette fabuleuse aventure et qui me poussait toujours à vivre ces moments bons ou mauvais avec la même intensité.

Merci à tous.

General Introduction

The digestive system, at the edges between our internal milieu and the external environment, harvests energy from our surrounding to sustain our body needs. Extremely compartmentalized, it accomplishes this task through a succession of specialized organs such as the stomach and his gastric juice, the ileum with its intestinal walls filled with villi and crypts, or the colon and its large community of micro-organism: the digestive tract has a regionalized anatomy and accomplishes many biological functions. Within the digestive system, all exchanges are realized through the intestinal epithelial barrier.

Biological barriers are the gatekeepers of all living organisms. They protect us against outside threats, are the site for a developing immunity, and harvest a large variety of nutrients to fulfill the organism needs. The shape of the gut epithelium reflects the organ function: composed of villi and crypts to optimize the surface of absorption and harvest most of the energy from the consumed diet, it can also be covered by one and sometimes two layers of viscous mucus, filled with antimicrobials and IgA to protect against pathogens. Gut epithelium also harbors an important community of microorganisms, called the microbiome, which influences greatly the state of biological barriers, as well as the homeostasis of the entire body. Intestinal epithelial barriers are locally characterized by their associated microbiota which complement the digestive system functions with their large metagenome, a genetic toolbox constituted by the hologenome.

Constantly renewed, the intestinal epithelium lasts four to five days in humans. It is maintained by migration, proliferation, differentiation, and cell death functions but also, to sustain a structural identity and still allows exchanges with the environment, it should preserve a certain permeability. The constant renewal of the epithelium participates in gut homeostasis through the adaptation of barrier functions exposed to a continual flow of environmental challenges.

Across intestinal epithelial barrier, homeostasis is regulated by an interaction between layers of specialized cells and their associated microbiota. Subjected constantly to environmental threats, host-microbiota interactome must evolve to overcome these challenges and maintain host health. Studying gut microenvironments and their interactions involve the exploration of large communities of micro-organisms and host regional responses. There is a growing need of global approaches to study the set of interaction between gut microenvironments leading to the maintenance of homeostasis. Using high throughput sequencing techniques and bioinformatic multi-omics pipeline we propose new systemic analyses to study this interactome.

Gut homeostasis is constantly challenged and the ability of the intestinal epithelium to adapt to stressors is essential to maintain the homeostasis of the intestinal epithelial barrier. When impaired, this lack of adaptation lead to a default in restoration processes and can ultimately promote the development of chronic diseases. Indeed, alteration of intestinal barrier permeability induced by psychological stress is known to contribute negatively to the evolution of chronic pathology such as irritable bowel syndrome (IBS), inflammatory bowel disease (IBD), or colorectal cancer (CRC), where we observe a disruption of homeostasis, a complete switch between a healthy equilibrium to a deleterious stable state. In this state of chaostasis, only the

symptomology of the pathology can be treated. If characterization of gut physiopathology and associated dysbiotic microbiota has increased dramatically within the past few years for these diseases, the installation of the rupture in homeostasis induced by psychological stress is barely studied. Indeed, this rupture is a distinctive property of chronic diseases initiations and occurs in the pre-symptomatic phases. The passage between a balanced homeostasis and its rupture is difficult to capture and require systemic methods to identify the factors involved in this mechanism. Therefore, using psychological stress as a key environmental factor contributing in a deleterious fashion in the initiation and development of chronic diseases, it can be used as a tool to study the dynamic phases of the rupture in homeostasis. Psychological stress is also known to influence gut microenvironment as it modifies barrier permeability, turn-over rate but also alter the diversity and composition of the gut microbiota. However, its regional effects along gut biogeography are not characterized, especially between the luminal microbiome, localized in the lumen of the digestive track, and the mucosal microbiome, in close relationship with the epithelial barrier and embedded in the mucosal layer. In this context, there is a growing need to better understand the mechanism of intestinal epithelial barriers and their microenvironment responses to chronic psychological stress. Identifying therapeutic targets involved in host-microbiota interactome can ultimately lead to development of strategies to restore homeostasis within the intestinal epithelial barrier and its close environment.

Therefore, the current thesis aims to characterize the impact of psychological stress upon the host-microbiota interactome. It will be divided in two parts: in the first one, we will expose the development of bioinformatics strategies to study multi-omics features – associations between datasets containing different biological entities (e.g., genes, proteins, mRNA …). Then, using these tools, we will present an in-depth characterization of the stress response within gut organs, and describe how organs' physiology, epithelial gene expression and regional microbiota are affected, to, eventually, extract host-microbiota biomarkers signature associated to stress.

Introduction Générale

Le tube digestif, à la frontière entre notre milieu interne et externe, récolte l'énergie de notre environnement pour subvenir aux besoins de notre corps. Extrêmement compartimenté, il accomplit cette tâche grâce à une succession d'organes spécialisés tels que l'estomac et ses sucs gastriques, l'iléon avec ses parois intestinales couronnées de villosités et de cryptes, ou encore le côlon et sa grande communauté de micro-organismes : le tube digestif possède une anatomie régionalisée et accomplit de nombreuses fonctions biologiques. Au sein du système digestif, tous les échanges sont réalisés à travers la barrière épithéliale intestinale.

Les barrières biologiques sont les gardiennes de tous les organismes vivants. Elles nous protègent contre les menaces extérieures, sont le siège du développement de l'immunité et récoltent une grande variété de nutriments pour répondre aux besoins de l'organisme. La forme de l'épithélium intestinal reflète la fonction de l'organe : parfois très sinueux pour optimiser la surface d'absorption et récolter la majeure partie de l'énergie de l'environnement, il peut aussi être recouvert d'une et parfois de deux couches de mucus visqueux, remplies d'antimicrobiens et d'IgA pour se protéger des agents pathogènes. L'épithélium intestinal abrite également une importante communauté de micro-organismes, appelée le microbiome, qui influence grandement l'état des barrières biologiques, ainsi que l'homéostasie de l'organisme entier. Les barrières épithéliales intestinales sont localement caractérisées par leur microbiote associé qui complète les fonctions du système digestif grâce à leur vaste métagénome. La combinaison du répertoire de gènes humain et microbien constitue une boîte à outils génétique aussi appelé l'hologenome.

Constamment renouvelé, l'épithélium intestinal a une durée de vie de quatre à cinq jours. Son maintien est assuré par les fonctions de migration, de prolifération, de différenciation et de mort cellulaire mais aussi, pour maintenir une identité structurelle et permettre les échanges avec l'environnement, il doit conserver une certaine perméabilité. Ce renouvellement constant de l'épithélium participe à l'homéostasie intestinale par l'adaptation des fonctions de barrière exposées à un flux continu de défis environnementaux.

À travers la barrière épithéliale intestinale, l'homéostasie est régulée par une interaction entre des couches de cellules spécialisées et leur microbiote associé. Soumis en permanence à des menaces environnementales, l'interactome hôte-microbiote doit évoluer pour surmonter ces défis et maintenir la santé de l'hôte. L'étude des microenvironnements intestinaux et de leurs interactions implique l'exploration de vastes communautés de micro-organismes et des réponses régionales de l'hôte. Il existe un besoin croissant d'approches globales pour étudier l'ensemble des interactions entre les micro-environnements intestinaux autour du maintien de l'homéostasie. En utilisant des techniques de séquençage à haut débit et un pipeline bioinformatique multi-omique, nous proposons de nouvelles analyses systémiques pour étudier cet interactome.

L'homéostasie intestinale est constamment remise en question et la capacité de l'épithélium intestinal à s'adapter à des stress environnementaux est essentielle pour maintenir l'homéostasie de la barrière épithéliale intestinale. Lorsqu'elle est altérée, ce manque d'adaptation conduit à des défauts dans les processus de restauration et peut finalement favoriser le développement de maladies chroniques. En effet, l'altération de la perméabilité de

la barrière intestinale induite par le stress psychologique est connue pour contribuer négativement à l'évolution de pathologies chroniques telles que le syndrome du côlon irritable (SII), les maladies inflammatoires de l'intestin (MICI), ou le cancer colorectal (CCR), où l'on observe une rupture de l'homéostasie, un basculement complet entre un équilibre sain et un état stable délétère. Dans cet état de chaostasie, seule la symptomatologie de la pathologie peut être traitée. Si la caractérisation de la physiopathologie intestinale et du microbiote dysbiotique associé s'est considérablement accrue ces dernières années pour ces maladies, l'installation de la rupture de l'homéostasie induite par le stress psychologique est peu étudiée. En effet, cette rupture est une propriété distinctive de l'initiation des maladies chroniques et se produit dans les phases pré-symptomatiques. Le passage entre une homéostasie équilibrée et sa rupture est difficile à capturer et nécessite des méthodes systémiques pour identifier les acteurs impliqués dans ce mécanisme. Ainsi, en utilisant le stress psychologique comme un facteur environnemental clé contribuant de manière délétère à l'initiation et au développement des maladies chroniques, il peut être utilisé comme un outil pour étudier les phases dynamiques de la rupture de l'homéostasie. Le stress psychologique est également connu pour influencer le microenvironnement intestinal car il modifie la perméabilité de la barrière, le taux de renouvellement mais aussi la diversité et la composition du microbiote intestinal. Cependant, ses effets régionaux le long de la biogéographie intestinale ne sont pas caractérisés, notamment entre le microbiome luminal, localisé dans la lumière du tube digestif, et le microbiome mucosal, en relation étroite avec la barrière épithéliale et intégré dans la couche muqueuse. Dans ce contexte, il est de plus en plus nécessaire de comprendre le mécanisme des réponses des barrières épithéliales intestinales et de leurs microenvironnements au stress psychologique chronique. L'identification de cibles thérapeutiques impliquées dans l'interactome hôte-microbiote peut conduire à terme au développement de stratégies visant à restaurer l'homéostasie de la barrière épithéliale intestinale et de son environnement proche.

Cette thèse vise donc à caractériser l'impact du stress psychologique sur l'interactome hôte-microbiote. Elle sera divisée en deux parties : dans la première, nous exposerons le développement de stratégies bioinformatiques pour étudier les caractéristiques multi-omiques de l'interactome - associations entre des ensembles de données de nature biologique différente (genes, ARNm, protéines…). Ensuite, en utilisant ces outils, nous présenterons une caractérisation approfondie de la réponse au stress dans les organes de l'intestin, et nous décrirons comment la physiologie des organes, l'expression des gènes épithéliaux et le microbiote régional sont affectés, pour, finalement, extraire la signature des biomarqueurs hôte-microbiote associés au stress.

CONTENTS

List of Figures:

Abbreviations

5HT: Serotonin
ACTH: Adrenocorticotropic hormone
APC: Adenomatous polyposis coli
ASV: Amplicon sequence variant
ATP: Adenosine triphosphate
BMP: Bone morphogenetic proteins
CBC: Crypt base columnar
CBG: Corticosteroid-binding globulin
CCorA: Canonical correlation analysis
CDK: Cyclin-dependent-kinases
CFU: Colony forming unit
Chra: Chromogranin-a
CK1: Casein kinase 1
CRC: Colorectal cancer
CRH: Corticotropin-releasing hormone
DAMP: Danger-associated molecular pattern
DHP: Dihydropyridine
EEC: Entero-endocrine cell
EGF: Epidermal growth factor
EGFR: Epidermal growth factor receptor
ENS: Enteric nervous system
FGF: Fibroblast growth factor
FMT: Fecal matter transplant
FXR: Fanesoid x receptor
GR: Glucocorticoid receptor
GSK3: Glycogen synthase kinase 3β
IAP: Inhibitor of apoptosis protein
IBD: Inflammatory bowel disease or **MICI**: Maladie inflammatoire chronique de l'intestin
IBS: Irritable bowel syndrome or **SII**: Syndrome de l'intestin irritable
IEB: Intestinal epithelial barrier or **BEI**: Barrière épitheliale intestinale
IEC: Intestinal epithelial cell
Ihh: Indian hedgehog
ISC: Intestinal stem cell
JAM: Junctional adhesion molecule
KGF: Keratinocyte growth factor
KLF4: Kruppel-like factor 4
MAM: Multiple adversity model
MAMP: Microbe associated molecular pattern
MCOA: Multiple co-inertia analysis
MHC: Major histocompatibility complex
ML: Machine learning

MS: Maternal separation
MSA: Multiple sequence alignment
MUC2: Mucin 2
OTU: Operational taxonomic unit
PCA: Principal component analysis
PCoA: Principal coordinate analysis
pRB: Phosphorylates retinoblastoma protein
PS: Psychological stress
PTSD: Post-traumatic stress disorder
REG3: Regenerating islet-derived protein 3
RS: Restrain stress
Rspo: R-ponding
SCFA: Short chain fatty acids
SDR: Social disruption
SFB: Segmented filamentous bacteria
Shh: Sonic hedgehog
SNF: Similarity network fusion
Spp: Species
TGF- β: Transforming growth factor β
TJ: Tight junction
UMI: Unique molecular identifier
VIP: Vasoactive intestinal peptide
WAS: Water avoidance stress
WGCNA: Weighted gene correlation network analysis
WIRS: Water immersion restraint stress
ZO: Zonula occludens

Introduction

1 THE DIGESTIVE SYSTEM

From the mouth to the anal cavity, the digestive system is a succession of specialized organs responsible for the transport, digestion, and absorption of nutrients to sustain our body metabolic needs, but it is also responsible for the protection against pathogens and the development of immunity.

Digestive organs are defined by their functions and anatomy. Five major structures can be distinguished: the mouth, esophagus, stomach, small intestine, and colon/rectum, separated by sphincters. From the esophagus to the rectum the digestive system conserves approximately the same tissue organization: a superposition of different tissue layers (Figure 1). From the inside of the lumen, toward the outside we can find:

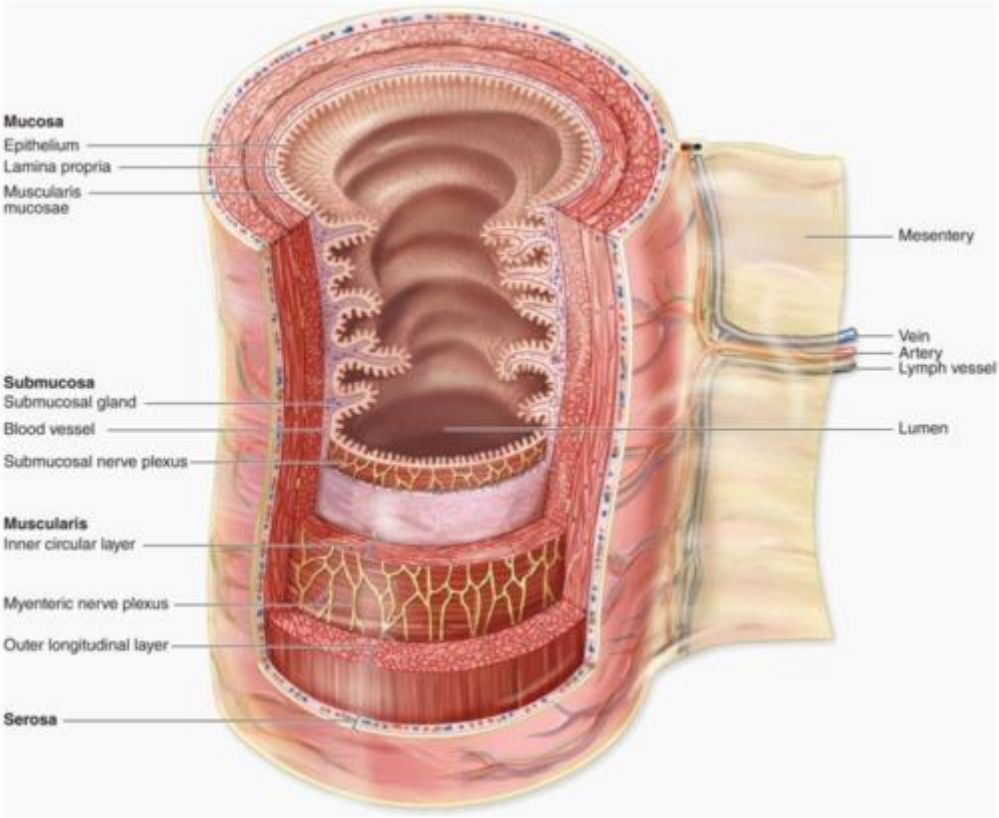

Figure 1 Digestive tract tissular organization: the digestive system is divided into 4 main superimposed layers of tissue. At the center the mucosa contains the intestinal lumen surrounded by the epithelium, the lamina propria and a layer of muscles called the muscularis mucosae. Then, the submucosa is a layer of conjunctive tissue composed of a vascular and a nervous system. The last layer is muscular and can be divided into a ring of circular muscles surrounded by another ring of longitudinal muscles (figure from [1]*).*

1) The mucosa surrounding the intestinal lumen is subjected to nutrient flow. The mucosa contains the gut epithelium: the first line of cells separating the luminal content from the inner body, the lamina propria, a conjunctive tissue, and the muscularis mucosae, a ring of muscle cells.

2) The submucosa, is also a conjunctive tissue layer, is highly vascularized and contains the myenteric plexus.
3) Around the submucosa is a muscular layer containing on the inner side a series of circular muscles surrounded by longitudinal muscles. It also includes part of the myenteric plexus.
4) Finally, the serosa is composed by the mesentery vascularized by mesenteric veins, arteries and lymph vessels.

1.1 THE MOUTH

7 to 10 meters long, the digestive system begins in the mouth where the mastication occurs, helped by the secretion of saliva by the salivary glands embedded within the buccal cavity. Saliva has many antalgic and antiseptic properties and contains mucins with other antimicrobial substances to neutralize micro-organisms and potential pathogens [2]. In the mouth, the combination of mechanical chewing and the secretion of salivary amylase and lipase initiate the breakdown of Starch into Maltose and Triglycerides into Glycerol and Fatty Acids [3]. The product is a bolus of food transported to the stomach via the esophagus, animated by the force of peristalsis (Figure 2).

1.2 THE ESOPHAGUS

The demarcation between the mouth and the esophagus is the upper esophageal sphincter. The esophagus is a 2 centimeters wide and 18-25 centimeters long tube, which ends up in the stomach. Its primary function is the transport of the food bolus to the stomach. The esophagus is surrounded by a spiral of muscles, which prevents gastric reflux via peristaltic contractions and guides nutrients downward. Peristalsis is a type of esophageal motility characterized by the sequential contraction of circular and longitudinal muscles embedded in the digestive tract [4]. The esophagus is the sole organ of the digestive system with a pluri-stratified squamous epithelium. It ends with the cardiac sphincter, a small muscle which opens into the stomach [5] (Figure 2).

1.3 THE STOMACH

The stomach mixes the bolus of food coming from the esophagus and digests macromolecules within the secreted gastric juice. Its structure can be divided in three regions: the cardia is located at the most proximal end of the stomach and constitute 5% of the total organ surface. The body or fundus composes the upper region of the stomach, contains most of the gastric glands (~75%) and is therefore, highly involved in chemical digestion and secretion of gastric enzymes. The last section is the antrum. It controls the release of the chyme into the small intestine and performs mechanical mixing [6].

The stomach applies both mechanical and chemical digestion to the bolus. Within the gastric juice are secreted pepsinogen enzymes, transformed by the hydrochloric acid present in the stomach into pepsin, which, in this form, can breakdown proteins into smaller peptides. Mechanical digestion is performed via the mixing process. Mixing highly depends on the ingested particle size and distribution (3 types of mixing are defined: solid-solid, solid-liquid, liquid-liquid). Mixing involves either phasic contraction of the antrum, diffusion of gastric secretion or both [7].

The stomach is also the first site of absorption for some nutrients: vitamin B12 is acquired by our body with the help of the secreted gastric intrinsic factor, as well as water, alcohol, or aspirin. The pyloric sphincter, at the end of the gastric pouch, is the limit between the stomach and the small intestine [8]. The release of food chyme to the duodenum is controlled and slowed by a process called the accommodation: it consists of relaxation of the proximal part of the stomach during the meal to accommodate a reservoir space for the incoming food [9] (Figure 2).

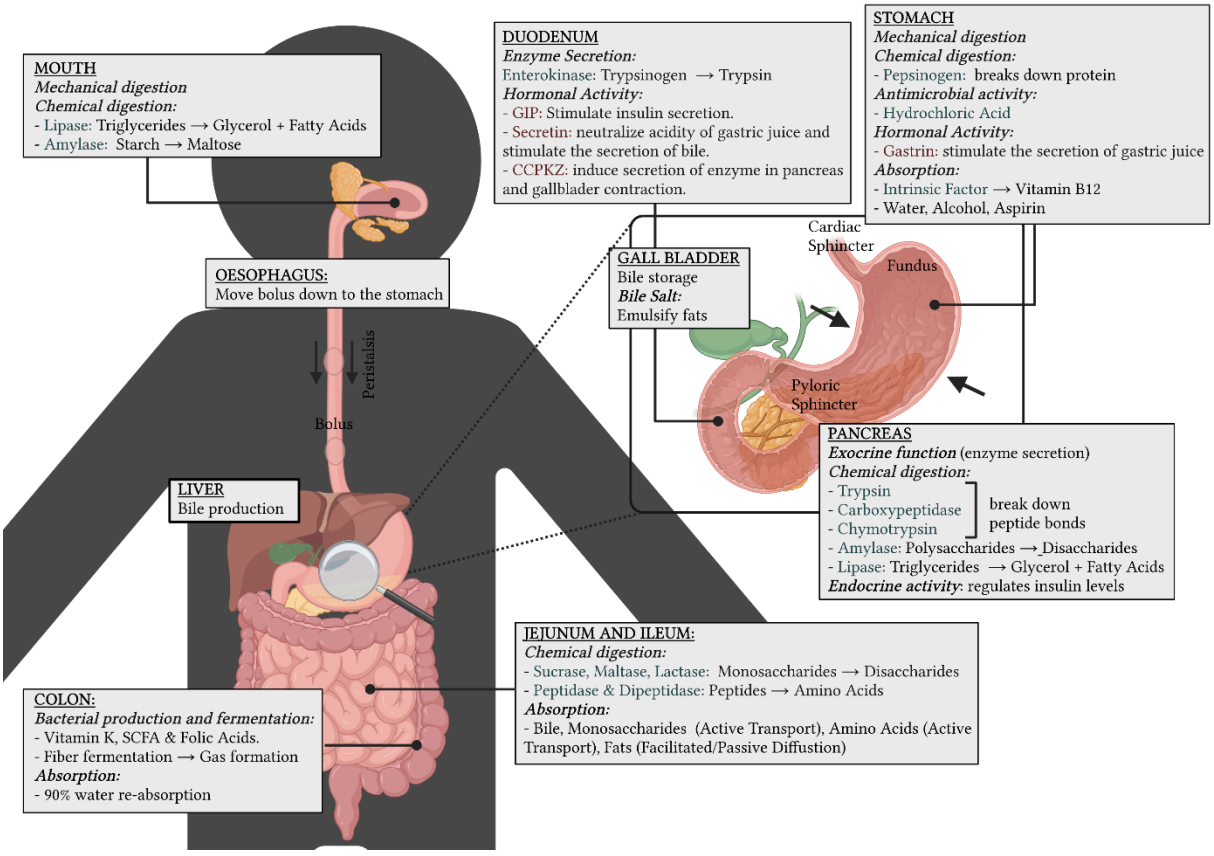

Figure 2 A representation of digestive system organs and their functions: The digestive system is composed of the mouth, the esophagus, the stomach, the small intestine (duodenum, jejunum, and ileum), the colon and the rectum. Accessory organs also participate in digestive functions such as the tongue, the salivary glands, the pancreas, the gallbladder, the liver, and the appendix.

1.4 SMALL INTESTINE: DUODENUM, JEJUNUM, AND ILEUM

The small intestine can be divided into three organs: the C-shaped duodenum, the jejunum, and the ileum. This part of the digestive tract is 3 to 6 meters long. It is optimized to absorb most of the nutrients provided by meals and redistribute them to the other organs of our body via the vascular system but also continues the digestion of nutrients. The intestinal walls of the small intestine are constituted of villi and crypts to optimize absorption [8].

Through the pyloric sphincter, the bolus, now transformed into an acidic chyme, is transported to the duodenum. The duodenum absorbs and digests nutrients but also communicates with the nearby accessory organs to secrete hormone, to neutralize the acidity of the chyme, and to regulate glucose levels in the body.

As nutrients are getting smaller and smaller, the chemical digestion is pursued in the jejunum, a major site of absorption for nutrients such as sugars, fatty acids, and amino acids. Disaccharides are further divided into monosaccharides by specialized enzymes (Sucrase, Maltase, Lactase) and small peptides are reduced to amino acids by peptidase and dipeptidase in this organ[8] (Figure 2).

In the ileum vitamin B12 is absorbed and bile acids are reabsorbed. In this organ, the immune system is extensively developed characterized by the presence of Peyers' patches. Ileum is therefore essential for the development of immunity [10].

Jejunum and Ileum can relocate bile back to the liver [3], actively transport monosaccharides and amino acids through the epithelial barrier, and passively diffuse fats into cells [8].

1.5 COLON

The demarcation between the small and large intestine is characterized by the ileo-cecal valve and a small organ called, in humans, the appendix. The vestigial appendix, is the equivalent of the cecum in other mammals and is much larger in rodents to perform specialized digestion of fibers [11].

The large intestine or colon is divided in three parts: the ascending (proximal in rodents), transverse and descending (distal in rodents) colon and is followed by the rectum. It is characterized by a less folded mucosa and composed only of intestinal crypts [12]. The colon hosts the largest number of microorganisms in our body. The colonic microbiota is responsible for the production of folic acids, vitamin K or short chain fatty acids essential for our health, as well as the formation of gas after the fermentation of fiber. Furthermore, the large intestine is the site where 90 % water is reabsorbed within the body (Figure 2) [8].

2 THE INTESTINAL EPITHELIUM

2.1 COMPOSITION OF THE INTESTINAL EPITHELIUM

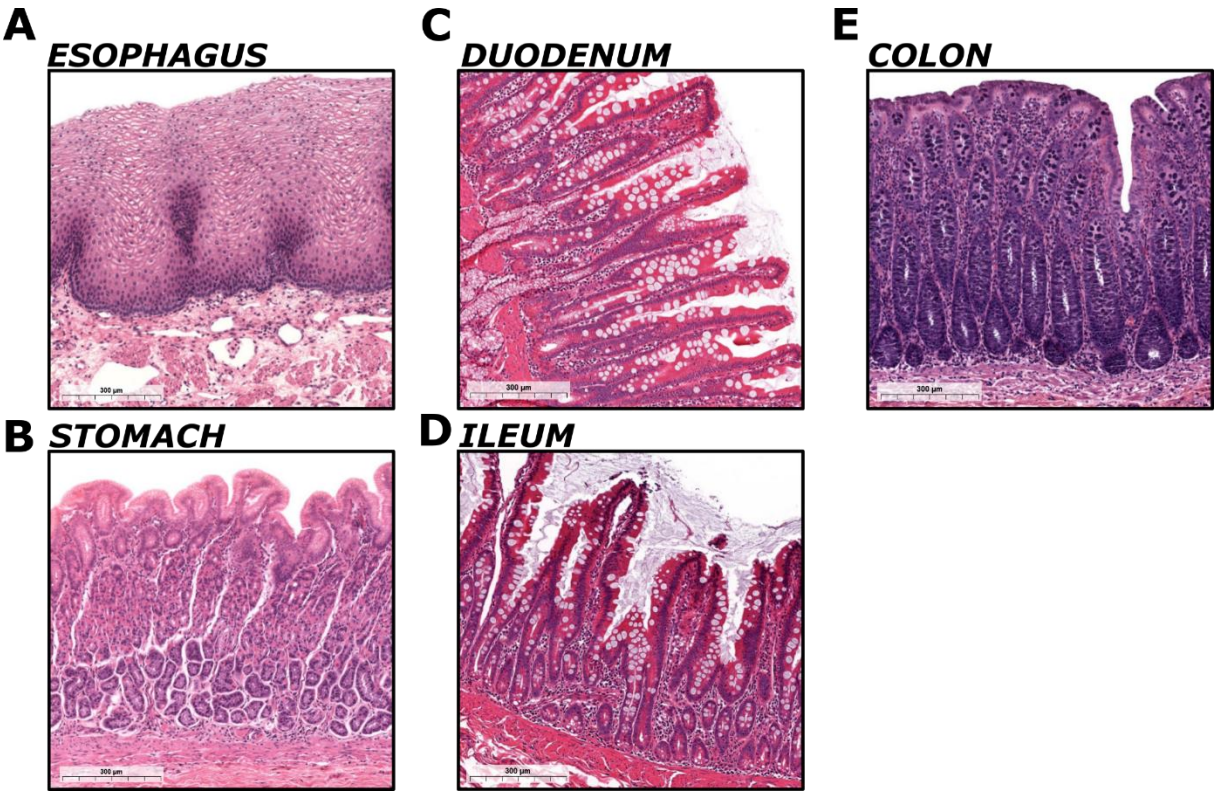

Figure 3 Histological sections from gut epithelial regions. Tissue sections of the A. esophagus, B. stomach, C. duodenum, D. ileum, and E. colon highlight the diversity of gut epithelial structure, organization, and composition within the gut. (histological slides from [13]*)*

The gut epithelium endorses many roles, but its main functions are exchanges with the environment and protection against toxins or pathogens. It forms a semipermeable barrier, where cells are bound together by intercellular junction proteins (tight junctions, anchoring junctions and GAP junctions described below in the 2.3.2 section) [14]. The functionality, composition and the structure of the gut epithelium is specific to each organ (Figure 3). In the esophagus, for instance, where the primary function is the transport of the food bolus, the epithelium is squamous and pluri-stratified [5] to optimize protection and motility. The stomach squamous epithelium is lined with gastric pits embedded in the mucosa. It is composed of highly specialized cells: mucous cells, parietal cells (producers of hydrochloric acid and intrinsic factor), chief cells (which secrete peptin) and enteroendocrine cells G (involved in gastrin secretion) [15]. The small intestine contains villi and crypts and is lined with columnar enterocytes characterized by the presence of microvilli on their apical surface to optimize absorption. Differences can be observed between the duodenal, jejunal and ileal mucosa such as the presence of Brunner's glands (producers of a specific alkaline mucus) only present in the

duodenum [16] or the number and size of Peyer's patches [17]. The colonic epithelium only contains intestinal crypts and possesses two mucus layers as it hosts a large microbial community [18]. In this section, we will describe the major cell types of intestinal and colonic epithelium, their localizations, and their functions.

2.1.1 Intestinal stem cells (ISCs)

Intestinal stem cells can be found along the digestive system and are localized, in the small intestine and the colon, at the base of crypts.[19].

The gut epithelium is renewed every 4-5 days in homeostatic conditions. ISCs are responsible for the constant renewal of the gut epithelium. Their division triggers a migration toward a zone of transit-amplification where cells can further migrate upward the crypt-villus axis to differentiate into enterocyte, goblet, tuft or entero-endocrine cells (EECs) or can migrate downward where they become Paneth cells. [20] (Figure 4).

Their number within intestinal crypts was discussed for a long time since two divergent hypotheses, called the "+4 position" and "Stem cell zone" models, were opposed on this subject [21]. The "+4 position" model is based on early evidence highlighting the presence of label retaining cells at the +4 position from crypt's bases. In this model only cells at this position are considered as stem cells and their asymmetric division results in one remaining stem cell and one newly differentiated cell. Below, at crypt's bases, only Paneth cells can be found in the '+4 position' model [22]. The more recent "Stem cell zone" model is based on the discovery of Crypt Base Columnar (CBC) cells (approximately 15 cells per crypts [21]), intercalated between Paneth cells at the crypt's bases. This model was validated with a clonal migration experiment where long cycling and slow cycling cells were distinguished [23].

Another debate was raised on the distinction between subtypes of stem cells. Since stem cells are essential for cell proliferation and renewal, their replenishment is important for intestinal homeostasis. Therefore, two models were proposed for the replenishment of stem cells: the "reserve intestinal stem cell" and the "plasticity" models [21]. The "reserve intestinal stem cell" hypothesizes that a reservoir of cells exists at a quiescent state (rISCs) and can replace active ISCs in case of barrier impairment [24]. The "plasticity" model states that many already differentiated cells can return to the stem cell state, such as EEC [25] or Paneth cells [26]. This plasticity mechanism, also observed in the stomach with mature chief cells for instance [27], does not exclude the possibility of reservoir stem cells but rather temporizes it.

Markers of stemness are highly studied and the most known in ISCs is the Lgr5 marker in both small intestine and colonic epithelium [28]. Bmi1, a rare marker in intestinal crypt cells, was proposed as a potential candidate for rISC identification [29] but is now questioned since it was also found expressed in CBCs [30]. In the stomach, there are also many gene candidates such as Axin2 [31] or CCK2R [32].

2.1.2 Enterocytes

Enterocytes represent the main cell type of the gut epithelial barrier. Presents along the crypt-villus axis, above the transit-amplifying zone in the intestine they are called colonocytes in the colon [33]. (Figure 4)

They form a semi-permeable membrane responsible for the absorption of nutrients and water. Polarized, with an apical and basal pole, they present to the luminal surface a membrane with a brush border to improve their capacity of absorption [34]. Their surface is covered with mucins and other glycolipids which form the glycocalyx, a first layer of protection surrounded by mucus [35]. Moreover, the regulation of tight, anchoring, and GAP junctions by enterocytes, controls intestinal permeability [36]. Indeed, these cells play a major role in immunity since they possess TLR receptors, and can scan their surrounding environment for the presence of bacteria [37]. They also act as a mediator between the lumen and the immune system by presenting antigens to dendritic cells in the lamina propria [38].

Approximately 90% of the intestinal epithelium is composed of enterocytes [39] and the marker Kruppel-like factor 4 (KLF4) is commonly used to identify these cells [40].

2.1.3 Goblet cells

Goblet cells are localized in the gut epithelium, above the transit-amplifying zone in the small and large intestine and form the major line of defence of the intestinal mucosa. (Figure 4)

The primary function of goblet cells is to secrete mucins, the principal component of mucus [41]. Mucus is a hydrophobic viscous liquid and constitutes a physical and chemical barrier to protect the intestinal epithelium from the surrounding microbiota. If, in the small intestine, there is only one mucus layer, the colon contains two layers: the outer one less viscous than the inner one [42]. Mucus prevents most of the bacteria to adhere to the gut epithelium, however some can still enter this viscous fluid due to their motility and their capacity to digest mucins [43]. The participation of Goblet cells in the development of immunity is not resumed to their capacity to form mucosal layers but also, to their frequent transport of luminal antigens to antigen-presenting cells, localized in the lamina propria to probe constantly the luminal content of the intestine [44].

Goblet cells comprise up to 15% of cells in the intestinal epithelial barrier and become more and more numerous as we descend the digestive tract from the duodenum to the colon [45].

Since goblet cells produce about 50 different types of mucins, among which Mucin 2 (MUC2) is the major component, they can be identified with MUC2 gene expression [46].

2.1.4 Enteroendocrine cells

EECs also reside in the intestinal epithelium and are present from the stomach to the colon. Produced by pluripotent stem cells, they undergo differentiation after migrating through the transit-amplifying zone. They are, then, randomly distributed along villi and crypts where they are in direct contact with the lumen, except for a subset of EECs which express the CCK gene marker and migrate back to the bottom of crypts [47] (Figure 4).

They secrete hormones and enzymes to facilitate the communication between organs and digestion [48]. Thus, their primary function is endocrine. They are involved in the regulation of intestinal motility, secretion, glucose or fats absorption and storage but also, the regulation of appetite. Enterochromaffins constitute a subtype of EECs specialized in the secretion of serotonin (5-HT). In the stomach, gastric juice composition and secretion are influenced by EECs

since subtype G can produce gastrin, one of its components, and subtypes D and K secrete respectively somatostatin and GIP, both regulators of gastric juice secretion. EECs activity is regulated by the rate of absorption of the intestinal epithelial epithelium as they can detect the presence of macronutrients and adapt their hormonal secretion depending on their availability. They are also impacted by the secretion of regional associated gut microbiota [49].

They are less numerous than the other cell types embedded in the epithelium, as they constitute only 1% of the gut epithelium [50]. The nomenclature of EECs was based on their hormonal secretions and named with alphabetic letters but is now revisited [51], with evidence from single cell sequencing [52, 53] which revealed their complex metabolism dependent on their organ location and the species.

The markers used to identify EECs can be Claudin-4 [54] or Chromogranin-A (Chrga) [53].

2.1.5 M cells

M cells are found in the intestinal epithelium associated with Peyer's patches themselves attached to follicle-associated epithelium. They are only present in follicle-associated crypts [55] (Figure 4).

These cells do not possess normal intestinal microvilli, in contrast to normal intestinal enterocytes. Their primary function is to survey and to sample the environment from which they can acquire luminal antigens. These antigens will be, then, presented to the immune system. Via their transport through Peyer's patches where they trigger an effective immune response, they can also facilitate the invasion of microorganisms through the intestinal barrier [56].

M cells are not numerous as they constitute only 4% of follicle-associated epithelium but their abundance increases during inflammation [55].

They are characterized by the presence of several surface markers: GPL2, PrP^{C}, and sIgA, all involved in bacterial recognition and uptake [57].

2.1.6 Tuft cells

Tuft cells are distributed along the gut from the stomach to the large intestine, above the transit-amplifying zone in crypts and villi [58]. (Figure 4)

They play a crucial role in immunity as they survey the presence of protists and parasitic helminths via specific receptors on their apical surface covered by microvilli [59]. High level of succinate secretion by Protozoan species can be recognized by the SUCNR1 receptor present on Tuft cells' membrane and triggers the release of IL25 in the lamina propria to activate an immune response [60].

The transcriptomic landscape of Tuft cells is relatively conserved among species and organ regions, but single cell transcriptomic studies revealed several subtypes. For instance, 2 subtypes exist in the small intestine: Tuft-1 cells express more genes implicated in neuromodulation whereas Tuft-2 cells are involved in immunological processes [61].

Tuft cells are rare and constitute only 0.4% of intestinal barriers [62].

The identification of Tuft cells can be realized using IL-25, ChAT and TRPM5 reporter genes [58].

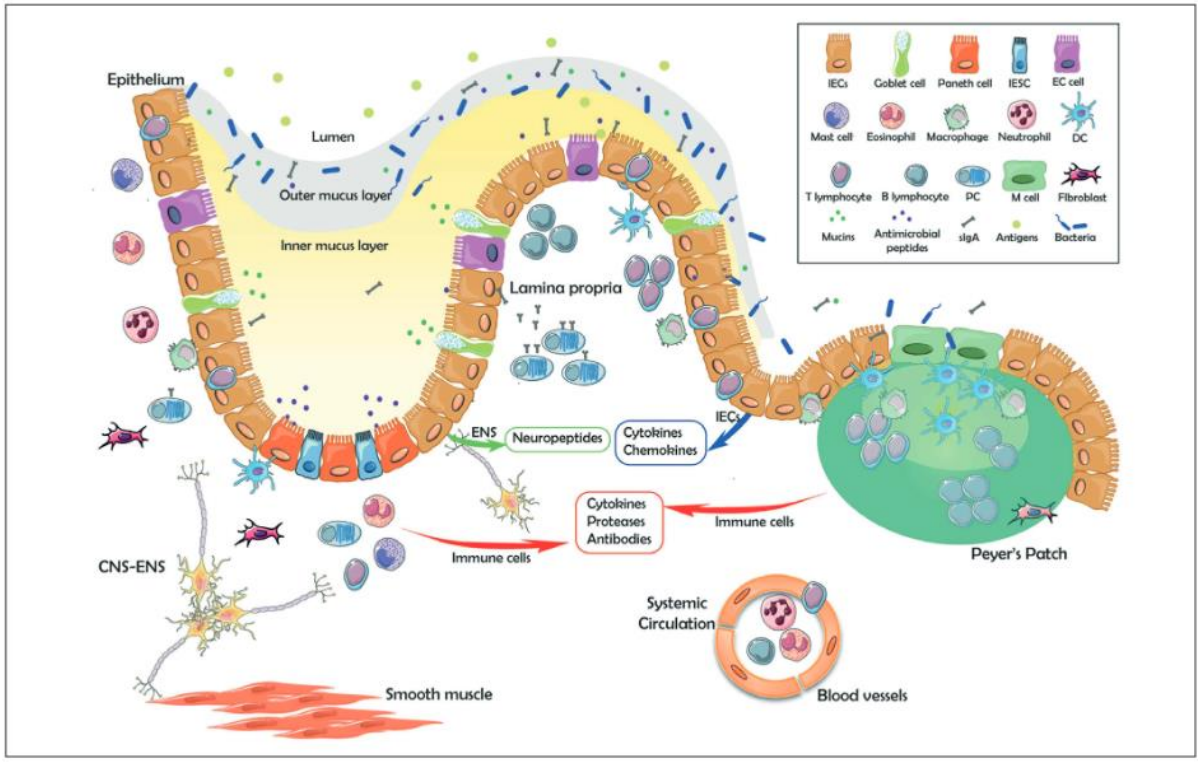

Figure 4 Intestinal epithelial barriers are constituted of different cell types. The repartition and function of these different cell types is responsible for the maintenance of intestinal barrier's functions and homeostasis. The gut epithelium is composed of intestinal epithelial cells (IECs) also called enterocytes constituting the physical barrier and responsible for absorption, Goblet cells responsible for mucus secretion, Entero-Endocrine cells (EECs) secreting hormones and other modulators, Paneth cells at the base of the crypts having a role in antimicrobial secretion and cell differentiation, and Intestinal stem cells (ISCs) pluripotent, and able to renew the gut epithelium in 4-5 days. The gut epithelium separates the outer environment composed of the microbiota and layers of mucus (one in the small intestine and two in the colon), from the inner environment, the lamina propria, which is constituted of the immune system (Macrophages, dendritic cells (DC), lymphocytes) but also fibroblast and the enteric nervous system (ENS) in relationship with the central nervous system (CNS). The lamina propria is surrounded by a layer of muscles called the muscularis mucosae. (figure from [14]*)*

2.1.7 Paneth cells

Paneth cells are located at the bottom of intestinal crypts as neighbors of intestinal stem cells (ISCs). They are exclusively present in the small intestinal crypts, and aberrant expression of these cells in colonic crypts can be associated to pathological states such as Inflammatory Bowel Diseases (IBD) [63]. After differentiation they are the unique cell type to migrate downward the intestinal crypts and reside there, intercalated between ISCs [64] (Figure 4).

Their primary function is to protect the gut epithelium and internal microenvironment (i.e., immune system, enteric nervous system) by secreting antimicrobial peptides. With their larger endoplasmic reticulum and Golgi apparatus, they deliver an important production of α-defensin, phospholipases-A2, lysozymes C, and Regenerating islet-derived (REG) 3α proteins, all important for the regulation of microorganisms [65]. They also support cell proliferation and participate actively in the Wnt/β-catenin pathway by secreting Wnt ligands to the neighboring ISCs [66]. They participate in epithelial repair and can reprogram into Intestinal Stem Cells in case of injury [26].

Paneth cells are approximately as numerous as ISCs (5-12 cells per crypt). They can be easily recognized with their pyramidal shape and since they are composed of numerous granules - the transporters of antimicrobial compounds [67] . In opposition to other cell types found in the gut, their life expectancy can last a month [68].

Their molecular signature is characterized by Sox9 expression [69], a typical marker of secretory lineage, and CD24 [70].

2.2 INTESTINAL EPITHELIUM HOMEOSTASIS

As the gut epithelium is renewed every 4-5 days in humans, homeostasis is reached by achieving a balance between cell proliferation, differentiation and death along intestinal crypts and villi. This equilibrium is maintained via the secretion of molecular mediators along the crypt-villus axis to finely tune and regulate all these processes.

2.2.1 Mediators regulating gut epithelium homeostasis

The architecture of the gut epithelium is decomposed between the stem cell zone, the transit-amplifying zone where cell proliferation occurs, the differentiation zone and the apoptosis zone. This architecture is maintained by gradients of ligands (e.g., TGF-β, BMP, Hedgehog, Notch, Wnt) [71–73] (Figure 6). The functions of these key mediators will be described in the next paragraphs.

2.2.1.1 Wnt/β-catenin

The Wnt/β-catenin pathway is the main regulator of proliferation within the gut epithelium and targets the LGR5+ ISC [74]. In the cell, β-catenin is constitutively phosphorylated and, therefore, targeted for degradation. But binding of the Wnt glycoprotein to its Frizzled receptor, and LRP5/6 co-receptor [75], prevents β-catenin constitutive phosphorylation by the axin, adenomatous polyposis coli (APC), kinases glycogen synthase kinase 3β (GSK3) and casein kinase I (CK1) complex. When Wnt is bound to its receptor, β-catenin can, therefore, translocate to the nucleus where it binds to the TCF/LEF transcription factor and induces the transcription of downstream genes involved in cell cycle regulation, cell migration and cell differentiation [76] (Figure 5B). An example of Wnt/β-catenin targeted genes are c-Myc and Cyclin-D1, both important regulators of the cell cycle [77]. They will be discussed in the Cell Proliferation Section below.

The Wnt/β-catenin pathway can be regulated to control/limit cell proliferation. In particular, the binding of DKK1 to the LRP5/6 receptor prevents further binding of Wnt to Frizzled [75] or the ubiquitination of Frizzled and LRP5/6 receptors by the transmembrane complex ZNRF3/RNF43, signals the degradation of both receptors [74]. The binding of Wnt to Frizzled receptors counteracts the ZNRF3/RNF43 ubiquitination by activating R-ponding (RSPO) which binds to LGR and ZNRF3/RNF43 and induces the ubiquitination of the latest (Figure 5B) [78].

The switch between cell proliferation, differentiation, and death, and therefore the fate of ISCs within intestinal crypts is controlled by the level of Wnt and β-catenin. When subjected

to high levels of β-catenin, ISCs tend to follow the path of apoptosis, while low levels lead to cell differentiation. Thus, only the adequate amount of Wnt and β-catenin allows cell proliferation [79]. This level is maintained by the secretion of Wnt2b and Wnt3 by respectively, the neighboring mesenchymal and Paneth cells [66, 80]. (Figure 5A).

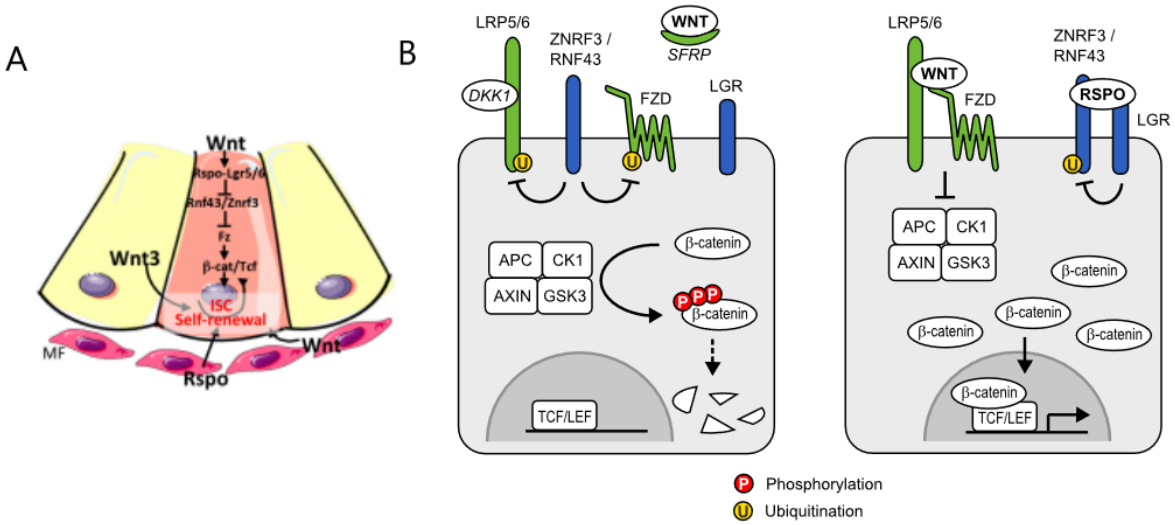

Figure 5 Cell proliferation in intestinal crypt is regulated by the Wnt/β-catenin pathway. A. Wnt is secreted by mesenchymal cells located below intestinal crypt and the surrounding Paneth cells and triggers the Wnt/β-catenin cascade in active ISCs (figure from [81]*). B. Wnt binds to Frizzled receptor and LRP5/6 Co-receptor to prevent the phosphorylation of β-catenin by the APC/CK1/AXIN/GSK3 complex. β-catenin can then bind to the TCF/LEF transcription factor and active the expression of downstream genes. Wnt/β-catenin cascade can be prevented by the binding of DKK1 to LRP5/6 co-receptor or the ubiquitination of Frizzled and LRP5/6 by the ZNRF3/RNF43 receptor usually blocked by R-ponding proteins (figure from* [74]*).*

2.2.1.2 TGF-β family: a focus on BMPs

Bone morphogenetic proteins (BMPs) belong to the Transforming Growth Factor β (TGF-β) family. They are cytokines and antagonists of Wnt pathway. TGF-β pathways always end with the phosphorylation of Type I serine/theorine kinase receptors, mediated by type II receptor activation and, finally, trigger SMADs' phosphorylation [73]. Their downstream signaling is dependent of the phosphorylated SMADS: if SMADs phosphorylated via BMP pathways are involved in cell differentiation, it is not the case of SMADs phosphorylated by TGF-β cytokines which induce cell proliferation or repair mechanisms [82]. For instance, TGF-β signaling induces SMAD2/3 phosphorylation and the formation of the SMAD2/3/4 complex, now able to translocate to the nucleus where it promotes the transcription of pro-regenerative genes [83]. Moreover, TGF-β members can prevent proliferation and their expression is often decreased in colorectal cancer models where Type II serine/theorine kinase receptors are inactivated [84]. BMP activates the Hedgehog pathway via phosphorylated SMAD-1, -5, and -8 and prevents the formation of ectopic crypts [85] (Figure 6).

2.2.1.3 Hippo

Hippo is a kinase which inhibits both Wnt mediated cell proliferation and apoptosis and is overall highly involved in regeneration processes [73, 86]. Indeed, it triggers the

phosphorylation of YAP proteins and prevents their translocation to the nucleus. In the cytoplasm, phosphorylated YAP proteins prevent both proliferation and apoptosis [87].

Therefore, the crypt-villus axis organization is dependent of TGF-β, BMP, Hedgehog, Hippo and Wnt gradients which dynamically promote or prevent cell proliferation, differentiation, apoptosis and wound healing along intestinal epithelium zones [73] (Figure 6).

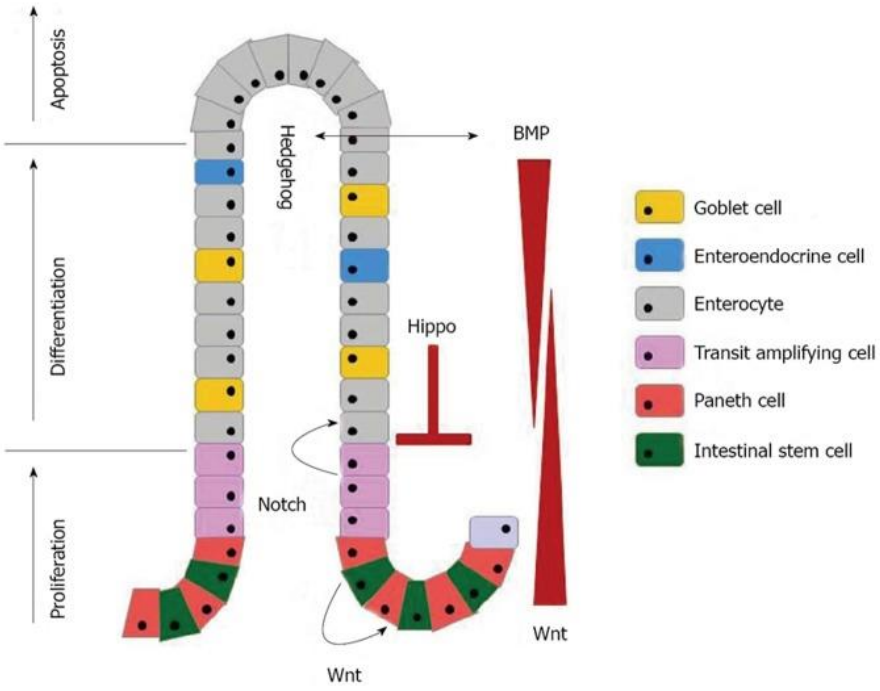

Figure 6 Gut epithelium architecture is regulated by major pathways: gradient of Wnt promotes proliferation. BMP and Hedgehog pathways shape colonic crypts' size and shape by antagonizing Wnt. Hippo plays an essential role in tissue regeneration and blocks both apoptosis and cell proliferation. Notch induces cell differentiation toward the secretory lineage. (figure from [73]*)*

2.2.2 Cell proliferation

Proliferation is a driving force of self-renewal in the gut epithelium. As cells produced by the active ISCs migrate to the transit-amplifying compartment of intestinal crypts, they are subjected to a decreasing secretion of Wnt.

To proliferate, cells need to divide and enter the different phases of the cell cycle called G1, S, G2 and M. For a cell to divide into two daughter cells, it requires growth (G1 phase) and the replication of its DNA (S phase). The G2 phase is a second growth period and prepare the cell for mitosis (M phase). After mitosis, daughter cells return to a quiescent state called G0.

Upon β-catenin binding in the cell nucleus, the transcription of downstream genes is activated and especially the transcription of Cyclin D1 and c-Myc - respectively involved in the G1 and S phases of the cell cycle (Figure 7). To exit the G0 phase and to undergo cell mitosis the presence of growth factors is required. All cell cycle phases are regulated by Cyclins and Cyclin-Dependent-Kinases (CDK). But the passage between each cell cycle phase is highly controlled [88]. The cell remains in the G0 phase as long as p21 and p27 are presents and inhibit Cyclin D1 [89]. C-Myc is therefore necessary for the G1/S phase transition since it can both promote Cyclin D1 [90] and repress p21 and p27 [91]. However, Cyclin D1 is also tightly regulated by GSK-3β protein. GSK-3β can phosphorylate and translocate Cyclin D1 from the nucleus to the cytoplasm where it will be degraded. GSK-3β protein can itself be

phosphorylated by the PI3K-AKT pathways and therefore be inhibited [92]. The passage between G1 and S phases is controlled by Cyclin D1/Cdk-4 complex which can phosphorylate retinoblastoma protein (pRB). pRB upregulates the expression of Cyclin E necessary for the next cell cycle phase [88, 93].

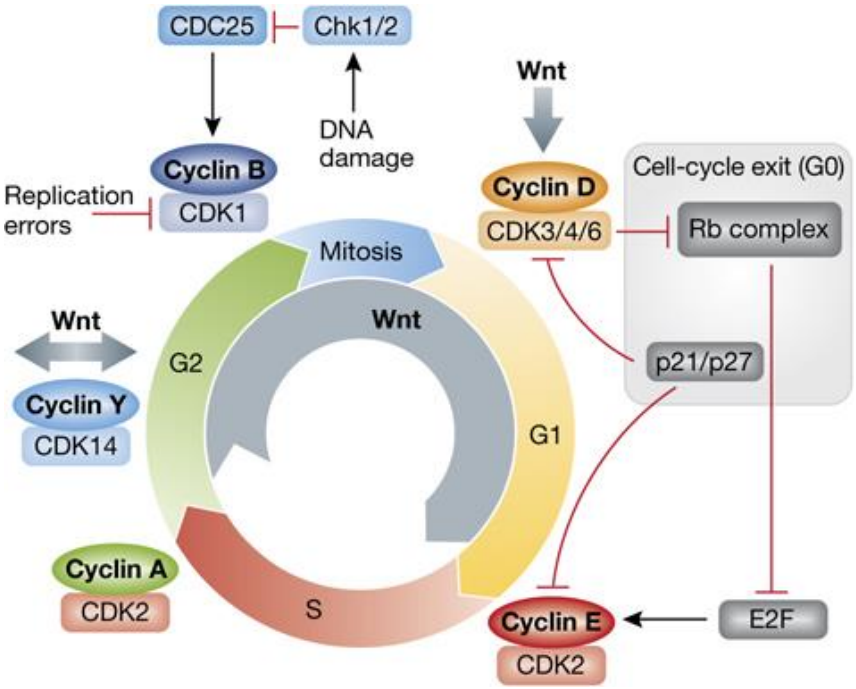

Figure 7 Wnt signaling mediates the transition between G1/S phase and peaks during the G2 phase of the cell cycle. All phases of the cell cycle are induced by Cyclin/Cyclin-Dependent-Kinase complexes. During the G1 phase, CyclinD1 usually inhibited by p21 and p27, can phosphorylate the Rb complex and therefore prevent re-entry in the G0 phase. Repression of p21 and p27 is mediated by c-Myc, another downstream gene of the Wnt/ 6-catenin pathway. Wnt signaling peaks at the G2 phase and promotes cell growth prior to mitosis (figure from [93]*).*

The β-catenin concentration oscillates during the cell cycle but peaks at the G2 phase. During this phase Cyclin Y/CDK14 can induce the phosphorylation of the LRP6 co-receptor and maximize Wnt signaling [93].

Cell cycle also implies cytoskeleton rearrangements, especially during the growth phase. These rearrangements require, prior to mitosis, that the cell loses its polarity. After the loss of polarity, actomyosin skeletal components are moved by Rac and Rho under the supervision of Arl4c (a transcription factor activated by the combined action of Wnt/ β-catenin signaling and growth factors). After mitosis, the cell is eventually repolarized [94].

Cell proliferation does not only depend on Wnt signaling pathway but also requires the prevention of cell death. Molecular actors have been identified and play a role in cell death prevention such as Birc6, an inhibitor of apoptosis protein (IAP) [95]. In the S phase, many actors are also involved in DNA synthesis and chromatin condensation and cohesion like Nipbl [96].

2.2.3 Cell differentiation

As levels of BMP, Hedgehog and Hippo maintain a separation between the differentiation and transit-amplifying compartments, the determination of cell fate can be divided into two categories and depends on Wnt/Notch gradients: the absorptive lineage includes the enterocytes; the secretory lineage includes Goblet, Paneth and EECs (Figure 8).

2.2.3.1 Enterocyte differentiation

Enterocyte specification is induced by exposure to high concentration of Notch ligands. If Wnt is secreted by Paneth cells and mesenchymal cells surrounding the intestinal crypts [66, 80], Notch signaling requires the activation of Notch1 and Notch2 within ISCs triggered by Notch ligands DLL1 and DLL4 (Delta Ligand 1 and 4) secreted by Paneth [66, 72]. When exposed to Notch, cells within the transit-amplifying compartment activate the expression of HES1, a transcription factor, which further inhibits the secretion of ATOH1 (also called MATH1), and become enterocytes [72, 97].

Enterocyte's differentiation is also a result of a process called lateral inhibition which triggers the amplification of enterocyte specification by cells from the secretory lineage. It involves, ATOH1, a transcription factor involved in the secretion of Delta Ligands and the expression of other secretory lineages specific transcription factors such as SPDEF [98–100] (Figure 8). If differentiated enterocytes inhibit Notch expression (via ATOH1 inhibition), differentiated secretory cells secrete ATOH1, thus express the Delta Ligands DLL1 and DLL4, and further reinforce Notch signaling in the surrounding cells [98].

2.2.3.2 Paneth Differentiation

The combination of high Wnt concentration and low Notch signaling induces Paneth cell differentiation. These conditions are met around the crypts' base, when Paneth cells are not abundant and, thus, cannot sustain Notch gradients usually present. The exposure to high levels of Wnt signaling induces the expression of SOX9 and provokes Paneth cell specification. Following differentiation, they migrate downward and intercalate between ISCs [69, 72]. If some mediators of Paneth cell specification have been identified, their mechanism of differentiation remains highly uncharacterized. Moreover, mechanism involved in their migration processes and responsible for their survival (up to one month) are unknown. Sox9 functions are still unresolved however, some authors hypothesize that Paneth cells capacities are partially explained by their label-retaining nature [101, 102].

2.2.3.3 Goblet differentiation

Cells exposed to neither Notch nor Wnt signaling can differentiate into goblet cells. Above the transit-amplifying zone, KLF4 factors, usually repressed by Notch signaling [103, 104], induces cell cycle arrest. Maturation into Goblet cell lineage is further induced by the activation of SPDEF (Figure 8) mediated via ATOH1 [45]. Foxa1 and Foxa2 are also activated and associated with Muc2 secretion [105]. KLF4, SPDEF Foxa1, Foxa2 are all involved in goblet cell

differentiation however the exact mechanism of their specification is currently unknown. Goblet cells are characterized by fast division in opposition to EECs differentiation [100].

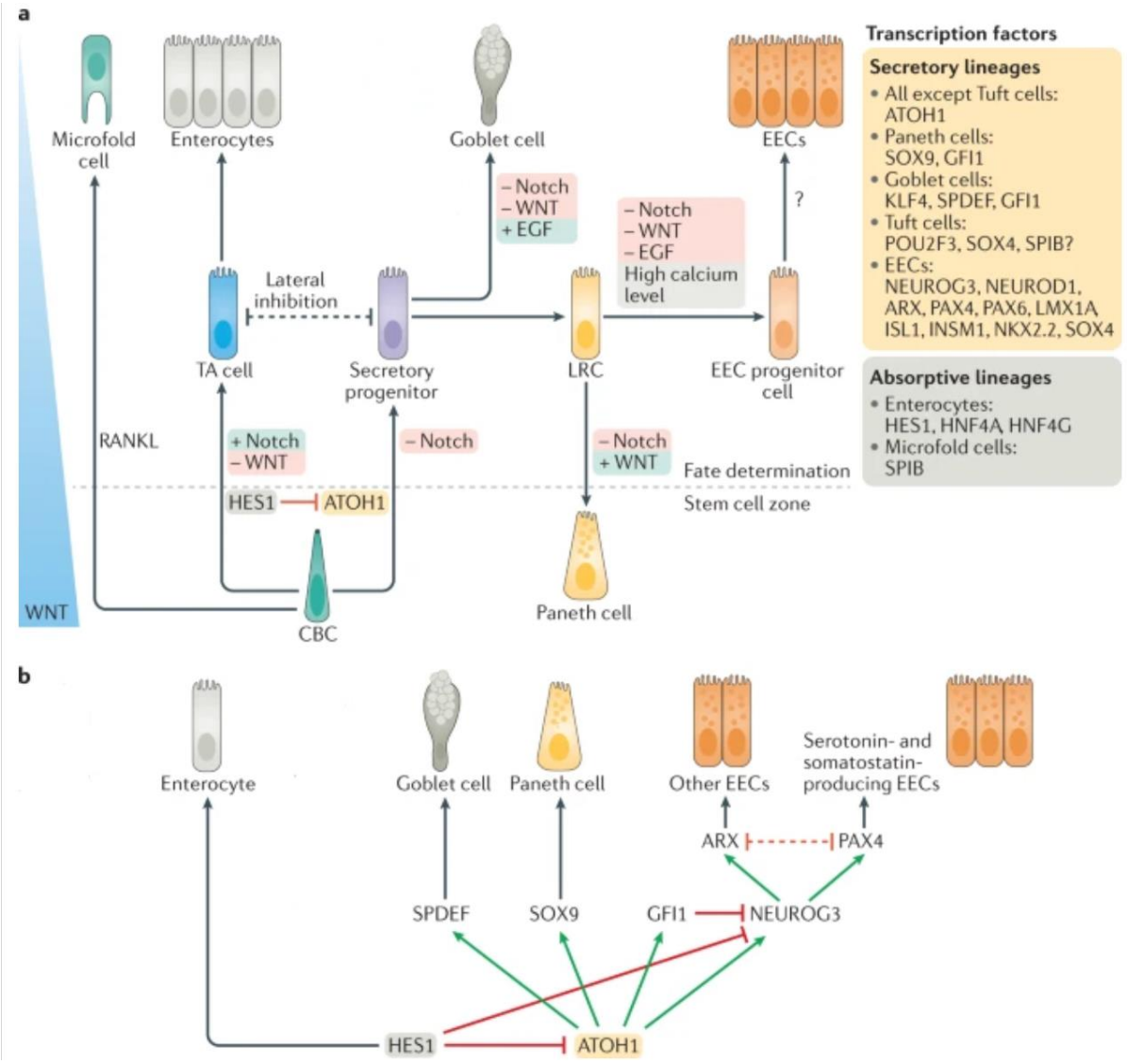

Figure 8 Cell differentiation into secretory and absorptive lineage is controlled by gradient of Wnt and Notch ligands. Lateral inhibition is another important process and promotes enterocyte development. Further differentiation toward goblet or EECs is triggered by their label retaining natures. (figure from [72]*)*

2.2.3.4 Enteroendocrine cell differentiation

The differentiation of EECs is a long process controlled by a large diversity of transcription factors specific to each subtype of EECs. As for goblet cells, cell differentiation into EECs requires the absence of both Notch and Wnt ligand. In the absence of Notch, HES1 is absent and, therefore, cannot inhibit the expression of NEUROG3. Then, the sequential activation of different transcription factors assures cell specification toward the EEC lineage [72]. Especially BETA2 (also called NeuroD1), Pax4 and Pax6, along with NEUROG3 are transcription factors responsible for the secretory capacities of EECs and can induce the arrest of the cell cycle [106]. The specification of EECs' subtypes was recently characterized by single cell analysis and

revealed a sequential activation of many mediators and a plasticity between subtypes differentiation [107].

Another difference in their differentiation process compared to other secretory lineage cells is their label-retaining nature: a cell capacity to segregate asymmetrically their DNA during, generally, long-lasting mitosis. It is characteristic of EECs, and explains their low abundance in gut epithelium (1% of the intestinal barrier) [108]. Moreover, as NEUROG3 is inhibited by cyclins involved in cell cycle, differentiation into EECs is prevented by fast cell division [109].

2.2.4 Cell death

Cell death is an essential process involved in the maintenance of the intestinal epithelium homeostasis. This process can take many forms and includes apoptosis, necrosis, anoikis and pyroptotic extrusion depending on the place and the cellular actors involved [110] (Figure 9).

Apoptosis and Anoikis occur in homeostatic conditions. Apoptosis can be mediated by extrinsic and intrinsic pathways. Via intrinsic pathway, the signalization of DNA damages to Caspase 9 signaling cascade induces mitochondrial permeabilization by Bcl2, the release of Cytochrome c and SMAC into the cytoplasm and the formation of apoptotic bodies (vesicles enclosing cellular contents to prevent the propagation of cellular wastes to surrounding tissue) [110, 111]. In the extrinsic pathway, the binding of TNF ligands to TNF receptors (TNFR1, TRAIL…) triggers the caspase 8 signaling cascade [112]. Both intrinsic and extrinsic pathways end with the activation of caspase 3 and 7, effectors responsible for the cleavage of DNA and the externalization of phosphatidylserine. This signal will be recognized by macrophages to remove cell apoptotic bodies from the environment [113].

Anoikis is a process specific to monolayers of epithelial cells and occurs at the top of colonic crypts or small intestine villi. As apoptosis, this process takes place in homeostatic conditions. It is triggered by mechanical forces which provoke cell extrusion. It regulates the constant proliferation of cells issued from the transit-amplifying zone by ISCs [110]. Within the cells, the loss of ligation by integrins signals caspase 9 or Bax cascade and induces the unification of adherens proteins in neighboring cells, closing the formed gap in a zipper-like movement [114]. As gut epithelium is renewed every 4-5 days, cell turn-over is frequent, driven by the proliferative forces of the ISCs embedded in the colonic crypts.

Both pyroptotic extrusion and necroptosis are cell death mode inducing pro-inflammatory conditions. Pyroptotic extrusion is provoked by pathogens and signals an intrusion within the cell [115]. Necroptosis occurs when caspase signaling cascades are blocked [116]. Both ends with the leaking of cell wastes into surrounding tissues. These wastes generally include Damage-associated molecular patterns (DAMPs) which are recognized by the immune system in the lamina propria and ultimately trigger a pro-inflammatory response [110]. They are heavily studied in pathology as IBD or colorectal cancer (CRC) [117, 118]. In IBD, for instance, a delay in apoptotic bodies cleansing by macrophages is thought to induce secondary necroptosis and therefore exacerbate the pro-inflammatory response [110, 119].

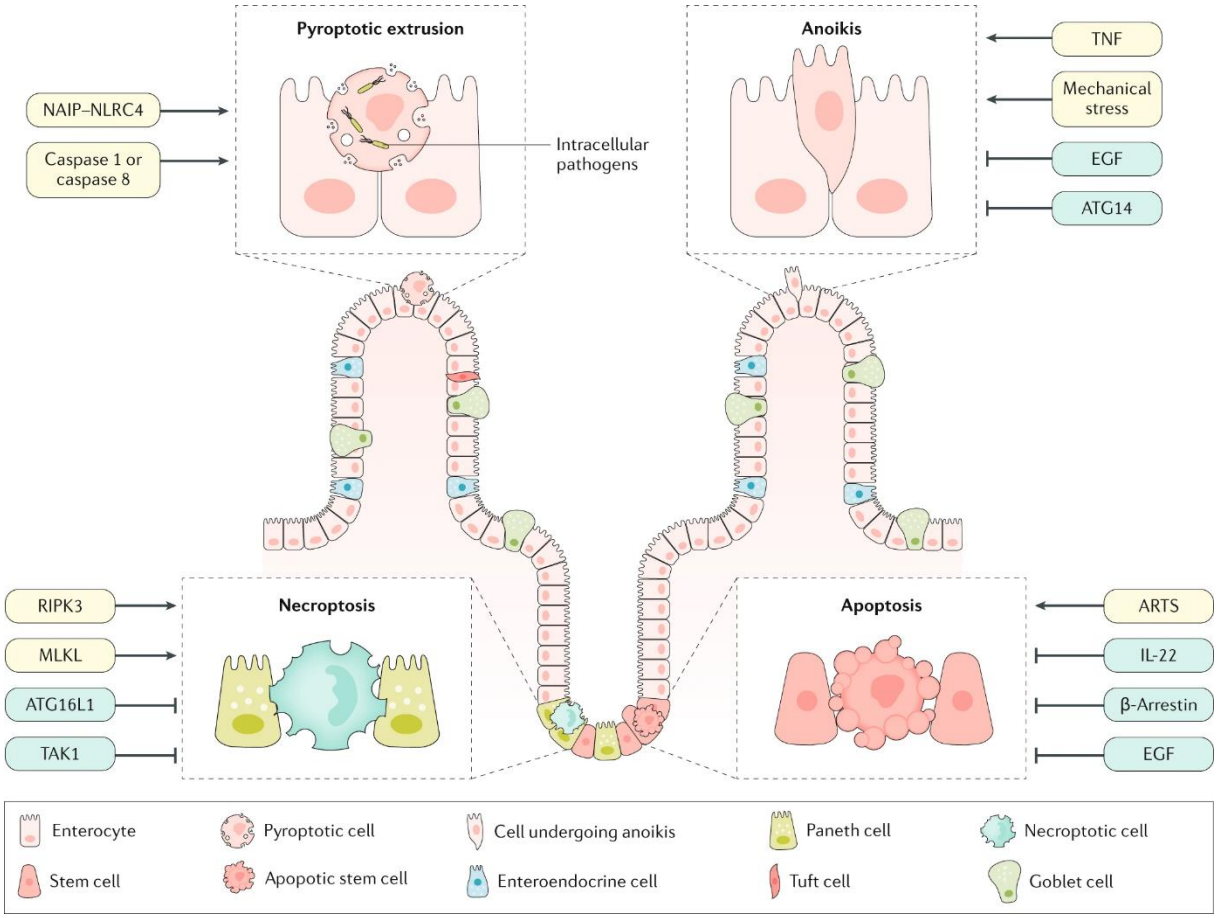

Figure 9 Pyroptotic extrusion, anoikis, necroptosis, and apoptosis are four types of cell death occurring in the gut epithelium. In homeostatic condition, the most common cell death mechanism is apoptosis. Both extrinsic and intrinsic pathways lead to the activation of caspases, the externalization of phosphatidylserine to signal cell death and provoke endocytosis by surrounding macrophages. Anoikis occurs at the top of villi in the small intestine and at the top of the crypts in the colon and is driven by mechanical forces. Both pyroptotic extrusion and necroptosis lead to pro-inflammatory conditions as they trigger the release of cell wastes into the external milieu (figure from [110]).

2.2.5 Wound Healing

Even in homeostatic conditions, parts of the intestinal barrier can be damaged [120] for instance following mechanical insult induced by the bolus [120]. Therefore, epithelial repair is a physiological function contributing to gut homeostasis and is performed occasionally to replenish the pool of epithelial cells in crypts and villi.

This process can be divided into 3 phases: restitution, proliferation, and differentiation [121]. Restitution is a form of migration, where cells surrounding the wound are directed toward the hole to fill it. This process prevents the impairment of the barrier and the passage of potential toxins [122]. It lasts between minutes to hours and is mediated by TGF-β [123]. This factor induces cells around the wound to form pseudopodia-like structures and to migrate [124].

Following restitution, proliferation occurs to replenish the gut epithelium at the site of the wound. This process is mediated by various growth factors including epidermal growth factor (EGF), keratinocyte growth factor (KGF), and fibroblast growth factor (FGF) [125, 126].

2.3 INTESTINAL EPITHELIAL BARRIER FUNCTIONS

Intestinal epithelial cells are responsible for the exchange of compounds between the lumen and the internal microenvironment of the host [14]. The acquisition of nutrients and electrolytes from this external environment can take two roads: the paracellular or transcellular.

2.3.1 Transcellular permeability

The transcellular permeability is a function allowing the transport through the cell. This transport can be done via passive/facilitated diffusion for lipophilic compounds or ions, via active transport for amino acids, or antigens, and also, through endocytosis for larger proteins or bacterial by-products (Figure 10) [127].

Passive or facilitated diffusion requires no expense in energy: to maintain osmolarity between the external milieu and cell cytoplasm, ions, or liposoluble vitamins can simply diffuse through the plasma membrane and follow gradients of solute from high to low concentrations [128]. Ions are generally diffused through ion channels and can be used to facilitate the passage of larger molecules or to generate energy via secondary active transport [129].

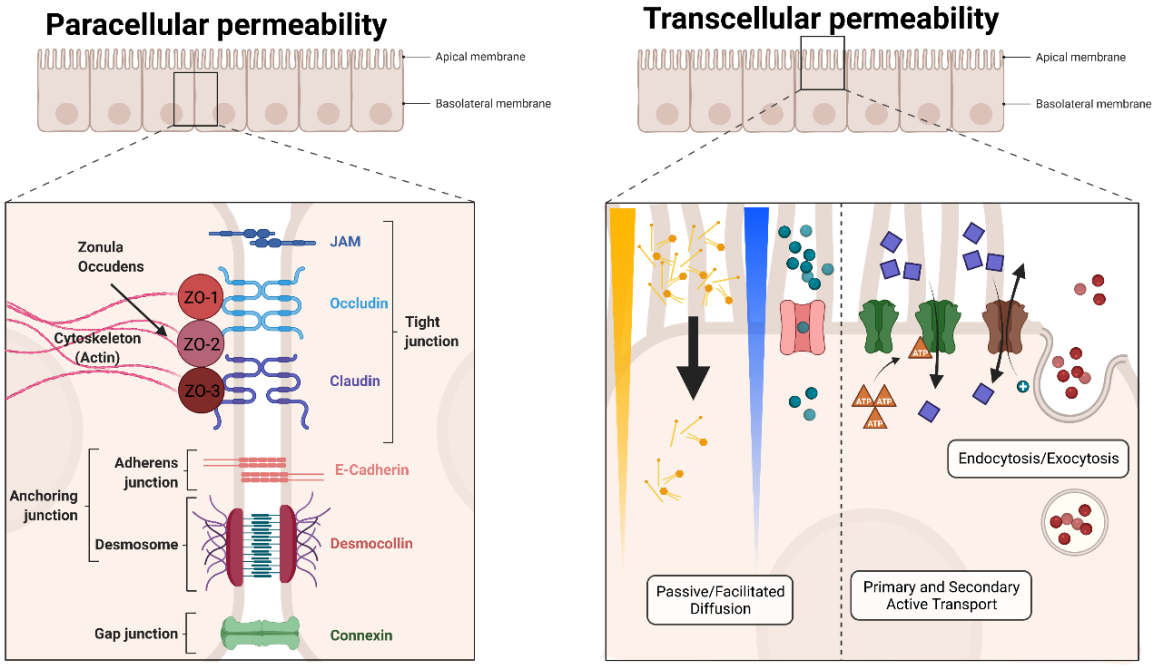

Figure 10 The intestinal epithelium permeability: paracellular permeability is regulated by 3 types of intercellular junctions: Tight, anchoring junctions (desmosomes and adherens junctions) and GAP junctions. Transcellular permeability can be performed through passive/facilitated diffusion, primary or secondary active transport and endocytosis/exocytosis.

Active transport consumes energy (often in the form of Adenosine triphosphate (ATP)). It can also be performed by creating electrochemical gradients via the transport of ions as stated before [130]. The movement of compounds is specific and depends on a large diversity of transporters. For instance, the receptor SGLT-1 is required for the transport of glucose [131].

Finally in endocytosis, vesicles are fused to the plasma membrane and their content is discharged within the cell. In exocytosis, it is the opposite: contents from the cell are packaged

into vesicles upon their exit in the external milieu. However, during the endocytosis/exocytosis, most of the absorbed contents are degraded in the process and exit at the basal pole of the cell, transformed. This degradation concerns approximately 90% of the compounds absorbed by endocytosis and only 10% can be found intact in the lamina propria [132]. This rare process of transcytosis is mediated by specific endosomes bearing the major histocompatibility complex (MHC) class II molecules [133]. Endocytosis may also be mediated by IgA, IgG or Ige [134].

2.3.2 Paracellular permeability

The paracellular permeability regulates the passage between cells via the assembly and regulation of inter- and intra-cellular junction proteins, a series of intermembrane proteins which controls the interval space between epithelial cells. There exist 3 major types of intercellular junction proteins (Figure 10):

2.3.2.1 Tight junctions (TJs)

2.3.2.1.1 Occludins

Occludins are important for TJ assembly and disassembly [14]. Their phosphorylation level is associated with their cellular location (highly phosphorylated occludins are stable and located at the junction between cells, while without phosphorylation, occludins are unstable and are located in the cytoplasm) [135]. Moreover occludins participate in cell differentiation since, in their absence, no parietal cells are found in the stomach [136], and are also important for cell polarity [137].

2.3.2.1.2 Claudins

There are 24 known isoforms of Claudin distributed differentially along the digestive tract [138]. Claudins form a channel for the passage of molecules and ions [139]. Therefore, the regionalization of paracellular permeability is a result of tight junctions' claudins composition since claudins' isoform are also regionalized [140]. Anion's passage is regulated by claudins-10a, -17, while cation's is associated with claudins-2, -10b and -15 [141, 142]. If they are effectors of paracellular permeability, they also exert different roles: for instance, claudins-1, -2, and -3 participate in cell adhesion [136] while claudin-11 is involved in cell cycle regulation [143]. Together, claudin-4 and occludins mislocated in the cytosol can trigger cell death signaling cascade [144].

2.3.2.1.3 Junctional adhesion molecules (JAMs)

JAMs are globulins. They help in the assembly of TJs and the establishment of cell polarity [145]. JAMs family involves many proteins (e.g., JAM-A, JAM-B, JAM-C, JAM-L and JAM-4) distributed differentially across organ regions. They participate in tight junction complex formation. While claudins are specialized in the paracellular permeability to ions, JAMs are involved in the regulation of macromolecule passage [146]. They are also implicated in various functions aside permeability [147]. JAM-A is, for instance, associated with cell proliferation via

inhibition of Akt/β-catenin activation [148] and JAM-C, is involved in cell differentiation of hematopoietic stem cells into myeloid cell progenitors [149]. JAM-L and its CAR co-factor are also related to wound healing as they trigger growth factor expression in T-cells in the periphery of the gut epithelium [150].

2.3.2.1.4 Zonula occludens (ZO)

All TJs are tightly linked to the cytoskeleton by Zonula Occludens proteins (ZO-1, ZO-2 and ZO-3). They are specialized in the establishment of plaque for the assembly of tight junction complexes. Their ability to polymerase claudins and occudins also participates in their ability to regulate paracellular permeability [151]. For instance, ZO-1 is also a stabilizing agent of junction assembly via the phosphorylation of Occludins [135]. Moreover they play an important role in both cell adhesion and cell migration since they are able to transmit signal from the inside of the cell to the periphery [14, 151]. If they regulate TJs assembly [152] they also relate to different biological functions.

As ZO-1 gets redistributed prior to cell shedding in the intestinal epithelium, it serves as a determinant marker of cell shedding [153].

ZO-2 is involved in the anchoring of TJs to the cytoskeleton as it stabilizes the cytoskeletal structure via the regulation of Rho proteins [154]. It also modulates cell homeostatic functions as it can inhibits Wnt pathway and, therefore reduce cell proliferation and promotes apoptosis [155].

ZO-3 was also studied in the context of cell proliferation and acts as a protective scaffold for cyclin D1 to prevent its degradation prior to mitosis [156].

2.3.2.2 Anchoring junctions

Anchoring junctions link the cytoskeleton of two cells to maintain a structural integrity and are located below TJs [157]. This category can be further subdivided into Adherens junctions and Desmosomes (Figure 10).

Adherens junctions include actin and E-cadherin proteins. They regulate cell adhesion via the exchange between the actin receptor at the cell surface and E-cadherin filaments linked to the cytoskeleton [14].

Desmosomes (desmocollin, desmoglein) are also linked to cells' cytoskeleton and allow a more stable cell-cell adhesion [158]. Via their connection to intermediate filaments in each cell, they allow transcellular communication [14].

2.3.2.3 GAP junctions

At the bottom, GAP junctions (connexin) are a way of communication between two neighboring cells as they create porous channels with hexameric structures [159, 160] (Figure 10). Through these channels, ions and cAMP can be exchanged between two neighboring cells [161, 162]. They play an important role in cell cycle, especially during cell differentiation and growth [163, 164].

3 THE (MICRO)ENVIRONMENT OF INTESTINAL EPITHELIAL CELLS

Intestinal epithelial cells homeostasis and functions are regulated by various soluble factors produced by cells directly surrounding or at distance from the epithelium. These originate from the host itself or from the external milieu (e.g., gut microbiota, nutrients).

The internal microenvironment of the epithelium is constituted, among others, by fibroblast, immune cells, and enteric nervous system reside and contribute to the regulation of epithelial functions [14]

A first component of the internal microenvironment is the immune system which constitutes both the innate and adaptive immune response. It is involved in the survey and protection against external threats in gut epithelium [165]. Indirectly, via the recognition and tolerance of commensal microorganisms, it participates in gut homeostasis and promotes colonization by SCFAs producers [166, 167]. But direct interactions between the immune system and the intestinal epithelium also occur. For instance, Th2 cells can secrete cytokines able to participate in wound healing as they induce cell proliferation mediated by macrophages [168, 169].

A second component of the gut microenvironment is the enteric nervous system (ENS). It regulates intestinal motility and barrier functions. Its network of neurons and glial cells, organized into two plexuses, run through the lamina propria and submucosal layer. The remodeling of intestinal barrier and homeostatic functions by the ENS, studied during the past 10 years, is mediated by the secretion of distinct and specific mediators by glial and nervous cells and contribute differentially to the regulation of these functions [170–173].

Finally, other cellular actors participate in gut homeostasis and are part of the internal microenvironment. Mesenchymal cells, seen previously in chapter 2.2.3, signal Wnt and BMP at crypt bases and promote cell proliferation and differentiation. Myofibroblasts and fibroblasts form together a syncytium below intestinal crypt and villi. Connected via α-smooth muscle actin and GAP junctions, their paracrine secretions are involved in cell proliferation and cell differentiation [174, 175]. They have recently been associated with wound healing because they can act as a guide for cell migration processes occurring during cellular restoration [176].

The immune system, ENS, mesenchymal and fibroblasts are all important actor of the gut internal environment; however, they will only be mentioned in the current thesis since they were not studied in our work.

The epithelium can also be modulated by factors produced at distance by other organs. The ‘prototypical organs’ involved in such regulation is formed by the hypothalamic-pituitary-adrenal (HPA) axis where communication between brain and adrenal gland lead to humoral regulation of barrier functions. This regulation will be described in detail later in this thesis.

The intestinal epithelium state is not only regulated by internal microenvironment but also by the external milieu and especially the gut microbiota.

3.1 DEFINITION OF THE GUT MICROBIOTA

The gut microbiota is an assembly of bacteria, phages and fungi distributed along the digestive system. Their abundance and composition are dependent on the organ region. Overall, the number of bacteria colonizing human body sites ($3.8 \cdot 10^{13}$) is quasi-equivalent to the number of host cells in adults' tissues ($3.0 \cdot 10^{13}$) [177]. The number of bacterial genes was recently estimated to be 400 times larger than the number of human genes [178].

Perceived as ecosystems, gut microbiomes represent the assembly of microorganism colonizing the digestive tract and their genome. They are described and characterized through the prisms of their ecological diversity and stability over time [179]. All bacterial taxa are organised into kingdom, phylum, order, class, family, genus, species, strain. They describe with an increasing precision the nature of any micro-organisms. Composed of 5 major phyla (*Bacteroidetes*, *Firmicutes*, *Actinobacteria*, *Proteobacteria*, and *Verrumicrobia*) [180], the gut microbiota reflects individual signatures of host's habits, story, and successive colonization events [181]. This description of the gut microbiota at the phylum level is mainly articulated around the *Bacteroidetes*/*Firmicutes* ratio which can be modulated through age and in health and disease [182, 183]. Therefore, we use taxonomic diversity to measure and describe the evenness and richness of a microbial community or to compare two bacterial communities [179]. The phylogenetic composition in large cohorts revealed the existence of enterotypes. Enterotypes are global variations of gut microbiota composition characterized in healthy adults. In human, 3 enterotypes exist: one governed by the *Bacteroidetes* Phylum, the second, by the *Prevotella* phylum and the last one, by the *Ruminococcus* phylum [184]. However, the mechanism of speciation is, nowadays, largely discussed in prokaryotes and especially bacteria, mostly due to their large population, their ability of homologous recombination and lateral gene transfer [185, 186]. Thus, gut microbiomes are more and more characterized using their functional diversity instead of their taxonomic diversity to measure the variety and richness of functions available in microbial communities [179].

From birth to elderly days, in health and diseases, changes in microbial diversity reflect host diet and lifestyle even if the microbiome remains capable of a certain plasticity to stress events or antibiotic consumption [187]. Newborns have a highly variable gut microbiota, influenced by delivery mode and lactation. Their microbiome stabilizes around the age of three and adopts an adult-like composition. Between birth and 3 years old, it will however go through transitional stages marked by large changes in their diet (lactation promotes a dominance of *Bifidobacterium* while the consumption of solid food changes microbiota composition toward an adult-like microbiome composed of *Bacteroidetes* and *Firmicutes*) [188, 189]. During development, the gut microbiota is essential, especially for the development of immunity [190], but also in the ENS formation [191, 192]. With age, the diversity of the microbiota increases and adopts gender-specific microbial species during puberty associated with hormonal secretion and influenced by the brain-gut axis formation [193, 194]. It, finally, becomes stable at the adult stage, except during pregnancy where it diversifies [195, 196]. In elderly, the gut microbiota is reduced and becomes more and more variable, highly associated with the health status of its host. (Figure 11) [196].

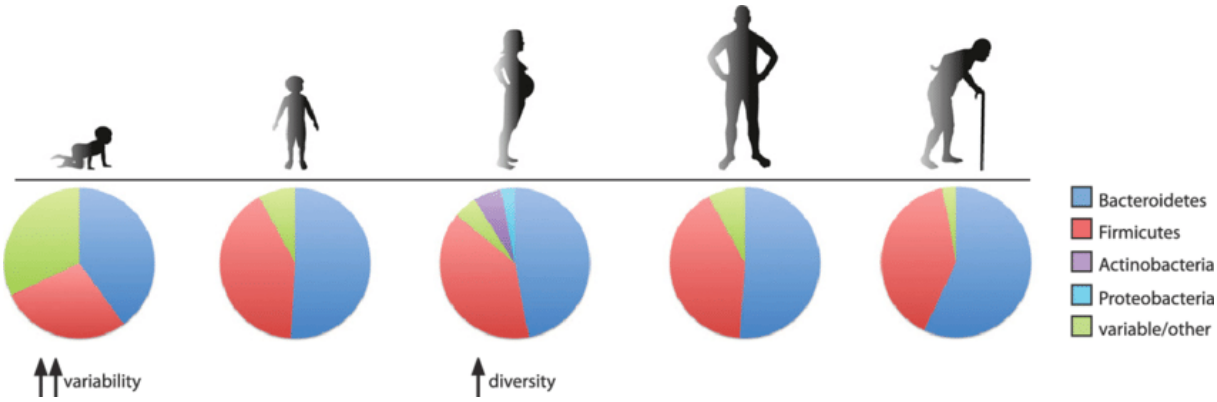

Figure 11 Gut microbiota diversity and composition evolve with host age. The gut microbiota is highly variable in newborn and overcomes diet transition periods. During puberty it is influenced by sex-related hormones which induce colonization by gender-specific microorganisms. Gut microbiota diversity stabilizes at the adult stage although it reaches its maximum during women's pregnancy. Then, the gut microbiota is reduced with years, becomes more and more variable in elderly and is highly associated with host health status (figure from [196]*).*

Changes in gut microbiome taxonomic, functional diversity and composition occurs during the lifetime of their host. However, the exposure to external threat such as antibiotic consumption, drastic diet changes, invasion of pathogenic species, introduce larger perturbations. Depending on the amount and the perception of these external interferences by gut ecosystems, gut microbiota can either permanently shift toward a new potentially detrimental equilibrium or return to their original state. The capacity of gut microbiome to overcome perturbation is called resilience [179].

3.2 THE GUT MICROBIOTA COMPOSITION ACROSS ORGAN REGIONS

The digestive system is composed, of different organs with diverging physiologies and creates a series of different ecosystems for the colonizing microbiota. It is possible to distinguish two types of microbiomes: the luminal microbiota includes micro-organisms living in the lumen of the digestive system, and the epithelial-associated (or mucosal) microbiota resides in the mucosal layer and in close relationship with the gut epithelium. The adherence of some commensal bacteria to the epithelial surface is even considered as a protection for the host against pathogens since these microorganisms prevent further colonization by occupying the available space [197]. Mucosal surfaces, crypts, interfold regions are also seen as protected environments in case of a harmful event. Bacteria inhabiting these niches are considered as reservoir species which can refill the endangered luminal microbiota during environmental challenges [198].

In this section, the biogeography of the gut luminal microbiota will be surveyed with a focus on, what we call the epithelial-associated microbiota in the small intestine and colon paragraphs (Figure 12 and 13).

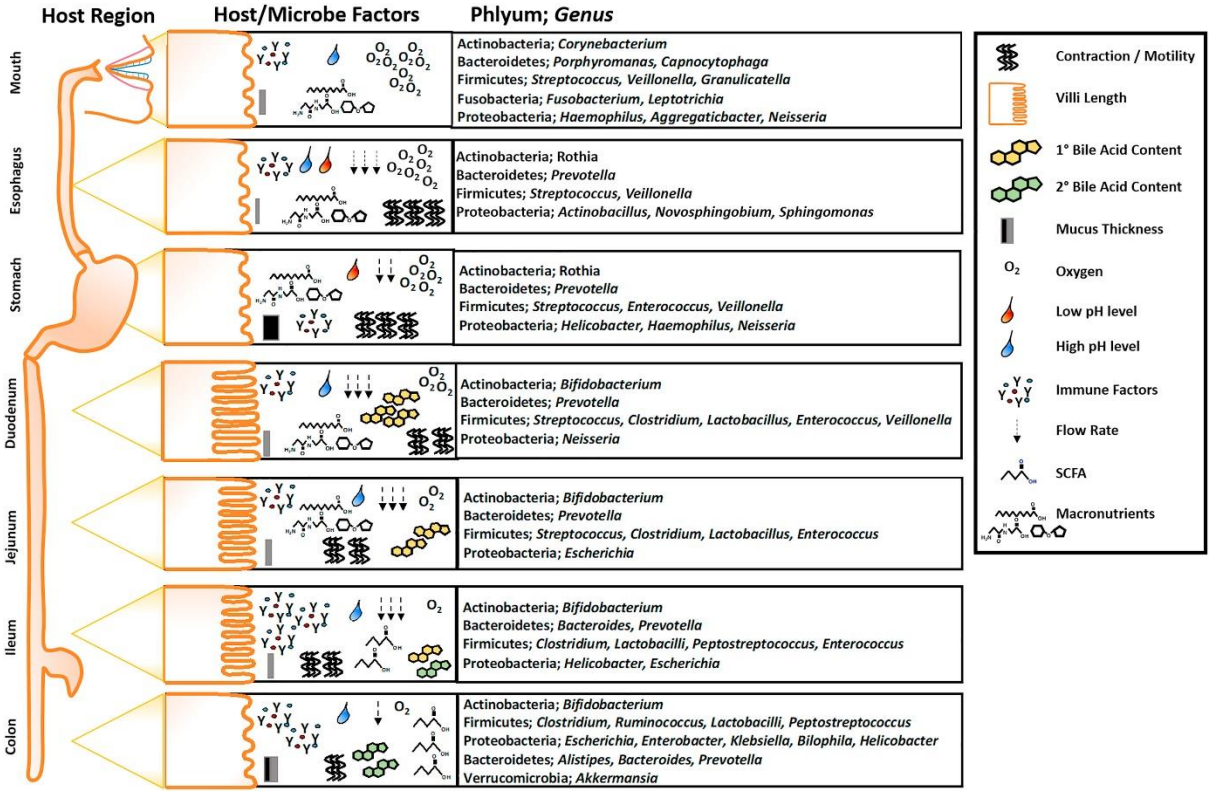

Figure 12 Gut microbiota biogeography: distribution of bacterial genera across the digestive system. The distribution of gut microbiota across organ regions depends on a combination of environmental and host factors which includes diet, pH, motility, oxygen, and mucus thickness. (figure from [199])

3.2.1 Mouth

In the mouth 10^9 bacteria coexist per mL content [199].

The mouth microbiota is diverse and influenced by saliva composition (mucins and immune factors), excretion and the access to oxygen [199].

The phyla diversity in the mouth is large and comprise *Actinobacteria*, *Bacteroidetes*, *Firmicutes*, *Proteobacteria* and *Fusobacteria*. At the genus level, a well-known resident of the mouth microbiota is *Corynebacterium*, which participates in plaque formation [200]. Other commensal bacteria can be cited like *Veillonella*, *Streptococcus*, and *Granulicatella gingiva*. They participate in the immune development of the mouth ecosystem [201]. The mouth microbiota participates in the transmission of bacteria to the lower gut regions [202].

3.2.2 Esophagus

The exact number of bacterial species inhabiting the esophagus is currently unknown, even if it is thought that 10^{11} bacteria are traveling through this organ per days [203]. The esophagus bacterial composition resembles the mouth microbial diversity and is mainly colonized by *Actinobacteria*, *Bacteroidetes*, *Firmicutes*, *Proteobacteria* at the phylum taxonomic level and *Prevotella*, *Veillonella*, *Sphingonomas* and *Rothia* at the genus taxonomic level [204].

The esophageal microbiota is mainly influenced by the diet but also by the motility generated by peristalsis. However, its implication in host homeostatic functions and the development of chronic diseases is currently unknown [199].

3.2.3 Stomach

The stomach microbial abundance lies between 10^1 and 10^3 CFU/mL

Gastric secretion, acidic pH and peristalsis, all shape the diversity of the stomach microbiota [199]. However, the still hosts diverse bacterial phylum such as *Actinobacteria*, *Bacteroidetes*, *Firmicutes*, *Proteobacteria* and includes *Prevotella*, *Streptococcus*, *Veillonella*, *Rothia*, and *Haemophilus* genera [205].

These bacteria may also play a role in ghrelin secretion and the regulation of appetite [206].

3.2.4 Small intestine

In the duodenum, where the bioavailability of nutrients is crucial for host metabolism, the microbiota is sparse (approximately 10^3 CFU/mL [199]), similar to the stomach microenvironment and characterized by low pH levels and large amounts of antimicrobial compounds (bile acids especially) regulating the presence of bacteria [207].

Composed mainly of *Actinobacteria*, *Bacteroidetes*, *Firmicutes*, *Proteobacteria* phyla and *Bifidobacterium*, *Clostridium*, *Lactobacillus*, *Prevotella*, *Veillonella* genera [199], the duodenum microbiota is a competitor for carbohydrates and lipids metabolism [208].

In the jejunum the microbial abundance increases (between 10^4-10^7 CFU/mL [199]). It harbors the same phylum diversity compared to the duodenum but is partially dissimilar in terms of genus diversity (presence of *Escherichia* and *Enterococcus* in the jejunum) [207].

The ileum bacterial abundance was reported approximately similar compared to the jejunum's one (between 10^3-10^8 CFU/mL [199]. it is composed by the same phylum compared to the duodenum and jejunum and mainly constituted, at the genus level, by *Bacteroides*, *Clostridium*, *Enterobacteria*, *Enterococcus*, *Lactobacillus*, and *Veillonella* [209].

As its terminal portion is specialized in the development of immunity, several studies reported the beneficial role of *Segmented Filamentous Bacteria (SFB)* colonizing these regions. These bacteria are involved in the recruitment of interleukin and the stimulation of Th17 cells [210, 211].

In the mucosal layer of the small intestine, the epithelial-associated microbiota is constituted of *SFB* (*Firmicutes*), *Lactobacillaceae* (*Firmicutes*), *Helicobacter spp*. (*Proteobacteria*) [43, 180, 212]. The epithelial-associated microbiota of the small intestine produces propionate and indole. [213]

Gradients of pH, oxygen, and antimicrobial levels induced the development of two successive types of microbial populations: in the upper intestinal tract, are found fast growing facultative anaerobes such as *Lactobacillaceae* (*Firmicutes*), *Erysiopelotrichaceae* (*Firmicutes*), or *Enterobacteriaceae* (*Proteobacteria*) while the colon harbors fermentative polysaccharide-degrading anaerobes like *Bacteroidaceae* (*Bacteroidetes*), *Prevotellaceae* (*Bacteroidetes*), *Rikenellaceae* (*Bacteroidetes*), *Lachnospiraceae* (*Firmicutes*) or *Ruminococcaceae* (*Firmicutes*) [214] described in the next section (Figure 12).

3.2.5 Colon

The colon harbors the largest community of microorganisms estimated at 10^{10}-10^{12} CFU/mL content. Colonic diversity is represented at the phylum level by Actinobacteria,

Bacteroidetes, Firmicutes, Proteobacteria and Verrumicrobia. At the genus level, a large variety of bacteria can be observed and include Bifidobacteria, Lactobacilli, Ruminococcus, Clostridium, Alistipes, Prevotella, Akkermansia.

The colonic microbiota is an extensive producer of SCFAs [199]. For instance, acetate, propionate, butyrate, and valerate are produced by *Roseburia*, *Clostridia* and *Eubacteria* species via the fermentation of indigestible fibers [215, 216].

Overall, we observe in this organ ,a shift in bacterial population are more pronounced between the lumen which contains a higher proportion of *Bacteroidaceae*, *Rikenellaceae* and *Prevotellaceae* (all *Bacteroidetes*) compared to the epithelial-associated microbiota which comprises more *Lachnospiraceae* and *Ruminicoccaceae* (all *Firmicutes*) [212, 217, 218].

In the mucosal regions of the colon the diversity of microorganism is more important compared to the small intestine mucosal layer and is divided between the outer and inner mucus layers. This dual mucus layer respects a gradient of increasing viscosity (Figure 13) [219] and decreasing oxygen concentration [218]. Therefore, studies report the presence of *Bacteroides Acidifaciens* (*Bacteroidetes*), *Bacteroides Fragilis* (*Bacteroidetes*), *Bifidobacteria* (*Actinobacteria*), and *Akkermensia Muniniphila* (*Verrumicrobia*) in the outer mucus, while the inner mucus is mainly constituted by *Bacteroides Fragilis* (*Bacteroidetes*) and *Acinetobacter spp.* (*Proteobacteria*) (Figure 13) [180]. However, *Bacteroides*, a dominant phylum in the gut [220], is also present in the epithelial-associated microbiota and was associated with mucosal colonization, development of immunity and barrier function in gut epithelium [166, 221]. The distribution of *Bacteroides* strains displays a regional pattern: *B. thetaiotaomicron* and *B. fragilis* abundances decrease gradually from the ileum to the rectum and *B. faecis* is present locally in the transverse colon [213]. In the transverse colon, carotenoid biosynthesis is also performed locally by a subset of bacterial strains *(B. vulgatus* and *Akkermensia muciniphila*) and is involved in vitamin A absorption, and IgA production [213, 222]. Of particular interest, the colonic microbiota, enriched in SCFAs producers such as *F prausnitzii*, *Eubacterium Rectale* or *A. Muciniphila* play a major part in the modulation of gut homeostatic functions [216, 223].

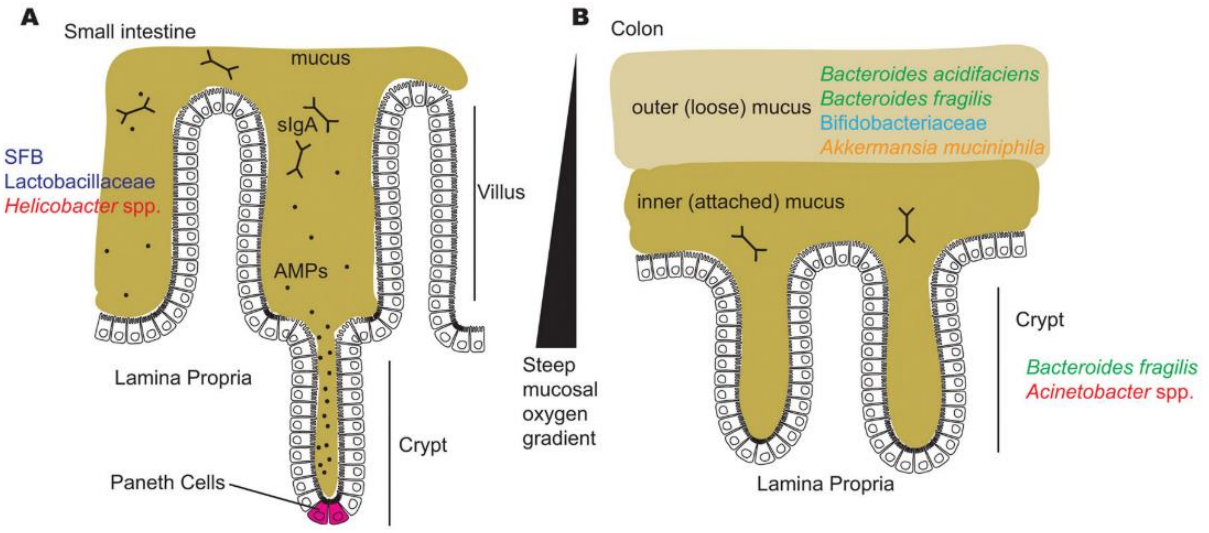

Figure 13 Epithelial-associated microbiota distribution in small and large intestines. Factors influencing epithelial-associated microbiota mucosal regionalization include the structure of the mucosal layer, the oxygen gradient, and the secretion of antimicrobials (increased in the small intestine). (figure from [180]*)*

The distribution of the gut microbiota across organ regions and between luminal and mucosal layers governs the type of interactions between the host and its associated microbiota. The regional host-microbiota interactions depend on the overall organ function and environmental factors.

3.3 THE IMPACT OF EPITHELIAL CELL AND GUT FACTORS UPON UPON MICROBIOTA COMPOSITION

The physiological succession of jejunal, ileal, cecal and colonic environments is governed by an increasing pH, a decreasing oxygen and antimicrobial concentration and, especially throughout the colon, an increasing viscosity [180]. All these parameters influence greatly the regional composition and diversity of the gut microbiota. But gut microbiota composition is also largely influenced by environmental factors such as diet.

3.3.1 Environmental factors: host diet and carbon sources

The access to carbon sources extracted from the host diet is a principal factor shaping the regional composition of the gut microbiota. Indeed, these carbon sources are the primary energy sources of bacteria. As the digestive tract digests and absorbs simple carbohydrates and lipids, a competition for nutrients occurs between the gut epithelium and its associated microbiota, especially in the upper portion of the intestine. In this region, the pH acidity, the secretion of antimicrobials, and the structure of the mucus layer, regulate the presence of microorganisms [180].

To overcome these challenges, the gut microbiota evolved strategies. Some like *Bacteroides Thetaiotaomicron* are generalists: their large genome gives them the ability to harvest multiple carbon sources [224]. Some can degrade specific limiting nutrients like *Bacteroides Vulgatus* or *Bacteroides Fragilis*. They can create durable niches as they induce colonization resistance (a process preventing the colonization by other species by occupying the available space) [225]. Eventually, some like *Bacteroides Muciniphila*, are able to consume Mucins, the principal component of mucus [226].

3.3.2 Antimicrobials

Antimicrobials are secreted by Paneth cells and the immune system present in the gut epithelium to regulate the presence of bacteria residing in the digestive tract. Their concentration is higher in the upper portion of the intestine and decreases along the digestive system. Antimicrobials reach their minimum concentration in the colon where microbial diversity and richness is at the highest.

Antimicrobials diffuse through the mucus layer and principally prevent bacteria from invading the space close to the gut epithelium. For instance, REGIII are a C-type lectin family of antimicrobials mostly represented by REGIII-α, REGIII-β and REGIII-γ [227]. They target gram-positive bacteria and disrupt their membrane upon binding to extruding glycans or peptidoglycans. The release of REGIII lectins is triggered by the presence of commensal microorganisms [228].

Another example of antimicrobials is the defensins family, and especially α-defensins secreted by Paneth cells. They target both gram-positive and gram-negative bacteria, fungi, viruses, and protozoans [229]. They employ many different mechanisms to induce cell death but mostly, they can create channels in bi-lipidic plasma membranes [230] and disrupt ion fluxes via the permeabilization of microbial envelopes [231].

Secreted IgA is an immune actor with multiple facets: sIgAs can prevent pathogens or toxins to access gut epithelium using agglutination mechanisms [232]. Via maternal transmission they induce tolerance toward commensal microorganisms [233] and even promote biofilms formations [234]. Upon endocytosis by M-cells, they can activate Dendritic cell activation [235, 236].

Finally, bile acids, synthesized by the pancreas and stored in the gallbladder, have an antimicrobial effect upon release [237]. Their concentration decreases gradually throughout the duodenum and the ileum. They help create a pH gradient which regulates microbial colonization in the upper portion of the digestive tract [238]. They also play a role in the establishment of gut microbiota in newborns [239].

Therefore, antimicrobial gradients and mechanisms shape gut microbiota from birth to elderly days (Figure 12).

3.3.3 Gut motility

The impact of gut motility upon gut microbiota composition was illustrated by several studies.

On one hand, the Bristol scale measured on healthy volunteers is an indicator of feces morphology. It is associated with transit and humidity content, and was identified as the largest predictive variable of microbiota composition and richness compared to other parameters (e.g., body index mass, age, cholesterol or triglyceride concentration, red blood cell count…) [240].

On the other hand, the impact of transit upon gut microbiota composition was further illustrated in experiments with modulation of gut motility. Indeed, when subjected to opioids treatments [241], known to inhibit intestinal transit and to delay gastric emptying [242], gut microbiota composition and diversity were modified and became enriched in potential pathogenic species. Bacterial communities related to stress tolerance or bile acids metabolism were greatly impacted [241].

Therefore, gut motility represents a key variable to describe changes in bacterial composition. This effect is thought to be mediated by the amount of time nutrients spend in each section of the digestive tract during gastro-intestinal. [180] (Figure 12).

3.3.4 Gut oxygen availability

The oxygen concentration in each section of the digestive tract and along the crypt-villus axis is another parameter influencing gut microbiota diversity and composition since O_2 can be deleterious for the growth of some bacterial species called anaerobes (Figure 12) [180].

Densely vascularized especially at crypt bases, the intestinal mucosa diffuses O_2 into gut lumen (Figure 13B). Most of the gut microbiota is composed of strict anaerobe species. Their growth is supported by a pool of aerobic species residing in the mucosa and able to use the

available oxygen, such as *Bacteroides Fragilis* or *Acinetobacter* [180, 212]. But oxygen availability also modulates microbial composition along the gastrointestinal tract.

For instance, bacterial distribution influenced by oxygen availability is well illustrated in a study in pigs [243], where members of the *Clostridiales* order (*Clostridium spp*., *Sarcina spp*. and *SMB53 spp*.), known to be obligate anaerobes, are associated to the proximal colon and display an opposite distribution pattern compared to *Campylobacter spp.* (*Proteobacteria*), a microaerophilic bacterium present in the duodenum.

3.4 GUT MICROBIOTA REGULATION OF GUT EPITHELIUM HOMEOSTASIS

The gut homeostatic and barrier functions are influenced by the gut microbiota. The effect of gut microbiota upon the intestinal epithelium can be mediated through two distinct mechanisms such as: the synthesis and secretion of bioactive metabolite and via microbial-derived components such as parts of their membrane (LPS), flagellin or DNA, recognized microbe associated molecular patterns (MAMPs) and danger associated molecular patterns (DAMPs) receptor embedded in epithelial cell membrane [244–246].

The involvement of gut microbiota in the modulation of intestinal epithelial cells proliferation and permeability, was confirmed in germ free animal models in which cell proliferation is regionally affected [247, 248], and permeability is increased and characterized by a decrease of claudins-1 and occludins junctional protein [249]. Fecal matter transplant (FMT) experiments result in partial restoration of epithelial barrier homeostasis and functions. This restoration is induced by the replacement of potential pathogenic bacteria and dysbiotic microbiota with a healthy microbiome and the re-colonization by commensal bacteria. The transplant of a healthy microbiome resolves the established pro-inflammatory state, paracellular permeability and induces epithelial repair via an increased production of SCFAs, especially butyrate but also by indirect immunomodulation [249–251]. Therefore, the gut microbiota is an actor of intestinal homeostasis and functions.

We will next focus on the effect of microbial-derived metabolites, especially bile acids and SCFAs metabolism upon the regulation of intestinal epithelial cells functions.

3.4.1 Microbial metabolites

3.4.1.1 Short chain fatty acids

SCFAs comprise butyrate, acetate and propionate and result from the metabolism of undigested polysaccharides [252]. The most abundant produced SCFA is acetate: in the colon. It represents 60% of the total SCFAs production while butyrate and propionate both account for 20% of SCFAs production respectively [253]. Although acetate can be used for butyrate production [254].

Propionate and acetate are produced by *Bacteroidetes* [255] and butyrate is synthesized mainly by *Firmicutes* [256] and especially *Butyricicoccus* species, and some *Lachnospiraceae* species [257, 258]. Their production displays region specific patterns: for instance, Propanoate

and Butanoate are produced by *Clostridiales* members present in the terminal Ileum, and butyrate is metabolized by *Butyrivibrio* spp located in the proximal colon [243].

SCFAs affect intestinal barrier and homeostatic functions. Butyrate promotes cell proliferation in healthy intestinal epithelial cells, but supplementation with sodium butyrate prevents growth in cancer cell lines via PKC and JNK dependent mechanisms. In addition, it induces cell differentiation and even apoptosis in these cell lines [259]. The role of butyrate in colorectal cancer is therefore questioned as it is involved in cell proliferation and can either promote or prevent it depending on environmental conditions [260]. This dual role of butyrate was confirmed *in vitro* in different cell cultures. The pro-proliferative effect of butyrate was found dependent on the presence of glucose in the milieu [261]. Butyrate modulation of intestinal epithelial cell functions is dependent on environmental factors present and the state of the epithelial barrier. Butyrate also influences intestinal barrier permeability and prevents bacterial invasion both *in vivo* [262, 263] and *in vitro* in Caco2 cell culture [264]. This metabolite is associated with mucus thickness in colon [265] and is the principal energy source of colonocytes [255].

Part of gut epithelium homeostasis, propionate regulates cell migration in intestinal crypts and villi [266]. As butyrate and propionate, acetate is also known for its proliferative and anti-inflammatory effect upon intestinal epithelium [253].

Overall, SCFAs are essential for gut epithelium homeostasis and highly studied in the context of diseases such as IBD. Their influence upon the gut-brain axis is highly investigated [253, 267].

3.4.1.2 Bile acids

They are two types of bile acids: primary and secondary. Primary bile acids originate from cholesterol metabolism and are mainly composed of chenodeoxycholic acid (CDCA) and cholic acid (CA). Primary bile acids CA and CDCA can be deconjugated by the gut microbiota into secondary bile acids such as deoxycholic acid (DCA) or lithocholic acids (LCA) [268].

Bacterial species responsible for bile acids deconjugation an 7α-dehydroxylation remain poorly identified except for *Clostridium scinden* present in the ileum.

Bile acids impact epithelial homeostasis via the activation of the TGR5 receptor located on Lgr5+ ISCs membrane [269, 270] but also via interaction with the epidermal growth factor receptor (EGFR) and fanesoid X receptor (FXR). Both are involved in cell proliferation mechanisms [271].

3.5 THE MICROBIOTA-GUT-BRAIN AXIS:

How the gut microbiota interacts with our body has become a central question. If the implication of microorganims in digestion and intestinal epithelial functions are increasingly characterized, their effect on the central nervous system is also being unraveled. There is a bi-directional dialogue between the gut microbiota and the central nervous system named the gut-brain axis and several communications route have been discovered between these two distant organs (Figure 1.5) [54].

- Connecting the central nervous system to the enteric nervous system embedded in the submucosa and lamina propria of the gut, the vagus nerve, with its afferent and efferent communication road, operates the bidirectional communication between the brain and the intestine [55].

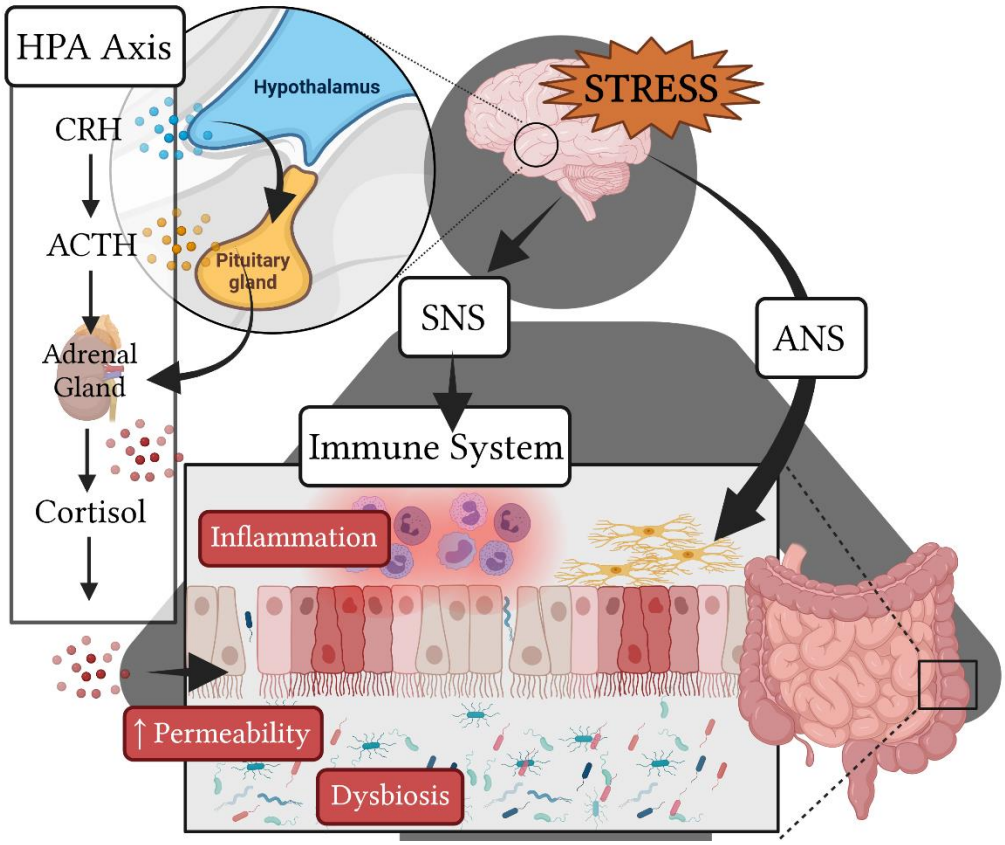

Figure 14 Mediation of the stress response: Stress response is translated thought 3 roads: the HPA-axis, the Autonomic Nervous System (ANS), and indirectly with the Sympathetic Nervous System (SNS) affecting the immune system. At intestinal barrier sites, stress induces an increase in permeability, a low-grade inflammation, abnormal cell migration and secretion, and dysbiosis of the associated microbiota.

- The immune system is directly influenced by gut microbiota which may activate it but also induce the secretion of interleukin or cytokine having direct effects on the central nervous system [56]. Especially IL-6 and IL-1, under the influence of the gut microbiota, can trigger the release of CRH [57], a component of the HPA axis.
- The HPA axis. Involved in the stress response, this axis initiates in the hypothalamus with the secretion of CRH which triggers the subsequent release of ACTH in the anterior pituitary gland, which in turn activates the systemic release of cortisol by the adrenal gland in the entire body. The gut microbiota can activate the HPA axis and is also influenced by its action [58–61].
- Neurotransmitters can be directly secreted by the gut microbiota and represent a bi-directional route of communication in the gut-brain axis [62–64]. For instance, Tryptophan production, a necessary amino acid for the synthesis of serotonin, regulated by the gut microbiota [65, 66].

- SCFAs are essential for the host metabolism and can cross the brain barrier and affect the central nervous system [67, 68].

As we slowly untangle the diversity of brain-gut-microbiota interactions, we uncover the causal relationships regulating body homeostasis in the holobiont. At the center of gut epithelial barrier, a thin equilibrium between health and disease is governed by host-microbiota interactions.

4 ENVIRONMENTAL FACTORS MODULATE BARRIER HOMEOSTASIS: PSYCHOLOGICAL STRESS

4.1 HISTORY OF PSYCHOLOGICAL STRESS:

The term *"stress"* in physiology appeared during the 20th century. We owe its modern use to the first definition of an internal biological equilibrium and the concept of *milieu intérieur*, brought by Claude Bernard in 1872 [272]. It is based on this notion that Walter Cannon defined the idea of homeostasis [273]. At that time, the scientific community was studying body functions from a reductionist perspective. Through this approach, organs were considered to operate independently, and the system was viewed as the sum of its individual components [274]. Walter Cannon, following the steps of Claude Bernard, supported a coordinated, adaptive response of the internal milieu to the external environment. Its definition of homeostasis is based on the *milieu intérieur* principle (an internal equilibrium carried by several interdependent components belonging to the same system in response to an external stimulus) and focused on the dynamic properties of biological systems: to some extent, they can modify their individual components in an adaptive response to the environment [274].

Bernard and Cannon had then brought a definition of the equilibrium in physiology. But what about disequilibrium and where lies the frontiers between health and disease?

It is in later work that Cannon linked emotions to physical symptoms and exposed the *fight-or-flight* response. He, then, proposed adrenaline as an effector molecule of acute stress: a compound able to maintain a relative homeostasis through a perturbation [275]. But the modern use of the world *"stress"* should be granted to Hans Seyle in 1936 [276], who borrowed this term from Physics, to describe what he first called the syndrome of general adaptation or the disease of adaptation [277]. If in mechanics, stress designs the sum of forces applied to an object, with the potential ability to distort it, it is defined in physiology as a state of threatened homeostasis [278]. Taking over Walter Cannon's work, years of research allowed him to discover the role of the HPA axis and glucocorticoids in the stress response [279]. His writing also led to a more precise definition of physical and psychological stress and highlighted the work of Lenard Levi on positive (eustress) and negative (distress) stress [280, 281]. His work emphasized the difference between, what we call today, chronic, and acute stress and demonstrated that a punctual and short exposure to a stressor could have a positive effect on the body while long-term, repeated exposure could become harmful and initiate/aggravate a pathological state. The infatuation of stress research took roots in a period of war: at that time, many soldiers would come back from combat with post-traumatic stress disorder (PTSD). Uncharacterized then, doctors did not know how to treat symptoms with no visible physical origin [278].

However, the growing interest around the stress response only occurred with the research of the psychologist Richard Lazarus. In opposition with the general adaptation syndrome, which aims to find a common physiological signal for the expression of stress, Lazarus defended the weight of individuality in the stress response [282]. In this matter, he

supported the variability of the emotional response in humans toward a situation, depending on their own evaluation of the external threat [283].

As research on the stress response is becoming more and more popular, rising its definition to a central pillar in physiology in less than a century, the concept of stress crosses the boundaries between domains [284]. Its study is becoming a trans-disciplinary challenge opening new horizons for systemic research and the understanding of disease development.

4.2 ACUTE VS CHRONIC STRESS

The response to stress can be acute or chronic depending on the type of stressor, the duration of the stress period and the genetic background of the individual [285].

In the acute response to stress, the exposure to stressors is short and triggers what we call the 'fight or flight' response [286]. Both the sympathetic adrenomedullar system (SAM) and HPA axes are activated to provide an adaptive response to a perceived external threat. In the acute stress response, physiological changes induced by stress are increasing until they reach a peak followed by a recovery period (Figure 14) [287].

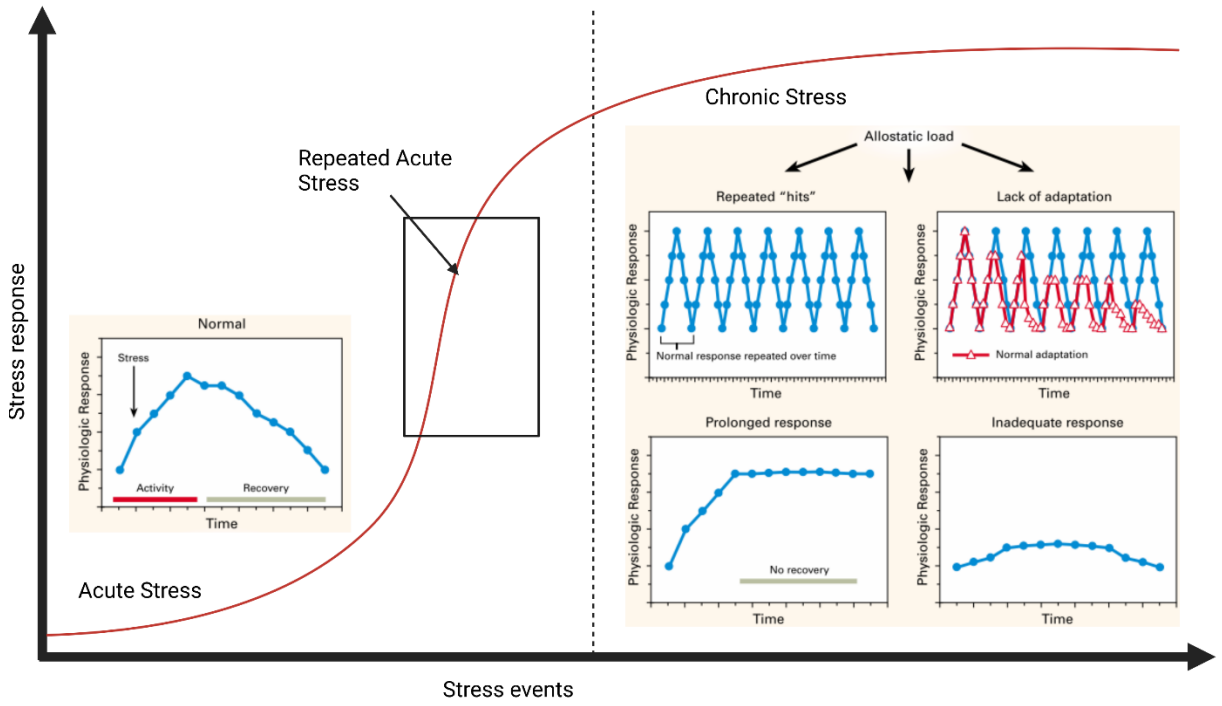

Figure 15 From acute to chronic stress response: the chronicity of the stress response depends on the exposition to environmental stressors (duration and repetition of stress events) and the perception of the threat. Acute stress induces a period of physiological activity followed by a recovery phase. Chronic stress is initiated in early phases of repeated acute stress and is representative of the passage between homeostasis and chaostasis. In chronic stress the allostatic load triggers impairment of the stress response which can be illustrated by abnormal repetition of stress response, a lack of adaptation to a known stressors, a prolonged stress response with no recovery phase or an inadequate response to the perceived threat with decreased expression of stress effector molecules (figure modified from [287]*).*

In the chronic response, the exposure to stressors is long and repeated and causes what we call an allostatic load - a cumulative effect which results in a detrimental physiological

response [287]. It results in an impairment of the HPA axis which can be translated by attenuation or stimulation of the cortisol negative feedback loop or a decreased expression of glucocorticoids receptor and cortisol [288–290]. During developmental phases, chronic stress can trigger hypersecretion of CRH and overactivation of the HPA axis [286, 291]. Chronic stress response can be illustrated by a shift between the perceived threat and the physiological response: in some cases, instead of a single stress hit, the physiological response is repeated over time [292]. Otherwise, when subjected to a known threat, adaptation is impaired and stress levels remain elevated [293]. The allostatic load can also prevent the usual recovery phase [294], or, on the contrary, be represented by a decreased physiological response to stress [287, 295] (Figure 14). We will see in the next section how chronic stress is implicated in the initiation and development of many chronic diseases.

If the response to acute stress or chronic stress is highly studied, the passage between these two states is difficult to capture. However, it is within this pre-symptomatic phase that chronic stress may be established or reversed. Therefore, there is a need to characterize the biomarkers involved in these precursor phases and involved in the establishment of chronic stress (Figure 14).

4.3 MEDIATION OF THE STRESS RESPONSE

The main stress response systems are the HPA-axis and the SAM-axis.

4.3.1 SAM axis

The sympathetic adrenomedullar system SAM, results in a fast physiological response triggered by the release of catecholamine (e.g., epinephrine, norepinephrine) by the adrenal medulla and sympathetic nerves [296, 297]. The amygdala, a pool of nucleus located in the median temporal lobe, is a brain region implicated in the integration of emotional responses is in interaction with the locus coeruleus where the SAM axis originates (brainstem nucleus receiving the information from the periphery). The locus coeruleus, as it roots within the sympathetic nervous system through the spinal cord, has an essential role in the orchestration of behavioral and biological response to stress in the brain and the rest of the body [296]. The amygdala and locus coeruleus are interconnected with their reciprocal neuronal projections and trigger a prompt activation of the brain. After a first phase of unconscious perception, the activation of the amygdala is, in a second phase, modulated by its neuronal connections, first with the prefrontal cortex – a determining region for the evaluation of the received cognitive information – and then, by the hippocampus – key structure for the collection of similar experienced memory. The intervention of these cerebral structures largely contributes to the individual variability observed in the stress response [296].

The stimulation of the locus coeruleus activates the prefrontal cortex via its numerous noradrenergic projections. The stimulation of the amygdala triggers a fast release of neurotransmitters (e.g., dopamine, acetylcholine, serotonin, and noradrenaline) and corticotropin releasing hormone (CRH). The cells producing CRH, and these neurotransmitters are interconnected with the locus coeruleus. These factors are responsible for an increased

vigilance, the treatment of the received information, and ultimately lead to the choice of the optimal strategy to confront the stressor [296].

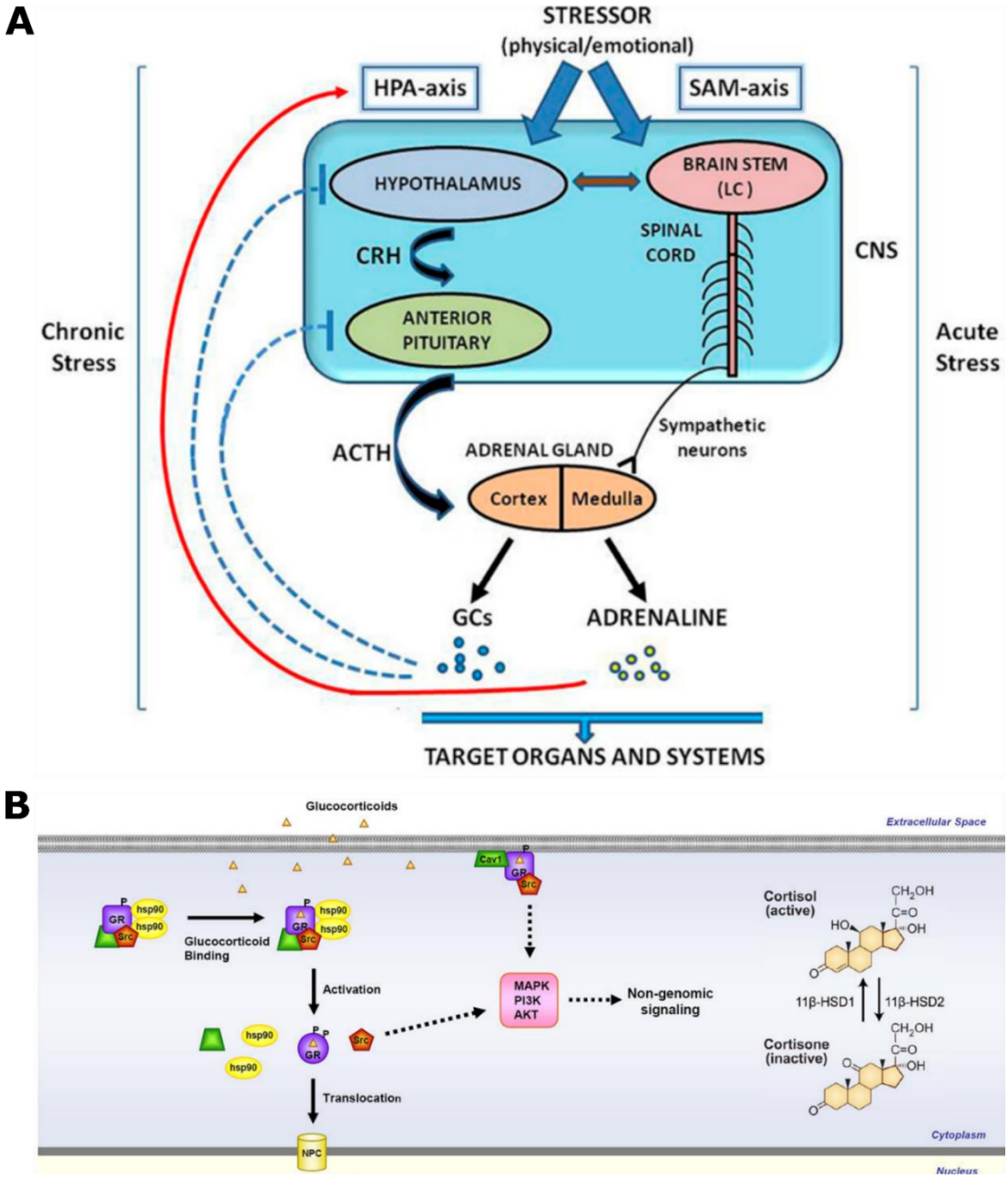

Figure 16 Mediation of the stress response: A. Stress is mediated mainly by the SAM axis and the HPA axis. The SAM axis originates in the Locus coeruleus and signals through the spinal cords to trigger the release of catecholamines. The HPA axis is initiated in the hypothalamus with the release of CRH, which triggers the release of ACTH in the circulation. ACTH, in the adrenal gland, triggers the secretion of cortisol (Figure from [296]*). B. Cortisol can be transported across the bi-lipidic plasma membrane of cells where it binds to GRs in the cytoplasm. It triggers the translocation of GRs to the nucleus and the activation of GRE loci located in DNA (figure from* [298]*).*

The physiological stress response propagates in the rest of the body via the action of CRH. Produced in the locus coeruleus, CRH leads to the synthesis and release of adrenaline and noradrenaline by the adrenal glands' medulla, and the release of noradrenaline by sympathetic nerves across the body [296].

The action and duration of the response is regulated by the autonomic nervous system in direct contact with the enteric nervous [284, 299]. Adrenaline and noradrenaline interact with α- adrenergic and β-adrenergic receptors in smooth muscle cells' plasma membrane [300]. Through the release of adrenaline and noradrenaline from the adrenal glands part of the humoral response, SAM axis can directly inhibit the ENS, or modulate sphincter functions by modulating their contractile ability [296].The SAM system occurs prior to the HPA axis response and prepares the body for the 'fight or flight' acute stress response (Figure 15A) [296].

Therefore, the SAM axis is a short-term action mechanism in contrast with glucocorticoid receptors involved in the HPA axis regulating the expression of transcription factors.

4.3.2 HPA Axis

In parallel, the HPA axis is activated: the stimulation of the amygdale activates the corticotropic axis and lead to the synthesis of CRH in the hypothalamus. CRH and other secreted hormones such as the arginin vasopressin (AVP) are transported from the hypothalamus to the pituitary gland via the portal system and will lead to the release of adrenocorticotropic hormone (ACTH) in the circulation. ACTH can, then, stimulate the synthesis and the liberation of glucocorticoids (cortisol in humans and corticosterone in rodents) from the cortex of the adrenal glands (Figure 15A) [296].

CRH ligands bind preferentially to CRHR1, a G-protein coupled receptors found in the anterior pituitary gland while other CRH peptides such as urocortin II and III have greater affinity toward the CRHR2 receptor [301]. Upon CRH binding, the adenylyl cyclase is activated and further induces cAMP expression. cAMP is then able to activate PKA, which initiates a transduction pathway involving the entry of calcium in the cell via voltage-dependent L-type calcium channels (or DHP (dihydropyridine) channels) and eventually, the activation of ERK1/2 transcription factor. After the translocation of phosphorylated ERK1/2 within the nucleus and the establishment of a complex with Nur77 and Nurr1, POMC is expressed [302] and can further be cleaved by prohormone convertase into ACTH and β-lipotropin [303]. ACTH is then released in the circulation and travels to the adrenal gland where it triggers de novo synthesis and release of cortisol and adrenaline. Cortisol can also, via a feedback loop, prevent the long-term activation of the HPA axis [304].

Cortisol is a glucocorticoid and key effector molecule of the stress response. Once released by the adrenal gland, it is transported by corticosteroid-binding globulin (CBC) and distributed in a systemic fashion in the body [298]. It can passively cross cell membranes and bind to glucocorticoid receptors (GR) located in the cell cytoplasm [305]. Activation of GR by cortisol allows its translocation to the GRE locus [306] within the nucleus and initiates the transcription of genes (sometimes 10%-20% of the cell's genes are expressed after the GRE loci activations [307]). GRE loci are numerous in the nucleus and not all occupied by GR upon cortisol activation implying that there is a tissue-specific binding pattern [308]. The glucocorticoid response can also be modulated by the bioavailability of GRs since GRE loci require different quantities of GRs to be activated [309] (Figure 15B).

Cortisol can also, via a negative feedback loop, prevent the long-term activation of the HPA axis [304]. Therefore, the HPA axis is a systemic route of the stress response and influences, in a tissue-specific manner, cell response.

4.4 STRESS AND CHRONIC DISEASES

Psychological stress is increasingly recognized as a key environmental factor involved in the onset and development of many chronic diseases.

4.4.1 Role of stress in digestive diseases

For instance, it is an important constituent of irritable bowel syndrome (IBS) physiopathology. The motility of the lower digestive tract was found similarly affected in stressed and IBS animal models [310]. Psychological stress also influences the development of the disorder by delaying the activity of the autonomic nervous system [311]. In addition, it also plays a role in the evolution of IBD, via different mechanisms. The increase of barrier permeability [312], the subsequent activation or reactivation of an inflammatory response [313, 314] induced by psychological stress was associated to a modification in the host-microbiota interactome [315–318] and all participate in the establishment of a detrimental colitis. Finally the effect of psychological stress was also reported in the development of CRC where glucocorticoids administration increased the development of tumors and their size [319]. Indeed, some effector molecules of the HPA axis have been associated with CRC development. The initiation and progression of CRC is partially mediated by an impairment of the internal immune microenvironment. CRH family members, known pro-inflammatory mediators, are found significantly increased in inflamed regions of the colon and may participate in the establishment of a suitable environment for cancer onset [320]. But activation of CRH receptors mediates multiple effects depending on the intestinal region. CRHR2 receptor, is drastically reduced in CRC, and is, upon activation, responsible for the inhibition of endogenous Ucn2 and Stat3. Therefore, CRHR2 can prevent pro-inflammatory pathways by engaging cells into cell cycle and wound healing processes [321].

4.4.2 Role of stress in neurodegenerative and behavioral diseases

Psychological stress is also often associated with the development of neurological or behavioral diseases. It is systematically implicated in the development of depressive-like symptoms [322] and, in established depression, accompanied with abnormality of the HPA-axis such as hypercortisolemia or changes in glucocorticoid receptors function [323]. Recent papers report its implication in Alzheimer disease. The hyper-phosphorylation of the tau-protein triggered by glucocorticoids can participate in the establishment of the disorder [324, 325] and high urine cortisol concentration can become a predictor of Alzheimer disease onset [326]. Another study also reported an increase in symptoms' relapses in autoimmune encephalomyelitis induced by psychological stress [327]. As stress hormones are also implicated in appetite and food preference (CRH induces appetite loss [328] while glucocorticoids are positively associated to fats and sucrose consumption [329]), a bidirectional relationship between stress and obesity was highlighted in the past few years [330]. It was characterized by an increased long-term cortisol secretion [331] or altered GR sensitivity [332].

4.5 STRESS MODELS IN ANIMALS

Building the right protocol to study stress is a real challenge of today's research since, as we saw previously, there is not one route for stress response and its expression highly depends on the individual's own evaluation and emotional interpretation of the situation. As the perception of the stress threat is dependent on the individual, the question of genetic factors predisposing to stress response was raised. Heritability of PS susceptibility was reported moderate in twin studies. Single Nucleotide Polymorphisms (SNPs) were found in serotonin transporter (SLC6A4), for instance, or pituitary adenylate cyclase-activating polypeptide (PACAP) an upstream promoter of CRH [285].

Thus, there is not one animal model to study the stress response but many corresponding to different stressful conditions, time of exposition to the stressor, and the individual genetic background [333]:

4.5.1 Maternal separation

Maternal separation procedure (MS) and multiple early adversity model (MAM) are representative of early stress occurrence, childhood-trauma such as abuse, or parental loss [334]. In this model, the pups are separated daily for at least two hours from their mother nest during the postnatal period essential for the development of the HPA axis [335, 336]. Early-stress events participate in the development of several chronic diseases such as IBS [337] or depression [338].

4.5.2 Social stress

Social stress models are conditioned by fear and relate to IBS [339] or PTSD [340]. The main model used is the social disruption test (SDR) and is induced by introducing a dominant aggressor in the animal cage [341]. After an initial fight followed by the defeat of the submissive, the animal is left alone [342] and displays an activation of the HPA-axis with elevated glucocorticoids release and changes in its behavior [343].

Another model of social disruption is a psychosocial stress induced by isolation. This stress model implies the solitary housing of individual mice. It is however contested since it requires a long isolation period to induce long-term effect and the persistence of the endocrinial stress response is questioned [333].

4.5.3 Water avoidance and restraint test

In water avoidance stress (WAS) the animal is placed on a small platform at the center of a basin, surrounded by water [344]. In restraint stress (RS) tests, animals are immobilized in a perforated tube [345]. Both stress models are extensively used to address the study of IBS since they can trigger a hypersensitivity of the gut after only one occurrence [344, 346, 347].

4.5.4 Physical Stress

Physical stress models include Forced Swim test (the animal is forced to swim and sometimes submerged) and Footshock electrical trauma (the animal is subjected to electric

shock of variable intensities, or imprisoned on an electrified grid) and aim to recreate life-threatening trauma representative of PTSD [348].

4.5.5 From acute to chronic stress

Models of acute stress were first used to evaluate the immediate effect of stress upon gut functions [349, 350]. The acute response can be triggered by a single stressful event such as a WAS or RS event [344, 345]. Both stress models can trigger a hypersensitivity of the gut after only one occurrence [346, 347].

In between acute and chronic stress is an intermediate stress model in which an acute stress is repeated several times, but the allostatic load is still insufficient to trigger abnormalities in the physiological response.

The repetition of a single acute stress event daily can induce chronic stress. Therefore models of chronic stress are, most of the time, acute stress models repeated over time [344]: for instance, WAS applied daily for several consecutive days can be considered as a chronic stress model while a single exposure to WAS is considered as acute stress. In between successive WAS exposure are considered to be repeated acute stress or early chronic stress [351, 352]. Recent advances in stress models have shown that diversifying the type of stress avoids habituation and can be more representative of daily life chronic stress [348, 353, 354].

These models are sometimes used to induce depression, PTSD like syndrome in animals or even IBS [334, 335, 339, 344]. The experimental design (type of stress applied and number of stress events) is related to the strength and the long-lasting effect of the stress response [348]. However, studying the tip-point between homeostasis and chaostasis remains a challenge due to the individuality of the stress response.

4.6 STRESS AND THE EPITHELIAL BARRIER

The intestinal epithelium response to psychological stress is increasingly recognized as a key physiopathological process involved in evolution of not only digestive but also extra digestive chronic diseases. This central hypothesis is based on the overall concept that psychological stress induces an alteration in major barrier functions (e.g., increased permeability, defect in mucus composition) leading to a moss of barrier integrity [284, 355]. This loss of barrier integrity will favour the passage of pathogens, bacteria composition, antigens that will induce a local or more systemic inflammation contributing to organ dysfunctions or relapses in genetically susceptible or not individuals [356]. Therefore, understanding of the intestinal epithelial barrier responses in terms of key epithelial homeostatic functions is of major interest.

In this part, we briefly described the impact of PS upon cell homeostasis gained using various animal models of stress. For the sake of space we choose not to describe the in vitro impact of various stress related mediators.

4.6.1 Gut epithelial homeostasis

4.6.1.1 Cell proliferation

Cell proliferation was often reported impaired in response to various stressors [352, 357, 358]. However, the variety of stress applied to animal models have shown different and often opposite results.

In acute stress models, rats subjected to a single event of short-term (2h) and long-term (12h) cold restraint stress showed a reduced cell proliferation in duodenal and ileal crypts [357]. In contrast, using acute forced swim test provoked an increased cell proliferation in the jejunum [359].

Intermediate stress model, like WAS repeated 5 days was sufficient to promote cell proliferation in rats ileum [352].

In chronic models, results appear highly dependent on the type of stress applied. Physical stress like electric shock inhibited jejunal epithelial cell proliferation [358]. However, social stress like isolation stress had no effect on epithelial cell function [360] .Finally, another study on WAS models unraveled an increase in cell proliferation in the ileum after 10 days [352].

Therefore acute, intermediate, and chronic stress models all can modulate intestinal epithelial cell proliferation. This response appears to be highly dependent on the type and number of stress events. The literature, however, often highlights differential modulation of cell proliferation induced by stress depending on the organ region and there is a lack of systemic studies characterizing the effect of PS across organs' gut epithelium. Indeed, only one study described changes induced by PS upon cell proliferation in more than one organ and showed localized decrease in gastric cell proliferation, increase of jejunal cell proliferation but no differences in the duodenum or the colon after acute forced swim test [359]. It is, to the best of our knowledge the only study observing cell proliferation changes induced by stress in the colon. This organ remains barely studied with regards to stress induced modulation of epithelial intestinal cells' homeostatic functions.

Stress response in *in vivo* animal models is complex since major pathways are involved and probably multiple mediators are released following stress events. Therefore, the effects of stress effectors remain different depending on the organ region, type of stress and the number of stress events. Mechanism underlying the modulation of cell proliferation by PS is still largely uncharacterized.

4.6.1.2 Cell differentiation

Stress hormone can also modulate intestinal cell differentiation. However *in vivo* studies are less abundant and only report impact upon cell differentiation during postnatal development. In this period, the HPA axis is thought to play an extensive role in intestinal epithelial development via changes in cell differentiation and digestive enzyme maturation [361]. Indeed, the passage between lactation and early weaning is associated to changes in corticosterone and glucocorticoid receptor activity: these changes are partially associated to the transition between mucous neck cells and fully differentiated zymogenic cells in the gastric isthmus for instance [362].

But the direct involvement of stress hormones in the regulation of cell differentiation is discussed as the effect of stress might only be an indirect effect, modulated by the formation and maintenance of a durable basement membrane and internal microenvironment [363].

4.6.1.3 Cell death

If PS affects cell proliferation it also provokes changes in cell death regulation. Indeed, after 5 days of WAS, rats showed an increased level of apoptotic cells whereas, after 10 days, cell death ratio returned to basal levels when cell proliferation constantly increased [352]. A study observed no changes in the number of apoptotic cells in the jejunum following an acute long-term isolation stress event [360]. In acute and chronic water immersion restraint stress (WIRS), cell apoptosis was found increased by stress in the small intestine [364].

Stress can induce an increase of cell apoptosis but remains highly dependent of the stress model. If acute stress triggers an increase in cell apoptosis, the response of intestinal epithelial cells following chronic stress is variable.

4.6.2 Impact of stress upon intestinal permeability

Stress can also modulate permeability directly via modification of intercellular junction proteins, presence/absence in the junctional complex, or their phosphorylation [365, 366]. The increase in intestinal permeability was associated with an exacerbated low-grade inflammation mediated by the passage of toxins [367–369].

Regional studies on transcellular and paracellular permeability all reported an increased barrier permeability in several gut regions. In acute stress models, restraint stress after only one occurrence was able to increase jejunal and colonic permeability [370, 371]. Both WAS and maternal separation acute stress were also able to promote ileal permeability [372]. In intermediate WAS model (5 successive days), the paracellular and transcellular permeability were both increased in the jejunum and the ileum [352, 372] Finally, intestinal epithelial cells showed an increased permeability in the ileum and the colon but not in the jejunum following a chronic WAS (10 successive days) [352, 373].

In the colon especially, the increase in gut permeability is accompanied by changes in tight-junction protein expression a decrease in ZO-1, occludin, and claudin-1 [373] and an increase of claudin-2 were reported accompanied by a decrease in GR expression following 10 days of WAS [374]. However, these changes in gene transcription were not reported in the small intestine.

The response to stress at barrier sites observed in the literature shows a regionality of the response along the intestinal length, but also changes epithelial homeostasis dynamics over time and gut epithelial regions. The type of stress applied (physical/psychological and duration) also has different physiological implications.

4.7 STRESS AND GUT MICROBIOTA

Numerous studies report that psychological stress can modulate gut microbiota composition and functions. Models have mainly characterized the feces microbiota. Studies

aimed at describing changes of gut microbiota induced by stress at the regional level and at the level of the epithelial associated and luminal microbiota are sparse.

4.7.1 Reported changes in bacterial composition

Following stress events a decrease in fecal microbiota diversity is often observed[375, 376], even if one study observed no changes[342]. In several studies, characterization of the differentially abundant bacteria was performed and highlighted modifications of several genera and families (listed Table 1). They will be discussed in this section.

Even a single event of acute stress (2h of social defeat stress (SDR)) is able to modify the α-diversity (but not the β-diversity) of the luminal colonic microbiota and both the α-diversity and β-diversity of the mucosal colonic microbiota. It can trigger microbial changes and decrease in abundance of *Parabacteroides* and *Lactobacillus* genera as well as the *Porphyromonadaceae* Family in the mucosa of the colon [342].

More intermediate models were developed (grid floor, restrain stress and SDR) to evaluate the impact of stress upon the gut microbiota. In these models, stress was repeated each day, but the number of stress events were not sufficient to trigger a chronic response with physiological abnormalities of the HPA axis. Both SDR and restraint stress induced decrease in microbial diversity in the small intestine, the cecum, and the colon [377, 378]. However, they highlighted divergent changes in bacterial abundance in the cecum. For instance, grid Floor was associated to an increase of *Alistipes* and *Odoribacter* genera [379] while restraint stress showed a decrease in *Tannerella* Genus [377], and SDR induced a decrease in *Bacteroidetes spp.*, *Pseudobutyrivibrio spp.*, or *Clostridium spp*. at the genus level [378] (Table 1). Therefore, even in the same organ, the type of stress influences the changes in bacterial abundances and does not modify the same bacterial genera and species.

Modifications of bacterial communities were mainly studied in chronic stress models (e.g., water immersion restraint stress (WIRS), water avoidance stress (WAS), maternal separation (MS)). If some similar results were observed between stress models like *Clostridium spp.* decreased in both MS and WAS challenges [376, 380] or the *Lachnospiraceae* family modulated by WIRS (increased) and WAS (decreased) [381, 382], different papers evaluating the same stress often highlighted diverging changes in bacterial abundances [380, 382]. Overall the bacterial composition was found impacted by chronic stress: we can cite the decrease in abundance of *Butyricicoccus*, *Parasutterella*, *Ruminococcus* and *Romboutsia* genera in the colon for instance [376] (Table 1). Studies reporting the preceding results mostly observed fecal samples, but some explored the ileal or cecal microbiota. However, none investigated the difference in the epithelial-associated microbiota on a large sequencing scale.

If stress induced changes in gut microbiota composition are not always reproducible, it can be due to multiple factors in the sequencing process (bias induced by different extraction kits, PCR amplification, sequencing error, contamination and bioinformatic pipeline). These limitations render the comparison of bacterial dysbiosis difficult between studies [383, 384].

4.7.2 Reported changes in bacterial derived metabolites

Aside changes in bacterial composition, stress-related modifications were also explored in terms of anaerobic/aerobic microbial composition or SCFAs producers. A study showed an

increase in the proportion of facultative anaerobes in several gut regions potentially induced by the presence of a low-grade inflammation [378].

Moreover, another paper demonstrated that chronic WAS stress (10 consecutive days) reduced the concentration of total SCFAs (acetate, propionate and butyrate) in feces. They highlighted the role of SCFAs in colonic motility via G-protein coupled receptor and could restore it with SCFAs administration [385]. These findings are consistent with the previously discovered family and genera modified by the stress response since most of them are SCFAs producers.

All in all, psychological stress can impact bacterial diversity and abundance in several organs of the digestive system. These differences are dependent on the organ region, the type of stress and the number of stress events.

Table 1 List of bacteria taxa already reported differentially abundant in stress model experiments

Bacteria	Taxonomic Rank	Collection Site	Differential Changes	Stress Model	Literature
Acute Stress Models					
Lactobacillus	Genus	Colonic (Adherent)	Decreased	Acute SDR	Galley et al., 2014
Parabacteroides	Genus	Colonic (Adherent)	Decreased	Acute SDR	Galley et al., 2014
Porphyromonadaceae	Family	Colonic (Adherent)	Decreased	Acute SDR	Galley et al., 2014
Intermediate Stress Models					
Odoribacter	Genus	Caecal	Increased	Grid Floor	Bangsgaard Bendtse et al., 2012
Alistipes	Genus	Caecal	Increased	Grid Floor	Bangsgaard Bendtse et al., 2012
Porphyromonadaceae	Family	Caecal	Decreased	RS	Bailey et al., 2010
Tannerella	Genus	Caecal	Decreased	RS	Bailey et al., 2010
Bacteroides spp.	Genus	Caecal	Decreased	SDR	Bailey et al., 2011
Coprococcus spp.	Genus	Caecal	Decreased	SDR	Bailey et al., 2011
Dorea spp.	Genus	Caecal	Decreased	SDR	Bailey et al., 2011
Pseudobutyrivibrio spp.	Genus	Caecal	Decreased	SDR	Bailey et al., 2011
Clostridium Spp.	Genus	Caecal	Increased	SDR	Bailey et al., 2011
Chronic Stress Model					
Lachnospiraceae	Family	Fecal	Increased	WIRS	Li et al. 2017
Porphyromonadaceae	Family	Ileal	Decreased	WAS	Yang et al., 2020
Clostridium Spp.	Genus	Colonic	Increased	rWAS	Watanabe et al., 2016
		Colonic	Decreased	MS	Enqi et al., 2021
		Colonic	Decreased	MAM	Enqi et al., 2021

Enterobacteriaceae	Family	Colonic	Increased	rWAS	Watanabe et al., 2016
Bacteroidales S24-7	Family	Colonic	Decreased	rWAS	Watanabe et al., 2016
Prevotellaceae	Family	Fecal	Increased	WAS	Zhang et al., 2019
Peptococcaceae	Family	Fecal	Decreased	WAS	Zhang et al., 2019
Lachnospiraceae	Family	Fecal	Decreased	WAS	Zhang et al., 2019
Spirochaetaceae	Family	Ileal	Decreased	WAS	Yang et al., 2020
Rikenellaceae	Family	Ileal	Decreased	WAS	Yang et al., 2020
Treponema	Genus	Ileal	Decreased	WAS	Yang et al., 2020
Alloprevotella	Genus	Colonic	Increased	MS	Enqi et al., 2021
				MAM	Enqi et al., 2021
Corynebacterium	Genus	Colonic	Increased	MS	Enqi et al., 2021
Rothia	Genus	Colonic	Decreased	MS	Enqi et al., 2021
Elusimicrobium	Genus	Colonic	Decreased	MS	Enqi et al., 2021
Ruminococcus	Genus	Colonic	Decreased	MS	Enqi et al., 2021
				MAM	Enqi et al., 2021
Romboutsia	Genus	Colonic	Decreased	MS	Enqi et al., 2021
Butyricicoccus	Genus	Colonic	Decreased	MS	Enqi et al., 2021
				MAM	Enqi et al., 2021
Allobaculum	Genus	Colonic	Decreased	MS	Enqi et al., 2021
Parasutterella	Genus	Colonic	Decreased	MS	Enqi et al., 2021
Turicibacter	Genus	Colonic	Decreased	MS	Enqi et al., 2021
				MAM	Enqi et al., 2021
Vampirovibrio	Genus	Colonic	Increased	MAM	Enqi et al., 2021
Butyricimonas	Genus	Colonic	Decreased	MAM	Enqi et al., 2021

5 FROM OMICS TO MULTI-OMICS

5.1 MULTI-OMICS ANALYSIS TO STUDY THE HOST-MICROBIOTA INTERACTOME

This thesis aims to study the impact of psychological stress upon the host-microbiota interactome in the gut. We used a repeated acute stress to remain in an intermediate stress model representative of the transition between balanced and unbalanced state. Our objectives were:

1) To characterize the regional changes in gut barrier functions.
2) To describe the regional transcriptomic response of the intestinal epithelial cells.
3) To identify the regional changes in abundances of adherent or luminal microbiota.
4) To extract adherent/luminal bacterial signatures associated to the transcriptomic changes induced by psychological stress.

Therefore, the first part of this thesis was designed to identify and develop analytic tools for the exploration of this systemic study and the extraction of biomarkers associated with the PS response. This section is dedicated to the description of the bioinformatic pipeline employed (3' end sequencing, 16S RNA sequencing and multi-omics analyses) which ultimately led to the development of MiBiOmics, an interactive platform and stand-alone application for the integration of multi-omics data using graph-based and ordination approaches.

5.2 3'END RNA SEQUENCING STANDS FOR TRANSCRIPTOMICS

5.2.1 Principle and comparison to classical RNA sequencing

5.2.1.1 Classical mRNA sequencing

5.2.1.1.1 Data collection

The goal of mRNA sequencing is to survey the transcriptome of a cell population. Cells are first isolated and spliced, and their mRNAs are collected [386]. In this process, the isolation of cell populations is crucial since, once spliced, we only keep a bulk mRNA mixture of the entire cell community. If different types of tissue are gathered during the isolation process, the transcriptome will reflect the mean gene expression of the tissue collection [387].

5.2.1.1.2 Shearing and priming

In a typical mRNA sequencing, once the mRNAs of a cell population are gathered, they are randomly sheared into smaller reads. These reads are approximately 100 nucleotides long and are processed to create a cDNA library. With this approach, reads are mixed with random primers sequences (primers are small nucleotidic sequences able to complement the strand of interest) which can bind randomly to the reads[388]. Reverse transcriptases, present in the

solution, build the complementary strand of the reads, and constitute the cDNA library. This library is then amplified using PCR (Figure 19) [388].

5.2.1.1.3 Amplification

During amplification, in next generation sequencing, all the reads are plated on the same surface, exposed to nucleotides associated with fluorophore. At each cycle, one nucleotide is added to the complementary strands of the reads and emits a signal. The milieu is cleansed to remove aberrant signals and the information about the added nucleotide is captured. New nucleotides are added again, and a new cycle begins until the complementary strand is built (Figure 18) [389].

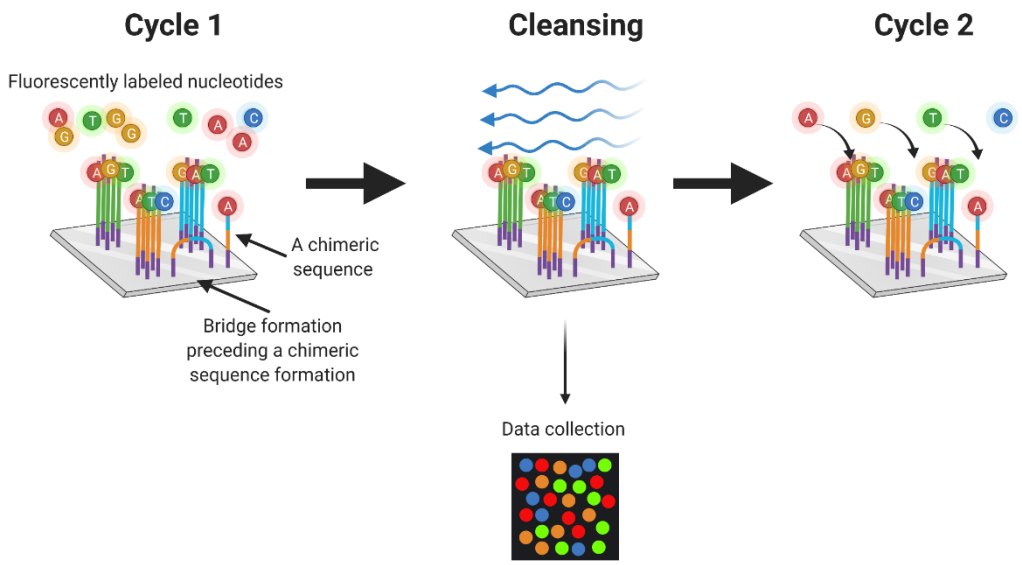

Figure 17 Next Generation sequencing amplification process: Within cycles of amplification, the complementary strand is built by adding nucleotides associated to fluorophore. The milieu is cleaned prior to data collection and the beginning of a new cycle.

If this method can capture the gene expression of a cell population and identify the proportion of expressed exonic sequences in a mRNA, one crucial piece of information is missing. After rounds of amplification and reverse transcription, the initial quantity of each read is lost: the resulting amount can be only interpreted as a proportion of the entire reads present in the mixture and is subjected to PCR amplification errors which can falsify the real quantity [390].

5.2.1.2 Comparison to 3'end RNA sequencing

To overcome this limitation, 3'end mRNA sequencing was developed: with this method, the initial mRNAs are not sheared, and the priming is targeted toward the polyA tail located at the end of the mRNA [388]. The primer is attached to a unique molecular identifier (UMI) which identifies each mRNA present in the solution with a unique sequence [390]. The polyA tail primers, composed of a series of approximately 30 tyrosine nucleotides, serve as an anchor for reverse transcriptase to build the complementary strand. After one round (single-end) or

several rounds of reverse transcriptase activity (paired-end), the cDNA library is amplified with PCR. During the primary analysis, the number of reads will be corrected using the UMI (Figure 19) [391].

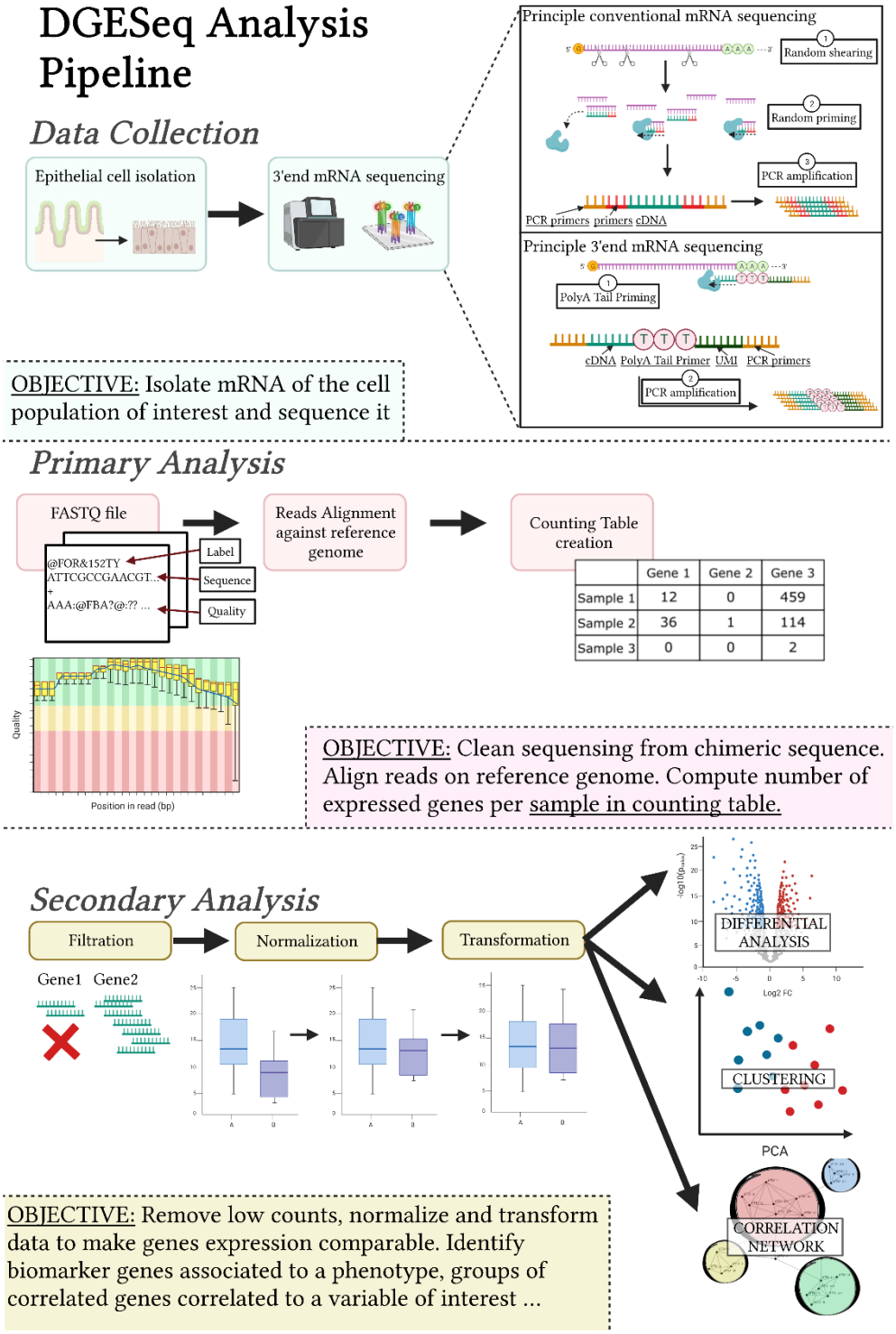

Figure 18 A typical analysis pipeline for 3'end mRNA sequencing data. The cell population of interest is isolated and sequenced. In primary analysis, reads are aligned on the reference genome and the sum of expressed genes per sample is computed. Eventually, a secondary analysis is performed to filter, normalize, and transform the

data and clustering method, differential analysis or correlation network are realized to identify biomarkers associated with a phenotype.

With this method, only the last nucleotides of each mRNA are sequenced and amplified: the alternative splicing cannot be explored [392]. However, the use of the UMI associated with the polyA tail primers allows a semi-quantitative exploration of the cell population gene expression and avoids the analyst to work with compositional data. The gathered transcriptomic information is close to the biological reality in terms of quantity [391].

After the sequencing, a bioinformatic pipeline is required to obtain the gene expression of each sample (primary analysis) and determine the biomarkers associated with a phenotype (secondary analysis) (Figure 19).

5.2.2 Primary Analysis: from raw reads to gene expression

5.2.2.1 FastQ files

Collected reads are listed in fastq file - a specific file format to gather sequence information. Reads are described across 4 lines: the first is the unique barcode associated to the read, the second is the sequence by itself, the third contains only a '+' and the last one describes the quality of each sequenced nucleotide [393]. FASTQ files can be visualized in quality control plots where the mean quality per nucleotide is displayed: it resumes the quality of the sequencing process and allows the analysis to cut parts of sequences subjected to errors with tools like multiQC (Figure 19) [394].

5.2.2.2 Sequence alignment

Once reads are sequenced and organized in FASTQ files they can be aligned. First built with de novo sequencing, the reference genomes of many different organisms are available on online databases. They are now used as template to align the raw reads extracted after sequencing, to identify which gene they express, and filter the chimeric sequences created by the sequencer after rounds of amplifications (chimeric sequences are created when two different reads localized on the same area of the plate bind together during an amplification due to their proximity and create a combination of the two reads. See Figure 18) [395, 396]. After reads are assigned to genes through the alignment process, the information can be resumed in a gene counting table: this data-frame recapitulates the quantity of expressed individual genes for each sample. It is the basis for secondary analysis and the identification of biomarkers (Figure 18) [397].

5.2.3 Secondary Analysis: extracting knowledge from sequencing

The first objective of the secondary analysis is to render the sequenced samples comparable. From the raw counting table, many systemic biases could intervene in the experimental process and render the comparison between samples difficult [395]: sometimes different samples are amplified on different sequencing plates and introduce a batch effect. Even the experimental procedure can introduce small measurable differences between samples: have they been processed on the same day? By the same person? The design of the

experimental procedure is, therefore, essential to reduce these biases but bioinformatic algorithms may correct them to a small extent [398, 399].

5.2.3.1 Filtration

First, a step of filtration is realized to remove low count genes present in only a small portion of the samples: these genes can only slow the analytic process, they can be ignored chimeric sequences, and are detrimental for some algorithms such as the functional enrichment [400].

5.2.3.2 Normalization

Following the filtration procedure, a normalization is performed to correct systemic bias. In the DESeq2 method for differential analysis, the systematic difference in samples' gene expression is computed and called a size factor. The size factor is then used to correct gene expression across the samples. DESeq2 is an example of a normalization method but many others exist and depend on the type of data [401–403].

5.2.3.3 Transformation

Normalization is generally followed by a transformation. In the cell, genes are not expressed with the same abundance depending on their functions: for instance, some called housekeeping genes are always present in high quantity while genes participating in signaling processes are often expressed in low quantity and occasionally. These differences in abundance of some expressed genes create a high variance within samples and render their comparison difficult. To overcome this limitation, transformation procedures aim to stabilize the variability between gene expressions within each sample. The effects of the normalization and transformation processes are synthesized in figure 19 [404].

After the filtration, normalization and transformation, gene expressions between samples are comparable [405, 406]. Many methods are available to explore and unravel differences in gene expression between two conditions, sources of variability in datasets, correlated gene clusters associated with a phenotype of interest.

5.2.3.4 Clustering

Clustering methods, such as principal component analysis, were developed to extract the main axis of variance within sequencing data. They project the integrity of the expression data in multi-dimensional spaces and, in this multi-dimensional space, look for the axis which maximizes the variance between samples. The samples are then reordered on a PCA plot according to the principal axes of variance of the dataset. Samples can be colored according to their phenotype, their metabolite concentration... and sometimes the variance can be explained by different experimental conditions (Figure 20) [407, 408].

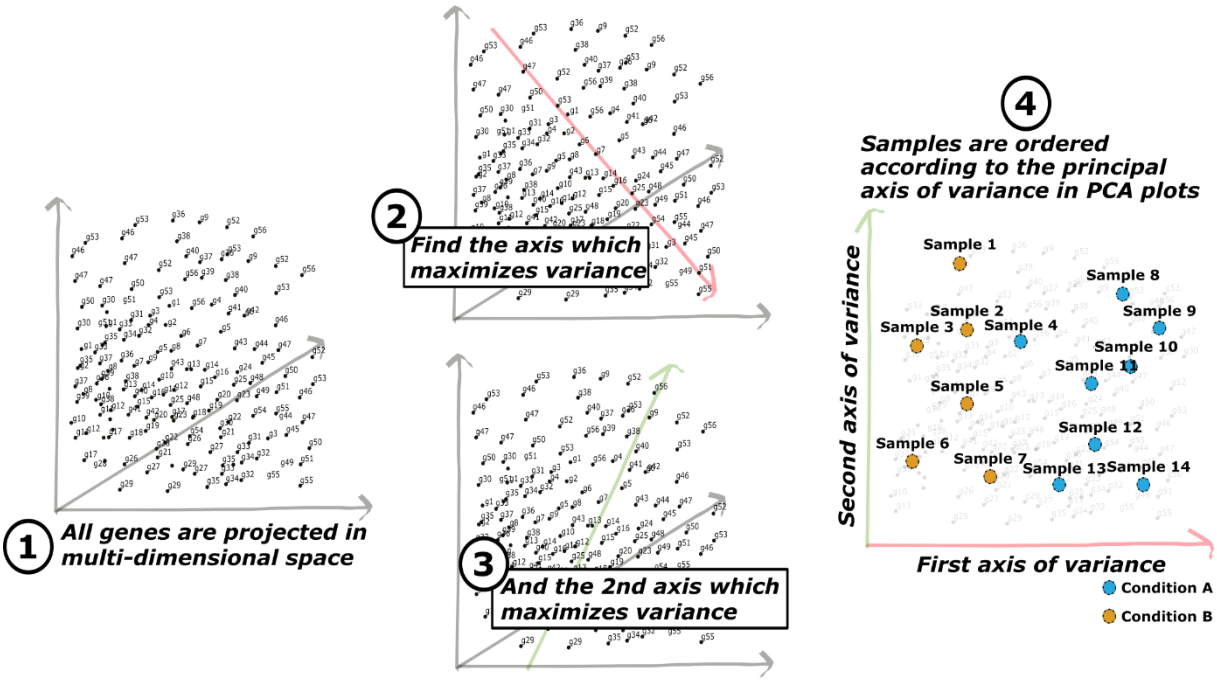

Figure 19 Principle of principal component analysis (PCA): In PCA, gene expression data is projected in multi-dimensional space and the main axes of variance are searched. Samples are then ordered according to these principal axes of variance.

5.2.3.5 Correlation networks

The inference of correlation networks can also be performed to deduce clusters of correlated genes and associate them to a parameter of interest, the evolution in the concentration of a metabolite for example. Both correlation and principal component analysis are exploratory methods: they project the data independently of a prior hypothesis, they are a good way to observe large trends in omics datasets without bias [409, 410]. More interpretative methods can be used to infer biomarkers associated with a phenotype and, therefore, can only be performed after the statement of a prior hypothesis. Correlation networks will be detailed later in this thesis with the example of the WGCNA algorithm.

5.2.3.6 Differential analysis

For instance, one interpretative technique, used to discriminate experimental conditions in transcriptomic analysis is the differential analysis. Differential analyses can be performed to determine the set of differentially expressed genes between two groups [395]. This method is based on fold change, a measure of the difference in gene expression between two conditions A and B [402].

$$FC = {mean(Gene1)_{condB}}\Big/{mean(Gene1)_{condA}}$$

A fold change of 1 indicates no changes in gene expression between two conditions. Between 0 and 1, the gene is under-expressed in condition B compared to condition A. Above 1, the gene is over-expressed in condition B compared to condition A. To better represent the difference in fold change, a log transformation can be performed. Since the operation is realized on each gene and accompanied by a statistical test, a p-value correction must be computed to remove false positives induced by multiple testing.

Many p-value correction procedures can be used. Bonferroni method, for instance, correct the α prior of testing (α = 0.05 means the result of a statistical test has 5% chances to be false) by the total number of tests realized (n) [411]:

$$\alpha_{Bonferroni} = \frac{\alpha}{n}$$

If ten tests are realized with an accepted 5% chances to fail, the real used α value would be $^{0.05}/_{10} = 0.005$ with Bonferroni correction. All p-values above this threshold will be rejected as a null-hypothesis.

Benjamini-Hochberg, another method to adjust p-value, orders them from the highest to the lowest and corrects each of them according to their rank and the number of tests.

$$AdjustedPvalue = pvalue_{rank} \times \frac{rank}{N}$$

where *rank* is the rank of the ordered p-value and N is the total number of tests realized [412].

After computing the fold change and its associated adjusted p-value for each gene, the results are displayed in volcano plot, with genes ordered according to their fold change on the x-axis and their adjusted p-value on the y-axis and colored only if they are significantly differentially expressed, with an absolute fold change above a desired threshold.

5.2.3.7 Functional enrichment

Discovering a list of genes associated to a phenotype, or changes in metabolite concentration is the first step in the interpretation of the results and the resolution of the hypothesis. Uncovering biological processes associated with these genes can be laborious work, and functional enrichment analysis can be performed to confront these genes to prior knowledge by projecting their expression on mapped identified pathways stocked in ontology database (e.g., KEGG, GO) [413–415].

Many types of transcriptomic analyses exist nowadays to overcome the challenges of sequencing and get as close as possible to the biological truth. For instance, some RNA sequencing technologies are used to survey microbial diversity by targeting a very specific RNA strand called rRNA.

5.3 16S rRNA SEQUENCINGS STANDS FOR MICROBIOMICS

Carl Woese, in the 70s', discovered the hidden advantages of ribosomal RNAs. These small strands of ribonucleic acids constitute the subunits of ribosomes and are highly conserved between species. Originally exploring the diversity of the 5S rRNA units across different species, Carl Woese discovered their potential as an evolutionary probe. He began to classify species and create an evolutionary tree according to their 5S rRNA sequences but soon, was limited by the shortness of the 5S rRNA strand (which measure about a hundred nucleotides). He decided to continue his laborious exploration using 16S rRNA strands which measure a thousand nucleotides in length. Since sequencing technologies were only emerging, most of the classification was performed by hand by Woese. But this long process was rewarding in the end as he discovered a new domain of life: the archaebacteria [416].

At first, 16S rRNA sequencing served as a measure for evolutionary time, and biological barcoding for living organisms impossible to differentiate macroscopically [417]. Nowadays it is mostly used to unravel the diversity of a biological environment: in the ocean it led to the discovery of the composition of microbial ecological niches but also allowed to explore how microbial distribution was impacted by temperature, pH, or access to light [418]. 16S rRNA sequencing helped reveal the relationship between microorganisms and their environment. Indeed, the discovery of the gut microbiome, but also, the skin, mouth, vagina, microbiome led to the concept of the holobiont: a vision of men intertwined with their microbiota [419].

If the sequencing process resembles the classical mRNA sequencing workflow, there are some differences in the treatment of the data (Figure 21).

5.3.1 Sequencing and primary analysis

5.3.1.1 Amplifying 16S rRNA

Without a polyA tail, the sequencing of 16S rRNA targets variable regions named V1-V9 dispersed on a 1400 nucleotides long strand. It uses the conserved sequences as a site for primers [420, 421]. Most of the time region V3, V4 or both are amplified with PCR for all the collected 16S rRNA collected in an environmental sample. As classical mRNA sequencing, the analysis is not quantitative: amplified rRNAs are a proportion of the original biological material present, and the data is compositional [422].

5.3.1.2 Demultiplexing and denoising

Typical workflows such as QIIME2 [423], first demultiplex the sequences: using the initial adapter barcodes they sort the sequences by samples in organized files [424].

16S rRNA can be performed in single-end or paired-end sequencing. In paired-end sequencing, each rRNA strand is sequenced both ways: from the 3'end to the 5'end and, from the 5'end to the 3'end. In paired end, a merging must be realized to reunite both sequences, a step performed sometimes before the denoising sometimes after depending on the algorithm.

The denoising can be performed by algorithms like DADA2 or Deblur: they remove the noisy sequences; the ones containing unknown nucleotides, or chimeras. This process is essential: sequences with high levels of resemblance are clustered together [425, 426]. A 97% identity between two sequences was the original threshold to determine the belonging to the same operational taxonomic unit (OTU) [427]. But OTUs are just a threshold: two sequences from the same OTU can still belong to different species. DADA2 and Deblur are two algorithms capable of better resolution to remove sequencing artifacts and to identify the different strain of bacteria at a level of identity called amplicon sequence variants (ASV). For instance, Deblur uses error models to first filter the sequences. It, then, compares sequences with the Hamming distance on a smaller subset, subjected to dereplication (dereplication removes identical copies of the same sequence) with removed singletons (sequences only present once in the entire subset: they are more susceptible to be chimeras) and known sequencing errors collected in databases [425]. DADA2, on the other hand, denoises the sequence prior to the merging in paired-end sequencing, and only keeps the one with exact overlapping sequences [426]. We cited, in this introduction, two tools for ASVs inference and denoising, but others exist like

FROGS [428]. The result of the denoising process is the counting table which describes the list of frequencies of each present ASVs for all the samples (Figure 21).

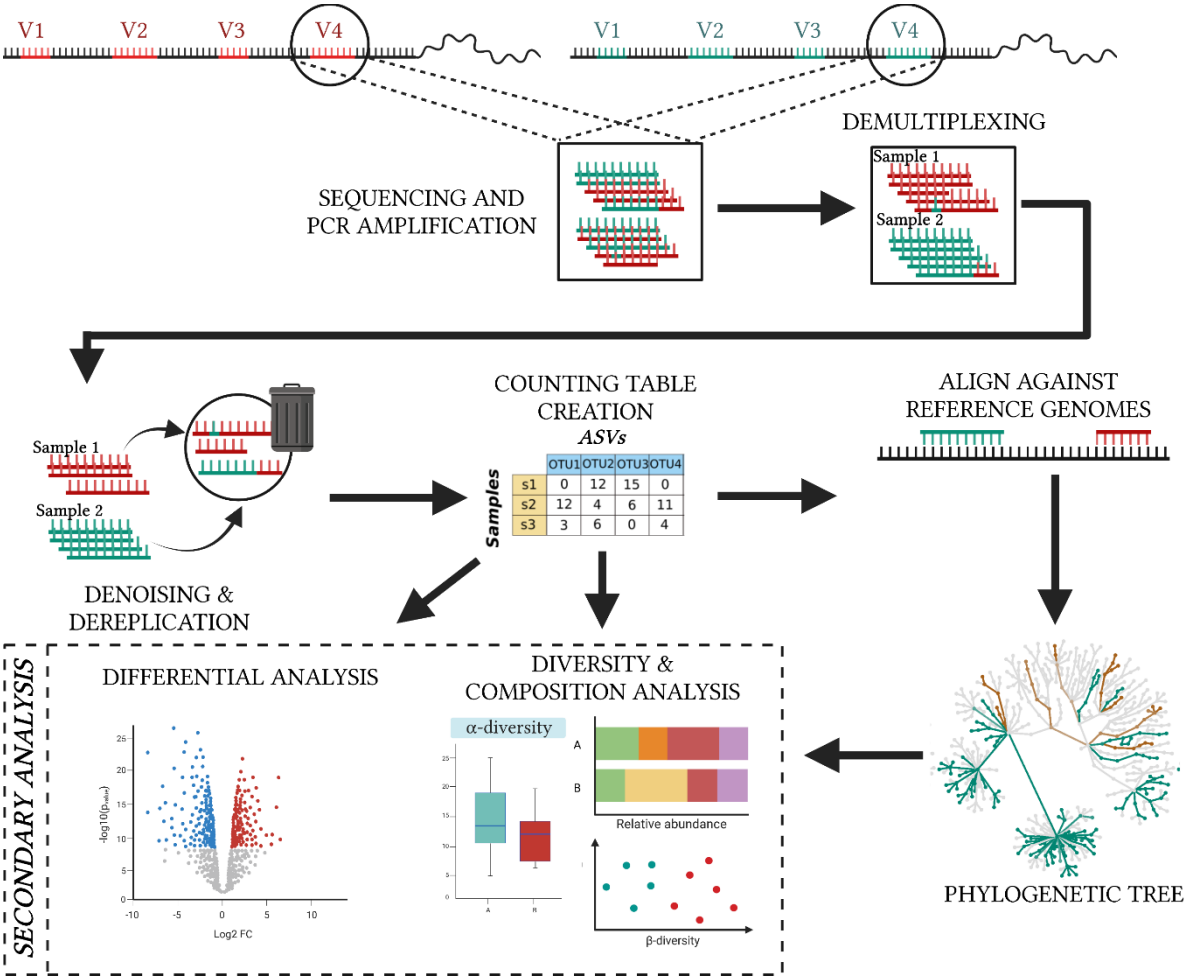

Figure 20 16S rRNA sequencing analysis pipeline: After the sequencing and PCR amplification of a variable 16S rRNA region (generally V3 or V4), the sequences are demultiplexed, denoised, dereplicated. A counting table is constructed and after sequence alignment against reference genomes a taxonomic table and a phylogenetic tree are also built. They can be used to perform diversity (α and βdiversity indexes) and composition analyses. Differential analysis can also be performed on microbial abundances.

5.3.1.3 Alignment and phylogenetic tree inference

Reads can then be aligned to full-length reference sequences stored in dedicated databases (GreenGenes or SILVA). These databases are often updated with new species, and new taxonomic arrangements found by de novo sequencing or shotgun metagenomic sequencing [429, 430]. From the taxonomic assignment, a tree can be constructed to represent the phyla, orders, classes, families, genera, and species present and the evolutionary distance between each of them. Phylogenetic trees are built from multiple sequence alignments (MSA) [431, 432]. Using both the frequency of each ASVs present and their taxonomic assignment, diversity measurement can be performed.

5.3.1.4 Assessing microbial diversity

Diversity measurements assess the richness and evenness of an environment: Does environment A contain more species than environment B? Are species in each environment equally abundant? α-diversity measures the intra-environment composition while β-diversity compares inter-environments composition. β-diversity can be based on the raw count matrix in Bray-Curtis dissimilarity index but can sometime use the phylogenetic tree: instead of measuring the number of differences between two environmental species compositions, it computes the number of shared branches between the two environments' taxonomic trees (Figure 21) [433, 434].

Characterizing microbial environments is one goal of 16S rRNA sequencing, but other analyses can be realized to find the statistical differences between two communities.

5.3.2 16S rRNA data is compositional

16S rRNA sequencing only produces compositional data: the final frequency of each ASVs is highly dependent on the instrument size and capacity and can only be expressed as a proportion of the initial samples' environment. Therefore, analysts must be very careful performing some type of analysis where raw abundances are particularly important. β-diversity measures are subjected to this limitation since they compare the abundance of species across ecosystem, but differential analysis too [422].

Comparing microbial quantities across samples can be complex when all abundances are a proportion of one another. In the example of figure 22, we clearly see that two highly different ecosystems like B and C can display the same proportion of species blue and red when both species are less abundant in ecosystem B in reality. Thus, differential analysis strategies must be adapted, in normalization and transformation strategies to overcome the limitation of compositional data.

One approach is to work on log-ratio:

$$G(x) = \sqrt[n]{x_1 \times x_2 \times x_3 \dots \times x_n}$$

$$x_{clr} = \left[\log\left({}^{x_1}/_{G(x)}\right), \log\left({}^{x_2}/_{G(x)}\right), \log\left({}^{x_3}/_{G(x)}\right), \dots, \log\left({}^{x_n}/_{G(x)}\right)\right]$$

where G(x) is the geometric mean of n ASVs of frequency x. Using log-ratio render samples comparable since their sample space is not proportional to one another but become real numbers [435].

Aldex2 and ANCOM are two differential analysis methods based on the *center-log-ratio* (clr) transformation but are more fit to large studies with many samples [176, 436]2. To find differences in rare variants, the *variance-stabilizing-transformation* (vst), used by DESeq2, can also be used [437].

The study of microbial ecosystems remains a challenge, even with the improvement of sequencing technologies. It is mostly due to their compositional nature but also to other factors such as the sampling procedure or the presence of rare, top-chain microbes which are often considered as singletons or filtered as low counts and removed from the analysis [438]. Moreover, microbiomes are an integral part of an ecosystem. The characterization of this ecosystem and their interactions are becoming a challenge, especially when the habitat of the microbiota is the human body with complex association strategies to maintain the health of the

host symbiont [439]. Studying the host-microbiota through omics datasets remains a challenge since each type of data is different in nature, but also in their sequencing process.

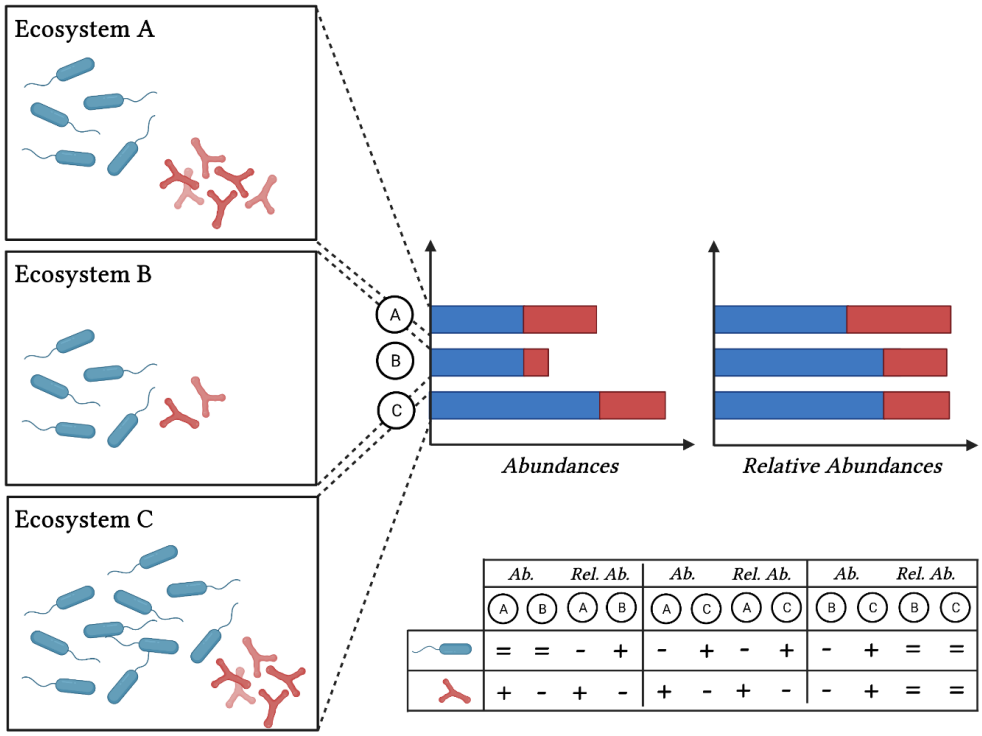

Figure 21: 16S rRNA data are compositional: Differential Analysis applied on compositional data are limited. Using proportion can falsify the original differences in raw abundances.

5.4 MULTI-OMICS ANALYSIS: AN INTEGRATIVE VIEW OF DATA

With the extensive use of data sequencing in biological experiments, multi-omics analyses are more and more employed. However, as the interest in the multi-omics field has grown drastically from 2005 to 2020, the number of algorithms and strategies has also increased over the years [440] (Figure 23). In systemic environments such as body organs or the ocean, single omics analyses are now considered as oversimplistic, only considering one biological entity in interaction with many others. Multi-omics aims to combine data from diverging omics types but describing the same set of samples to capture interactions between different biological layers. However, they are confronted with multiple issues: adding omics layers is mostly appending new variables to an already large quantity, all describing a rather small number of samples. Moreover biological data are considered noisy and multi-omics data gathering can exacerbate this trait [441]. The normalization of data with different origins is also a challenge. Eventually, there are a multitude of multi-omics strategies but no gold standard procedure [442].

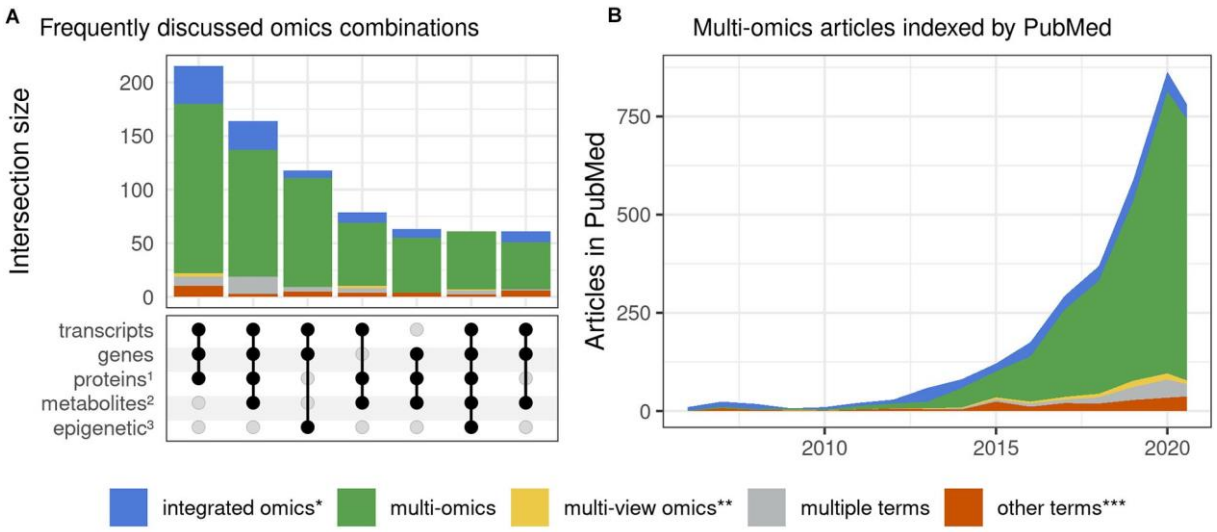

Figure 22 Overview of the multi-omics field over the past few years: A. The most common multi-omics combination employed. B. Number of articles referencing multi-omics analyses or related terms between 2005 and 2021 (Figure from [440]*).*

In this section we will describe the different multi-omics strategies. They are classified over many criteria. When, within the pipeline, omics data are integrated, defines if the analysis is an early, mixed, intermediate, late, or hierarchical integration. The method employed for integration can be network-based, clustering, or machine learning approaches. The methodology's choice is intimately related to how the results will be interpreted and can be exploratory, interpretative, or even discriminative.

5.4.1 From early to late integration

When the data are integrated in a multi-omics pipeline is determinant for the method employed and the results of the analysis (Figure 24).

- In early integration, the first step of the analysis is the integration of the datasets to create a large multi-omics framework. With this method, the limitations of multi-omics analysis discussed earlier are not treated. Thus, early integration is more adapted to dimensionality reduction approaches to remove the excess noise of the combined omics datasets.
- Mixed integrations perform independent analysis on each dataset before combining them. These analyses aim to transform the data first into new comparable mathematical relationships (e.g., networks, similarity matrices…). In this new form, the data from each omics can be fused together.
- Intermediates resemble mixed integrations as they jointly analyze the two separate omics layers to find common latent patterns and produce a common multi-omics representation from this joint analysis.
- In late integrations, data analyses are performed separately to produce independent results which can be interpreted together.
- Eventually hierarchical analyses use the biological nature of the omics data to use one omics to interpret the other omics layer: the pipeline is therefore performed sequentially, the results of one -omics analysis serves for the second omics dataset.

Between early to late integration, the different strategies are used to overcome the limitations of multi-omics analyses (such as mixed and intermediate integration which aims to account the noisy nature of these datasets), or to take advantage of the nature of biological data to interpret the other omics layer (in the example of hierarchical integration).

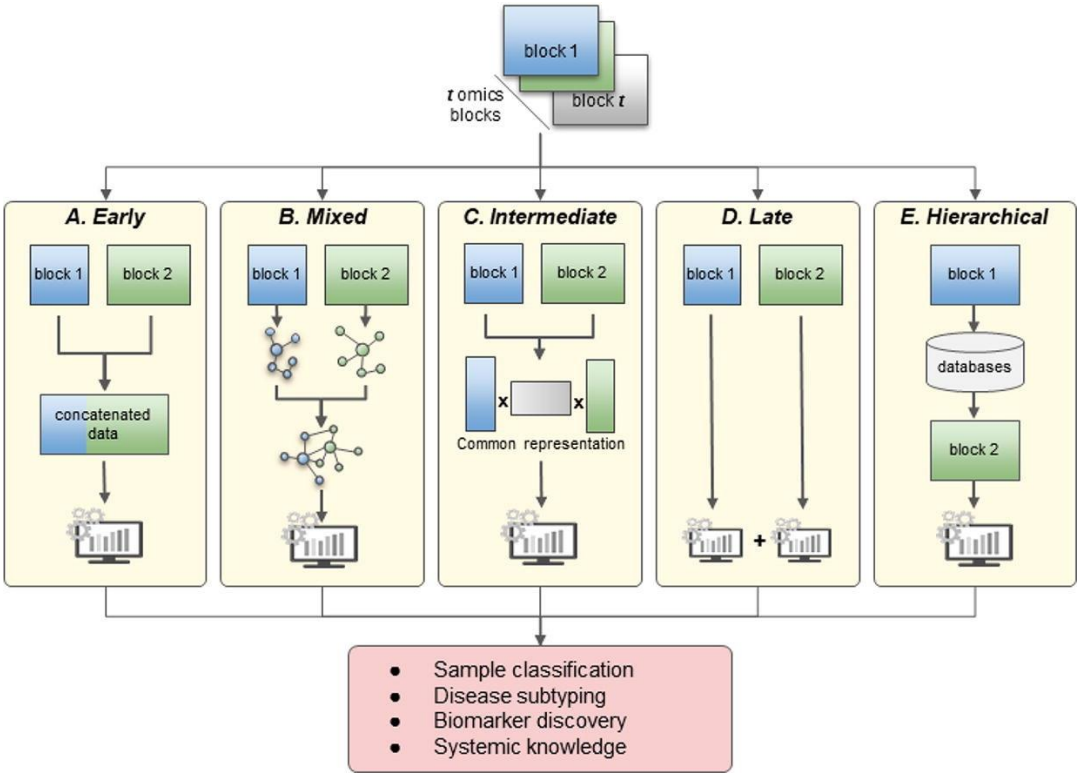

Figure 23 Early, mixed, intermediate, late or hierarchical strategies can be employed to perform multi-omics analysis. They discriminate multi-omics analyses based on when and how -omics datasets are integrated together (Figure from [441]*).*

5.4.2 Methods employed in multi-omics

Several methods are employed to extract multi-omics features: in this section we will discuss clustering, network-based, ordination, and machine learning approaches but many others exist.

5.4.2.1 Machine Learning

Machine learning (ML) techniques comprise a wide range of algorithms based on learning from previous data. The models are constructed from, what we call, a 'training' subset to classify the dataset of interest. Principal ML models include Kernel Learning to find similarity measures between samples based on linear, gaussian, polynomial relationships; Neural networks are based on connection between artificial neurons for decision-making; or random forests build decision trees based on variables values to unravel common experimental outcomes.

ML approaches are more adapted to early or late integration pipeline and available in platforms like mixOmics, specialized in multi-omics analyses and providing ready-to-use and generalized framework to work with all -omics types.

The limit of ML algorithms is that they require a prior decision from the analyst: the number of latent variables, classes, or iterations. If methods are developed to help in parameterization, a deep knowledge of the data, their nature and their possible associations is required to use these algorithms [443]. Therefore, they are not adapted for biologists without computing skills.

5.4.2.2 Ordinations

Ordination techniques are a way, when confronted with a really large number of variables, to order the samples according to new synthetic axes. The construction of these axes is dependent on the method employed.

One example is CCorA (canonical correlation analysis). It, basically, associates each pair of variables belonging to multiple -omics datasets and aims to find the ideal combination of pairs to maximize the association between the different omics layers [444]. A simple approach with limitations since correlation does not imply causality.

Other ordination methods utilize other types of metrics. For instance, multiple co-Inertia analysis (MCOA) is based on variance. This approach was originally developed for ecological purpose to study species-environment relationships. With this method, all -omics data frames are projected in separate multi-dimensional spaces. In both spaces, the axis maximizing the covariance between both datasets is searched. When the samples are scaled according to these two axes their correlation is maximized. The samples can also be scaled on a typical biplot, using the factorized F1 and F2 axes, the 2 axes to maximize the variability of each dataset in each multidimensional space. Samples are then scaled two times: one projection is their position according to the F1 and F2 axes of the first -omics multidimensional space, the other is their position according to the F1 and F2 axes of the second -omics multidimensional space. The distance separating both projection is often represented as an arrow: the length of the arrow is proportional to the distance separating both samples projection through their -omics layers. MCOA is useful to find the samples with highly different expression and behavior in different -omics layer but also to extract variables from each -omics datasets driving the covariance. (Figure 25) [445]

Procrustes analysis, finally, is also an ordination technique but factorizes the multi-dimensional spaces without correlation or covariance but based on shape comparison. It optimizes the superimposition between dimensional space to find common data structure between -omics layers [446, 447].

If CCorA is an early integration method, both MCOA and Procrustes are intermediate integration analyses.

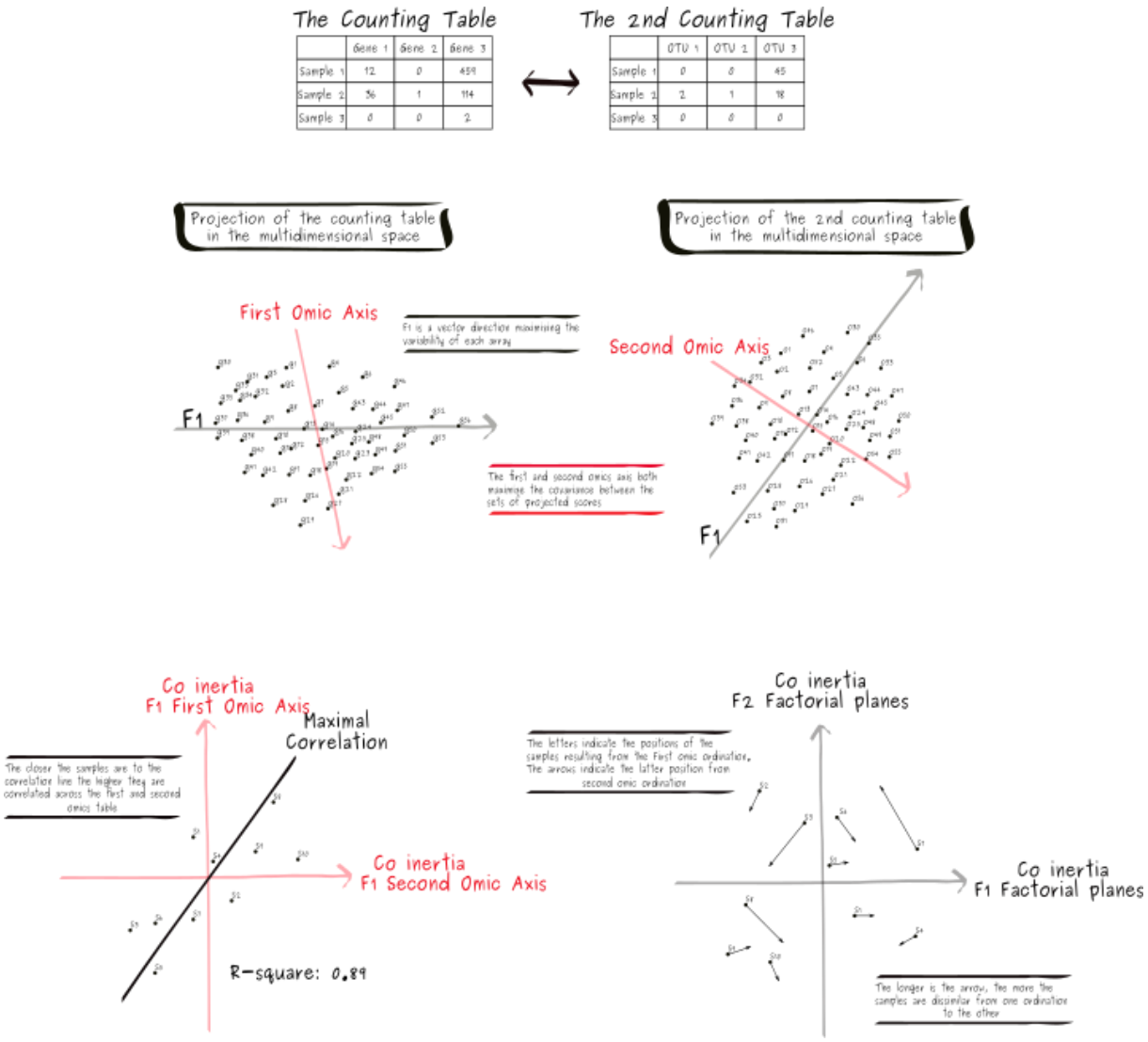

Figure 24 Ordination techniques: the example of multiple coinertia analysis: In MCOA, -omics datasets are projected in separate multidimensional spaces and the axes maximizing their co-variance are found. Samples can be plotted in biplots using the F1 and F2 axes, the two axes maximizing the variability in each -omics layer and the distance in their expression across omics datasets can be observed (Inspired from [445]*).*

5.4.2.3 Network-based

Networks can be used to illustrate the relationships between samples or omics variables. similarity network fusion (SNF) is, for instance, a tool used to cluster samples using multi-omics variable information. In this pipeline, networks are inferred from each omics dataset in which nodes are samples and the edges represent the weight of each omics similarity matrix. After the inference of each individual network, they are fused together iteratively to obtain a sample network based on the multi-omics datasets [442, 448] (Figure 26).

Another completely different usage of network-based approaches can be illustrated with the tool COSMOS. COSMOS is restricted to certain types of data (e.g., transcriptomic, phosphoproteomics, metabolomics) and uses prior knowledge to project the results of a separate differential analysis on directed knowledge networks [449]. If COSMOS is restricted in terms of data type, it is powerful to infer causal hypotheses from multi-omics datasets.

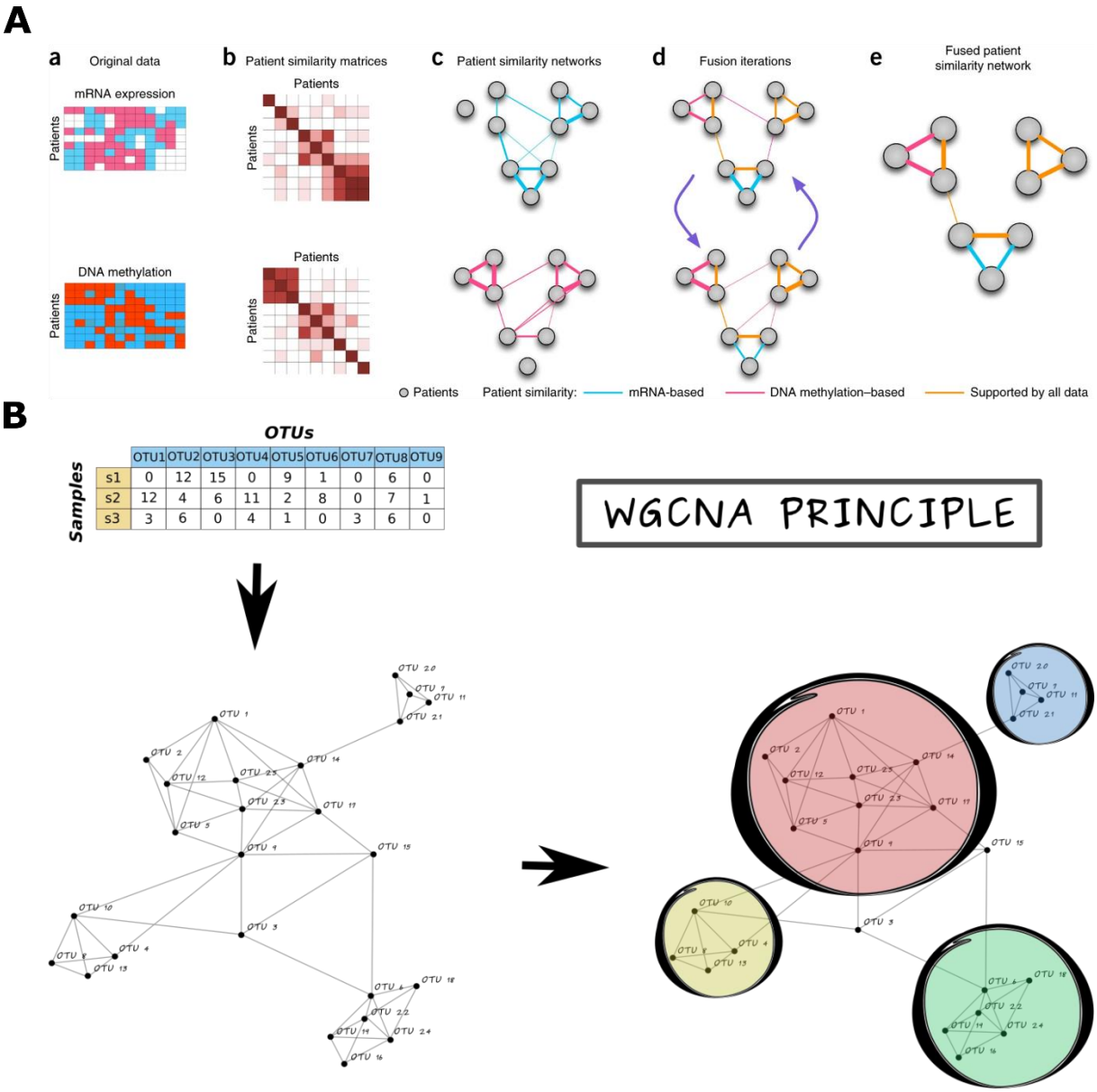

Figure 25 Two examples of network-based approaches: A. Similarity Network Fusion method infer sample relationships based on each -omics similarity matrices. The inferred -omics networks are fused over several iteration based on common edges patterns (Figure from [448]*) . B. WGCNA also infers networks from a similarity matrix computed from the original dataset. However, the nodes of the inferred networks are not the samples but the variables themselves. A clustering method is applied to the topology of the network to deduce modules composed of highly correlated variables and reduce the dimensionality of -omics datasets. The samples contributing to the formation of these module can be retrieved afterwards (Inspired by* [450]*).*

If correlations have limitations, they can be useful in network-based methods where they serve to reduce the dimensionality of the data. An example is the WGCNA (Weighted Gene Correlation Network Analysis) algorithm which uses correlation to infer networks and reduce the large subset of variables to modules of highly correlated variables restricted to a scale-free topology to approximate real biological interactions (Figure 26) [450]. But the WGCNA approach was not applied to multi-omics datasets until the development of our tool which will be presented in Chapter 1.

Objectives

As the concept of holobiont emerged in the literature, studying the bi-directional interaction between our body and its associated microbiota became a priority to untangle how homeostasis is regulated by and beyond our organs. In health, and in diseases as well, the inter-dependency within the hologenome is at stake, especially in the gut, this complex succession of digestive organs which coordinates many cell types and functions. With the development of high throughput sequencing, -omics studies revealed how host physiology or species abundances can be impacted by an environmental challenge. However, studying their interactions and how they can be influenced is still an issue: how data can gather and transcribe an interaction between different biological entities?

Psychological stress is at the frontier between homeostasis and chaostasis. As an environmental factor, it triggers systemic modifications, even after an acute event, and can be an actor in the initiation and the development of many chronic diseases. If its effects on the intestinal physiology and function were reported, its impact on the host-microbiota bi-directional interactome was never studied. Since the gut microbiota participates actively in the stress response via the HPA axis, and regulates many functions in the gut, its interactions with the epithelial barrier during a stress constitute a central query to unravel the systemic impact of the stress response.

Therefore, the current thesis aims to untangle the impact of psychological stress on the gut host-microbiota interactome, by developing new multi-omics approaches to explore the gut microbiota interactome. This work is divided into two axes:

- In the first part, we aimed to develop multi-omics approaches to explore associations within and between -omics dataset. The goal was to provide network and ordination-based methods to visualize and interpret multi-omics integration. Since multivariate analyses are barely accessible to biologists without programming skills, and lack visualization representation to interpret these complex associations, a secondary objective was to provide a guided platform to perform these algorithms. The development of these tools constituted the base for the further analysis of the gut-microbiota interactome submitted to a stress challenge. This work was published in BMC bioinformatics during the third year of my thesis (January 2021) as Zoppi J, Guillaume J, Neunlist M, Chaffron S. MiBiOmics : An interactive web application for multi-omics data exploration and integration. 2020;:1–11. It provides a ready to use web-application called MiBiOmics with a guided documentation to explore association within multi-omics datasets. The development of MiBiOmics will be discussed in Chapter 1 of this thesis.
- In the second part, the developed multi-omics tools were used to analyze the impact of psychological stress upon the host-microbiota interactome. In this study, mice were subjected to water avoidance stress (WAS) to provoke a generalized stress response and the physiology of 4 intestinal segments (the jejunum, ileum, proximal and distal colon) were investigated, as well as the regional gut epithelium transcriptome, epithelial-associated and luminal microbiota. Using combined in vivo studies and organoids with bioinformatical analysis tools, we aimed to characterize

the impact of stress upon the functional and transcriptomic response of gut epithelial and its interactions with microbiota composition and functional remodeling. This work is currently in preparation/submitted under the title: " Multi-omics and functional characterization of psychological stress induced modulation of microbiota host-interactions in colonic epithelial cells " The results of this study are referred to in chapter 2.

With this work, our goal was to offer new tools and systemic experimental framework to study the host-microbiota interactome in the context of the stress response. We were able to develop biological models and bioinformatical tools and to use these models to characterize the remodeling of intestinal barrier functions by stress. We hope our answer helped characterize the regional bi-directional interactome around gut barrier and how it can be impacted by an external factor.

Article 1: MiBiOmics: an interactive web application for multi-omics data exploration and integration

RESUME FRANÇAIS DU PREMIER ARTICLE

Alors que les approches expérimentales multi-omiques deviennent une pratique courante dans le domaine biomédical, la caractérisation multi-échelle des systèmes biologiques nécessite le développement de nouveaux algorithmes et méthode intégrative pour élargir nos connaissances sur le fonctionnement des organismes et des écosystèmes naturels [451]. Faciliter les associations entres couches -omiques (la (méta-)génomique, (méta-)transcriptomique, métabolomique...) et inclure différentes magnifications de l'organisme (cellules, organes, holobiont, communautés) est un défi dans divers domaines, notamment l'écologie microbienne [452], la génétique [453] et la médecine personnalisée [454]. De plus, la multi-omique, capable de capturer des sources supplémentaires de variabilité à travers les différentes entités biologiques étudiées, permettrait d'identifier des séquences d'évènements conduisant à un phénotype ou une condition. Sans prédire les mécanismes sous-jacents, elle pourrait tout de même à délimiter les acteurs clés dans certains processus biologiques sur plusieurs échelles du vivant [455].

Aujourd'hui, si plusieurs méthodes intégratives ont été développées, elles se restreignent souvent à l'étude de couches omiques spécifiques [456], certains schéma expérimentaux, et s'appliquent grâce à des connaissances préalable en projetant sur des voies biologiques connues et décrites par la littérature[457]. Il existe des pipelines bio-informatiques plus généraux tels que mixOmics qui n'offrent cependant que des méthodes semi-supervisées et peu accessibles à la communauté, car elles nécessitent des compétences de programmation [443].

L'objectif de ce premier article de thèse est de fournir des méthodes exploratoires basées sur l'inférence de réseaux de corrélation et des techniques d'ordinations qui peuvent être appliquées de façon plus générale aux différentes données -omics. De plus, MiBiOmics, présenté à la fois sous forme de site web et d'application autonome, donne accès à plusieurs librairies R et à de nouveaux outils de visualisation visant à mieux interpréter la complexité des associations multicouches. Cet outil permet de révéler des signatures robustes dans des ensembles de données à haute dimension par le biais d'une interface utilisateur et à l'aide de tutoriaux guidés, rendant accessible aux scientifiques sans compétences informatiques plusieurs techniques multi-omiques.

MiBiOmics permet d'étudier de façon individuelle et complémentaire jusqu'à trois jeux de données à haute dimension simultanément. Il met à disposition deux techniques principales: l'inférence de réseaux multi-omics basé sur la méthode WGCNA [450] et une méthode

d'ordination appelée la co-inertie multiple[445]. L'application est divisée en plusieurs sous-sections: la préparation des données (qui permet de télécharger les différents jeux de données, de les filtrer, normaliser et transformer), l'exploration des données (qui met à disposition des analyses en composantes principales (PCA), de réaliser des dendrogrammes et découvrir les principaux axes de variabilités dans chaque jeux de données), l'inférence de réseaux (qui guide pas à pas l'utilisateur pour réaliser un réseau WGCNA pour chaque couche omique en respectant la topologie scale free), l'exploration de ces réseaux (après la réduction de dimensionnalité pour chaque jeux de données en module de variable fortement inter-corrélées, l'utilisateurs peut explorer chaque sous-partie des différents réseaux et les associer à des paramètres externes d'intérêt), et enfin l'analyse multi-omics (qui permet de réaliser des ordinations telles que la co-inertie multiple et de corréler les modules des différents réseaux entre eux pour dégager des signatures de biomarqueurs multi-omiques).

L'application MiBiOmics, à travers son interface visuelle, permet l'exploration et l'extraction de variables multi-omiques avec une méthode prête à l'emploi et la génération de nombreuses figures publiables. Cet outil permet la réduction de dimensionnalité de larges jeux de données haut débit via des méthodes d'exploration qui requiert peu de paramétrage. Il propose une adaptation de la méthode WGCNA pour l'échelle multi-omique.

La comparaison des outils multi-WGCNA et de la co inertie multiple de MiBiOmics au pipeline DIABLO de mixOmics très largement reconnu en matière d'analyse multi-omiques a montré la complémentarité des trois approches. Sur une étude comparative d'un même jeu de données (les données de l'atlas des génomes cancéreux TCGA), même si une partie des variables extraites était commune aux trois analyses, les trois outils ont permis d'identifier des résultats très complémentaires. Les valeurs prédictives de ces biomarqueurs dans la distinction du type de tumeurs, bien que très fortes pour les trois méthodes étaient meilleures pour les outils fournis par MiBiOmics. Cependant, DIABLO démontre de meilleures performances sur certaines couches omiques comme la protéomique où le nombre de biomarqueurs identifiés étaient bien supérieurs. Cette différence de résultats entre chaque outil peut s'expliquer par la nature fondamentalement différente de chaque méthode dans leur extraction et sélection de variables. En revanche, à travers cette analyse comparative, nous avons pu démontrer que MiBiOmics était capable de générer de nouvelles hypothèse à l'échelle multi-omique grâce à l'association de la protéine SYK, très connues en cancérologie[458], à plusieurs miRNAs non identifié jusqu'à maintenant qu'il a été le seul à identifier: une interaction possible entre plusieurs entité biologique qui nécessitera cependant une validation expérimentale pour être validée.

En conclusion, MiBiOmics met à disposition un ensemble d'outil multi-omique à travers une plateforme facile d'accès et d'une documentation guidée et permet la génération d'hypothèse à l'échelle multi-omique. Il offre un pipeline original et complémentaire aux méthodes précédemment développées. Cependant des efforts doivent encore être fait pour généraliser l'analyse multi-omique et améliorer les méthodes existantes pour se rapprocher de la description précise de mécanismes biologiques et potentiellement s'affranchir de la validation expérimentale.

Zoppi *et al. BMC Bioinformatics* (2021) 22:6
https://doi.org/10.1186/s12859-020-03921-8

BMC Bioinformatics

SOFTWARE Open Access

MiBiOmics: an interactive web application for multi-omics data exploration and integration

Johanna Zoppi[1], Jean-François Guillaume[2], Michel Neunlist[1] and Samuel Chaffron[3,4*]

*Correspondence:
samuel.chaffron@ls2n.fr
[3] CNRS UMR6004, LS2N, Université de Nantes, 44000 Nantes, France
Full list of author information is available at the end of the article

Abstract

Background: Multi-omics experimental approaches are becoming common practice in biological and medical sciences underlining the need to design new integrative techniques and applications to enable the multi-scale characterization of biological systems. The integrative analysis of heterogeneous datasets generally allows to acquire additional insights and generate novel hypotheses about a given biological system. However, it can become challenging given the often-large size of omics datasets and the diversity of existing techniques. Moreover, visualization tools for interpretation are usually non-accessible to biologists without programming skills.

Results: Here, we present MiBiOmics, a web-based and standalone application that facilitates multi-omics data visualization, exploration, integration, and analysis by providing easy access to dedicated and interactive protocols. It implements classical ordination techniques and the inference of omics-based (multilayer) networks to mine complex biological systems, and identify robust biomarkers linked to specific contextual parameters or biological states.

Conclusions: MiBiOmics provides easy-access to exploratory ordination techniques and to a network-based approach for integrative multi-omics analyses through an intuitive and interactive interface. MiBiOmics is currently available as a Shiny app at https://shiny-bird.univ-nantes.fr/app/Mibiomics and as a standalone application at https://gitlab.univ-nantes.fr/combi-ls2n/mibiomics.

Keywords: Multi-omics, Ordination, Biological networks, Data integration, R shiny

Background

The multi-scale characterization of biological systems is extending our knowledge about the functioning of organisms and natural ecosystems. Today, their multi-omics characterization is becoming standard, thus novel methodologies and easily accessible tools are required to facilitate the study of associations and interactions within and across omics layers [e.g. (meta-)genome, (meta-) transcriptome, metabolome] and scales (e.g. cells, organs, holobionts, communities). The analysis of single omics datasets has helped to identify molecular signatures associated to phenotypes of interest [1]. However, it usually does not allow to predict mechanisms underlying phenotypic variabilities [2]. Although multi-omics information is not sufficient to identify causes and consequences

of a biological process, it can contribute to delineate key players sustaining it [3]. Indeed, exploring a biological system across several omics layers enable to capture additional sources of variability associated with a variation of interest and potentially to infer the sequence of events leading to a specific process or state [4]. Within the last decade, multi-omics integrative approaches have been applied across various fields including microbial ecology [5], genetics [6] and personalized medicine [7]. As of today, several integrative methods have been developed, but are often specific to a given experimental design, data type or a precise biological question [8]. Indeed, tools such as MONGKIE [9], are based on prior knowledge and integrate data by projecting them on known metabolic networks and biological pathways. More generally, existing multi-omics pipelines are focusing on certain data types (Metabolomics with MetaboAnalyst [10]) or on disease-related mechanisms (MergeOmics [11]). More widely applicable methods exist, such as the R package mixOmics [12] that provides several semi-supervised methodologies often based on ordination techniques. Considering the multiplicity of existing techniques, the selection of an appropriate workflow is challenging for biologists, especially when it comes to the representation of several system-level omics layers and its interpretation. There is a clear need for accessible (web) tools to facilitate the integration, analysis and representation of multi-omics datasets through an intuitive and guided approach.

MiBiOmics aims to provide established and novel techniques to reveal robust signatures in high dimensional datasets [13] through a graphical user interface allowing to perform widely applicable multi-omics analyses for the detection and description of associations across omics layers. Available as a web-based and a stand-alone application, it gives access to several R packages and tools to help users who are not familiar with programming to load and explore their data in a simple and intuitive way. MiBiOmics allows the parallel study of up to three omics datasets, as well as the in-depth exploration of each single dataset. It also provides easy access to exploratory ordination techniques and to the inference of (multilayer) correlation networks enabling useful dimensionality reduction and association to contextual parameters. The user can then compare results from these different approaches and cross-validate multi-omics signatures to generate confident novel hypotheses.

Implementation

MiBiOmics is implemented in R (Version 3.6.0) as a Shiny app providing an interactive interface to perform each step of a single- or multi-omics data analysis (Fig. 1). MiBiOmics is also accessible as a standalone application that can be easily installed via Conda (Version 4.6.12). The application is divided into five sections as described below:

Data upload

Within MiBiOmics, the user can upload up to three omics datasets, allowing the data exploration and network analysis of a single- or multi-omics dataset. There must be common samples between omics datasets in order to perform all analyses provided by the application. An annotation table describing external parameters (e.g. pH, site of extraction, physiological measures) needs to be provided. These parameters may be quantitative or qualitative, and available for each sample. An additional taxonomic annotations

Fig. 1 The MiBiOmics framework. The MiBiOmics workflow can be divided into three main tasks: data preprocessing, data exploration, and multi-omics integration. The data preprocessing task is dedicated to data upload, data filtration, normalization, and transformation. The data exploration task implements classical clustering methods, PCA, PCoA and WGCNA correlation networks that can be applied to each omics dataset separately. Finally, the multi-omics integration task allows the user to perform multi-omics exploration, integration and analyses using ordination techniques (multiple co-Inertia and Procrustes analysis), and multi-omics network inference

table can be uploaded when one omics table corresponds to microbial lineages [e.g. as Operational Taxonomic Units (OTUs) or Amplicon Sampling Variants (ASVs)].

Following data upload, the user can filter, normalize and transform each data matrix using common methods, such as the center log ratio (CLR) transformation to deal with the compositional nature of sequencing data, or filtration based on prevalence. In this section, it is also possible to detect and remove potential outlier samples.

To allow new users to easily test the functionality of MiBiOmics, we provide two example datasets: the breast TCGA datasets from *The Cancer Genome Atlas* [14] allows to explore associations between miRNAs, mRNAs and proteins in different breast cancer subtypes; and a dataset from the *Tara* Oceans Expeditions [15, 16] to explore prokaryotic community compositions across depth and geographic locations.

Data exploration

In this section, two ordination plots [Principal Component Analysis (PCA), Principal Coordinates Analysis (PCoA)] [17] are dynamically produced to visualize and explore relationships between samples, and to identify main axes of variation in each dataset. When OTUs or ASVs are uploaded with their taxonomic annotations, it is possible to obtain a relative abundance plot describing the proportion of lineages at a given taxonomic level (e.g. Phylum, Family, Genus or Species) in each sample.

Network inference

The network inference section allows to perform a Weighted Gene Correlation Network Analysis (WGCNA [18]). Help sections are available to assist the user with parametrization, notably for optimizing the scale-free topology of the network. Here, WGCNA networks can be inferred for each uploaded omics dataset. We strongly advise users to read the WGCNA original publication and associated tutorials for this step of the analysis.

Network exploration

The network exploration section allows to compute and explore significant associations between subnetworks or modules (e.g. of genes, transcripts, metabolites), and communities (of lineages) delineated from each omics layer, which contain highly correlated features. Each module is associated to all external parameters provided in the annotation table and correlations are visualized as a heatmap (Fig. 2a). Modules associated to parameters of interest can be further analyzed. The user can also identify which samples are contributing the most to the delineation of a specific module (Fig. 2b), a method provided by the WGCNA R package, which computes modules eigenvalues and allows to quantify the relative contribution of a given sample to the inference of a module. In case an OTUs/ASVs table is provided with taxonomic annotations, the relative abundance of lineages contributing to each module can be visualized as bar plots.

In addition, OPLS (Orthogonal Partial Least Square) regressions [19] can be performed using a selected module component as features in order to estimate its capacity to predict a given contextual parameter, and are useful to cross-validate a module-parameter association. The results of this analysis are represented as hive plots with two axes. On the x-axis, the module features are ordered according to their Variable Importance Projection (VIP) score (a measure of their weight in the OPLS regression), while on the

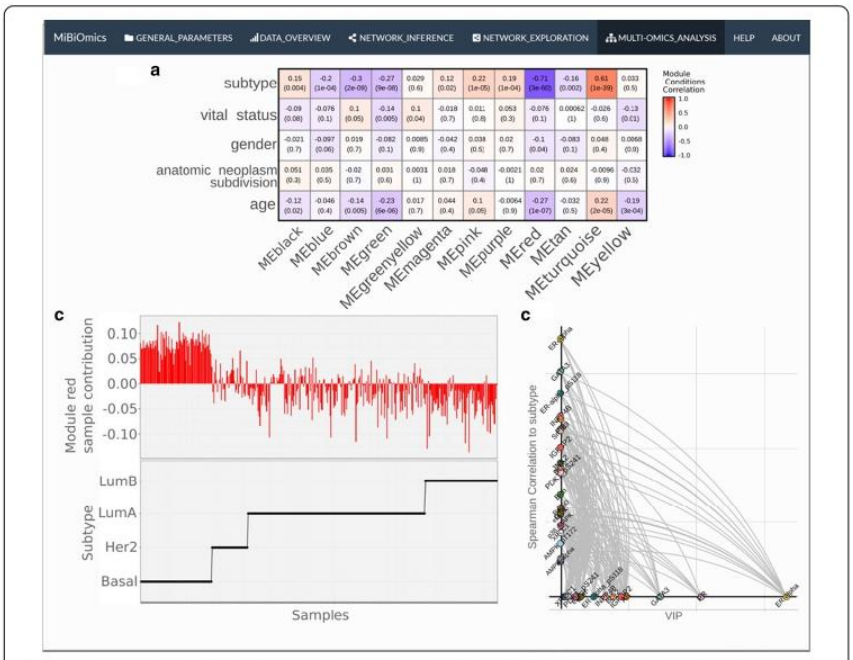

Fig. 2 MiBiOmics networks exploration. MiBiOmics networks analysis visualizations (network exploration section) from the analysis of the The Cancer Genome Atlas Network [14] breast cancer TCGA datasets. **a** Correlation heatmap displaying associations of interest between mRNA's WGCNA modules and contextual parameters. **b** The upper panel indicates the contribution of each sample in the red mRNA module delineation. Module eigenvalues are calculated for each sample and indicate how much they participate in the inference of each module. The lower panel indicates the corresponding subtype value for each sample. Here, Basal samples positively contribute to module red of mRNA, while Her2, LumA and LumB negatively contribute to the mRNA red module. **c** Hive plot displaying the protein red module's features according to their VIP scores, correlations to the subtype parameter and their relationships. In this hive plot, each point represents a variable of the protein WGCNA red module ordered, on the x-axis according to its VIP score, and on the y-axis according to its correlation to the subtype parameter. Edges linking proteins represent the actual edges of the WGCNA network. This representation is useful to distinguish central variables in the module (associated to many other variables) and predictive variables (features with a high VIP), and thus to assert whether central variables of the module are more associated to changes in the discriminant trait compared to predictive variables

y-axis they are ordered according to their correlations to an external parameter of interest (Fig. 2c).

Multi-omics analysis

Here, MiBiOmics allows users to detect and study associations across omics datasets. Multivariate statistical tools including Procrustes analysis [17] and multiple co-inertia [20] are useful to compute and visualize the main axes of covariance, to extract multi-omics features driving this covariance, and to assert how the distribution of multi-omics sets can be compared. This central section of MiBiOmics implements an innovative approach for detecting robust links between omics layers. Building upon the WGCNA pipeline we innovate here by providing an applied methodology to link groups of variables from different omics nature to external variables capturing a trait of interest. To

do so, all modules delineated within each omics-specific network are associated to each other by directly correlating their eigenvectors. Here, the dimensionality reduction of each omics dataset through module definition ensures a small number of correlations, thereby increasing the statistical power for detecting significant associations between omics layers. For visualization, a hive plot helps summarizing significant associations between each module as a multilayer network integrating links between omics-specific modules as well as their association to contextual parameters (traits or phenotypic characteristics). In this hive plot, each axis represents the network of a given omics layer. Corresponding modules are ordered on the axes according to their association to a contextual parameter of interest selected by the user. Modules with no significant associations are not depicted. Significant associations between omics-specific modules are represented, and individual associations between modules can also be visualized as heatmaps and data frame. Conveniently, the user can also select modules of interest to investigate pairwise correlations between modules' features and delineate groups of modules associated together and to an external parameter of choice. Following the identification of multi-omics modules related to a parameter of interest, the user can further investigate the pairwise correlations between variables of both modules inferred from different omics layers through the bipartite network represented in Fig. 3c or with the correlation heatmap.

Herein, we developed and implemented a novel multi-omics integration tool called multi-WGCNA. By reducing the dimensionality of each omics dataset in order to increase statistical power, multi-WGCNA is able to efficiently detect robust associations across omics layers. In addition, these multi-omics associations are linked to external traits (categorical or continuous) into a network of features for extracting robust biomarkers. We also implemented new visualization graphics to represent these multi-omics associations, an important addition in our opinion since representing multilayer associations is often challenging. Importantly, all figures generated by the application (PCA, PCoA, relative abundance plots, WGCNA outputs, hive plots, multiple co-inertia, Procrustes plots, correlograms, bipartite networks) can be downloaded (as svg or pdf files), as well as network features as csv files (WGCNA modules information, eigenvalues and co-inertia drivers).

Results and Discussion

MiBiOmics enables the exploration, integration, analysis and visualization of up to three omics datasets. Through the primary exploration of a dataset, the inference of biological networks and the extraction of multi-omics associated features, the application provides a ready-to-use analysis pipeline to interactively explore sources of variability and variables of interest in a given biological dataset, as well as associations between multi-omics features in multi-scale studies.

The inference of networks from omics features is useful to represent and model the complex architecture of putative interactions in biological systems. In addition, networks provide a way to reduce the dimensionality of a dataset by delineating cohesive groups of co-varying, often functionally related features, that can then be associated to contextual or phenotypic characteristics of interest [3]. A key functionality of MiBiOmics is the multi-omics adaptation of WGCNA [18] to explore association across omics

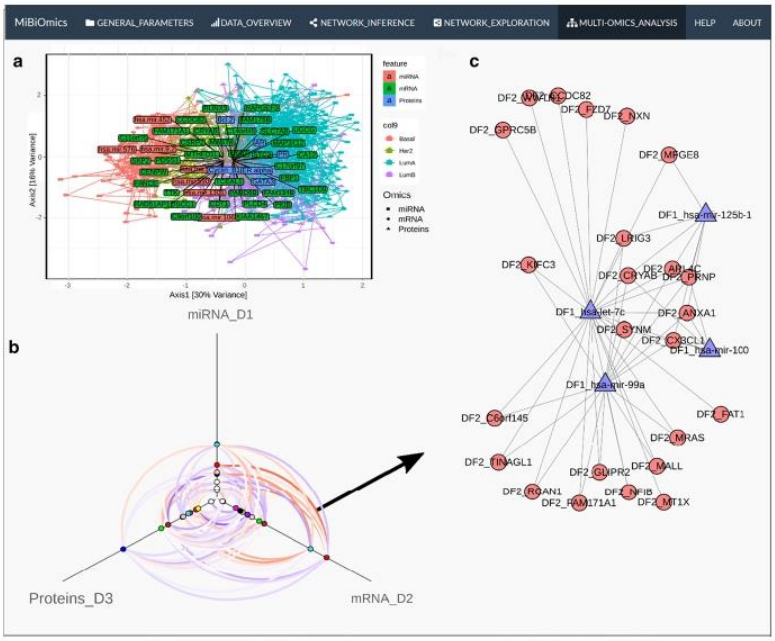

Fig. 3 MiBiOmics multi-omics integration. MiBiOmics visualizations (multi-omics integration section) from the analysis of the The Cancer Genome Atlas Network [14] breast cancer TCGA datasets. **a** A multiple co-inertia plot integrating 3 omics layers and extracted miRNA, mRNA and protein drivers. In the MiBiOmics 3-layers co-inertia analysis representation, each sample is represented by a triangle: the three vertices are the positions of the sample in each ordination space of the 3-layers co-inertia analysis. The edges linking these vertices indicate how each layer of the sample's covariate in each ordination space [27]. **b** Hive plot displaying modules of each omics network and their associations. Red edges represent positive associations, and blue edges negative associations. Edge color intensity reflects the correlation strength. **c** Bipartite network between mRNA features of the red mRNA module and miRNA features of the red miRNA module (Spearman Correlation > 0.35). When the user selects two modules of interest, variables belonging to both modules are correlated 2-by-2 and variables correlating significantly above a correlation threshold selected by the user are linked together with an edge

datasets via a network-based approach. As shown in Fig. 2a, the interface provides the ability to interactively probe associations in each omics layers of different breast cancer subtypes [14] within each network and their association to patient parameters. We further used these associations to external parameters to infer relation across multi-omics modules. The original WGCNA outputs are provided by the application to deepen the analysis between modules and external parameters (Fig. 2b). In addition, we provide the user with the possibility to perform an OPLS regression for modules of interest to evaluate the robustness of these variables to predict a given trait or phenotype. Figure 2c is an example of an OPLS regression using WGCNA module variables as features. On the x-axis the features of the red module are ordered according to their VIP score (their importance for the module), and on the y-axis according to their correlation to the subtype parameter. This figure highlights how central features of a WGCNA module relate to an external parameter.

The exploratory multi-omics analysis allows to study the main axes of covariance across omics profiles and give the ability to discover and select variables implicated

in an association between omics datasets. The concomitant application of (multiple) co-inertia (Fig. 3a) and/or Procrustes multivariate techniques with the exploration of multi-omics correlations between WGCNA modules of distinct omics layer (Fig. 3b), provides a complementary vision of multi-omics relationships. The MiBiOmics interface allows to explore WGCNA modules of interest to directly infer significant associations between features from distinct omics layers (Fig. 3c). In a multi-omics adaptation, WGCNA can be used to delineate a group of modules associated together and to a parameter of interest and extract features of different omics nature but related to each other. While an interactive version of WGCNA already exists [21], MiBiOmics goes beyond by providing a multi-omics strategy to identify correlated modules across omics layers and generate novel hypotheses. Associating modules across different datasets has already been performed in the original WGCNA article [18] and reproduced in several studies. For example, the overlap of modules between transcriptional profiles of different tissue [22] was assessed, as well as a comparison between proteomics and gene expression profile of modules in a cohort of Alzheimer patients [23]. In both cases, the association between modules was determined by overlapping identical features (e.g. same genes in a given reference genome) within each module, a method which is not applicable when omics datasets do not contain similar data types or refer to the same biological system. In MiBiOmics, we enable the inference of relationships between omics layers within an entire biological system (e.g. holobiont) or ecosystem (e.g. the plankton), which makes it more widely applicable and especially suited for omics-based environmental studies.

We compared methods integrated in MiBiOmics (see Additional file 1 for details) to the mixOmics DIABLO methodology [24]. Within MiBiOmics, the multiple co-inertia analysis and the multi-WGCNA procedures provide the user with two integrative and exploratory methods, which can be applied to any type of data, and associated to not only categorical traits, but also quantitative traits. To highlight the complementarity of our application with DIABLO, we performed an in-depth comparison of biomarkers extracted by each method when analyzing the TCGA dataset. Only few multi-omics features associated to breast cancer subtypes in the TCGA dataset were extracted by all three methods (n = 32, Fig. 4a). Both methods integrated in MiBiOmics (i.e. multiple co-inertia and multi-omics WGCNA) and DIABLO extracted mostly distinct features (Fig. 4a) underlining the probable complementarity of these multi-omics integrative strategies. Scores attributed by each method to the common set of extracted features were also dissimilar (Fig. 4b–d and Additional file 1: Table S1). This may be explained by the fact that these methods implement fundamentally different approaches to features extraction and selection, which confirms the complementary nature of each analysis. For comparing the predictive power of models integrating features extracted by each method, we performed Sparse Partial Least Square Discriminant Analysis (sPLS-DA) and computed the corresponding mean AUC scores (Fig. 4a and Additional file 1: Figure S1). All models can be considered to be highly predictive of the cancer subtype phenotypes, with the miBiOmics multi-omics WGCNA methodology obtaining the highest AUC score (AUC = 0.9945), while the multiple co-inertia analysis performed very well too (AUC = 0.9903). Features extracted by the DIABLO method from mixOmics resulted into a lowest score (AUC = 0.9808) but

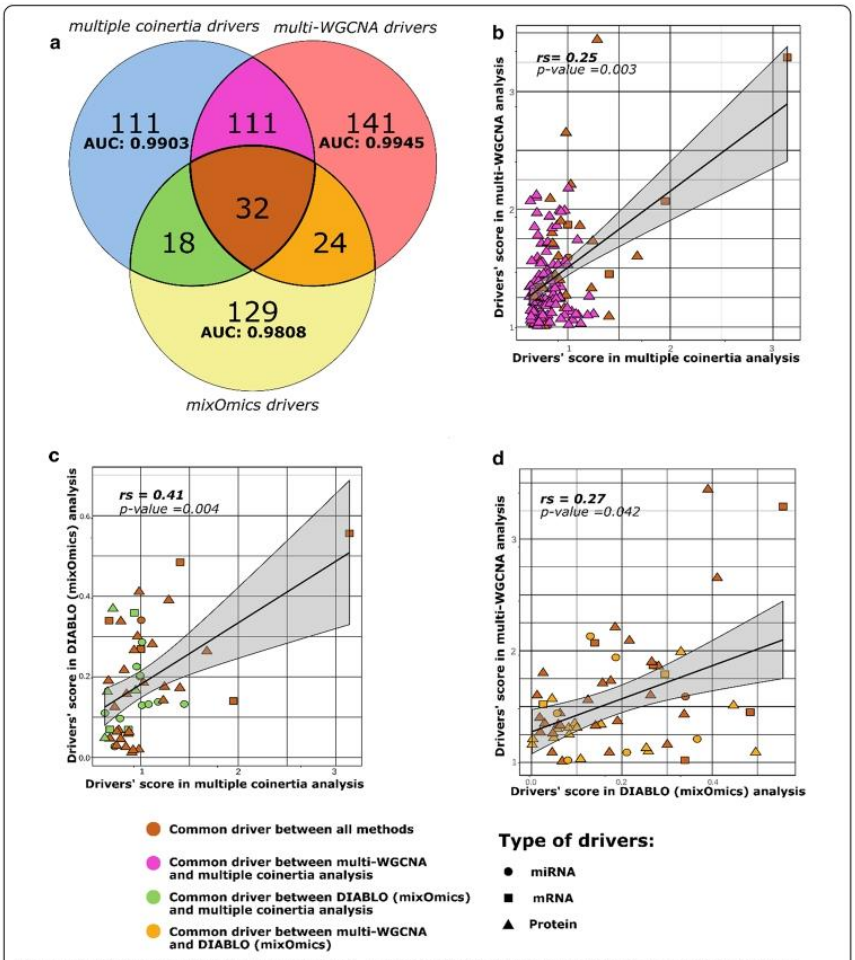

Fig. 4 MiBiOmics and mixOmics comparison. **a** Venn diagram displaying common and distinct features extracted by DIABLO (mixOmics), multiple co-inertia and multi-omics WGCNA (MiBiOmics). Area under the curve (AUC) scores were computed to compare features selection and model performance of each method. **b** Selected features' weights comparison between multiple co-inertia and multi-WGCNA on their common subset of features. **c** Selected features' weights comparison between multiple co-inertia and DIABLO (mixOmics) on their common subset of features. **d** Selected features' weights comparison between DIABLO (mixOmics) and multi-WGCNA method on their common subset of features

remained highly predictive. Generally, these methods may benefit from an enrichment method applied to the list of extracted drivers [20].

Through a gene-disease functional enrichment analysis (see Additional file 1), only the multi-WGCNA and multiple co-inertia methods were able to extract several biomarkers significantly associated to breast cancer while DIABLO found no mRNA related to breast cancer (Fig. 5a). In proportion, MiBiOmics tools extracted more mRNAs related to several stage of breast cancer development or tumor type (Fig. 5a). Some of these terms, such as the Carcinoma breast stage IV, were only retrieved by mRNAs extracted via multi-WGCNA. Also, the results obtained with the multiple co-inertia were more specific with close to 40% of mRNAs related to breast cancer (Fig. 5a). We performed a

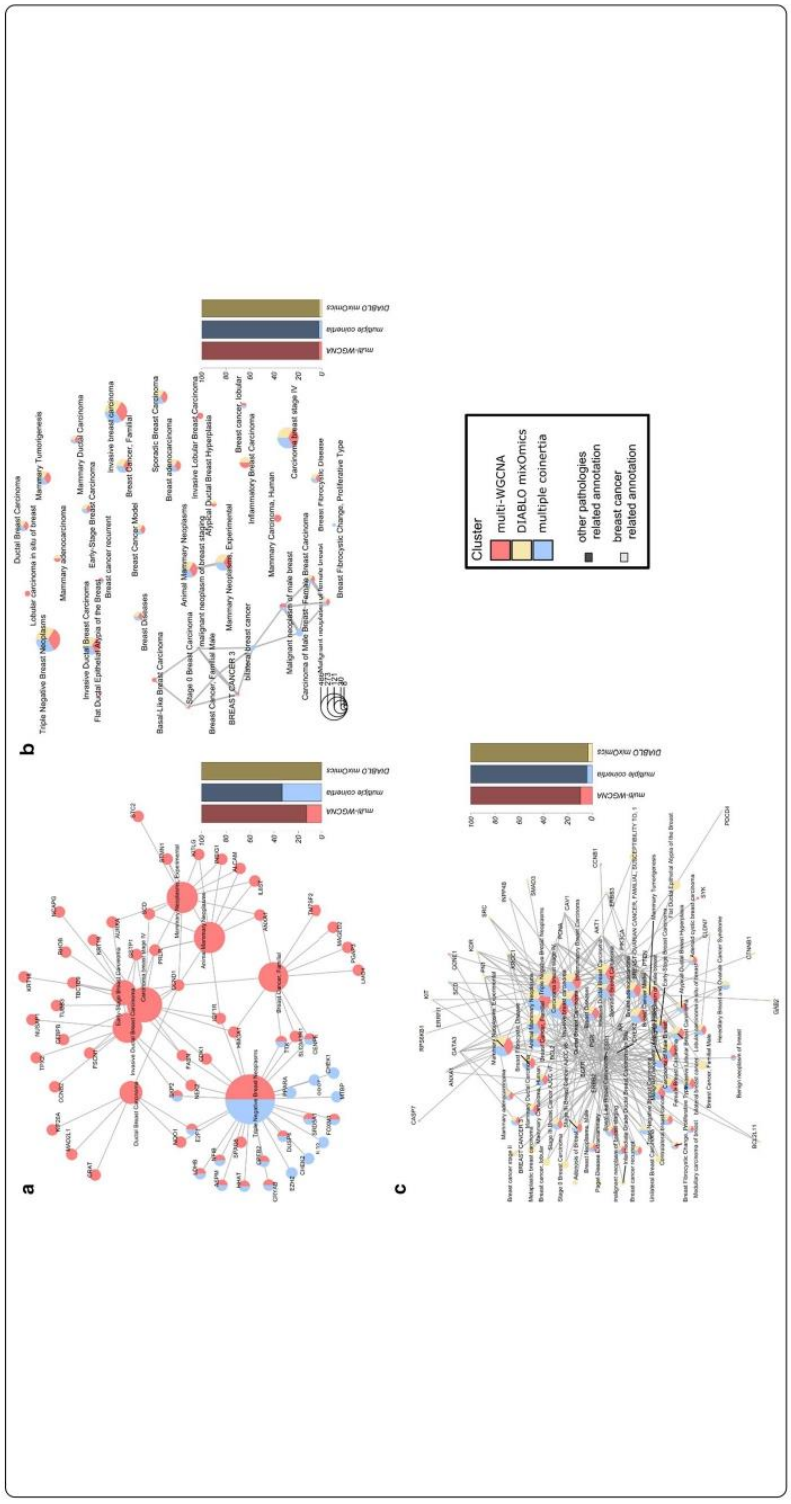
a
b
c
multi-WGCNA
multiple coinertia
DIABLO mixOmics
Cluster
multi-WGCNA
DIABLO mixOmics
multiple coinertia
other pathologies related annotation
breast cancer related annotation

(See figure on previous page.)
Fig. 5 Comparison of extracted features by DIABLO (mixOmics), multi-WGCNA (MiBiOmics) and multiple co-inertia analyses (MiBiOmics). To compare the performance of each method, a gene enrichment analysis was performed using ClusterProfiler [28] and the DisGenNet (DGM) database [29]. **a** Diseases annotations from the DGM database and their corresponding genes associated to each subset of mRNA extracted features (DIABLO in yellow, multi-WGCNA in pink and Multiple co-inertia analysis in blue). **b** Diseases annotations from the DGM database associated to each subset of validated targeted genes by miRNA extracted features (DIABLO in yellow, multi-WGCNA in pink and multiple co-inertia analysis in blue). **c** Disease annotations from the DGM database and their corresponding proteins associated to each subset of protein extracted features (DIABLO in yellow, multi-WGCNA in pink and Multiple co-inertia analysis in blue). In each plot, the side bar plot indicates the proportion of breast cancer related annotations compare to the other pathologies associated terms

similar analysis on extracted miRNA features by retrieving their targeted genes. Similarly, for subsets of validated gene targets, we performed a functional enrichment analysis to find their association to diseases (Fig. 5b). Here, most breast cancer associated terms were found by all three methods. Notably, both multi-WGCNA and multiple co-inertia analyses were also able to highlight specific annotations related to male disposition in breast cancer or basal-like phenotype of breast tumor. The ratio of breast cancer related terms against other pathologies related terms was low for all methods but may be explained by the generally wide targeting nature of miRNAs. The functional enrichment analysis on extracted proteins by DIABLO (mixOmics), multi-WGCNA and multiple co-inertia analysis (MiBiOmics) (Fig. 5c) was also performed, and most of the breast related annotations were found by all three methods. However, DIABLO extracted several proteins associated to additional terms related to different stage of breast cancer evolution, while multi-WGCNA extracted the highest proportion of breast cancer related proteins compare to other pathologies.

This comparison of disease related annotations of extracted features showed the complementarity of the three methods. While the analyses extracted mostly different features related to tumor type, all of them were found highly predictive of the tumor subtype and were often associated to the same disease. Features extracted exclusively by one of the three method also participated in the enrichment of specific breast cancer stage annotations, and highlighted the potential of these methods in complementing each other in the analysis and characterization of multi-omics associations. We also evaluated the potential of each method to extract mRNAs, miRNAs, and proteins related to breast cancer annotations by computing the accuracy, recall, and F1-score for each method and each omics data type (See Additional file 1 and Additional file 1: Table S1). The performance of each method was found dependent of the nature of the data and both pipelines performed differently in terms of accuracy to extract features associated to breast cancer. Overall, the multi-WGCNA approach was found more accurate with regards to the mRNA features extraction associated to breast cancer, while DIABLO was found more accurate in extracting proteins associated to breast cancer (Additional file 1: Table S1).

Overall, MiBiOmics provides two complementary methods to extract associated variables between omics layers and in relationship with a trait of interest. Both multi-WGCNA and multiple co-inertia analyses highlighted specific protein biomarkers that were not identified by DIABLO. For example, both multi-WGCNA and multiple co-inertia analyses highlighted specific annotations related to male disposition in breast cancer

or basal-like phenotype of breast tumor. A more specific example is the identification of the SYK protein only by the multi-WGCNA method. The SYK protein appears to have a dual role: depending on the alternative splicing of the mRNA it may act as a pro-oncogene or a tumor suppressor protein, and can interact differentially with its targeted genes [25]. The mechanisms surrounding this dual role of the SYK protein are still being largely studied [26]. Here, the multi-omics hive plots and bi-partite networks provided by MiBiOmics can be useful to generate new hypothesis on the associations and potential interactions between SYK and specific genes and miRNAs linked in the multi-omics network. While MiBiOmics may be useful to generate new hypotheses about molecular processes, it cannot infer causal mechanisms between omics features and phenotypes. This would require experimental validations, which can actually be guided by MiBiOmics results. To provide an exploratory and integrative framework for multi-omics studies, MiBiOmics distinguishes itself by providing a powerful dimensionality reduction and unsupervised method combining both ordination and graph-based techniques, which enables to study complex biological systems as a whole. Importantly, it also integrates contextual information by linking multi-omics signatures to qualitative and quantitative contextual parameters.

Conclusion

MiBiOmics is an interactive web-based (and standalone) application to easily and dynamically explore associations across omics datasets. Through an innovative network-based integrative strategy, it can help biologists to identify putative mechanisms of interactions and generate novel hypotheses. The core of the application lies behind the reduction of dimensionality across omics datasets to efficiently link them at the molecular level, and to identify biomarkers associated with a given trait or phenotype. The MiBiOmics pipeline facilitates the exploration, integration, and analysis of multi-omics datasets to a broad audience by providing scientists a powerful way to predict and explore putative molecular mechanisms underlying complex phenotypes across a wide range of biological scales and systems.

Availability and requirements

Project name: MiBiOmics

Project home page: https://gitlab.univ-nantes.fr/combi-ls2n/mibiomics

Operating system(s): Platform independent

Programming language: R

Other requirements: for the local installation Conda 4.6.12 or Docker

License: AGPL-3

Any restrictions to use by non-academics: No restrictions

Supplementary Information

The online version contains supplementary material available at https://doi.org/10.1186/s12859-020-03921-8.

Additional file 1. Supplementary material (methods, table S1, and figure S1).

Abbreviations
ASV: Amplicon sequence variant; AUC: Area under the curve; DGN database: Disease gene network database; DIABLO: Data integration analysis for biomarker discovery using latent variable approaches for omics studies; OPLS: Orthogonal partial least square; OTU: Operational taxonomic unit; PCA: Principal component analysis; PCoA: Principal coordinates analysis; sPLS-DA: Sparse partial least square discriminant analysis; TCGA database: The cancer genome atlas database; VIP: Variable importance projection; WGCNA: Weighted gene correlation network analysis.

Acknowledgements
The authors wish to thank Mélanie Fouesnard, Damien Eveillard, Philippe Bordron, Gaëlle Boudry, Catherine Michel and Simon Beck for their useful feedback while testing and using the application. We also thank the bioinformatics core facility of Nantes (BiRD—Biogenouest) for providing computing resources and support.

Authors' contributions
JZ and SC participated equally in the design and development of MiBiOmics as a standalone web-application and writing the manuscript. MN contributed to the writing of the manuscript. JFG was responsible for the distribution and maintenance of MiBiOmics webserver at https://shiny-bird.univ-nantes.fr/app/Mibiomics. All authors read and approved the final version of the manuscript.

Funding
This work has received financial support from the Region Pays de la Loire (MiBioGate 2016-11179 to M.N.), the French National Institute of Health and Medical Research, and the CNRS through the MITI interdisciplinary program ***Modélisation du Vivant*** [GOBITMAP to S.C.].

Availability of data and materials
The datasets provided as example within MiBiOmics application are available in the data repository, at https://gitlab.univ-nantes.fr/combi-ls2n/mibiomics.

Ethics approval and consent to participate
Not applicable.

Consent for publication
Not applicable.

Competing interests
The authors declare that they have no competing interests.

Author details
[1] INSERM, TENS, Université de Nantes, Nantes, France. [2] CHU Nantes, Inserm, CNRS, SFR Santé, Inserm UMS016, CNRS UMS 3556, Université de Nantes, 44000 Nantes, France. [3] CNRS UMR6004, LS2N, Université de Nantes, 44000 Nantes, France. [4] Research Federation (FR2022) Tara Oceans GO-SEE, Paris, France.

Received: 26 June 2020 Accepted: 2 December 2020
Published online: 06 January 2021

References
1. Chakraborty S, Hosen MI, Ahmed M, Shekhar HU. Onco-multi-OMICS approach: a new frontier in cancer research. BioMed Res Int. 2018;2018:9836256. https://doi.org/10.1155/2018/9836256.
2. Subramanian I, Verma S, Kumar S, Jere A, Anamika K. Multi-omics data integration, interpretation, and its application. Bioinform Biol Insights. 2020;14:7–9.
3. Hasin Y, Seldin M, Lusis A. Multi-omics approaches to disease. Genome Biol. 2017;18:1–15.
4. Li Y, Wu F-X, Ngom A. A review on machine learning principles for multi-view biological data integration. Brief Bioinform. 2016. https://doi.org/10.1093/bib/bbw113.
5. Heintz-Buschart A, May P, Laczny CC, Lebrun LA, Bellora C, Krishna A, et al. Integrated multi-omics of the human gut microbiome in a case study of familial type 1 diabetes. Nat Microbiol. 2016;2:1–12. https://doi.org/10.1038/nmicrobiol.2016.180.
6. Zhang B, Gaiteri C, Bodea LG, Wang Z, McElwee J, Podtelezhnikov AA, et al. Integrated systems approach identifies genetic nodes and networks in late-onset Alzheimer's disease. Cell. 2013;153:707–20. https://doi.org/10.1016/j.cell.2013.03.030.
7. Chen R, Mias GI, Li-Pook-Than J, Jiang L, Lam HYK, Chen R, et al. Personal omics profiling reveals dynamic molecular and medical phenotypes. Cell. 2012;148:1293–307. https://doi.org/10.1016/j.cell.2012.02.009.
8. Paliy O, Shankar V. Application of multivariate statistical techniques in microbial ecology. Mol Ecol. 2016;25:1032–57.
9. Jang Y, Yu N, Seo J, Kim S, Lee S. MONGKIE: an integrated tool for network analysis and visualization for multi-omics data. Biol Direct. 2016;11:1–9. https://doi.org/10.1186/s13062-016-0112-y.
10. Chong J, Soufan O, Li C, Caraus I, Li S, Bourque G, et al. MetaboAnalyst 4.0: towards more transparent and integrative metabolomics analysis. Nucleic Acids Res. 2018;46:W486–94.
11. Shu L, Zhao Y, Kurt Z, Byars SG, Tukiainen T, Kettunen J, et al. Mergeomics: Multidimensional data integration to identify pathogenic perturbations to biological systems. BMC Genomics. 2016;17:1–16. https://doi.org/10.1186/s12864-016-3198-9.
12. Rohart F, Gautier B, Singh A, Lê Cao KA. mixOmics: an R package for 'omics feature selection and multiple data integration. PLoS Comput Biol. 2017;13:1–19.

13. Guidi L, Chaffron S, Bittner L, Eveillard D, Marin M, De RSB. Plankton networks driving carbon export in the oligotrophic ocean. Nature. 2016;532:465–70.
14. Network CGA. Comprehensive molecular portraits of human breast tumours. Nature. 2012;490:61–70.
15. Sunagawa S, Coelho LP, Chaffron S, Kultima JR, Labadie K, Salazar G, et al. Ocean plankton. Structure and function of the global ocean microbiome. Science (New York, NY). 2015;348:1261359. https://doi.org/10.1126/science.1261359.
16. Mariette J, Villa-vialaneix N. Integrating TARA oceans datasets using unsupervised multiple kernel learning. bioRxiv. 2017; 1–16. https://doi.org/10.1101/139287.
17. Dixon P. VEGAN, a package of R functions for community ecology. J Veg Sci. 2009;14:927–30.
18. Langfelder P, Horvath S. WGCNA: an R package for weighted correlation network analysis. BMC Bioinform. 2008;9:599.
19. Wehrens R, Bjørn-Helge M. The pls package: principal component and partial least squares regression in R. J Stat Softw. 2007;18:1–24.
20. Meng C, Kuster B, Culhane AC, Gholami AM. A multivariate approach to the integration of multi-omics datasets. BMC Bioinform. 2014.
21. Sundararajan Z, Knoll R, Hombach P, Becker M, Schultze JL, Ulas T. Shiny-Seq: advanced guided transcriptome analysis. BMC Res Notes. 2019;12:432. https://doi.org/10.1186/s13104-019-4471-1.
22. Xiao X, Moreno-Moral A, Rotival M, Bottolo L, Petretto E. Multi-tissue analysis of co-expression networks by higher-order generalized singular value decomposition identifies functionally coherent transcriptional modules. PLoS Genet. 2014;10:e1004006.
23. Seyfried NT, Dammer EB, Swarup V, Nandakumar D, Duong DM, Yin L, et al. A multi-network approach identifies protein-specific co-expression in asymptomatic and symptomatic Alzheimer's disease. Cell Syst. 2017;4(60–72):e4. https://doi.org/10.1016/j.cels.2016.11.006.
24. Singh A, Gautier B, Shannon CP, Vacher M, Rohart F, Tebbutt SJ, et al. DIABLO: an integrative approach for identifying key molecular drivers from multi-omics assays. Bioinformatics. 2019;35:3055–62.
25. Krisenko MO, Geahlen RL. Calling in SYK: SYK's dual role as a tumor promoter and tumor suppressor in cancer. BBA Mol Cell Res. 2015;1853:254–63. https://doi.org/10.1016/j.bbamcr.2014.10.022.
26. Lamb DJ, Rust A, Rudisch A, Glüxam T, Harrer N, Machat H, et al. Inhibition of SYK kinase does not confer a pro-proliferative or pro-invasive phenotype in breast epithelium or breast cancer cells. Oncotarget. 2020;11:1257–72.
27. Dolédec S, Chessel D. Co-inertia analysis: an alternative method for studying species–environment relationships. Freshw Biol. 1994;31:277–94.
28. Yu G, Wang LG, Han Y, He QY. ClusterProfiler: an R package for comparing biological themes among gene clusters. OMICS. 2012;16:284–7.
29. Piñero J, Ramírez-Anguita JM, Saüch-Pitarch J, Ronzano F, Centeno E, Sanz F, et al. The DisGeNET knowledge platform for disease genomics: 2019 update. Nucleic Acids Res. 2020;48:D845–55.

Publisher's Note

Supplementary information for:

MiBiOmics: An interactive web application for multi-omics data exploration and integration

Johanna Zoppi, Jean-François Guillaume, Michel Neunlist and Samuel Chaffron.

Details about multi-omics data analysis methodologies we compared in the article (Figure 4) are described below. Both methods implemented in MiBiOmics (multi-WGCNA and multiple co-inertia) were compared to DIABLO [1] integrated in the mixOmics R package.

mixOmics DIABLO

We performed a DIABLO analysis on the whole breast TCGA dataset to extract multi-omics features associated to the tumor subtype parameter. Following the DIABLO tutorial [1], we choose a design where all the omics blocks (mRNA, miRNA and proteins) are connected with a link of 0.1. For selecting the final model we choose the centroid distance with 4 components, and identified an optimum number of extracted features per components using the function tune.block.plsda. A total of 203 non-redundant features were selected using this protocol, which we compared with both methods implemented in MiBiOmics.

MiBiOmics multi-WGCNA

For the integration of multi-omics datasets, MiBiOmics allows the inference of multi-layer networks based on the WGCNA methodology developed by Langfelder and Horvath in 2008 [2]. This multilayer network is built by detecting significant associations between WGCNA subnetworks or modules delineated for each omics dataset. In addition, association to contextual information is also integrated by detecting modules of the multi-layer network significantly associated to a given trait or phenotype. To extract multi-omics features associated to a contextual parameter of interest (here the tumor subtype in the TGCA dataset), the following protocol was implemented:

- WGCNA signed networks are inferred for all omics datasets (miRNA, mRNA and protein datasets). Here, we used a biweight midcorrelation (or bicor), and choose soft powers of 16, 8 and 10 with a minimum module size of 4, 6 and 4 for the miRNA, mRNA and protein datasets, respectively. For these parametrization steps (soft power and minimum module size), we strongly advise users to follow protocols and instructions associated to the WGCNA article [2].

- Modules associated to our trait of interest (tumor subtype) were selected based on the Spearman correlation (and associated p-value) between the parameter and the modules eigenvalue (abs(cor.) > 0.5 and p-value < 0.001). Based on these criteria, three modules were selected: the mRNA red and turquoise modules, and the protein green module.

- Starting from this first set of modules we delineated a group of modules significantly associated together. The hive plot in the MiBiOmics 'multi-omics analysis' section allows to visualize how eigenvalues of each module correlate to each other across omics layers. This step allows to detect significant associations between modules and thus between omics layers. Here, we selected modules associated to the first set of modules directly associated to the trait of interest (the red and turquoise from the mRNA network, and the green from the protein dataset; Spearman abs(cor.) > 0.5 and p-value < 0.001. Using this procedure, we obtained a multi-layer network or network of modules associated to a given

trait. At this stage, the following additional modules were selected: blue and turquoise from the miRNA network, brown, red and turquoise from the mRNA network and blue and green from the protein network.

- For each module, the list of features, their VIP scores, correlations to the subtype parameter and associated p-value were downloaded via the 'Network Exploration' tab, after setting the appropriate number of components for each sPLS-DA (the optimum number of components is identified by the first minimum local on the Root Mean Square Error of Prediction (RMSEP) plot.

- Given some modules may contain many features, we selected these features weighted by their importance in the module (based on the VIP score), and their association to the parameter of interest (tumor subtype). Here, we selected only features that obtained a VIP score above 1 and an associated p-value below 0.05.

Using this protocol, 308 features were selected across the mRNA, miRNA and protein datasets to be significantly related together and/or associated to the tumor subtype.

MiBiOmics multiple co-inertia

Using the TGCA multi-omics dataset, we performed a multiple co-inertia as implemented in MiBiOmics with the ade4 R package, and extracted drivers on the first axis of co-variance (we selected the first axis of the multiple co-inertia along which samples were ordered according to their respective subtype). These drivers or features are ranked according to how much they participate to the co-variance on this axis. Here, we selected the top 30% features with the highest absolute score in the first axis of the total covariance.

Following this procedure, a total of 272 multi-omics features were extracted.

Comparing the predictive power of each method

In order to compare the capacity of these methods to extract features associated to a parameter of interest we performed a Sparse Partial Least Squares Discriminant Analysis (sPLS-DA) using each method features associated to the tumor subtypes using the mixOmics plsda function. The appropriate number of components was chosen using the recommended value of the perf mixOmics function and the more accurate distance metric (the selected number of components for the sPLS-DA was 6, 7 and 3 for the multiple co-inertia, multi-WGCNA and DIABLO features, respectively). The AUC was computed, and ROC curves were plotted for each sPLS-DA (Figure S1) to estimate and compare the predictive power of each method according to the tumor subtype parameter. The AUC indicated a strong predictive power for all three methodologies (DIABLO-AUC = 0.973, multi-WGCNA-AUC = 0.999, multiple co-inertia-AUC = 0.990) but using distinct extracted features.

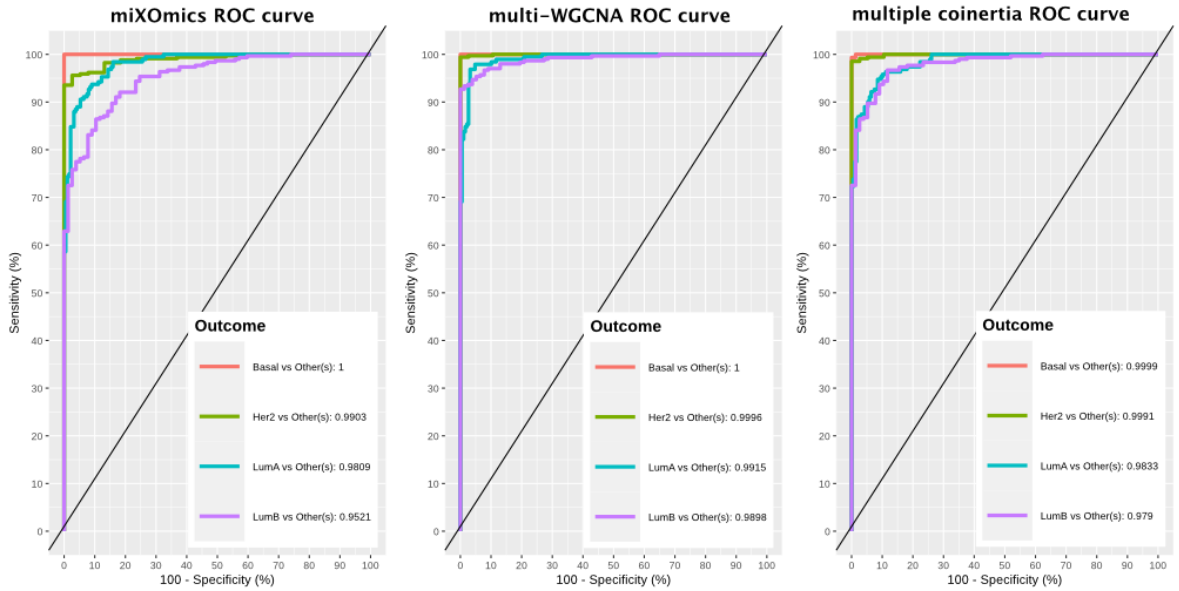

Figure S26 : Predictive power of DIABLO (mixOmics), multi-WGCNA (MiBiOmics) and multiple coinertia (MiBiOmics) for the tumor subtype parameter of the TCGA dataset. ROC curves and AUC were obtained using sPLS-DA models built using extracted features associated to the tumor subtype parameter by the three methods (DIABLO from mixOmics, multi-WGCNA and multiple co-inertia from miBiOmics).

Comparing the extracted biological features and their relation to breast cancer subtype

Because each set of extracted features was found highly correlated to the breast cancer subtype and still different from each other, we analyzed their implication and relationship relative to breast cancer. For this analysis, we used the DGN (Disease Gene Network) database assisted with the ClusterProfiler R package for the functional enrichment and visualization tools. For the mRNA and protein extracted sets, we recovered the corresponding entrezID and performed a functional enrichment independently on the subsets of mRNAs and proteins extracted by each method (DIABLO mixOmics, multi-WGCNA MiBiOmics, and multiple coinertia analysis MiBiOmics). For the miRNA, we first recovered their targeted genes and ran the analysis on the entrezID of these targeted genes.

We described the accuracy of each method by looking at the number of breast cancer related terms compare to the total number of pathology annotations recovered by each method. We also calculated a score to evaluate the precision and sensibility of each method:

	Condition Positive	Condition Negative
Predicted condition positive	**True Positive:** mRNA/miRNA/Protein **contributes** to at least to one breast cancer associated term and **was extracted** by the method.	**False Positive:** mRNA/miRNA/Protein **does not contribute** to at least to one breast cancer associated term and **was extracted** by the method.

Predicted condition negative	**False Negative:** mRNA/miRNA/Protein **contributes** to at least to one breast cancer associated term and **was not extracted** by the method.	**True Negative:** mRNA/miRNA/Protein **does not contribute** to at least to one breast cancer associated term and **was not extracted** by the method.

$$F1 - score = \frac{True\ Positive}{True\ Positive + {}^{1}/_{2}\,(False\ Positive + False\ Negative)}$$

$$Accuracy = \frac{\sum True\ Positive + \sum True\ Negative}{\sum Total\ Population}$$

$$Recall = \frac{\sum True\ Positive}{\sum Condition\ Positive}$$

The resulting F1-score, accuracy and recall values are listed below:

Table 2 F1 score, accuracy and recall to evaluate the associations between the extracted features by each tools (DIABLO mixOmics, multi-WGCNA and multiple coinertia MiBiOmics) and breast cancer annotations.

		DIABLO mixOmics	Multi-WGCNA	Multiple coinertia
F1 score	mRNA	0	0.17	0.08
	miRNA (targeted genes)	0.31	0.31	0.29
	Protein	0.54	0.13	0.20
Accuracy	mRNA	0.77	0.72	0.73
	miRNA (targeted genes)	0.20	0.27	0.33
	Protein	0.55	0.39	0.41
Recall	mRNA	0	0.15	0.07
	miRNA (targeted genes)	0.99	0.94	0.86
	Protein	0.39	0.07	0.11

References

1. Singh, A., Gautier, B., Shannon, C.P., Vacher, M., Rohart, F., Tebbutt, S.J., Lê Cao, K.A.: DIABLO: anintegrative approach for identifying key molecular drivers from multi-omics assays. Bioinformatics35(17),3055–3062 (2019)

2. Langfelder, P., Horvath, S.: WGCNA: An R package for weighted correlation network analysis. BMCBioinformatics (2008). doi:10.1186/1471-2105-9-559

Article 2: Multi-omics and functional characterization of psychological stress induced modulation of microbiota host-interactions in colonic epithelial cells

RESUME FRANÇAIS DU DEUXIEME ARTICLE

Le stress psychologique (SP) chronique est de plus en plus reconnu comme un facteur clé contribuant à l'apparition et à l'évolution des maladies chroniques. Il est associé de manière récurrente à des maladies affectant l'intestin comme le syndrome du côlon irritable (SCI) [1, 2], mais aussi aux maladies inflammatoires de l'intestin (MII) [3], aux allergies alimentaires [4] et plus récemment au cancer colorectal (CCR) [5, 6], mais aussi à d'autres organes comme le cerveau dans la sclérose en plaques [7]. Par conséquent, une meilleure compréhension des mécanismes qui sous-tendent les effets des PS sur les maladies chroniques a des effets thérapeutiques majeurs. En particulier, il convient de caractériser les effets des SP à la frontière entre le stress aigu et le stress chronique, où la charge allostatique (l'effet cumulatif des événements de stress sur la physiologie de l'organisme [8]) déclenche des anomalies de la réponse physiologique [9].

Il a été suggéré que les effets délétères du SP dans les maladies chroniques sont médiés, en partie, par des altérations des fonctions de la barrière épithéliale intestinale (BEI) telles qu'une perméabilité paracellulaire ou transcellulaire accrue [10, 11] et/ou des propriétés altérées du mucus [12]. Ces altérations sont considérées comme favorisant le passage d'agents luminaux (antigènes, LPS...) à travers la BIE qui, à son tour, favorise l'induction ou le maintien d'une inflammation intestinale ou systémique de bas grade contribuant négativement à l'évolution ou à l'apparition de la maladie [13]. De manière cohérente, les approches visant à restaurer ou à améliorer la perméabilité de la barrière ont démontré leur intérêt thérapeutique dans la prévention ou le traitement des maladies induites par le stress psychologique [14, 15]. Des modifications de la perméabilité de la BIE induites par le SP ont été signalées dans diverses régions de l'intestin. Par exemple, le stress de contention a augmenté la perméabilité paracellulaire dans le jéjunum de rats Wistar [16], un effet reproduit par le protocole de stress d'évitement de l'eau (WAS) dans le même organe [11], mais pas dans une expérience plus récente où seule la perméabilité paracellulaire colique a été impactée alors que la perméabilité paracellulaire jéjunale est restée identique chez les témoins et les rats soumis au WAS. Dans un modèle de souris soumis au protocole WAS, la perméabilité paracellulaire était augmentée dans le jéjunum, l'iléon et le côlon par rapport au contrôle [17]. Les divergences observées

entre les études et les modèles de rongeurs suggèrent des effets fonctionnels et moléculaires spécifiques à chaque région [18]. Dans l'ensemble, les changements induits par les PS semblent être spécifiques à chaque région de l'intestin et ces changements fonctionnels, outre la perméabilité, restent à décrire et à comprendre. En outre, il reste à déterminer si les SP induisent un remodelage transcriptomique des cellules épithéliales intestinales spécifique à chaque région et qui explique les changements fonctionnels.

En effet, outre les changements de perméabilité, l'impact des PS sur d'autres processus homéostatiques clés de l'IEB, tels que la prolifération, la mort ou la différenciation cellulaire, peut contribuer collectivement à l'altération de la perméabilité [19] et est encore largement inconnu. Il est intéressant de noter que des études précédentes ont montré que les PS pouvaient moduler la prolifération cellulaire en fonction du type de stress effectué (aigu ou chronique) et de la région intestinale étudiée. Par exemple, le test de nage forcée aiguë a induit une augmentation de la prolifération cellulaire dans le jéjunum [20], tandis que le test de contrainte par le froid et les chocs électriques répétés ont réduit la prolifération cellulaire dans toutes les régions de l'intestin grêle (duodénum, jéjunum et iléon) [21, 22]. Plus récemment, il a été démontré que le WAS répété augmentait la prolifération cellulaire dans l'iléon [23]. Cependant, la réponse du côlon aux premiers stades du PS chronique en termes de prolifération des cellules épithéliales et de mort cellulaire reste actuellement largement inconnue, tout comme les voies impliquées dans ces effets putatifs.

En plus d'agir directement sur les cellules de l'hôte, de plus en plus de preuves suggèrent que les effets des PS sur les dysfonctionnements intestinaux sont médiés, au moins en partie, par le microbiote intestinal [24, 25]. On a constaté que les SP chroniques modifiaient la diversité et la composition bactériennes globales dans les régions iléale, cæcale, colique et dans les fèces [26-31]. Ces études ont révélé que, bien qu'aucun changement n'ait été signalé au niveau des embranchements [26, 28-34], des changements se sont produits dans l'abondance relative de familles bactériennes telles que Coriobacteriaceae, Lachnospiraceae, Porphyromonadaceae, Enterobacteriaceae, Peptococcaceae ou des genres (par exemple, Dorea, Pseudobutyrivibrio, Alistipes, Parasutterella, Romboutsia, Butyricicoccus). Si les changements microbiens liés au stress dans l'intestin sont de mieux en mieux caractérisés dans les différentes régions de la lumière intestinale [26, 28-34], on ignore actuellement si des changements bactériens se produisent aux premiers stades du stress chronique. En outre, les résultats peuvent difficilement être comparés en raison de la différence de stress et de protocole expérimental [35, 36]. Les modifications induites par le PS dans la composition et la diversité bactérienne associée à l'épithélium restent rares avec une seule étude montrant une diminution de la β-diversité du microbiote associé à la muqueuse colique [37]. En outre, l'impact simultané des PS sur le microbiote associé à la fois à la lumière et à l'épithélium et leur interaction avec la réponse épithéliale de l'hôte restent encore largement inconnus.

Compte tenu de la capacité des SP à induire des changements fonctionnels distincts et multiples (perméabilité, prolifération) chez l'hôte, mais aussi de leur capacité à modifier la composition du microbiote tant luminal qu'associé à l'épithélium, un effort important reste à faire pour identifier des signatures intégratives putatives associant les microbes intestinaux à la réponse transcriptomique et fonctionnelle de l'épithélium, suggérant des liens de causalité. Des stratégies multi-omiques ont récemment été développées par de grands consortiums pour étudier l'interaction entre l'hôte et le microbiote dans l'apparition des maladies inflammatoires

de l'intestin ou du diabète de type 2 [38]. Cependant, à notre connaissance, ces approches n'ont pas été utilisées pour étudier l'impact des SP sur l'"associatome" régional hôte-microbiote. En outre, ces approches restent limitées par l'absence de méthodes et d'outils de référence permettant l'intégration et l'analyse générales d'ensembles de données multi-omiques, afin d'identifier la signature corrélative entre l'hôte et son microbiote associé [39]. Cependant, de telles approches pourraient servir de base à l'identification de signatures bactériennes prédictives associées au remodelage fonctionnel ciblé des organes induit par le PS chronique. Ces signatures multi-omiques pourraient nous aider à identifier de nouvelles cibles thérapeutiques dans les caractéristiques de l'hôte et du microbiote pour la prévention des dysfonctionnements des BEI induits par les SP.

Par conséquent, en combinant des études in vivo et des organoïdes avec des outils d'analyse bioinformatique, nous avons cherché à caractériser l'impact des SP sur la réponse fonctionnelle et transcriptomique de l'épithélium intestinal et ses interactions avec la composition du microbiote et le remodelage fonctionnel induits par les SP.

Title: Multi-omics and functional characterization of psychological stress-induced modulation of microbiota host-interactions in colonic epithelial cells.

Zoppi J[1], Marchix J[1], Bordron P[1], Durand T[1], Bessard A[1], Aubert P[1], Eveillard D[2], Parnet P[3], Aymeric L[1], Mahe M[1], Chaffron S[2,*], Neunlist M[1,*]

[1] Université de Nantes, Inserm, TENS, The Enteric Nervous System in Gut and Brain Diseases, IMAD, Nantes, France

[2] Université de Nantes, CNRS UMR 6004, LS2N, F-44000 Nantes, France

[3] UN, INRAE, UMR 1280, PhAN, IMAD, Nantes, France

*MN and SC equally contributed to this work

Summary:

Chronic psychological stress (PS) is recognized as a critical factor that contributes to the evolution of many chronic diseases in a deleterious fashion. Although PS-induced gut dysfunctions, such as altered intestinal permeability, have been suggested to contribute to deleterious systemic effects, the putative contribution of PS to alterations of other key homeostatic intestinal epithelial barrier (IEB) functions such as cell proliferation, differentiation or cell death remains largely unknown. In this context, we combined *in vivo* multi-omics studies with organoid models to characterize the impact of PS upon the functional and transcriptomic response of gut epithelial cells and its interactions with PS-induced microbiota composition and functional remodeling.

Here we show that repeated acute water avoidance stress (WAS) induces region-specific remodeling of the gut epithelium transcriptome across four intestinal parts (jejunum, ileum, proximal and distal colon), with an upregulation of pro-proliferative/pro-regenerative functions in the distal colon. With *in situ* characterization of cell proliferation and cell death processes, we validated this pro-proliferative response and showed an additional pro-apoptotic profile of the colonic distal epithelium. Organoids grown from stressed mice colonic epithelium were less eccentric and had fewer budding structures than control. PS increased the luminal microbiota diversity and we observed changes in epithelial-associated and luminal microbiota composition. Moreover, the concentration of Short Chain Fatty Acids (SCFAs) in the cecum was significantly decreased. Multi-omics signatures associated with cell proliferation and cell death in the distal colon revealed specific sets of host genes, implicated in microtubule destabilization, actin structure and antimicrobial resistance, in bi-directional association with luminal and epithelial-associated bacteria in stressed mice. These results support a functional link between the microbiota and cell proliferation as we showed that fecal supernatant of stressed mice induced a significant increase in cell proliferation but not in cell death in HT-29 cell culture.

Altogether our results demonstrate that PS induces a pro-regenerative response driven by combined microbiota and intestinal epithelial transcriptome remodeling. This study set the basis for identifying combined bacteria and host gene targets to prevent PS-induced barrier dysfunctions that are increasingly recognized as key contributors to the evolution of major chronic diseases.

Keywords: Gut biogeography, host-microbiota interactions, multi-omics analysis, acute repeated stress.

Introduction

Chronic psychological stress (PS) is recognized as a critical factor contributing to the onset and evolution of chronic diseases. It is repeatedly associated with diseases affecting the gut, such as Irritable Bowel Syndrome (IBS) [1, 2], Inflammatory Bowel Disease (IBD)[3], food allergies [4], and more recently Colorectal Cancer (CRC) [5, 6], but also other organs such as the brain in multiple sclerosis [7]. Therefore, better understating mechanisms underlying PS effects upon chronic diseases is of major therapeutic interest. In particular, the effects of PS at the acute/chronic stress frontiers where the allostatic load (the cumulative effect of stress events upon body physiology [8]) triggers abnormalities in physiological response [9] need to be further characterized.

The deleterious effects of PS in chronic diseases have been suggested to be mediated, in part, by alterations in intestinal epithelial barrier (IEB) functions such as increased paracellular or transcellular permeability [10, 11] and/or altered mucus properties [12]. These alterations are considered to favor the passage of luminal agents (e.g., antigens, LPS) across the IEB , which favors the induction or maintenance of low grade intestinal or systemic inflammation contributing negatively to disease evolution or onset [13]. Consistently, approaches aimed at restoring or enhancing barrier permeability have demonstrated therapeutical interest in the prevention or treatment of diseases induced by psychological stress [14, 15]. Changes in IEB permeability induced by PS have been reported to occur in various regions of the gut. For instance, restraint stress increased paracellular permeability in the jejunum of Wistar rats [16], an effect reproduced by Water Avoidance Stress (WAS) protocol in the same organ [11], but not in a more recent experiment where only the colonic paracellular permeability was impacted [17]. In a mice model subjected to WAS protocol, the paracellular permeability was increased in the jejunum, ileum, and colon as compared to control [18]. Altogether, changes induced by PS appear to be gut region-specific, and these functional changes, besides permeability, remain to be described and understood. Furthermore, whether PS induces region-specific transcriptomic remodeling of intestinal epithelial cells that account for functional changes remain to be explore.

Indeed, besides changes in permeability, the impact of PS upon other key IEB homeostatic processes such as cell proliferation, cell death or cell differentiation can collectively contribute to altered permeability [19] and are still largely unknown. Previous studies showed that PS could modulate cell proliferation depending on the type of stress performed (acute vs chronic) and the gut region studied. For instance, acute force swim test induced an increase in cell proliferation in the jejunum [20], while cold restraint test and repeated electric shock reduced cell proliferation in all small intestine regions (duodenum, jejunum, and ileum) [21, 22]. More recently, repeated WAS was shown to increase cell proliferation in the ileum [23]. However, the response of the colon to early stages of chronic PS in terms of epithelial cell proliferation and death, as well as the pathways involved in these putative effects, remain currently largely unknown.

Besides acting directly on host cells, increasing evidence suggests that effects of PS upon gut dysfunctions are mediated, at least in part, by the gut microbiota [24, 25]. Chronic PS was found to alter the overall bacterial diversity and composition in ileal, cecal, colonic regions and in the feces [26–31]. These studies revealed that, although no change was reported at the phylum level [26, 28–34], changes occurred in the relative abundances of bacterial families such as *Coriobacteriaceae*, *Lachnospiraceae*, *Porphyromonadaceae*, *Enterobacteriaceae*, *Peptococcaceae* or genera (e.g., *Dorea*, *Pseudobutyrivibrio*, *Alistipes*, *Parasutterella*, *Romboutsia*, *Butyricicoccus*). While stress related microbial changes in the gut have been previously reported for different regions of the intestinal lumen [26, 28–34], it remains currently unknown whether these bacterial changes occur at the early stages of chronic stress. Moreover, these results can hardly be compared due to the difference in stress and experimental protocol [35, 36]. Modifications induced by PS in the epithelial-associated bacterial composition and diversity remain sparse with only one

study showing a decrease in colonic mucosal-associated microbiota β-diversity [37]. In addition, the simultaneous impact of PS upon both luminal and epithelial associated microbiota and their interaction with the host epithelial response have not been investigated so far.

Given the ability of PS to induce distinct and multiple functional changes (permeability, proliferation) in the host, but also its ability to change microbiota composition of both the luminal and epithelial-associated microbiota, a significant endeavor remains to identify integrative signatures linking gut microbes to epithelial transcriptomic and functional response. Multi-omics strategies have recently been developed to study the crosstalk between host and microbiota in the onset of Inflammatory Bowel Diseases or type 2 Diabetes [38]. However, such approaches, to the best of our knowledge, have not been used to study the impact of PS upon regional host-microbiota interactions. While these approaches remain limited by the lack of gold-standard methods for the integration and analysis of multi-omics datasets to identify host-microbiota signature [39], they can be particularly useful to identify predictive bacterial signatures associated with organ functional remodeling induced by chronic PS. These multi-omics signatures may help us identify novel therapeutical targets in both host and microbial features for the prevention of PS induced IEB dysfunctions. Here, by combining *in vivo* multi-omics characterization with organoids experiments and bioinformatics integration and analysis, we aimed to characterize the impact of PS upon the functional and transcriptomic response of gut epithelial cells, and its interactions with PS induced microbiota composition and functional remodeling.

Material and Methods

Lead contact and materials availability:

Further information or requests concerning data, code, or other resources, should be directed to the lead contacts Michel Neunlist (michel.neunlist@univ-nantes.fr) or Samuel Chaffron (samuel.chaffron@ls2n.fr).

Experimental model and subject details:

Animals

C57BL/6 mice were purchased from Janvier Labs and housed in pathogen-free conditions at the UTE animal facility of the Nantes' Medicine Campus. Experiments were conducted in the same facility on these 8-11 weeks old Male mice with the agreement of the C2EA, the Animal Ethics Committee of the region Pays de la Loire. The referral number for this experiment was 6751. Mice had free access to food and water. They were housed in cages with regulated temperature, humidity and light/dark cycle lasting 12h each. Twenty-four mice (n_{CT}= 12 and n_{WAS}= 12) were used for the *in vivo/ex vivo* functional exploration, and the *in situ* characterization of colonic epithelium realized across three different experimental runs. Twelve mice (n_{CT}= 6 and n_{WAS}= 6) were employed for the extraction and growth of organoids' culture, we collected the cecal content of 24 mice (n_{CT}= 12 and n_{WAS}= 12) to dose the SCFAs concentration and another 24 mice (n_{CT}= 12 and n_{WAS}= 12) for the preparation of fecal water supernatant.

Water avoidance stress

One hour WAS (08 am–09 am) was performed daily after ten days of acclimatization and during four consecutive days. Mice were placed on a platform (diameter, 10 cm; height, 10 cm) positioned at the center of a plastic tank (42 × 42 × 19 cm) filled with water at room temperature up to 1 cm of the top of the platform as seen in a previous study [7].

Functional exploration *in vivo*:

In vivo evaluation of total transit time:

Carmine red, which is not absorbed from the lumen of the gut, was used to study total GI transit time as previously described [40]. A solution of carmine red (60 mg mL−1) suspended in carboxymethyl cellulose sodium salt (CMC) 0.5% (vol/vol) was administered by gavage through a 24-gauge round-tip feeding needle (Fine Science Tools 18061-24). The volume of carmine red solution used for each animal was calculated based on animal weight (0.3 mg g−1). Fecal pellets were monitored at 5 min intervals for the presence of carmine red. Total GI transit time was considered as the interval between the initiation of gavage and the time of first observance of carmine red in stools.

In vivo evaluation of colonic motility:

Each animal was removed from its home cage and placed in a clean, clear plastic cage without food or water for two hours. Fecal pellets were collected immediately after expulsion and placed in sealed tubes. Fecal pellets were counted and weighed to obtain the wet weight of the stool, then dried overnight at 65 °C and weighed again to obtain the dry stool's weight. The percentage of water content was calculated as the difference between the wet and dry stool's weight/100.

In vivo assessment of paracellular permeability and transcellular permeability:

Animals received an oral gavage with 10 mg mL−1 sulfonic acid conjugated with fluorescein (F-SA) diluted in 0.5% (vol/vol) of CMC in EDTA. Blood was collected 10 and 30 min after gavage and plasma was

obtained following centrifugation for 20 min at 2000 g. Fluorescence intensity of the plasma was measured using a plate reader (Multilabel counter, Wallac 1420 Victor: PerkinElmer, Courtaboeuf, France).

Functional exploration ex vivo

Ex vivo evaluation of paracellular and transcellular permeability:

Ex vivo assessment of paracellular and transcellular permeability assessment was estimated from jejunum, ileum, distal colon biopsies mounted in Ussing Chambers. The quantification of F-SA and HRP (horseradish peroxidase) transport across the intestinal barrier was used to evaluate respectively both paracellular and transcellular, respectively, permeability following a previously established protocol [40].

Evaluation of cell proliferation and cell death *in situ*

Tissues collected from the distal colon were dehydrated, embedded in paraffin before being sliced and stained with hematoxylin and eosin to assess the size of the colonic crypt in control and stressed animals. We performed an immunohistoschemistry (IHC) staining with the Ki67 (Abcam, Rabbit polyclonal anti-Ki67, ref: ab15580, dilution: 1/500) and Caspase 3 (Casp3) antibodies (SIGMA Rabbit anti-caspase 3 (active form), ref: C8487, dilution: 1/200) to assess, respectively, the proliferative and apoptotic properties of the distal colonic epithelial barrier.

After cellular permeabilization and the blocking of non-specific sites, tissues were incubated in humid chambers with primary antibodies diluted in a buffer solution (PBS-NaN3 1X-HS) overnight, washed with PBS and incubated with Cy3 secondary antibody (Jackson ImmunoResearch Laboratories, Cy3-conjugated AffinityPure Donkey Anti-Rabbit IgG, red: 711-165-152, dilution: 1/500) diluted in the same buffer solution for two hours. Finally, a DAPI solution diluted 1:1000 (SIGMA reference: D9564) in PBS 1X was added and tissues were covered with Prolong for long-term conservation.

To analyze Ki67 IHC staining, we used the Axiozoom V16 Zeiss to count the number of immunoreactive (IR) cells (with ZEN 2 pro blue edition), and recorded their respective position in the colonic crypts. For Casp3 IHC staining, we measured the intensity profile along the colonic crypts with FIJI (using an in house developed routine), assessed the distribution of Casp3-IR cells along the colonic crypts and counted Casp3-IR cells when the intensity threshold was above a threshold of 3000. The classification of Casp3-IR cells distribution along the crypto-villus axis was realized with the Kohonen R packages (version 2.0.19)

Isolation of colonic crypts and organoids growth:

Organoid's extraction and culture

We isolated the distal colonic crypts of 6 control and 6 stressed mice to follow the growth of distal organoids for three weeks. After the sacrifice, the distal colon of the mice was everted, rinsed three times in PBS, and transferred in a solution of PBS/EDTA for 30min. We, then, performed a manual shaking of the everted colons and separated the intestinal crypts from the remaining tissue by filtering on a 100µm strainer. After a centrifugation step (10min, 4°C and 150g), we removed the supernatant and resuspended the pellet in Matrigel. The colonic crypts suspended in Matrigel were plated in a 24 wells plate with mIS medium and placed in an incubator. The medium was changed every four days for three weeks.

Microscopy and morphological analyses:

We captured organoids growth in 3-dimensional space with the INCELL analyzer 2200 (v7.2) each week. The stitching was realized with Developper Toolbox 1.6.2 and a house developed routine. We realized a Linear Stack Alignment with SIFT and Extended Depth of Field with the easy mode option with FIJI. Eventually we used Organoseq for the identification, contouring and morphological analysis (e.g., area, eccentricity:

($\frac{\sqrt{major\ axis^2 - minor\ axis^2}}{major\ axis}$)) of the organoids present in each well. Only the counting of organoids' buds was performed manually.

Fecal water preparation and exposition to HT-29 cells:

Fecal Water preparation:

The feces collected at the end of 4 days of WAS of 12 control and 12 stressed mice were kept at -80°C. We added HBSS (10mL HBSS for 1g of dry feces) and vortexed the solution. Then, the mixture was centrifuged (3000g at 4°C for 15min) and the supernatant was filtered on a 0.22µm strainer to sterilize the fecal water.

HT-29 cell culture and exposition to fecal supernatant

We plated HT-29 cells (1000 cells per well) in RPMI medium and waited 6 hours before adding the fecal water (diluted at 1/100). We added new fecal water each day during 96H. After fixation of the HT-29 culture, we exposed the cells to Ki67 primary antibody (Abcam, Rabbit polyclonal anti-Ki67, ref: ab15580, dilution: 1/500) and Casp3 primary antibody (SIGMA Rabbit anti-caspase 3 (active form), ref: C8487, dilution: 1/200) diluted in a buffer solution composed of PBS $NaNO_3$, Horse Serum and Triton for three hours. A Cy3 secondary antibody (Jackson ImmunoResearch Laboratories, Cy3-conjugated AffinityPure Donkey Anti-Rabbit IgG, red: 711-165-152, dilution: 1/500) was used and diluted in the same buffer solution for one hour. We eventually used DAPI (SIGMA reference: D9564, dilution: 1/1000) for 5 min to count the total number of cells, the Ki67 and the Casp3 IR cells after 96H of growth.

Microscopy and automated counting routine:

The immunoreactivity to Ki67, Casp3 and DAPI were captured with INCELL analyzer 2200 v7.2. With Python (version 3.7.10), opencv (version 3.4.2) and scikit-image (version 0.17.2), we developed a routine for the identification and contouring of IR cells. After applying a binary threshold, we applied the findContours function of the opencv library and selected the contours with an area above 40 to remove noise generated by cell fragments. After removing outliers with Grubs tests, we compare the number of immunoreactive Casp3, Ki67 and DAPI positive cells after 96h of incubation with the fecal supernatant using individual t-tests between control and stress groups. Data are presented as mean +/-SD.

Dissociation of intestinal epithelial cells.

A 2% isoflurane solution was utilized to anesthetize the animal before the euthanasia by cervical dislocation. The jejunum, ileum, proximal and distal colon were collected with care and conserved in a physiological solution. The luminal microbiota was extracted from each organ by pushing the content of each intestinal segment with a cotton swab in a cryotube and was immediately frozen in liquid nitrogen. Then, the organ tissues were, then, washed with ice-cold PBS to remove the excess of luminal content and incubated in EDTA solution for 30 min on orbital shakers with three interruptions to vortex each tube at full speed. The de-epithelized tissues were removed with forceps to keep only the epithelium which was centrifuged at 3000g for 10 minutes at 4°C. The supernatant was discarded, pellet washed with ice-cold PBS and centrifuged for another 10 minutes at 3000g and 4°C. After removing the supernatant, the pellet is placed in a cryotube with 600µL of RA1 + 1% β-mercaptoethanol and flash-frozen in liquid nitrogen.

RNA extraction, 3'SRP RNA sequencing and data analysis

RNA Extraction and sequencing:

From the extracted epithelium of each organ region, the host transcriptome was extracted with the Micro Rneasy RNA kit from QIAGEN (ref: 74004) and sequenced with the 3'SRP RNA sequencing protocol.

Libraries were prepared from 10ng of RNA after a quality control realized by TapeStation. During the library preparation, specific adapters were added to each mRNA to obtain a quantitative evaluation of the produced transcript by the sample: a well-specific adapter and a unique molecular identifier (UMI). A reverse transcription step followed the barcoding of each transcript. cDNAs were then pooled and purified with the Zymo Kit and amplified following the procedure described in [41]. The sequencing was then realized on an Illumina HiSeq 2500 with the rapid run mode by the Genobird Nantes platform.

Reads (58 basepair long) with a Phred score above 30 were aligned and filtered against Mus Musculus reference transcriptome (mm10) using srp pipeline based on [42] (https://gitlab.univ-nantes.fr/bird_pipeline_registry/srp-pipeline) which utilizes the bwa aligner. Reads showing multiple alignments against the reference genome were removed from the analysis. Samples with a minimum of 5'000 expressed genes and 200'000 assigned reads were analyzed and genes appearing in less than 9 samples were not considered. A count matrix was generated from mapped reads to perform the statistical analyses.

Statistical analysis:

Statistical analyses were performed using R version 4.0.2 or Python version 3.7.

In order to identify differentially expressed genes in each region of the digestive tube (jejunum, ileum, proximal and distal colon), we used the DESeq2 R package strategy (version 1.28.1) [43].The DESeq function was applied on the filtered genes matrix (genes expressed less than ten times across all samples were removed) to detect significant differences in gene expression between control and stressed mice. We corrected the batch effect induced by multiple runs performed during the sequencing using the DESeq formula. Because stress is not a pathological state and notable changes in gene expression were not expected, we selected all genes with a significant p-value after correction for multiple testing using the Benjamini-Hochberg procedure ($p\text{-value}_{adjusted} < 0.05$).

GO terms specific to the intestinal epithelium were obtained using a semantic web approach as described in [44]. We first extracted a set of GO terms and associated genes in the mouse genome, and only considered genes associated with the tissue 'intestinal epithelium' (UBERON_0001277) or the related sub-tissues (see table below) in BgeeDB [45]. We then conducted a standard enrichment analysis with the ontobio package (version 2.7) in python on this set of genes associated with intestinal epithelium specific terms.

Table of Uberon terms used to construct the GO specific intestinal epithelium terms. Each term here is a subclass of the term UBERON_0001277: intestinal epithelium

class	label
http://purl.obolibrary.org/obo/UBERON_0001277	intestinal epithelium
http://purl.obolibrary.org/obo/UBERON_0001278	epithelium of large intestine
http://purl.obolibrary.org/obo/UBERON_0022281	epithelium of crypt of Lieberkuhn of large intestine
http://purl.obolibrary.org/obo/UBERON_0000397	colonic epithelium
http://purl.obolibrary.org/obo/UBERON_0005636	caecum epithelium
http://purl.obolibrary.org/obo/UBERON_0009697	epithelium of appendix
http://purl.obolibrary.org/obo/UBERON_0013695	colon endothelium
http://purl.obolibrary.org/obo/UBERON_0013741	base of crypt of Lieberkuhn of large intestine
http://purl.obolibrary.org/obo/UBERON_0003354	epithelium of rectum
http://purl.obolibrary.org/obo/UBERON_0015716	anal canal epithelium
http://purl.obolibrary.org/obo/UBERON_0013742	wall of crypt of Lieberkuhn of large intestine
http://purl.obolibrary.org/obo/UBERON_0001902	epithelium of small intestine
http://purl.obolibrary.org/obo/UBERON_0013743	base of crypt of Lieberkuhn of small intestine
http://purl.obolibrary.org/obo/UBERON_0013744	wall of crypt of Lieberkuhn of small intestine
http://purl.obolibrary.org/obo/UBERON_0022280	epithelium of crypt of Lieberkuhn of small intestine
http://purl.obolibrary.org/obo/UBERON_0013636	epithelium of intestinal villus
http://purl.obolibrary.org/obo/UBERON_0008345	ileal epithelium

http://purl.obolibrary.org/obo/UBERON_0008346	duodenal epithelium
http://purl.obolibrary.org/obo/UBERON_0005643	foregut duodenum epithelium
http://purl.obolibrary.org/obo/UBERON_0005644	midgut duodenum epithelium
http://purl.obolibrary.org/obo/UBERON_0000400	jejunal epithelium
http://purl.obolibrary.org/obo/UBERON_0004693	Peyer's patch epithelium
http://purl.obolibrary.org/obo/UBERON_0011184	epithelium of crypt of Lieberkuhn
http://purl.obolibrary.org/obo/UBERON_0013739	base of crypt of Lieberkuhn
http://purl.obolibrary.org/obo/UBERON_0013740	wall of crypt of Lieberkuhn
http://purl.obolibrary.org/obo/UBERON_2005126	intestinal bulb epithelium

Luminal and epithelial-associated microbiota 16S rRNA gene amplification, sequencing and statistical analysis

16S rRNA gene sequencing

The luminal microbiota was extracted from each organ by pushing the content of each intestinal segment with a cotton swab in a cryotube and was immediately frozen in liquid nitrogen. For the epithelial-associated content, we used the recovered epithelial tissue in each organ region.

The DNA extraction was performed with the QIAamp PowerFecal DNA (ref: 51804) for the luminal microbiota and with the Duo Powerfecal RNA/DNA (ref: 80244). All samples were quantified with fluorimetry (Qubit® 3.0 Fluorometer, Invitrogen by Life technologies, Carlsbad, CA) and only the ones with more than 1 ng/µL of DNA were kept. A PCR amplification of the hypervariable V3 and V4 regions was realized. Libraries were constructed with the Nextera XT indexes kit, purified on magnetic beads and quantified. After normalization, libraries were denatured and sequenced with the Illumina MiSeq platform with the Miseq V2 kit Miseq for 2 x 250 paired-end by Biofortis Mérieux platform. A multiplexing was realized to reach 50000 raw reads per sample.

Using QIIME2 [46], reads were demultiplexed and a quality control step was realized to trim and truncate the sequences to keep only parts with a Phred score above 30. We used DEBLUR [47] to resolve ASVs (Amplicon Sequence Variants) by sequence denoising, filter predicted chimeras, and removed singletons. A phylogenetic tree was constructed using the mafft program in QIIME2 [48]. For each sequence, the taxonomic assignment was performed using a silva classifier (silva-132-99-nb-classifier) with a confidence level above 0.70. For diversity and differential analysis, we kept epithelial-associated microbiota samples with at least 2500 representative sequences, and luminal microbiota samples with at least 5500 representative sequences. We choose these thresholds to maximize both the number of representative sequences and the number of samples. For statistical analyses we only considered ASVs present in at least 20% of the samples in each organ region to improve statistical power.

Statistical Analysis

We used the DESeq2 R package (version 1.28.1) for differential analysis [49] on relative abundance matrices reconstructed for each organ region and for epithelial-associated and luminal microbiota. The differential analyses were performed at ASVs and Genus taxonomic levels (ASVs belonging to the same genus were grouped together). Using DESeq2 we estimated size factors with the *estimateSizeFactors* function and ran the *DESeq* function with the *poscounts* option, which is more adapted for sparse matrices. We considered taxa to be differentially abundant between control and stressed group when the associated adjusted p-value was below 0.05 (after controlling the FDR using the Benjamini-Hochberg procedure).

Multiple Co-inertia Analysis:

Multiple co-inertia analysis was performed using the R package omicade4 (version 1.28.2) [50] available on the MiBiOmics platform [51] on the common set of samples between the host transcriptome, the luminal

and the epithelial-associated microbiota. To identify the co-variance axis of interest, we identified the axis maximizing the separation of samples with a high proliferative/apoptotic number of cells from a low proliferative/apoptotic number of cells visually. On that axis of covariance, we then extracted drivers with the 10% highest scores. Using this subset of extracted drivers, we performed an Orthogonal Partial Least Square discriminant analysis (OPLS-DA) regression to extract significant features with a VIP score > 1 (Variable Importance Projection or VIP is a measure of variable weight in orthogonal partial least square (OPLS) regression) and significant p-values (p-value < 0.05), significantly contributing to predicting changes in levels of proliferative or apoptotic cells. The functional enrichment of multiple coinertia drivers was realized with the ClusterProfiler R package (version 3.17.4) [52].

Statistical analysis of biological data

Biological data (organoids analysis, cell proliferation *in vitro/in vivo*) were analyzed, (after removing outliers using Grubs tests) using two-way repeated measures ANOVA with adjusted Bonferroni p-values. The analysis compared organoids eccentricity, buddings and area across weeks and conditions. Individual t-tests were performed to compare control and stress group organoids eccentricity, buddings, area, the number of Ki67, Casp3 and the total number of immunoreactive cells in histological slides. Data are presented as mean+/- SD.

Results

Stress modulates intestinal epithelium transcriptome in an organ-specific manner

In a first step, we aimed at determining the transcriptomic response of enriched isolated epithelial cells obtained from mice jejunum, ileum, proximal and distal colon, after an *in vivo* acute repeated WAS period. Using 3'-End RNA sequencing, we showed that, as compared to control, stress induced region-specific changes in gene expression with the most significant changes observed in the small intestine as compared to the colon (Figure 1). In particular, 212 differentially expressed (DE) genes were found in the jejunum (Figure 1A) and 349 genes in the ileum (Figure 1B), while only 50 and 81 genes were found differentially expressed in the proximal (Figure 1C) and distal colon (Figure 1D), respectively. Furthermore, we showed that stress induced a transcriptomic response that was highly region-specific. In particular, in the small intestine, 70% and 78% of DE genes were specific to the jejunum and ileum, respectively. About 10% of DE genes were common to both organs while only about 2% of them were common to either proximal or distal colon. In the colon, 82% and 68% of DE genes were specific to the proximal and distal colon, respectively (Figure 1E). About 2% of DE genes were common to both organs while about 2% of them were common to jejunum and ileum.

Stress induces a pro-proliferative and pro-regenerative transcriptomic response in the distal colon.

Next, an automated gene annotation approach, selecting GO-Term's annotations specific to the gut epithelium was performed (see methods) to identify putative organ specific functions associated with genes potentially modulated by WAS. Interestingly, the distal colon was the organ in which the most significant number of functions were identified to be regulated by WAS as compared to the ileum, jejunum, or proximal colon (Figure 2A). In the distal colon, gene associated functions ranging from the downregulation of mitochondrial processes and aerobic respiration to the upregulation of tight junction protein assembly, cell differentiation and fatty-acid beta oxidation, were associated to the stress response (Figure 2B). In the jejunum, RNA processing functions were upregulated by stress while mitochondrial assembly and neuron-neuron synaptic transmission were downregulated in the ileum, as compared to control. No modification in any biological functions was reported in the proximal colon following GO term analysis (Figure 2B).

To gain more precise insights into putative functions regulated at the gene level in the distal colon, we performed a manual annotation of genes modulated by stress using published work and, especially, in articles referring to colonic and intestinal epithelium (Table 1 & Supplementary Table 1). Using this approach, we showed that 60 % of DE genes were associated with functions previously identified using the automated functional enrichment, while 21.2 % were associated with other functions related to epithelial homeostasis (e.g., cell death, cell migration). Finally, 18.4% of genes were unrelated to intestinal epithelial homeostasis function (e.g., ER-Golgi Trafficking, Protein, Amino Acids Transport), and 7.4% of genes had unknown associated functions.

The most extensive sets of genes, representing 55% of differentially expressed (DE) genes in stress, were associated with regulation of cell proliferation, differentiation and cell death, and migration, all critical processes involved in the regulation of intestinal barrier homeostasis. More specifically, about 16% of DE genes favored cell proliferation and were upregulated by stress, and 3.7% (Gptx1, Hoxb13 and Ap1m2) were inhibitors of cell proliferation and were downregulated by stress as compared to control. In particular, many genes were involved in the regulation of the Wnt/β-catenin pathway such as Pik3CA, Tnks2, Cpt1a, Setd2, Hoxb13, and Ptprd. We also found genes involved in the regulation of cell cycle, regulating cyclins (Med13L, Birc6) or checkpoints between cell cycle phases (Dpy30, Thoc2). 7,4 % of the genes were inhibitors of cell death and upregulated by stress. They are involved in the negative regulation of STAT proteins (A130077B15Rik, Nipbl) or Wnt/β-catenin (Zo-2). About 4,9% of the DE genes promoted cell migration (Arap2, Herc1, Nipbl and Rapgef6), while 2,5 % inhibited this process (Larp4b, Ptprd), and two upregulated genes

promoted wound healing (Rock 1 and Rock 2). Genes regulating intestinal epithelial permeability functions were also differentially expressed. In particular, Zo-2, Gcc2 were upregulated, while Rnf186 was downregulated, contributing theoretically together to the reduction of paracellular permeability following stress. Finally, cell adhesion genes were also DE by stress as Lmo7 and Rapgef6, constituent of adherens junctions were upregulated.

The second largest set of DE genes was constituted by activators of mitochondrial energy metabolism. All DE genes were downregulated by PS (13,5 % of DE genes). Most of them are part of the mitochondrial electron transport chain (Uqcrc1, Uqcrh) or more precisely the ATP synthase (Atp5d, Atp5j2, Atp5k, Atp5l). PS also impacted β-oxydation with 6,2% of DE genes impacted: 3.7% were downregulated by PS (Acat1, Cyb5r3, Fabp1), and 2,5% were upregulated by PS (Acadl, Cpt1a).

Stress modulates epithelial cells and barrier functions in the distal colon

We next aimed at determining whether pro-proliferative and pro-regenerative transcriptomic responses were associated with functional changes in the distal colon. First, we analyzed putative changes in colonic morphology in animals following stress as compared to control. No changes in crypt height (Figure 3K) nor intestinal epithelial cell density were induced by repeated acute stress. In contrast, using Ki67 to identify proliferating cells, we showed that repeated acute stress induced a significant 1,43-fold increase in the proportion of Ki67-IR cells (n_{CT} = 8, n_{WAS} = 12, p-value = 0,015; Figure 3I). In addition, the proportion of Ki67-IR cells was significantly positively correlated to the level of corticosterone in mice serum (Figure 3M). Concomitantly, changes in cell proliferation were associated with a significant increase in the proportion of active Casp3-IR epithelial cells (n_{CT} = 9, n_{WAS} = 11, p-value = 0,034). Also, the distribution of Casp3-IR cells along colonic crypts was altered by stress as compared to control. While in control mice Casp3-IR cells were mostly positioned at the top of crypts, no preferential distribution of Casp3-IR cells was observed in stressed mice, and they were more often positioned at crypt bases (Supplementary figure 1). To determine whether these cellular changes were associated with functional changes in colonic permeability, we investigated distal colon permeability using Ussing chambers (Supplementary figure 2C) and showed that stress significantly reduced permeability to F-SA. Interestingly, we showed that ASF flux across ileal mucosa was not altered in stressed animals as compared to controls (Supplementary figure 2B).

Stress modulates morphological parameters of colonic organoids derived from stressed animals as compared to control

In order to further explore functional changes in intestinal epithelial homeostasis induced by stress, we generated organoids derived from distal colonic crypts of stressed and control mice. Organoids grew in Matrigel and culture medium for 3 weeks (Figure 4A). Organoids morphological changes were analyzed weekly using an INCELL analyzer. First, organoids derived from stressed or control animals had a significant increase in their area between the first and the second week of culture (Figure 4C). While organoids derived from control mice showed a significant increase in the budding structure number over time, their number remained unchanged in organoids derived from stressed mice (Figure 4E). We also assessed organoids eccentricity as a measure of roundness, as it is a prominent morphological feature previously used to distinguish different phenotypes of organoids (e.g., enterocysts, mature organoids, regenerative organoids) [53]. We showed that control mice derived organoids displayed a significant decrease in their eccentricity measure between the first and second week of growth. Eccentricity remained unchanged over the three weeks of culture for organoids derived from stressed animals (Figure 4D). Altogether, these morphological findings point toward enhanced regenerative phenotype of organoids in those derived from WAS mice as compared to control.

Stress alters colonic luminal and epithelial-associated microbial diversity and evenness

In the next step, we aimed to determine whether changes in colonic barrier functions induced by stress were associated with changes in both luminal and epithelial-associated microbiota composition. In the distal colon, we first showed that stress did not modify evenness (Figure 5A) and β-diversity in both the luminal and epithelial-associated microbiota (Figure 5E and F). However, stress increased the α-diversity of the luminal (but not epithelial-associated) microbiota (Figure 5B). To determine whether these changes were specific to the distal colon, we performed a similar analysis in the proximal colon. In this organ, stress did not modify α- or β-diversity in both luminal and epithelial-associated microbiota as compared to control (Figure 5D and G-H). However, evenness was significantly increased by stress in the epithelial-associated microbiota as compared to controls (Figure 5C).

Stress modifies microbiota composition in the distal and proximal colon differentially

Next, we compared phyla composition in control and stressed mice in the distal colon (Supplementary figure 3). The epithelial-associated microbiota was characterized by a more significant proportion of *Firmicutes* (78% in control and 73% in stressed mice) compared to *Bacteroidetes* (17% in control and 22% in stressed mice). There was an opposite trend in the luminal microbiota where *Bacteroidetes* was the major bacterial phylum (55% in control and 48% in stressed mice). *Firmicutes* were the second largest phylum colonizing the lumen of the distal colon (37% in control mice and 44% in stressed mice). As for previous parameters [54], we also showed that in the proximal colon the epithelial-associated microbiota was also composed of a more significant proportion of *Firmicutes* (90% in control and 79% in stressed mice) compared to *Bacteroidetes* (7% in control and 17% in stressed mice). Unlike the composition of the luminal microbiota of the distal colon, in the luminal microbiota of the proximal colon the *Firmicutes* phylum constituted the most considerable portion of the microbiota (53% in control and 61% in stressed mice). In comparison, *Bacteroidetes* were the second largest phylum (39% in control and 33%).

Next, we performed a differential abundance analysis (see methods) to identify individual taxa modulated by stress in the distal colon. As current taxonomic annotation methods are usually not precise below genus annotations, we named the differentially abundant ASVs according to their respective genus. First, in the distal colon, we observed in the epithelial-associated microbiota a decrease in abundance of the *Lachnospiraceae NK4A136 g* induced by WAS as compared to control. Moreover, a significant increase in the luminal genus *Lachnospiraceae UCG-006*, a decrease in both the luminal genus *Coriobacteriaceae UCG-002g,* and an unassigned genus were observed in WAS as compared to control (Figure 6A).

In the proximal colon, we showed that the number of differentially abundant ASVs and genera associated to stress, compared to control, was more critical than the distal colon ones. Interestingly, similar to the distal colon, only one epithelial-associated taxa was differentially associated with stress, i.e., *Lachnospiraceae NK4136 g* genus, and was decreased by stress as compared to control. Next, analysis of the luminal microbiota revealed that 4 ASVs belonging to the *Lachnospiraceae NK4136 g* genus were significantly increased and only one ASVs belonging to the same genus was decreased by stress as compared to control. In addition, stress significantly increased ASVs assigned to the *Oscillibacter*, *Ruminococcaceae UCG-014*, *Alistipes* and *Butyricicoccus* genera as compared to control (Figure 6B). We also identified four genera (*Romboutsia*, *Parasutterella*, *Coriobacteriaceae UCG-002* and *Muribaculum*) significantly decreased in stress versus control. Finally, stress decreased the abundance of two unassigned genera and two unassigned ASVs, while it increased the abundance of two unassigned ASVs as compared to control (Figure 5J).

Host transcriptomic factors, epithelial-associated and luminal bacteria covary with levels of proliferation and cell death

Next, using computational analyses, we aimed at identifying integrated multi-omics signatures, that is microbiota changes associated with transcriptomic remodeling of epithelial cells involved in essential

epithelial physiological functions (in the distal colon), which were associated to stress, cell proliferation and cell death.

To capture individual co-variation in epithelial cells-microbiota associations across the luminal (777 ASVs) and epithelial-associated microbiota (713 ASVs), and the resulting host epithelial response in the distal colon (15147 epithelial gene expressions), we performed a multiple co-inertia analysis. The ordination of samples suggested that cell proliferation (8% of total covariance represented by the 8th axis) and death (11% of total covariance represented by the 2nd axis) are covarying (Figure 7B and 7D) between the luminal, epithelial-associated microbiota and the host transcriptomic response, in the distal colon. OPLS-DA analysis was performed on the drivers of this covariance to extract significant variables affected by changing ratios of proliferating cells and the number of cells undergoing apoptosis. The drivers associated with cell proliferation (Figure 7A) highlighted strong epithelial-associated signature (*Lactobacillus*, *Roseburia* and *Lachnoclostridium),* with one particular epithelial-associated ASV already found significantly decreased by stress as compared to control *(Lachnospiraceae NK4146 g*). Only 1 unassigned luminal ASVs was found in the multi-omics signature associated with cell proliferation. These bacteria were associated with a subset of 64 epithelial genes involved in various biological processes. Using a functional enrichment analysis, we identified gene functions such as tubule destabilization (Katnal1, Katnb1, and Epha1), growth factors activity (Fgf10), or phosphatase activity (Aptx, Impa2, Lpin3, Ubash3a) (Supplementary figure 4A). Then, performing in-depth manual annotation of these genes concerning to their putative role in colonic epithelial functions, we showed that 24% were related to epithelial homeostasis, 12,5% were involved in cytoskeleton remodeling, 7,8% participated in bacterial sensing (Nod1) of pro-inflammatory processes (Ackr2, Cops8, H2-Eb2, Nod1), 6,5% were related to Cell Migration (Cmtm3, Cplane1, Impa2, Lamc3), and 18,5% of them were currently unidentified. Among the drivers regulating epithelial cell proliferation, some were involved in mediating the crypto-villus establishment via the regulation of essential pathways such as Sonic Hedgehog (Cplane1), BMP4 (Dand5), TGF-β (Tubb2a, Zeb2), Pi3k/Akt (Pkib), or implicated in growth factors regulation (FgF10, EphA1). The drivers associated with cytoskeleton remodeling were involved in microtubule modulations as reported by the functional enrichment analysis (Aaas, Hdac6, Katnal1, Katnb1, Tubb2a) but also to actin modifications (Fgd3) or ciliogenesis (Cplane1, Rilpl1), all in line with cytoskeleton remodeling occurring during cell proliferation. Of particular interest, two genes were already reported as actors in host-microbiota associations and involved in cell proliferation: Pdgfrb promotes epithelial cell proliferation and is positively regulated by the *Lachnospiraceae* family, and Zeb2 is regulated by the microbiota and can induce Colorectal Cancer. Eventually, some genes were known to regulate cell death via lysing and removal of cell waste (C1qa, Cfp).

Next, we identified drivers associated with cell death. While 80% of bacteria in the multi-omics signature associated with cell proliferation were epithelial-associated, only 16% belonged to the epithelial-associated microbiota in the multi-omics signature linked to cell death (Figure 7C). Interestingly, we found both the epithelial-associated *Lachnospiraceae NK4A136g* and luminal *Parasutterella* ASVs belonging to the previously found genera in the differential abundance analysis. The multi-omics signature associated with cell death also included *GCA-900066575*, *Bilophila*, and unassigned ASVs. Interestingly, the functional annotation of the epithelial gene's associative signature was significantly different from that previously identified for cell proliferation. Indeed, it was highly enriched in terms of the humoral immune response (like Reg3a) and actin filament, microvillus, and cell adhesion (Supplementary figure 4B). The manual annotation of these genes identified 18,6% of genes involved in cytoskeleton modulation (Msn, Myo1g, Podxl, Borcs5, Mme, Fhl2, Gga3, Itgb1bp1), 14% related to paracellular permeability (Msn, Nectin1, Ptprcap, Rbm38, Reg3a, S1pr1), 9,3% participated in cell migration processes (Gga3, Itgb1bp1, Pitpnm3, Podxl) and 11,6% were involved in Immune system regulation (Ly6d, Fhl2, Il2rg, Reg3a, Klhl6). 44% of the drivers were related to other functions (e.g., post transcriptional mRNA modification, GTP hydrolysis, vitamin C uptake, Biosynthesis of CoA) and 14%

remained unidentified drivers. Within the subset of drivers involved in immune system alteration we found genes related to B-cells, T-cells or NK-cells promotions (Il2rg, Klhl6), and known antimicrobials (Fhl2, Il2rg, Reg3a). The genes associated with paracellular permeability were mostly regulators of E-Cadherin or Zo-1 (Msn, Nectin1, Ptprcap, Rbm38, Reg3a, S1pr1). Among the drivers associated with cytoskeleton modifications, we found many genes involved in focal adhesion (Fhl2, Gga3, Itgb1bp1, Myo1g, Podxl), actin (Msn, Myo1g, Podxl) and microtubule structure (Borcs5).

Stress modifies SCFAs profiles

To test whether changes in microbial composition induced by WAS were associated with changes in key bacteria-derived metabolites, such as short chain fatty acids, we quantified their abundance in cecum (see methods), as limited amount of feces were sampled in the distal colon. We showed that repeated acute stress significantly modified SCFAs concentration leading to a significant decrease of 25.8 % in total SCFAs, as well as individually measured SCFAs such as butyrate (25,1% decrease), acetate (22.7% decrease) and propionate (37,6% decrease), as compared to control (Figure 8A-D).

Fecal derived metabolites reproduce in part *in vitro* epithelial functional changes observed in stressed mice

Given this strong multi-omics bacterial/epithelial signatures suggesting the ability of stress induced changes in microbiota composition to mediate functional changes in cell proliferation and cell death, we performed experiments to determine the ability of fecal supernatant (FS) from stressed mice as compared to control, to regulate, at least in part, cell proliferation and cell death. Following, 96h exposition of HT-29 cells to FS isolated from control and stressed mice, we showed a significant increase in the number of HT-29 cells per well induced by FS of stressed mice as compared to controls. This effect was associated with a significant increase in the proportion of Ki67-IR cells, but no change in the proportion of Casp3-IR cells by FS of stressed mice as compared to control (Figure 9A-C).

Discussion:

By combining *in vivo* mice model, *in vitro* organoids model, *in situ* characterization of gut epithelial proliferative and apoptotic profiles, and bioinformatics analysis, we conducted a multi-omics and functional characterization of psychological stress-induced modulation of host-microbiota interactions in colonic epithelial cells.

We first showed that transcriptomic changes in the gut epithelium induced by repeated WAS were organ-specific, affecting all four considered regions of the gut differentially (jejunum, ileum, proximal and distal colon). Interestingly, we identified a subset of differentially expressed genes enriched in pro-proliferative/pro-regenerative genes in the distal colon. Next, *in situ* immunohistochemical analysis identified an increased epithelial cell proliferation cell death in the distal colon of stressed mice. In addition, distal colonic organoids derived from stressed mice revealed altered growth and budding processes. Furthermore, following 16s rRNA gene sequencing, we observed that stress increased luminal but not epithelial-associated α-diversity in the distal colon. The abundances of two genera (*Coriobacteriaceae UCG-002* and Unassigned) were significantly decreased while the *Lachnospiraceae UCG-006* genus was more abundant in stressed mice as compared to control. Notably, the epithelial-associated *Lachnospiraceae NK4A136 g* was largely decreased in stress. We also reported that stressed mice had a lower cecal concentration of short chain fatty acids than control. Finally, through computational analyses, we identified integrated multi-omics signatures of host epithelial genes, epithelial-associated and luminal microbiota, associated with the pro-proliferative and pro-apoptotic response of the distal colonic epithelium.

The first significant finding reported here was that repeated WAS induced region-specific changes in purified intestinal epithelial cells as compared to control, with the most extensive sets of genes being differentially regulated in the small intestine. The cause of these organ-specific differential responses remain largely unknown but could reflect various processes modulated by stress. As we performed bulk RNA sequencing, the individual cell specific response to stress could not be investigated and differences could, in part, be mediated by the differences in cell type composition of the studied regions [55]. Furthermore, this differential transcriptomic response could also reflect differences in receptor compositions mediating the effects of PS. In particular, in the gut, the differential regional expression for Corticotropin Releasing Factors (CRF) subtypes [56], Glucocorticoid Receptors (GR), Mineralocorticoid Receptors (MR) [57, 58], or GRE locus accessibility [59] have been previously reported and could thereby, upon their agonists binding, lead to activation of different pathways leading to different transcriptomic profiles. Such regional effects have for instance been reported for Glucocorticoids (GC), where systemic perfusion of GC induced a net increase in sodium transport in the colon but no differences in the ileum [60]. Organ-specific changes in bacterial composition induced by stress could also contribute to the differential regulations of transcriptomic response reported here. Altogether a different transcriptomic response to WAS in intestinal epithelial cells may contribute to differential organ specific functional changes reported by others [17, 20] and in our study, in particular concerning permeability. Indeed, paracellular permeability was reported not affected in the ileum but decreased in the colon. Such differential functional changes induced by stress in the gut have also been reported concerning motility. Indeed, in terms of motility, stress induces a delay in gastric emptying [61], inhibition of small intestinal motility [62], and an increase in colonic motility [63] also observed in our study (Supplementary Table 2).

The combination of an automated gene annotation approach with a manual annotation analysis revealed that the distal colon exhibited a strong pro-proliferative and pro-regenerative transcriptomic response to stress. Indeed, about 55% of DE genes in stress were associated with regulation of cell proliferation, differentiation, and cell death and migration. More specifically, upregulated genes such as Alr4c, Cpt1a, Pi3kca, Ptprd, Tnks2 were associated with activation of Wnt/β-catenin pathways [64–68], via the

stabilization of β-catenin by Pi3kca or Cpt1a [66, 67], the degradation of AXIN1 and AXIN2 both part of a complex inhibiting β-catenin by Tnks2 [64], or the regulation of downstream genes involved in tubulogenesis via Arlc4 [68], all leading to potential pro-proliferative/pro-regenerative response in the colon [69]. In addition, we also showed significant downregulation of anti-oncogenic genes contributing altogether to further favor a pro-proliferative response (Gpx1, Ap1m2, Hoxb13) [70–72]. Besides this concomitant increase in pro-proliferative activity, we also observed modulation of genes directly involved in the control of paracellular permeability. In particular, we observed an increase in ZO-2 and GCC2. Upregulation of these genes has been shown to reduce paracellular permeability [73–75]. From a functional point of view, this response could restore of barrier functions of newly generated epithelial cells following WAS. Furthermore, we did not observe significant changes in gene expression involved in cell death or apoptosis regulation, suggesting that genetic programming of cell death by stress could be an early process that we did not 'capture' when experiments were performed. This result is consistent with a previous study reporting that epithelial cell death occurs early in the ileum following chronic stress (i.e., day 5 of WAS) while, at later phases (i.e., day 10 of WAS), only a pro-proliferative response is maintained [23].

The study of organoids derived from stressed and control mice allowed us to identify differential time dependent morphological changes in the course of culture that are consistent with altered epithelial cell functions. In particular, we observed decreased eccentricity in organoids derived from stressed animals, associated with a reduced number of buds as compared to control. The difference in these parameters can be considered as markers of undifferentiated or regenerative organoids. Indeed, the presence of budding structures requires in organoids culture a primary event of symmetry breaking, characterized by changes in eccentricity, which are induced by the presence of differentiated Paneth cells and Wnt pathways [76], and is therefore a marker of proliferative processes in organoid culture experiments [77]. Surprisingly, organoids derived from control mice and stressed mice showed no more significant differences in area, budding or eccentricity after three weeks, indicating that the lack of proliferation and differentiation observed in stress derived organoids was only delayed and resolved at the mature organoid stage. This unexpected decrease in cell proliferation given the *in vivo* study, where a significant pro-proliferative response was observed, could be explained by the nature of the organoid culture, which does not recapitulate all signals provided by the epithelial microenvironment present *in vivo*. In particular, the absence of the gut microbiota that we identified as an essential driver of stress induced cell proliferation *in vivo* (see below), is absent in our culture.

An important finding of our study was that we observed concomitant changes in microbiota composition induced by stress of both luminal and epithelial associated ones. Of particular interest, in the distal colon, we observed a significant decrease in epithelia-associated *Lachnospiraceae NK4A136g*, a butyrate producer [78]. This result is also consistent with previous studies revealing a decrease in the family of *Lachnospiraceae* abundance induced by WAS [33], even if this particular genus was not identified. Furthermore, in the distal colon, we observed a significant increase in *Lachnospiraceae UCG-006* genus in the luminal microbiota of stressed animals but was negatively associated with both acetate and butyrate concentration [78, 79]. We also identified in the distal colon a decrease in the abundance of an unassigned genus and of the *Coriobacteriaceae UCG-002* genus whose family was already reported decreased in stress by a previous study [31]. In the proximal colon, stress was also associated to a decrease in abundance of epithelial associated *Lachnospiraceae NK4A136 g*. However, stress differentially modulated more bacterial abundances in the proximal colon than in the distal one with a more balanced regulation of butyrate-producing bacteria, i.e., decrease in *Parasutterella* Genus, *Romboutsia* Genus and increase in *Butyricicoccus* ASV and *Ruminococcus UGC-014* ASV. Of interest, the *Lachnospiraceae* group and *Ruminococcus UCG-014*, *Coriobacteriaceae* and *Butyricicoccus* were reported as decreased by stress in another study [31]. These modifications, observed in the feces, were sometimes in contradiction with our results (such as the increased

Ruminococcus UCG-014 and *Butyricicoccus* ASVs in response to stress reported in our study) but could be explained by the difference in regional microbial sampling.

Finally, through computational multi-omics integration and analysis, we identified distinct signatures of epithelial-associated and luminal microbiota as well as host epithelial genes that were associated with cell proliferation and cell death. In particular, we observed that changes in cell proliferation were primarily associated with epithelial-associated bacteria, whereas cell death multi-omics signature identified mostly luminal bacteria. Further reinforcing the specificity of the signature of cell distinct biological processes was the fact that among all drivers identified, none were common between the cell proliferation and cell death signatures. Interestingly, *Lachnospiraceae NK4136 g* ASV, that was identified in the cell proliferation multi-omics signature, was also significantly decreased by stress in the epithelial-associated microbiota, thus suggesting a central functional role of this ASV in mediated PS effects upon epithelial cell proliferation. Consistently, we found that changes induced by WAS in bacterial composition were associated with a change in the cecal concentration of SCFAs. The reduced concentration of SCFAs, and in particular of butyrate, observed in our study, might reflect the overall changes in butyrate producing bacteria observed in the epithelial associated and luminal microbiota of the distal colon. This decrease in SCFAs induced by stress is consistent with previously reported changes in the literature [80].

Analyzing genes predicted to be involved in cell proliferation, we identified functions involved in the regulation of cell proliferation in particular via the regulation of pathways such as Sonic Hedgehog (Cplane1), BMP4 (Dand5), TGF-β (Tubb2a, Zeb2), Pi3k/Akt (Pkib), FgF10, EphA1, all known to favor cell proliferation. In addition, our association study identified two genes, Pdgfrb and Zeb2, that were previously reported as actor in host-microbiota interactions and involved in the regulation of cell proliferation. Notably, Pdgfrb has been shown to be regulated by *Lachnospiraceae*, although the strains remain to be defined, and was shown to promote intestinal cell proliferation [81]. The identification of Zeb2 in the signature associated with cell proliferation is also of particular interest, and a recent study showed that microbiota dysbiosis associated with intestinal epithelial cells expression of Zeb2 promotes CRC development [82]. In order to further reinforce the functional relevance of this analysis, we showed that feces of stressed mice enhance HT-29 cell proliferation as compared to control. Such direct functional effect upon intestinal cell proliferation of fecal metabolites obtained from PS stressed animal has, to the best of our knowledge, never been demonstrated. FS-derived mediators responsible for these effects remain unknown. One hypothesis is that SCFAs, in particular butyrate, observed in our study to be reduced in stressed animals could contribute to these effects. Indeed, reduced butyrate concentration in FS could have favored cell HT-29 cell proliferation as butyrate was shown to reduce cell proliferation in cell lines such as HT-29 [83]. In contrast, no effects on cell death of FS were reported although a bacterial signature associated with cell death was observed. This absence of effect could be because the model used to test this hypothesis, i.e., HT-29-cells are particularly resistant to apoptotic processes [84].

Altogether our study demonstrated that PS induces a pro-regenerative response driven by combined microbiota and intestinal epithelial transcriptome remodeling. This study could set the basis for identifying combined bacteria and host gene targets to prevent PS induced barrier dysfunctions that are increasingly recognized as key contributors to the evolution of major chronic diseases.

Acknowledgement:

The authors wish to thank Thibaut Layssac for its useful feedback concerning image analysis, Emilie Durieux, Malvyne Derkinderen, Amelie Lê and Catherine Le Berre-Scoul for their advices on immunohistochemistry. We also thank the bioinformatics core facility of Nantes (BiRD—Biogenouest) for the 3'end RNA sequencing and for providing computing resources (SRP pipeline) and support. Finally, we would like to thank Biofortis Mérieux for the 16S rRNA sequencing and their feedback on the project.

Fundings:

This work has received financial support from the Region Pays de la Loire (MiBioGate 2016-11179 to M.N.).

Abbreviations:

ASV: amplicon sequence variant
Casp3: caspase 3
CMC: carboxymethyl cellulose sodium salt
CRC: colorectal cancer
CRF: corticotropin releasing factor
DE: Differentially expressed
FS: fecal supernatant
F-SA: Fluorescein conjugated sulfonic acid
GC: glucocorticoid
GR: glucocorticoid receptor
IBD: inflammatory bowel disease
IBS: irritable bowel syndrome
IEB: intestinal epithelial barrier
IEC: intestinal epithelial cell
IR: immunoreactive
MR: mineralocorticoid receptor
PS: psychological stress
SCFA: short chain fatty acid
WAS: water avoidance stress

Figures:

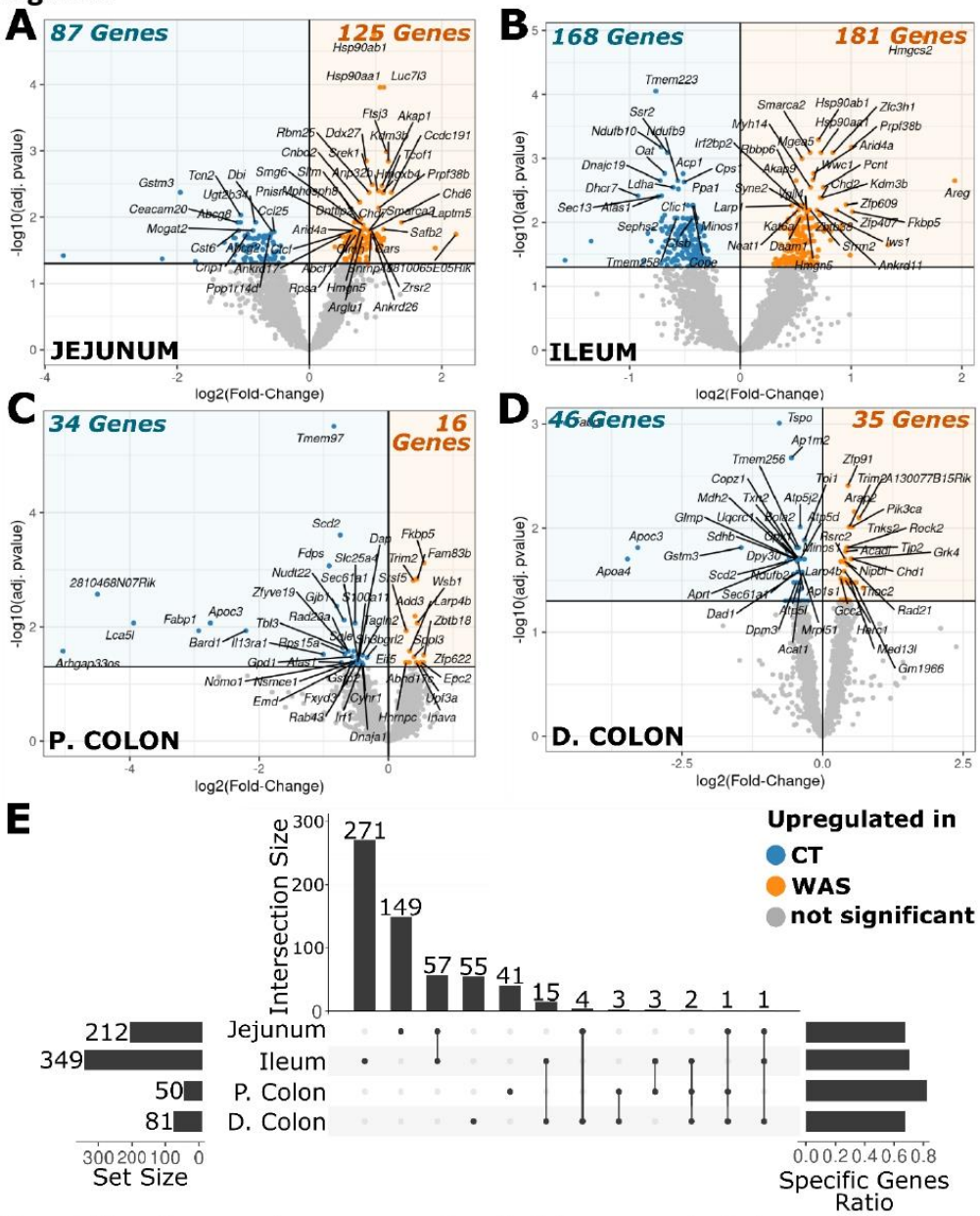

Figure 1 *Effect of a repeated acute stress on the epithelial gene expression in the mouse digestive tube: A, B, C and D. Volcano plot representation of differential expression between control and stressed mice in the epithelial genes of, respectively, Jejunum (A), the Ileum (B), the proximal colon (C) and the distal colon (D). Genes were colored when considered as differentially expressed, with adjusted p-value < 0,05 in blue when downregulated and in orange when upregulated, using the control condition as a reference. E. Upset plot indicating the number of common and uniquely differentially expressed genes between each organ region. The set size shows the number of differentially expressed genes in each organ and the Specific Gene Ratio indicates the percentage of uniquely differentially expressed genes in each region.*

A

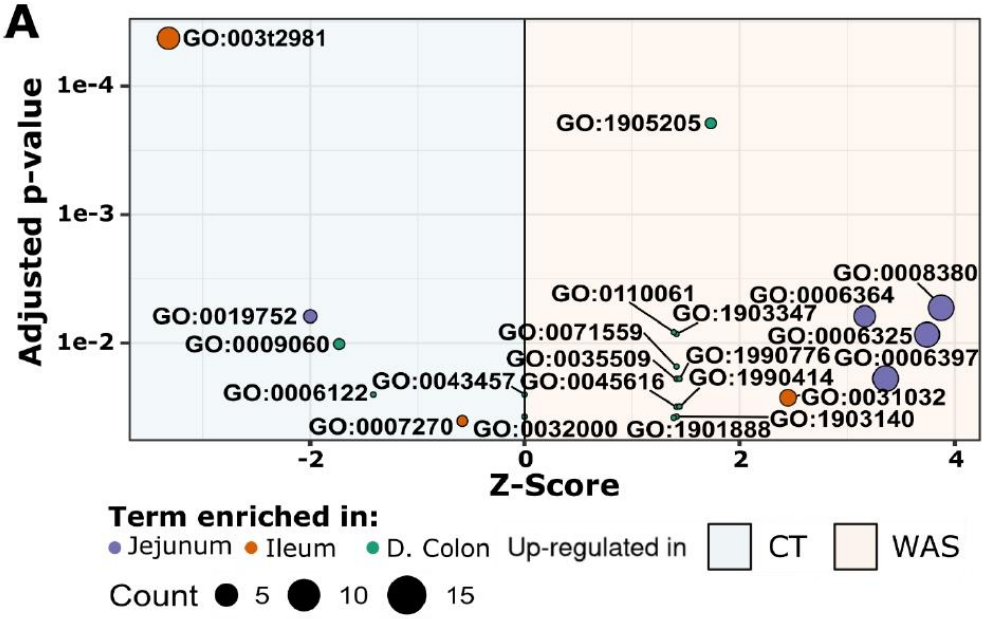

B

GO Terms	Adjusted P-value	Description	
GO:0008380	0.0053	RNA splicing	↗
GO:0006364	0.0062	rRNA processing	↗
GO:0019752	0.0062	Carboxylicacid metabolic process	↘
GO:0006365	0.0086	Chromatin organization	↗
GO:0006397	0.019	mRNA processing	↗
GO:0032981	0.000043	Mitochondrial respiratory chain complex 1 assembly	↘
GO:0031032	0.027	Actomyosin structure organization	↗
GO:0007270	0.040	Neuron-neuron synaptic transmission	↘
GO:0006122	0.025	Mitochondrial transport, ubiquinol to cytochrome c	↘
GO:0009060	0.010	Aerobic respiration	↘
GO:0032000	0.037	Positive regulation of fatty acid beta-oxydation	→
GO:0035509	0.019	Negative regulation of myosin-light-chain-phosphatase	↗
GO:0043457	0.025	Regulation of cellular respiration	→
GO:0045616	0.031	Regulation of keratinocyte differentiation	↗
GO:0071559	0.015	Response to transforming growth factor beta	↗
GO:0110061	0.0054	Regulation of angiotensin activated signaling pathway	↗
GO:1901888	0.023	Regulation of cell junction assembly	↗
GO:1903140	0.031	Regulation of establishmentof endothelial barrier	↗
GO:1903347	0.0054	Negative regulation of bicellular tight junction assembly	↗
GO:1905205	0.00019	Positive regulation of connective tissue replacement	↗
GO:1990414	0.019	Replication-born double-strand break repair via sister chromatid exchange	↗
GO:1990776	0.019	Response to angiotensin	↗

Up-regulated in ↘ Control ↗ Stress → Non significant

Figure 2: *Functional Annotation with epithelium specific filtered GO Terms on the subset of differentially expressed genes. A. Epithelium specific filtered GO terms of the Jejunum, Ileum, proximal and distal colon associated with the differentially expressed genes in each organ region represented according to their adjusted p-value (<0.05) and z-scores. B. their associated adjusted p-value, and their description.*

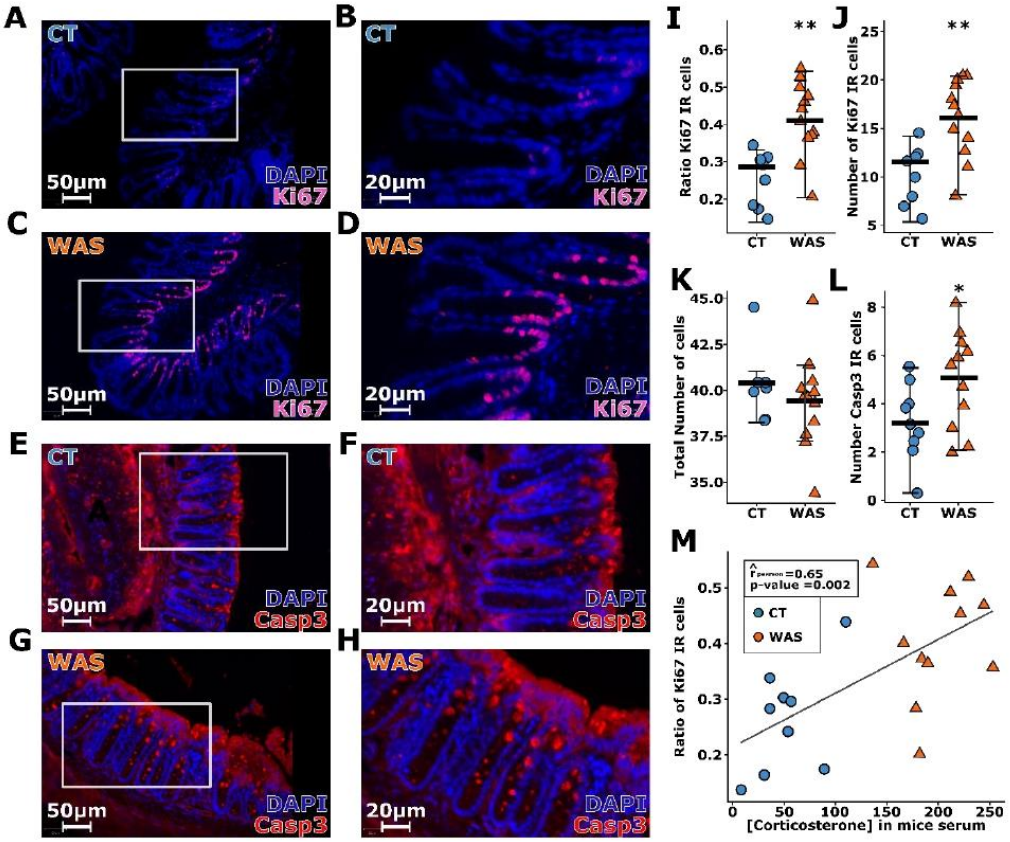

Figure 3: *Stress induces changes in cell turn-over rate in the distal colonic epithelium: The distal colonic crypts of control mice at A. 50 µm and B. 20 µm magnification and stressed control mice at C. 50 µm and D. 20 µm magnification were immunostained with Ki67 antibody and DAPI. The distal colonic crypts of control mice at E. 50 µm and F. 20 µm magnification and stressed control mice at G. 50 µm and H. 20 µm magnification were immunostained with Casp3 antibody and DAPI. I. Shows an increase in the Ki67-IR ratio in stressed mice compared to control mice (n_{CT} = 8, n_{WAS} = 12, p-value = 0,015). J. Shows an increase in the number of Ki67-IR cells in stressed mice compared to control mice (n_{CT} = 8, n_{WAS} = 12, p-value = 0,030). K. No modification in the total number of cells in colonic crypts between control and stressed mice (n_{CT} = 8, n_{WAS} = 12). L. Shows an increase in the number of Casp3-IR cells in stressed mice compared to control mice (n_{CT} = 9, n_{WAS} = 11, p-value = 0,034). M. Shows a positive correlation ($corr_{pearson}$= 0.65, p-value = 0.002) between the ratio of Ki67-IR cells and the corticosterone levels in control and stressed mice (n_{CT} = 8, n_{WAS} = 12).*

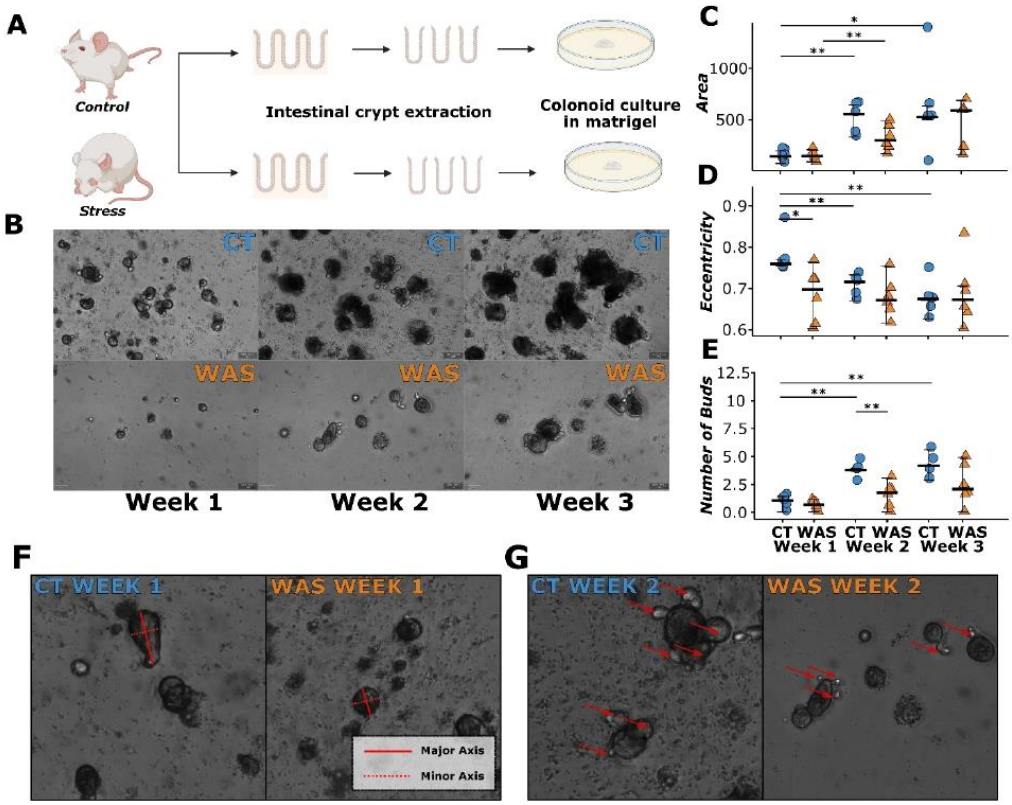

Figure 4: Organoids grown from control vs stressed colonic crypts showed a divergence in their eccentricity and differentiation state: A. Schematic representation of the experimental Workflow. The distal colonic crypts were extracted and cultured in Matrigel. Their growth was monitored after 1, 2 and 3 weeks of culture. B. Representative image of control (upper panels) and WAS (bottom panels) primo culture organoids after 1 week (left panels), 2 weeks (middle panels) and 3 weeks (right panels) of culture. C. shows a difference in organoids area between 1 and 2 weeks of growth in both control and WAS groups but no differences between experimental groups. D. Shows a difference between control and WAS organoids eccentricity in the first week of growth. Control organoids significantly decrease in eccentricity over the weeks while stressed organoids remain unchanged. E. Shows a difference between control and WAS number of buds in their organoids at week 2. In control organoids, the number of buds significantly increases over the weeks while, in stressed organoids, it remains unchanged. F. A representative image of difference in eccentricity between control derived organoids and stressed derived organoids after 1 week of culture. G. A representative image of difference in number of budding structures between control derived organoids and stressed derived organoids after 2 weeks of culture.

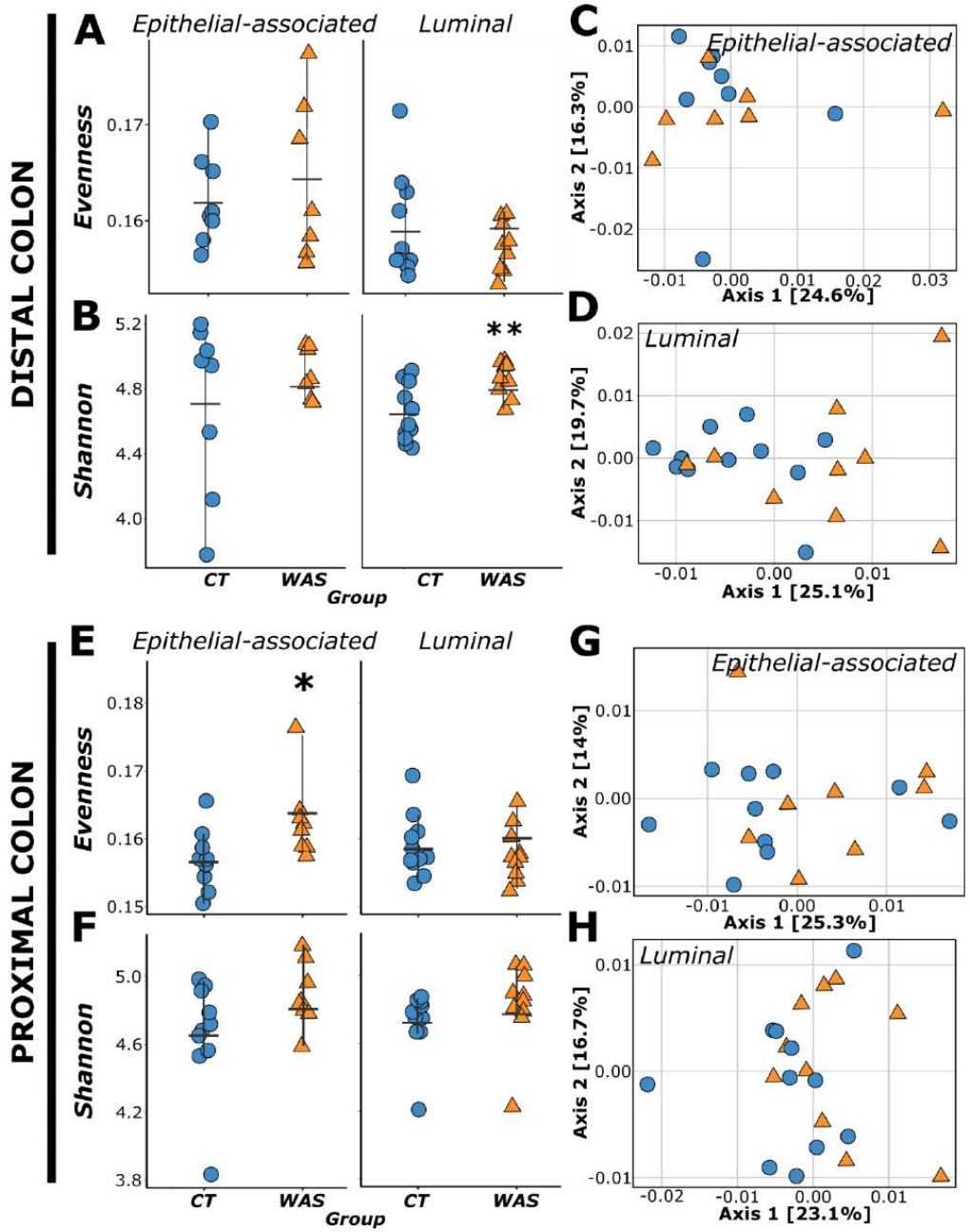

Figure 5 Microbiota diversity analysis in the colon between control and stressed mice: A. shows no difference in the evenness of the epithelial-associated (n_{CT} = 8, n_{WAS} = 7) and Luminal content (n_{CT} = 11, n_{WAS} = 9) of the distal colon. B. indicates an increase of shannon index of Luminal content of the distal colon (Test Mann-Whitney, n_{CT} = 11, n_{WAS} = 9, p-value = 0,006) but not in the epithelial-associated content (n_{CT} = 8, n_{WAS} = 7). C. shows an increase in the evenness of the epithelial-associated content of the proximal colon (test Mann-Whitney, n_{CT} = 10, n_{WAS} = 8, p-value = 0,011) and no modification of the luminal content evenness (n_{CT} = 11, n_{WAS} = 10). D. and no modification on the Shannon index of the epithelial-associated (n_{CT} = 10, n_{WAS} = 8) and luminal content (n_{CT} = 11, n_{WAS} = 10) of the proximal colon. E. F. shows the weighted Unifrac distance between control (blue) and stressed (red) samples in the epithelial-associated and luminal content of the distal and G. H. proximal Colon.

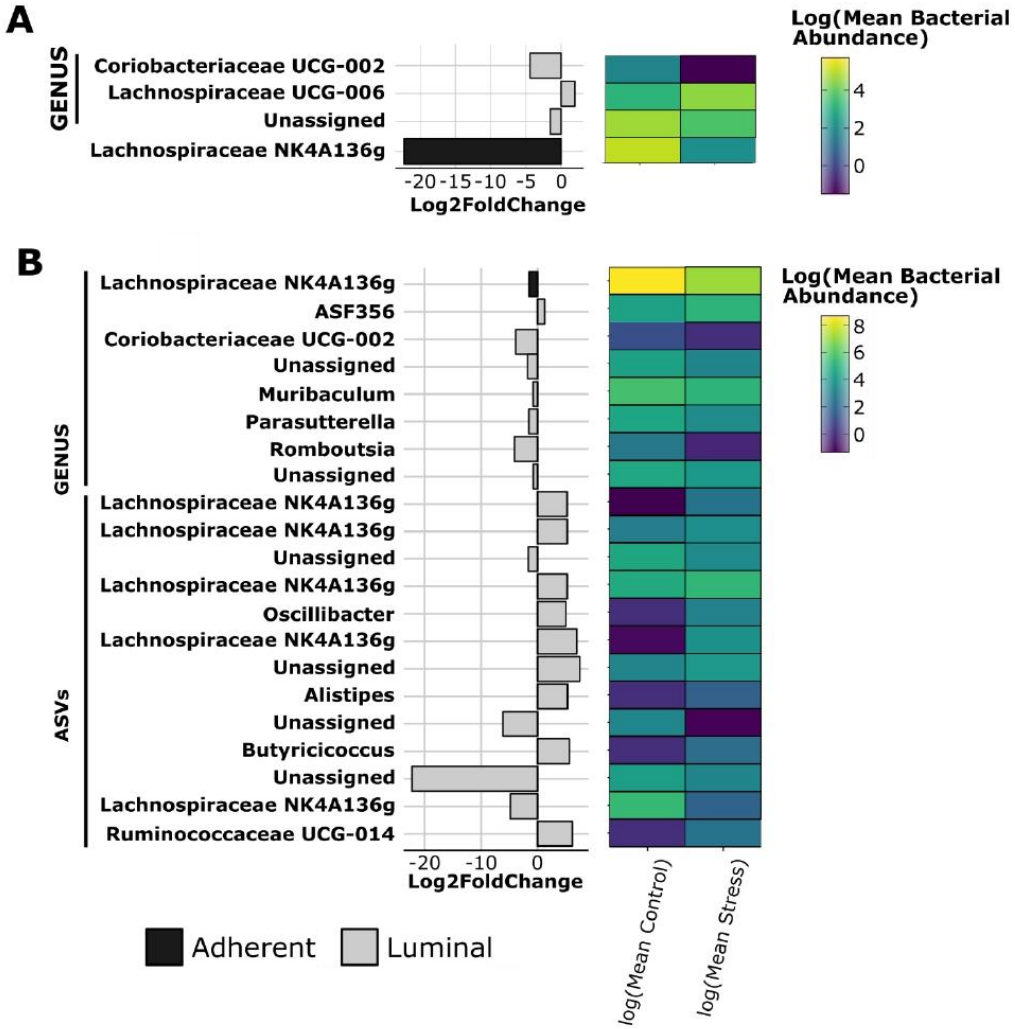

Figure 6 *Microbiota differential abundance analysis in the colon between control and stressed mice: A. indicates the log2 fold-change of the significantly differentially abundant amplicon sequence variants (ASVs) and genera and their respective mean abundance in control and stressed subjects. (DESeq2, adjusted Bonferroni p-value < 0.05) of distal colon and B. proximal Colon.*

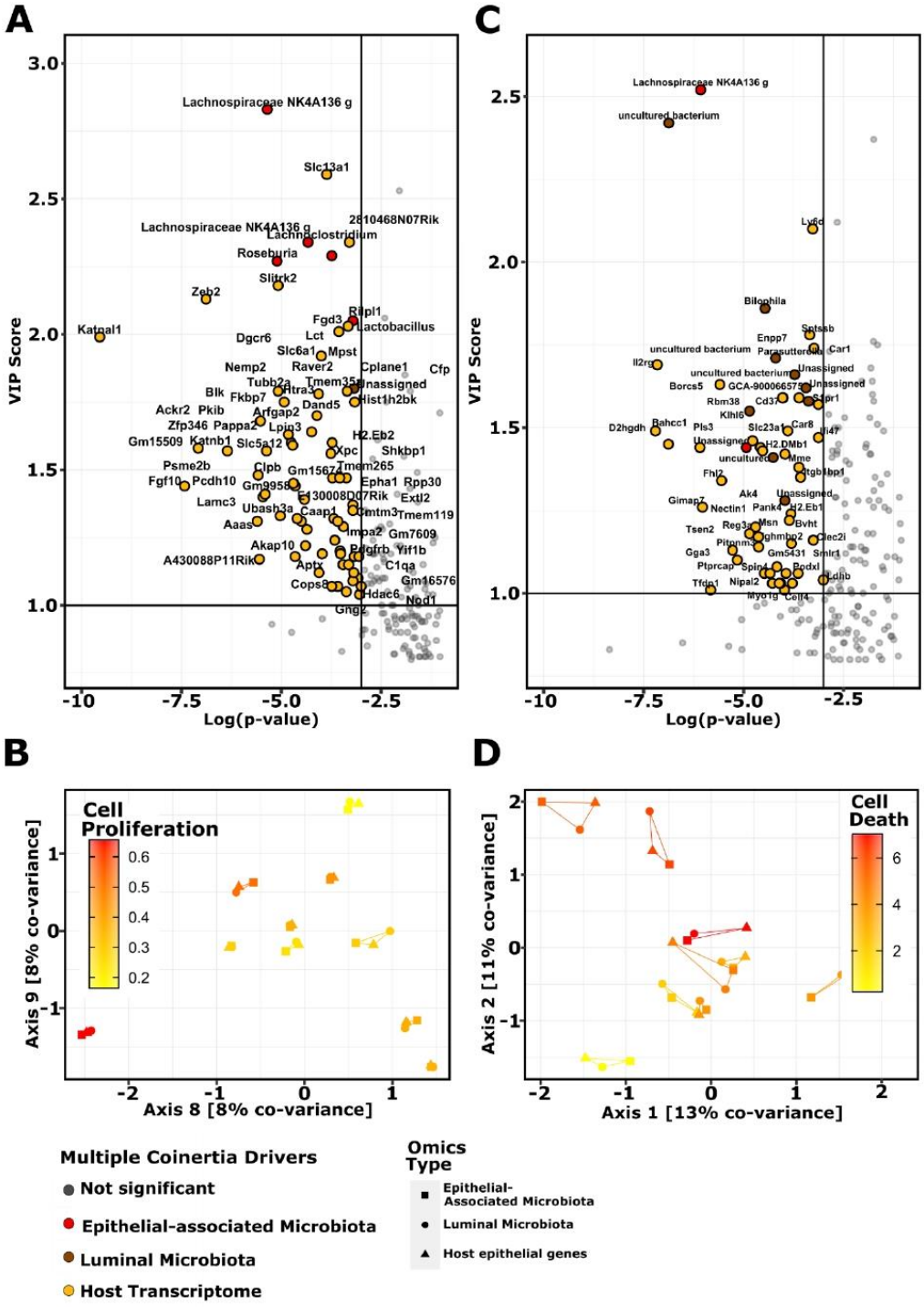

Figure 7: Integrative analysis revealing multi-omics signatures between the host epithelium, the epithelial-associated and the luminal microbiota in relation to cell proliferation and apoptosis: A. Significantly important drivers of the eight axis of the multiple co-inertia analysis (only variables with a VIP>1 and a p-value <= 0.05 are considered significantly important toward changes in ratio of Ki67-IR cells in colonic crypts) and B Multiple co-inertia analysis of the host epithelium, epithelial-associated and luminal microbiota in the distal colon. Samples are colored according to their ratio of Ki67-IR cells in colonic crypts. C. Significantly important drivers of the second axis of the multiple co-inertia analysis (only variables with a VIP>1 and a p-value <= 0.05 are considered significantly important toward changes in ratio of

Casp3-IR cells in colonic crypts) and D Multiple co-inertia analysis of the host epithelium, epithelial-associated and luminal microbiota in the distal colon. Samples are colored according to their ratio of Casp3-IR cells in colonic crypts.

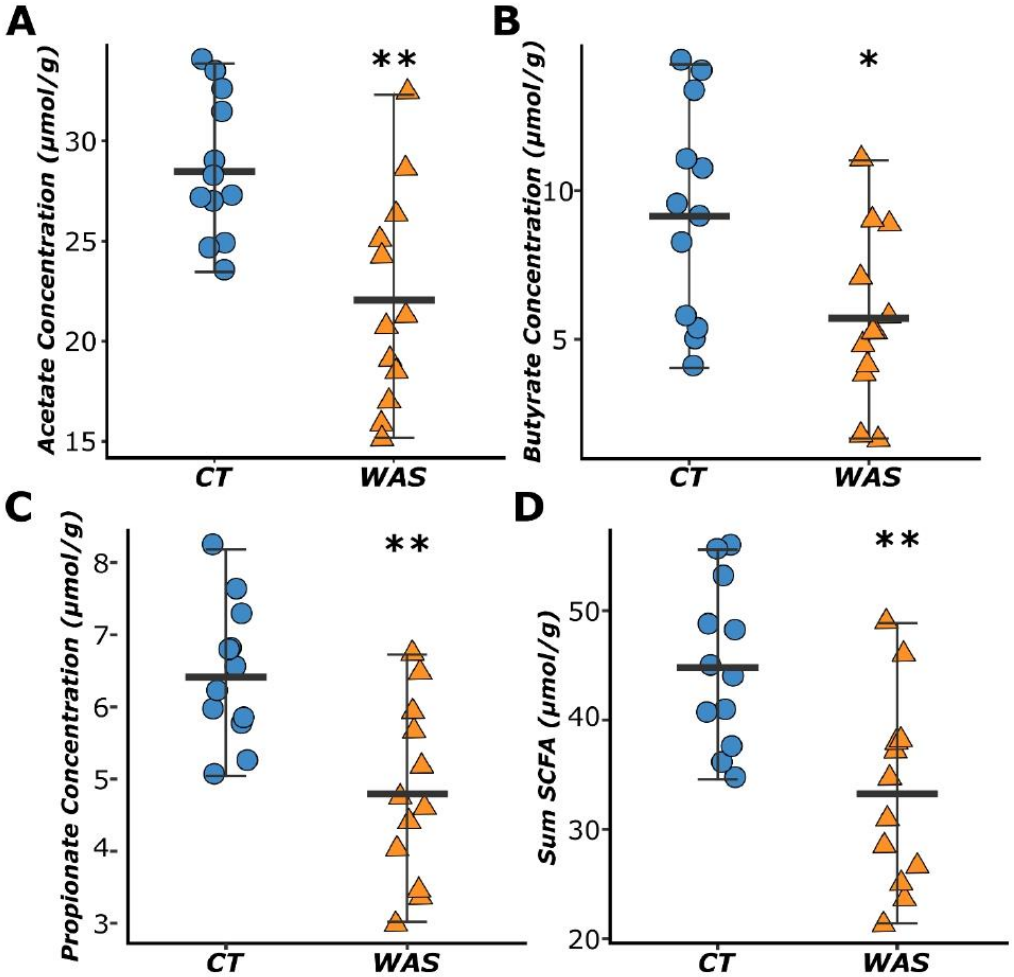

Figure 8 *Cecal concentration of SCFAs indicates a decrease in A. Acetate concentration (nCT = 12, nWAS = 12, t-test, p-value= 0.002) in WAS mice as compared to control. B. Butyrate concentration (nCT = 12, nWAS = 12, t-test, p-value= 0.018) in WAS mice as compared to control. C. Propionate concentration (nCT = 12, nWAS = 12, t-test, p-value= 0.002) in WAS mice as compared to control. D. total sum of SCFAs (nCT = 12, nWAS = 12, t-test, p-value= 0.002) in WAS mice as compared to control.*

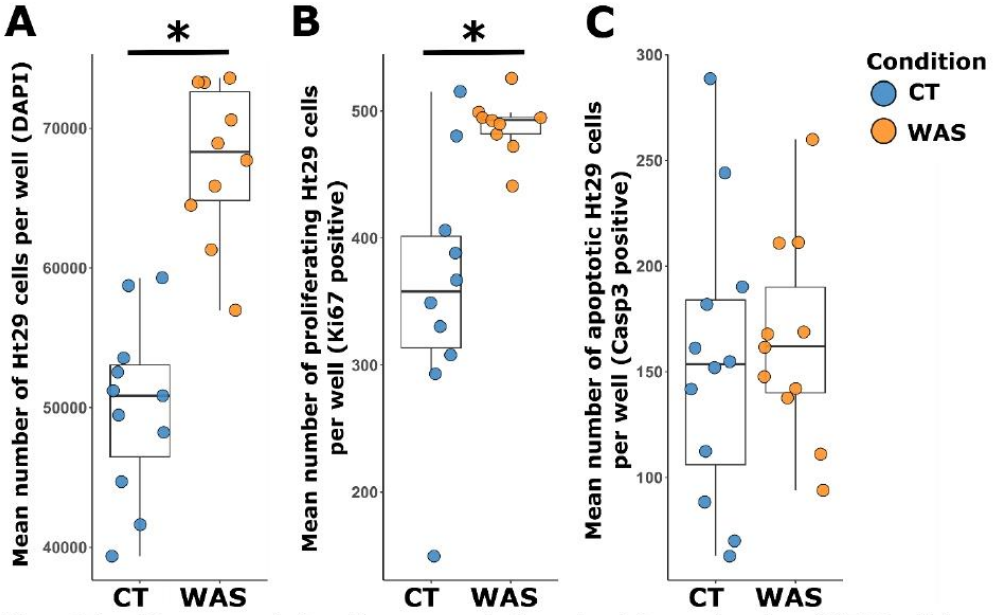

Figure 9 *Fecal Supernatant isolated from stressed mice reduced the total number of HT-29 cells in culture after 96H of exposition and induced changes in cell proliferation after 72h A. Number of HT-29 cells in culture after 96h of exposition to control or stressed mice fecal supernatant (nCT = 11, nWAS = 10, t-test, p-value= 1.667x10^{-6}). B. Number of proliferating HT-29 cells in culture (Ki67-IR) after 96h of exposition to control or stressed mice fecal supernatant (nCT = 11, nWAS = 11, t-test, p-value= 0.0029). C. Number of apoptotic HT-29 cells in culture (Casp3-IR) after 96h of exposition to control or stressed mice fecal supernatant.*

Tables:

Function	Downregulated	Upregulated
Activators of Cell proliferation	Dpy30, Fabp1 **(2,5%)**	Arl4a, Birc6, Cpt1a, Lmo7, Med13l, Nipbl, Phip, Pik3ca, Rad21, Thoc2, Tnks2, Trim2, Zfp91 **(16,0%)**
Inhibition of Cell proliferation	Gpx1, Ap1m2, Hoxb13 **(3,7%)**	Herc1, Klf6, Ptprd, Rsrc2, Setd2, Zo-2 **(7,4%)**
Inhibitors of Cell Differentiation		Rad21 **(1,2%)**
Activators of Cell death	Rnf186 **(1,2%)**	Zo-2, Gcc2 **(2,7%)**
Inhibitors of Cell death	Cyb5r3, Dad1 **(2,5%)**	A130077B15Rik, Birc6, Larp4b, Nipbl, Phip, Pik3ca **(7,4%)**
Enhancers of Cell migration		Arap2, Herc1, Nipbl, Rapgef6 **(4,9%)**
Inhibitors of Cell Migration		Larp4b, Ptprd **(2,5%)**
Enhancers of Wound Healing		Rock1, Rock2 **(2,5%)**
Decreases Paracellular permeability	AP1S1 **(1,2%)**	Zo-2, Gcc2 **(2,5%)**
Increase in Paracellular Permeability	Rnf186 **(1,2%)**	
Part of adherens Junction		Lmo7, Rapgef6 **(2,5%)**
Activators of Mitochondrial Energy Metabolism	Aprt, Atp5d, Atp5j2, Atp5k, Atp5l, Cisd1, Sdhb, Tspo, Txn2, Uqcrc1, Uqcrh **(13,5%)**	
Enhancers of beta oxydation	Acat1, Cyb5r3, Fabp1 **(3,7%)**	Acadl, Cpt1a **(2,5%)**
Activators in Lipid Metabolism	Apoa4, Apoc3, Scd2, Ebp **(4,9%)**	
Other functions unrelated to epithelial homeostasis	AP1M2, Bola2, Copz1, Dpm3, Sec61a1, Yipf1, Glmp, ***GSTM1, GSTM3,*** SLC25A39, Tpi1 **(13,5%)**	Mal2, Chd1, GRK4, Zmym5 **(4,9%)**
Unknown function		Nbeal1, Gm1966, BAZ2B, Jpt1, Tmem208, Tmem256 **(7,4%)**

Table 1*: Manual annotation of gene functions in colon distal*

Supplementary Figures:

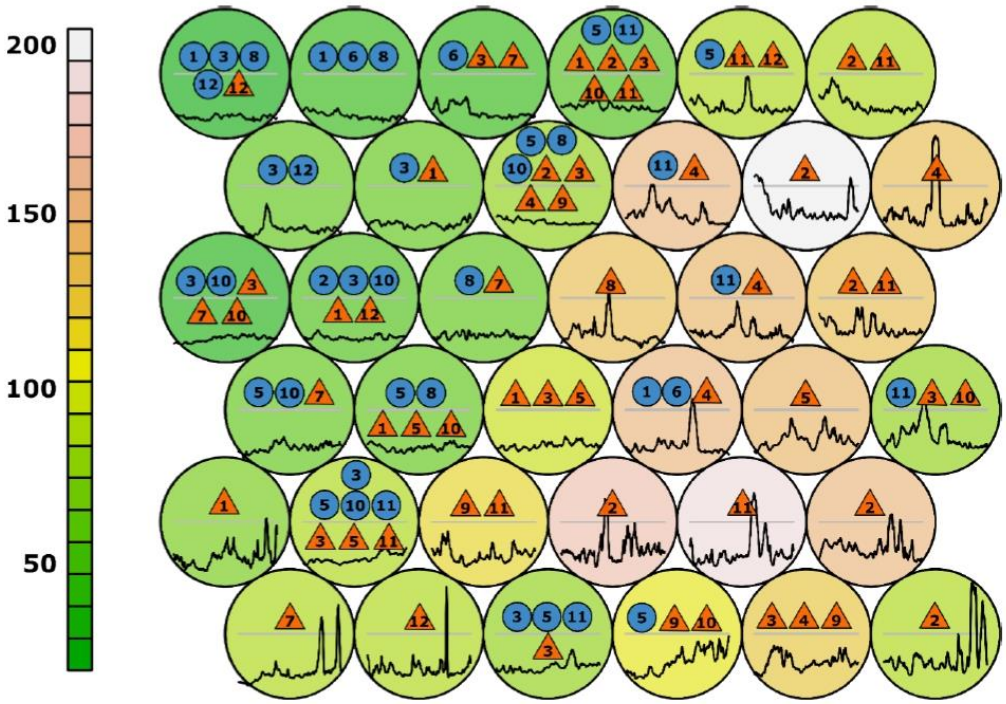

Supplementary Figure 1: Self Organizing Map (SOM) of the Casp3 Immunostaining distribution in colonic crypts: Cells are colored according to their difference to one another. Each cell contains the crypts of control (blue circle) or stressed (orange triangle) sample corresponding to their Casp3-IR cells distribution.

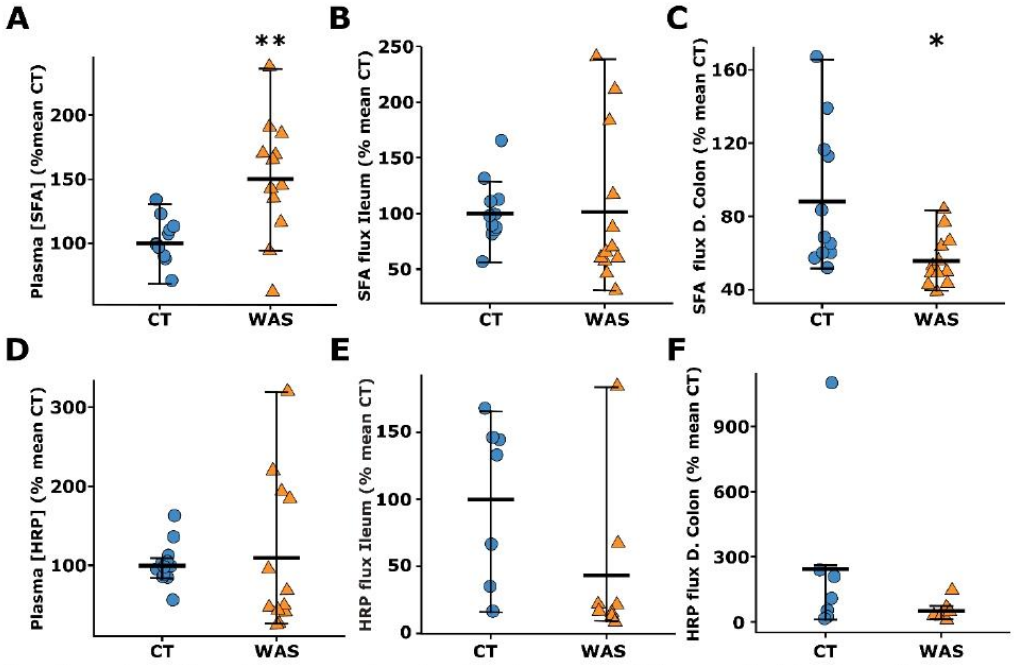

Supplementary Figure 2: *Changes in animal barrier permeability provoked by stress:* *A. shows an increase of in vivo permeability to fluorescein sulfonic acid (SFA) in stressed mice compared to control mice after 4 days of consecutive WAS stress (n_{CT}= 12, n_{WAS}= 12, p-value = 0,004), B. No modification in ex vivo permeability to fluorescein sulfonic acid (SFA) in the ileum between control and stressed mice n_{CT}= 11, n_{WAS}= 12), C. and a decrease in ex vivo permeability to fluorescein sulfonic acid (SFA) in the distal colon in stressed mice compared to control mice (n_{CT}= 11, n_{WAS}= 12, p-value = 0,023). D. shows no modification in vivo permeability to horseradish peroxidase (HRP) between control and stressed mice after 4 days of consecutive WAS stress (n_{CT}= 12, n_{WAS}= 12), E. in ex vivo permeability to horseradish peroxidase (HRP) in the ileum between control and stressed mice (n_{CT}= 7, n_{WAS}= 8), F. ex vivo permeability to horseradish peroxidase (HRP) in the distal colon between control and stressed mice (n_{CT}= 7, n_{WAS}= 6).*

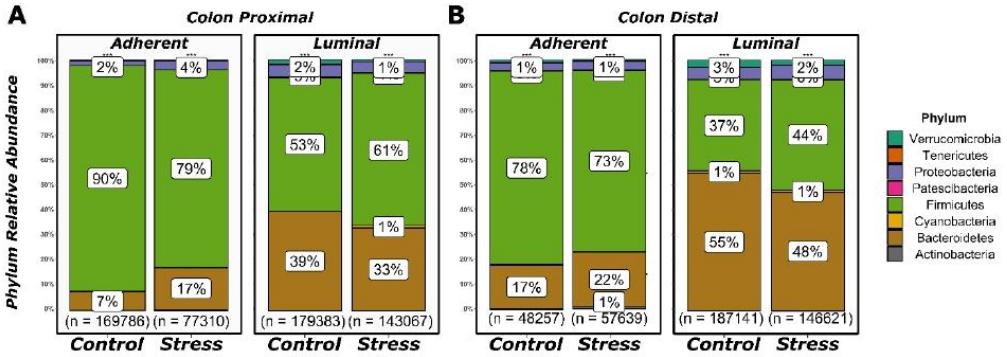

Supplementary Figure 3: Phylum composition of the epithelial-associated and Luminal microbiota in: A. Proximal and B. distal colon.

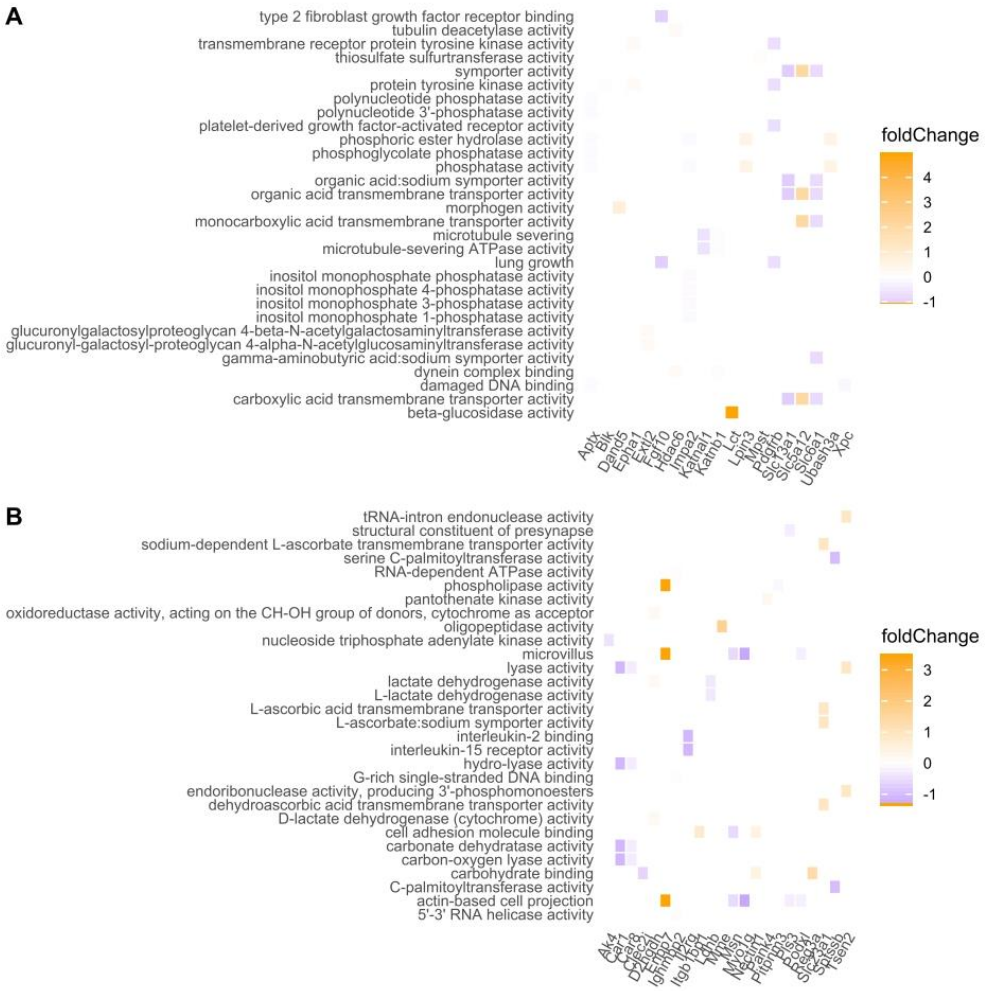

Supplementary Figure 4: *GO functional enrichment on host transcriptomic terms extracted from the subset of multiple coinertia drivers: A. GO Terms associated with cell proliferation in the distal colon are listed in the row of the heatplot. The genes participating each functional annotation are listed as rows. They are colored according to their log2(fold change) in the transcriptional analysis: orange when upregulated and blue when downregulated using the control condition as a reference. B. GO Terms associated with cell death in the distal colon are listed in the row of the heatplot. The genes participating each functional annotation are listed as rows. They are colored according to their log2(fold change) in the transcriptional analysis: orange when upregulated and blue when downregulated using the control condition as a reference.*

Supplementary Tables:

Functions	Downregulated Genes	Upregulated Genes
Activators of Cell proliferation	S100A11, Scd2 **(4%)**	Eif5, Hnmpc, Trim2 **(6%)**
Inhibition of Cell proliferation	Slc25A4 **(2%)**	Klf6, Ptprd, Setd2 **(6%)**
Prevents Cell Death	Dap **(2%)**	Eif5 **(2%)**
Increase in Intestinal Barrier Permeability	Scd2 **(2%)**	Add3, Inava **(4%)**
Promotes Lipid Metabolism	/	Abhd17c **(2%)**
Prevents Lipid Metabolism	Apoc3, Fabp1, Fdps, Scd2, Sqle **(10%)**	/
Promotes Mucosal inflammation	Fabp1 **(2%)**	Inava **(2%)**
Inhibition Mitochondrial Energy Metabolism	Slc25a4 **(2%)**	/

Supplementary Table 1 *Manual annotation of proximal colonic epithelial differentially expressed genes.*

Parameter	Mean Control Group	Mean WAS Group	P-value
Weight at Day 14 (g)	25 (n=12)	24,42 (n=12)	NS
Intestine Length (cm)	42,6 (n=10)	43 (n=12)	NS
Large Intestine length (cm)	7,76 (n=10)	7,83 (n=12)	NS
Small Intestine length (cm)	34,84 (n=10)	35,17 (n=12)	NS
Corticosterone Concentration	43,18 (n=12)	191,42 (n=12)	<0,001
Triglyceride concentration in serum	71,21 (n=12)	41,61 (n=12)	0,002
Cholesterol concentration in serum	76,39 (n=12)	75,07 (n=12)	NS
NEFAs concentration in serum	0,2 (n=12)	0,24 (n=12)	NS
Colonic Transit at day 14	100 (n=12)	274,8 (n=12)	<0,001

Supplementary Table 2: Changes in animal physiology provoked by stress: a list of anatomical parameters, lipids concentration, and permeability measure and how they are impacted by acute repeated stress.

References:

1. Mayer EA, Naliboff BD, Chang L, Coutinho S V. Stress and the gastrointestinal tract V. stress and irritable bowel syndrome. American Journal of Physiology - Gastrointestinal and Liver Physiology. 2001;280 4 43-4.
2. Larauche M, Mulak A, Taché Y. Stress-related alterations of visceral sensation: Animal models for irritable bowel syndrome study. Journal of Neurogastroenterology and Motility. 2011;17:213–34.
3. Mawdsley JE, Rampton DS. Psychological stress in IBD: New insights into pathogenic and therapeutic implications. Gut. 2005;54:1481–91.
4. Yang P, Jury J, So JD, Sherman PM, Mckay DM, Perdue MH. Chronic Psychological Stress in Rats Induces Intestinal Sensitization to Luminal Antigens. 2006;:104–14.
5. Baritaki S, de Bree E, Chatzaki E, Pothoulakis C. Chronic Stress, Inflammation, and Colon Cancer: A CRH System-Driven Molecular Crosstalk. Journal of Clinical Medicine. 2019;8:1669.
6. Li B, Wang Y, Yin L, Huang G, Xu Y, Su J, et al. Glucocorticoids promote the development of azoxymethane and dextran sulfate sodium-induced colorectal carcinoma in mice. BMC Cancer. 2019;19:1–10.
7. Fournier AP, Baudron E, Wagnon I, Aubert P, Vivien D, Neunlist M, et al. Environmental enrichment alleviates the deleterious effects of stress in experimental autoimmune encephalomyelitis. Multiple Sclerosis Journal - Experimental, Translational and Clinical. 2020;6.
8. McEwen BS, Karatsoreos IN. Sleep deprivation and circadian disruption: Stress, allostasis, and allostatic load. Sleep Medicine Clinics. 2015;10:1–10. doi:10.1016/j.jsmc.2014.11.007.
9. MacEwen BS. The physiologic response to stress. New England Journal of Medicine. 1998;338:171–9.
10. De Punder K, Pruimboom L. Stress induces endotoxemia and low-grade inflammation by increasing barrier permeability. Frontiers in Immunology. 2015;6 MAY:1–12.
11. Santos J, Benjamin M, Yang PC, Prior T, Perdue MH. Chronic stress impairs rat growth and jejunal epithelial barrier function: role of mast cells. American journal of physiology Gastrointestinal and liver physiology. 2000;278:G847-54. doi:10.1152/ajpgi.2000.278.6.G847.
12. Da Silva S, Robbe-Masselot C, Ait-Belgnaoui A, Mancuso A, Mercade-Loubière M, Salvador-Cartier C, et al. Stress disrupts intestinal mucus barrier in rats via mucin O-glycosylation shift: Prevention by a probiotic treatment. American Journal of Physiology - Gastrointestinal and Liver Physiology. 2014;307:420–9.
13. Labanski A, Langhorst J, Engler H, Elsenbruch S. Stress and the brain-gut axis in functional and chronic-inflammatory gastrointestinal diseases: A transdisciplinary challenge. Psychoneuroendocrinology. 2020;111 April 2019.
14. Ait-Belgnaoui A, Han W, Lamine F, Eutamene H, Fioramonti J, Bueno L, et al. Lactobacillus farciminis treatment suppresses stress induced visceral hypersensitivity: A possible action through interaction with epithelial cell cytoskeleton contraction. Gut. 2006;55:1090–4.
15. Vanhaecke T, Aubert P, Grohard PA, Durand T, Hulin P, Paul-Gilloteaux P, et al. L. fermentum CECT 5716 prevents stress-induced intestinal barrier dysfunction in newborn rats. Neurogastroenterology and Motility. 2017;29:1–12.
16. Kiliaan AJ, Saunders PR, Bijlsma PB, Cecilia Berin M, Taminiau JA, Groot JA, et al. Stress stimulates transepithelial macromolecular uptake in rat jejunum. American Journal of Physiology - Gastrointestinal and Liver Physiology. 1998;275 5 38-5:1037–44.
17. Zheng G, Wu SP, Hu Y, Smith DE, Wiley JW, Hong S. Corticosterone mediates stress-related increased intestinal permeability in a region-specific manner. Neurogastroenterology and Motility. 2013;25:1–21.
18. Cameron HL, Perdue MH. Stress impairs murine intestinal barrier function: Improvement by glucagon-like peptide-2. Journal of Pharmacology and Experimental Therapeutics. 2005;314:214–20.
19. Ahmad R, Sorrell MF, Batra SK, Dhawan P, Singh AB. Gut permeability and mucosal inflammation: Bad, good or context dependent. Mucosal Immunology. 2017;10:307–17.
20. Räsänen T. Fluctuations in the Mitotic Frequency of the Glandular Stomach and Intestine of Rat under the Influence of ACTH, Glucocorticoids, Stress and Heparin. Acta Physiologica Scandinavica. 1963;58:201–10.
21. Tutton PJ, D HR. Stress induced inhibition of jejunal crypt cell proliferation. Virchows Archiv B Cell Pathology. 1973;15:23–34.
22. Greant P, Delvaux G, Willems G. Influence of stress on epithelial cell proliferation in the gut mucosa of

rats. Digestion. 1988;40:212–8.
23. Boudry G, Jury J, Ping CY, Perdue MH. Chronic psychological stress alters epithelial cell turn-over in rat ileum. American Journal of Physiology - Gastrointestinal and Liver Physiology. 2007;292:1228–32.
24. De Palma G, Collins SM, Bercik P, Verdu EF. The microbiota-gut-brain axis in gastrointestinal disorders: Stressed bugs, stressed brain or both? Journal of Physiology. 2014;592:2989–97.
25. Kelly JR, Kennedy PJ, Cryan JF, Dinan TG, Clarke G, Hyland NP. Breaking down the barriers: the gut microbiome, intestinal permeability and stress-related psychiatric disorders. Frontiers in cellular neuroscience. 2015;9 October:392. doi:10.3389/fncel.2015.00392.
26. Bharwani A, Mian MF, Foster JA, Surette MG, Bienenstock J, Forsythe P. Structural and functional consequences of chronic psychosocial stress on the microbiome and host. Psychoneuroendocrinology. 2016;63:217–27.
27. Bailey MT, Dowd SE, Parry NMA, Galley JD, Schauer DB, Lyte M. Stressor exposure disrupts commensal microbial populations in the intestines and leads to increased colonization by Citrobacter rodentium. Infection and Immunity. 2010;78:1509–19.
28. Enqi W, Jingzhu S, Lingpeng P, Yaqin L. Comparison of the Gut Microbiota Disturbance in Rat Models of Irritable Bowel Syndrome Induced by Maternal Separation and Multiple Early-Life Adversity. Frontiers in Cellular and Infection Microbiology. 2021;10 January:1–12.
29. Bangsgaard Bendtsen KM, Krych L, Sørensen DB, Pang W, Nielsen DS, Josefsen K, et al. Gut Microbiota Composition Is Correlated to Grid Floor Induced Stress and Behavior in the BALB/c Mouse. PLoS ONE. 2012;7.
30. Yang CQ, Guo XS, Ji-Li, Wei ZB, Zhao L, Zhao GT, et al. Rifaximin Improves Visceral Hyperalgesia via TRPV1 by Modulating Intestinal Flora in the Water Avoidance Stressed Rat. Gastroenterology Research and Practice. 2020;2020:1–9.
31. Zhang J, Song L, Wang Y, Liu C, Zhang L, Zhu S, et al. Beneficial effect of butyrate-producing Lachnospiraceae on stress-induced visceral hypersensitivity in rats. Journal of Gastroenterology and Hepatology (Australia). 2019;34:1368–76.
32. Li S, Wang Z, Yang Y, Yang S, Yao C, Liu K, et al. Lachnospiraceae shift in the microbial community of mice faecal sample effects on water immersion restraint stress. AMB Express. 2017;7.
33. Watanabe Y, Arase S, Nagaoka N, Kawai M, Matsumoto S. Chronic psychological stress disrupted the composition of the murine colonic microbiota and accelerated a murine model of inflammatory bowel disease. PLoS ONE. 2016;11:1–18.
34. Bailey MT, Dowd SE, Galley JD, Hufnagle AR, Rebecca G, Lyte M. Exposure to social stressors alters the structure of the intestinal microbiota. Brain Behav Immun 2011 March ; 25(3): 397–407 doi:101016/j.bbi201010023. 2011;25:397–407.
35. Durazzi F, Sala C, Castellani G, Manfreda G, Remondini D, De Cesare A. Comparison between 16S rRNA and shotgun sequencing data for the taxonomic characterization of the gut microbiota. Scientific Reports. 2021;11:1–10. doi:10.1038/s41598-021-82726-y.
36. Brooks JP, Edwards DJ, Harwich MD, Rivera MC, Fettweis JM, Serrano MG, et al. The truth about metagenomics: Quantifying and counteracting bias in 16S rRNA studies Ecological and evolutionary microbiology. BMC Microbiology. 2015;15:1–14.
37. Galley JD, Nelson MC, Yu Z, Dowd SE, Walter J, Kumar PS, et al. Exposure to a social stressor disrupts the community structure of the colonic mucosa-associated microbiota. BMC Microbiology. 2014;14:1–13.
38. The Integrative HMP (iHMP) Research Network Consortium. The integrative human microbiome project: Dynamic analysis of microbiome-host omics profiles during periods of human health and disease corresponding author. Cell Host and Microbe. 2014;16:276–89. doi:10.1016/j.chom.2014.08.014.
39. Hasin Y, Seldin M, Lusis A. Multi-omics approaches to disease. Genome Biology. 2017;18:1–15.
40. Tasselli M, Chaumette T, Paillusson S, Monnet Y, Lafoux A, Huchet-Cadiou C, et al. Effects of oral administration of rotenone on gastrointestinal functions in mice. Neurogastroenterology and Motility. 2013;25:183–93.
41. Soumillon M, Cacchiarelli D, Semrau S, van Oudenaarden A, Mikkelsen T. Characterization of directed differentiation by high-throughput single-cell RNA-Seq. bioRxiv. 2014;:003236.
42. Xiong Y, Soumillon M, Wu J, Hansen J, Hu B, Van Hasselt JGC, et al. A Comparison of mRNA Sequencing

with Random Primed and 3′-Directed Libraries. Scientific Reports. 2017;7:1–12.
43. Love MI, Huber W, Anders S. Moderated estimation of fold change and dispersion for RNA-seq data with DESeq2. Genome Biology. 2014;15:1–21.
44. Peng J, Lu G, Xue H, Wang T, Shang X. TS-GOEA: A web tool for tissue-specific gene set enrichment analysis based on gene ontology. BMC Bioinformatics. 2019;20 Suppl 18:1–7. doi:10.1186/s12859-019-3125-6.
45. Bastian FB, Roux J, Niknejad A, Comte A, Fonseca Costa SS, de Farias TM, et al. The Bgee suite: Integrated curated expression atlas and comparative transcriptomics in animals. Nucleic Acids Research. 2021;49:D831–47.
46. Bolyen E, Rideout JR, Dillon MR, Bokulich NA, Abnet CC, Al-Ghalith GA, et al. Reproducible, interactive, scalable and extensible microbiome data science using QIIME 2. Nature Biotechnology. 2019;37:852–7.
47. Amir A, McDonald D, Navas-Molina JA, Kopylova E, Morton JT, Xu ZZ, et al. Deblur Rapidly Resolves Single-Nucleotide Community Sequence Patterns. American Society for Microbiology. 2016;2:1–7.
48. Katoh K, Misawa K, Kuma K, Miyata T. MAFFT: a novel method for rapid multiple sequence alignment based on fast Fourier transform. Nucleic acids research. 2002;30:3059–66.
49. Weiss S, Xu ZZ, Peddada S, Amir A, Bittinger K, Gonzalez A, et al. Normalization and microbial differential abundance strategies depend upon data characteristics. Microbiome. 2017;5:1–18.
50. Meng C, Gholami AM. Multiple Co-inertia Analysis of Multiple OMICS Data using omicade4. 2018;:1–6.
51. Zoppi J, Guillaume JF, Neunlist M, Chaffron S. MiBiOmics: an interactive web application for multi-omics data exploration and integration. BMC Bioinformatics. 2021;22:1–14. doi:10.1186/s12859-020-03921-8.
52. Yu G, Wang LG, Han Y, He QY. ClusterProfiler: An R package for comparing biological themes among gene clusters. OMICS A Journal of Integrative Biology. 2012;16:284–7.
53. Lukonin I, Serra D, Challet Meylan L, Volkmann K, Baaten J, Zhao R, et al. Phenotypic landscape of intestinal organoid regeneration. Nature. 2020;586:275–80. doi:10.1038/s41586-020-2776-9.
54. Donaldson GP, Lee SM, Mazmanian SK. Gut biogeography of the bacterial microbiota. 2016;14:20–32.
55. Bowcutt R, Forman R, Glymenaki M, Carding SR, Else KJ, Cruickshank SM. Heterogeneity across the murine small and large intestine. World Journal of Gastroenterology. 2014;20:15216–32.
56. Larauche M, Kiank C, Taché Y. Corticotropin releasing factor signaling in colon and ileum: regulation by stress and pathophysiological implications. Journal of physiology and pharmacology. 2009;60 Suppl 7:33–46.
57. Sheppard KE, Li KXZ, Autelitano DJ, Karen E, Dominic J. Dehydrogenase Isoforms in Rat Intestinal Epithelia. 1999;:541–7.
58. Sheppard KE. Nuclear receptors. II. Intestinal corticosteroid receptors. American Journal of Physiology - Gastrointestinal and Liver Physiology. 2002;282 5 45-5:742–6.
59. John S, Sabo PJ, Thurman RE, Sung M-H, Biddie SC, Johnson TA, et al. Chromatin accessibility pre-determines glucocorticoid receptor binding patterns HHS. Nat Genet. 2011;43:264–8. doi:10.1038/ng.759.Chromatin.
60. Ghishan FK, Meneely RL. Intestinal maturation: The effect of glucocorticoids on in vivo net magnesium and calcium transport in the rat. Life Sciences. 1982;31:133–8.
61. Tsukada F, Nagura Y, Abe S, Sato N, Ohkubo Y. Effect of restraint and footshock stress and norepinephrine treatment on gastric emptying in rats. Biological and Pharmaceutical Bulletin. 2003;26:368–70.
62. Cao SG, Xia XP, Wang WX, Zheng JJ, Xue ZX. Effects of psychological stress on small intestinal motility, somatostain and substance P levels in plasma and small intestine in mice. World Chinese Journal of Digestology. 2005;13:967–70.
63. Maillot C, Million M, Wei JY, Gauthier A, Taché Y. Peripheral corticotropin-releasing factor and stress-stimulated colonic motor activity involve type 1 receptor in rats. Gastroenterology. 2000;119:1569–79.
64. Ye P, Chiang YJ, Qi Z, Li Y, Wang S, Liu Y, et al. Tankyrases maintain homeostasis of intestinal epithelium by preventing cell death. PLoS Genetics. 2018;14:1–19.
65. Kim M, Morales LD, Jang IS, Cho YY, Kim DJ. Protein tyrosine phosphatases as potential regulators of STAT3 signaling. International Journal of Molecular Sciences. 2018;19:1–19.
66. Riemer P, Rydenfelt M, Marks M, van Eunen K, Thedieck K, Herrmann BG, et al. Oncogenic β-catenin and PIK3CA instruct network states and cancer phenotypes in intestinal organoids. Journal of Cell Biology.

2017;216:1567–77.
67. Xiong X, Wen YA, Fairchild R, Zaytseva YY, Weiss HL, Evers BM, et al. Upregulation of CPT1A is essential for the tumor-promoting effect of adipocytes in colon cancer. Cell Death and Disease. 2020;11. doi:10.1038/s41419-020-02936-6.
68. Matsumoto S, Fujii S, Kikuchi A. Wnt signaling: Biological functions and its implications in diseases: Arl4c is a key regulator of tubulogenesis and tumourigenesis as a target gene of Wnt - β-catenin and growth factor - Ras signalling. Journal of Biochemistry. 2017;161:27–35.
69. Kuhnert F, Davis CR, Wang HT, Chu P, Lee M, Yuan J, et al. Essential requirement for Wnt signaling in proliferation of adult small intestine and colon revealed by adenoviral expression of Dickkopf-1. Proceedings of the National Academy of Sciences of the United States of America. 2004;101:266–71.
70. MacK JA, Maytin E V. Persistent inflammation and angiogenesis during wound healing in K14-directed hoxb13 transgenic mice. Journal of Investigative Dermatology. 2010;130:856–65. doi:10.1038/jid.2009.305.
71. Takahashi D, Hase K, Kimura S, Nakatsu F, Ohmae M, Mandai Y, et al. The epithelia-specific membrane trafficking factor AP-1B controls gut immune homeostasis in mice. Gastroenterology. 2011;141:621–32. doi:10.1053/j.gastro.2011.04.056.
72. Short SP, Li C, Revetta FL, Washington K, Williams CS. Loss of Glutathione Peroxidase 1 Protects the Epithelium from Colitis and Inflammatory Tumorigenesis. Gastroenterology. 2019;156:S-127-S-128. doi:10.1016/s0016-5085(19)37107-0.
73. Han X, Mann E, Gilbert S, Guan Y, Steinbrecher KA, Montrose MH, et al. Loss of guanylyl cyclase C (GCC) Signaling leads to dysfunctional intestinal barrier. PLoS ONE. 2011;6.
74. Gonzalez-Mariscal L, Bautista P, Lechuga S, Quiros M. ZO-2, a tight junction scaffold protein involved in the regulation of cell proliferation and apoptosis. Annals of the New York Academy of Sciences. 2012;1257:133–41.
75. Umeda K, Ikenouchi J, Katahira-Tayama S, Furuse K, Sasaki H, Nakayama M, et al. ZO-1 and ZO-2 Independently Determine Where Claudins Are Polymerized in Tight-Junction Strand Formation. Cell. 2006;126:741–54.
76. Serra D, Mayr U, Boni A, Lukonin I, Rempfler M, Challet Meylan L, et al. Self-organization and symmetry breaking in intestinal organoid development. Nature. 2019;569:66–72.
77. Blutt SE, Klein OD, Donowitz M, Shroyer NF, Guha C, Estes MK. Use of organoids to study regenerative responses to intestinal damage. American Journal of Physiology-Gastrointestinal and Liver Physiology. 2019.
78. Meehan CJ, Beiko RG. A phylogenomic view of ecological specialization in the lachnospiraceae, a family of digestive tract-associated bacteria. Genome Biology and Evolution. 2014;6:703–13.
79. Li J, Wu T, Li N, Wang X, Chen G, Lyu X. Bilberry anthocyanin extract promotes intestinal barrier function and inhibits digestive enzyme activity by regulating the gut microbiota in aging rats. Food and Function. 2019;10:333–43.
80. Yuan F, Tan W, Ren H, Yan L, Wang Y, Luo H. The effects of short-chain fatty acids on rat colonic hypermotility induced by water avoidance stress. Drug Design, Development and Therapy. 2020;14:4671–84.
81. Chowdhury SR, King DE, Willing BP, Band MR, Beever JE, Lane AB, et al. Transcriptome profiling of the small intestinal epithelium in germfree versus conventional piglets. BMC Genomics. 2007;8.
82. Slowicka K, Petta I, Blancke G, Hoste E, Dumas E, Sze M, et al. Zeb2 drives invasive and microbiota-dependent colon carcinoma. Nature Cancer. 2020;1:620–34. doi:10.1038/s43018-020-0070-2.
83. Siavoshian S, Segain JP, Kornprobst M, Bonnet C, Cherbut C, Galmiche JP, et al. Butyrate and trichostatin a effects on the proliferation/differentiation of human intestinal epithelial cells: Induction of cyclin D3 and p21 expression. Gut. 2000;46:507–14.
84. Wilson CA, Browning JL. Death of HT29 adenocarcinoma cells induced by TNF family receptor activation is caspase-independent and displays features of both apoptosis and necrosis. Cell Death and Differentiation. 2002;9:1321–33.

Discussion and Perspectives

CHARACTERIZING THE REGULATION OF BARRIER AND HOMEOSTATIC FUNCTIONS OF THE INTESTINAL EPITHELIAL BARRIER INDUCED BY PSYCHOLOGICAL STRESS

In the current thesis, we characterized the impact of stress upon barrier and homeostatic functions in the distal colon. Although the effects of stress upon paracellular and transcellular permeability were already reported by the literature in various stress models, we identified new regulated functions and in particular cell proliferation, differentiation, and death in the distal colon.

The functional results are surprising with regards to previous studies considering a general increase in intestinal epithelial cells permeability *in vivo* and *ex vivo* in various intestinal organs However, the distal colon was never, to the best of our knowledge, studied separately from the proximal colon in this context. Proximal and distal colons are, although, known to possess different physiologies and differential gene expression that may lead to different proliferative, intestinal permeability profiles and susceptibility to CRC [459, 460]. Moreover, the observed decrease in intestinal permeability remains coherent with the capacity of glucocorticoids to reinforce intestinal epithelial barrier in pro-inflammatory contexts [461, 462]. These protective effects can be alleviated by chronic stress or other mechanisms inducing a decrease in glucocorticoids efficiency, in their production or their bioavailability, or a desensitization of secretagogue receptors (ACTH, CRH, AVP). They could also be mediated by a reduced response of targeted tissues characterized by a desensitization of cortisol receptors (GR, MR). The molecular mechanisms leading to the desensitization of receptors may probably originate from epigenetics [463].

We know that organ specific changes induced by PS are a result of differential chromatin remodeling and accessibility of GRE locus. To the best of our knowledge, if chromatin remodeling was studied and observed in brain regions, it was not studied at all in intestinal segments following a stress event [464]. Moreover, during injury, a phenomenon of plasticity and chromatin remodeling allow EECs or Paneth to dedifferentiate into ISCs but this phenomenon was not studied in terms of regulation of cell death, cell proliferation in enterocytes [465].

We also characterize the transcriptomic response of psychological stress in digestive organs and showed a regional specificity of this response. These organ dependent functions modulated by stress remain to be identified. The GO terms analysis highlighted interesting hypotheses regarding the modulation of gene expression by stress: synaptic remodeling in the ileum and mRNA post transcriptomic remodeling for the jejunum. Using data collected in 4 regions of the brain we could investigate gut brain axis association especially in the ileum and we will see later an example of analysis to be performed.

However, our work also highlighted the limit of functional enrichment analysis: they are restricted to database knowledge and general biological pathways, and they ignored regional functions of genes [415]. We need to rethink the way we study transcriptomic data expression: in our study we used for example a primary selection of enrichment terms related to the tissue/organ of interest. But we can think of other approaches. Since we observed the remodeling of homeostatic function an interesting development would be the integration, in the analysis pipeline, of selection and in-depth analysis of changes in transcription factors and co-factors [466].

All in all, the results of this transcriptomic analysis, partially validated with our *in situ* characterization of distal colonic tissue, and *in vitro* model of stress derived organoids, requires further qPCR analysis to confirm the presence of these genes, and KO experiments to unravel their implication in intestinal epithelial cell proliferation, differentiation and apoptosis.

THE ORGANOID MODEL AND ITS UTILITY TO STUDY STRESS-INDUCED MODULATION OF THE HOST-MICROBIOTA INTERACTOME

Through the culture of organoids derived from stressed and control animals, our objective was to identify a putative reprogramming or long term induced effects of PS upon colonic epithelium homeostatic functions. Following development of experimental protocol to obtain organ specific colonoids (i.e., proximal vs distal colon ones – unpublished data), we were able to observe significant morphological differences between control and stressed derived organoids. Surprisingly, our stressed derived organoids were less proliferative and more undifferentiated compared to control organoids based on morphological parameters analysis. We hypothesized that stress, in the organoid model, induced a delay in the proliferation/differentiation transition of the gut epithelium coherent with previous studies [467, 468]

The absence of pro-proliferative response induced by stress in our organoids could also be explained by the nature of organoids culture which does not include all the microenvironmental signals of *in vivo* models and especially the absence of the gut microbiota. This hypothesis is supported by the fact that, the fecal derived supernatant, containing certainly gut microbiota derived metabolite, was an important actor of cell proliferation induced by stress.

Organoids recapitulate intestinal functions and show in this experiment a long-term effect of stress upon intestinal epithelial homeostatic functions. These long-term effects are coherent with the previously hypothesized remodeling of chromatin induced by stress.

Another objective could be the generalization of organoid models to describe the dynamics of stress-induced gut epithelial homeostasis modulation. The limitation of the organoid model is that it is devoid of signals from surrounding tissue (fibroblast, ENS, immune system) and is not in contact with the microbiota anymore [469]. The exposition of organoids to glucocorticoids (or other host factors induced by stress: CHR, epinephrine…) could help identify how they participate in the remodeling of intestinal epithelial cells' functions.

Therefore, a perspective regarding organoid culture could be to characterize their morphological features when exposed to stressed mice fecal supernatant or the identified bacteria involved in the pro-proliferative response. We hypothesize that this exposition could resolved the delay in the proliferation/differentiation transition observed in stressed derived organoids. Indeed, organoid models can become a good model to study host-microbiota interaction [470]. In this model, we would use everted generated organoids, characterized by their apical surface facing the external milieu, itself filled with supernatant or the identified cultured bacteria of our study [471].

PERSPECTIVES TO STUDY THE MODULATIONS OF THE GUT MICROBIOTA TAXONOMIC AND FUNCTIONAL DIVERSITY INDUCED BY STRESS.

The impact of stress upon the distal colonic epithelial-associated and luminal microbiota was then performed using 16S rRNA sequencing on both luminal content and epithelial cells of the distal colon. The analysis revealed an increased α-diversity and changes in the abundance of one epithelial-associated bacteria and 3 luminal genera. The causes of these bacterial abundances changes induced by stress are not know but could partially be caused by the remodeling of mucus properties (and especially muc2) by corticosteroids [472].Another factor potentially involved in the effects of stress on the regional gut microbiota could be WAS effects on gut motility. Differential changes induced by WAS procedure in intestinal motility (slowing in proximal vs acceleration in distal part) could contribute to explain the differential regulation of proximal and distal microbiota by PS.

Taxonomic diversity and abundance analysis are a good tool to identify potential biomarkers/genera associated with a phenotype of interest. However, they are limited since they cannot resolve taxonomic information at the scale of the species. Moreover, the concept of species in prokaryotes is complex since horizontal gene transfer between species makes compartmentalization of genetic information difficult. The definition of the microbiota tends to become more and more functional with the generalization of shotgun metagenomic sequencing [384] and the discovery of new concepts like metabolic niches [473, 474]. However, studying the microbiota from a taxonomic perspective should not be stopped. We observed, in our results, differences in the epithelial-associated and luminal microbiota. A previous study showed that stress and external threat induced a dynamic exchange between the luminal and epithelial associated microbiota [198]. These dynamical changes should be therefore studied in time-series experiments. We also propose to describe the microbiota not only from the prism of diversity and abundance changes but with new measures including a concept of entropy between luminal and epithelial compartment or even between intestinal segments. Gut microbiotas are exchanged dynamically between segments and environmental challenges may not only modify their abundance but also change their distribution leading ultimately to regional loss of specific ecological niches in intestinal segments.

HOST-MICROBIOTA INTERACTOME VERSUS GUT-BRAIN-MICROBIOTA INTERACTOME

To infer associations between host epithelial cells and gut microbiota, the development of multi-omics tools was required. If multi-omics studies are more and more employed since 2005 [440], no gold standard methods emerged from the multiplicity of tools already developed [442]. Generalized methods applicable to all -omics combinations have been used like mixOmics [443] but remain non accessible to biologists without programming skills and only proposed discriminant techniques. We, therefore developed MiBiOmics, a web-based and standalone application, for exploratory multi-omics analysis using networks and ordination techniques. A comparison between MiBiOmics and mixOmics analysis pipeline showed complementary results, and complementary performance on different -omics datasets [477]. Since its development, MiBiOmics was already used to infer association between gut microbiota dysbiosis and hypothalamic variations induced by a Western Diet in rats. This tool highlighted the interactions of *E. fergusonii* and *F. plautii* and cecal metabolites involved in early hypothalamic oxidative stress [478]. MiBiOmics was also used in still unpublished work and could, thus, set the basis for the generalization of exploratory network-based approaches in multi-omics analysis. Future development in MiBiOmics includes the growth of memory resources and the integration of OPLS regression on subsets of multiple coinertia drivers. We also want to develop new visualization tools for the interpretation of multi-omics analysis results.

With MiBiOmics, we extracted a subset of significantly associated drivers to cell proliferation and cell death and observed distinct multi-omics signatures with no common epithelial genes, luminal or epithelial-associated microbiota between the two subsets of drivers. This multi-omics approach remains to be employed on other intestinal segments and in association with other functional parameters. We applied for instance, multi-WGCNA analysis on the proximal colon to identify epithelial-associated, luminal microbiota and epithelial genes related to changes in transcellular and paracellular permeability (See annex 1): The transcellular permeability found increased in the colon was associated in this analysis with two modules of epithelial associated microbiota and to a module of genes enriched in functions associated to modulation of the brush border membrane. However, this analysis needs to be further investigated to extract hypotheses and more importantly to confirm experimentally the generated hypotheses.

PS and its impact on intestinal host-microbiota is a fine example of modulation of the gut-brain-microbiota axis. We also propose to characterize regional gut-brain-microbiota interactions to identify biomarkers of these bidirectional interactions and infer hypotheses on the mechanistic behind gut-brain communications roads. Modulation of the gut-brain axis modulation by stress is still under investigation and is a short-term perspective of the project.

STRESS AND FUNCTIONAL PATHOLOGICAL CONSEQUENCES

Finally, to validate the implication of the gut microbiota in the remodeling of epithelial cell homeostatic functions induced by stress we exposed HT-29 cell culture to fecal supernatant retrieved from stressed animals. First, an effort should be done to validate the differential response observed in primary intestinal cell culture on organoid models since they possess different phenotypic and functional properties.

The identification of host-microbiota signatures implicated in the remodeling of epithelial homeostatic functions induced by stress set the basis for the characterization of host and microbial biomarkers involved in the onset and development of chronic diseases. As stress is recognized as a key contributor in intestinal chronic diseases, there is a need to unravel the mechanisms underlying its implication in barrier dysfunctions. Our results demonstrate a distinct regional upregulation of pro-proliferative processes in the distal colonic epithelium and identified host-microbiota interactions implicated in the development of CRC. If mediators of the stress response were positively associated with the development and growth of CRC [319–321], the effects of PS upon its induction remain uncharacterized. As an immediate perspective we, therefore, propose to describe how PS participates in the induction of CRC. Preliminary results were generated from an *in vivo* study, focused on the characterization of the effect of chronic stress upon tumorigenesis. They showed no difference in size or number of mature tumors in the colon of mice subjected to chronic WAS stress and AOM injections compared to control mice with AOM injections (Annex 3). However, the impact of stress upon tumor growth and development remains unknown in this model. We are currently characterizing the number of aberrant crypts in the colonic epithelium of stressed mice as compared to control to unravel how stress participates in the initiation of adenomas in colonic epithelium.

Moreover, using targeted multi-omics correlation networks available in MiBiOmics we could describe how brain regional gene expressions are involved in the regulation of intestinal epithelial genes and gut microbiota abundance. Analysis of prefrontal cortex, hippocampus, hypothalamus related to changes in host epithelial and microbial changes in the proximal colon are currently under study. Primary results show differential modulation of the gut-brain axis with modulation of synaptic transmission in the hippocampus stressed mice associated with the remodeling of mitochondrial energy metabolism in the epithelium of the proximal colon and the abundance of ASVs (See Annex 2).

With our combined approach, we showed that PS modulates regional gut epithelial homeostatic functions via the remodeling of host-microbiota interactions. PS induces a pro-apoptotic response in the early stage of acute stress followed by a pro-proliferative and pro-regenerative response characterized by changes of host-microbiota associations in the distal colon. This project opened new perspectives and showed the importance of designing new systemic method to study gut homeostasis and stress response. We were able, during these three years, to formulate hypotheses with bioinformatic tools and validate some of them with experimental approaches. This transversal approach remains to be applied to the other organ regions and the modulation of the gut brain axis by the stress response is still under-study.

General Conclusion

In this thesis, we were able to develop a tool to study associations between the host and its associated microbiota. We showed that stress modifies differentially the gene expression of gut epithelia between different digestive organ regions. We highlighted a pro-proliferative and pro-regenerative response specific to the epithelium of the distal colon. With an immunohistochemistry approach, we validated the increase in cell proliferation induced by stress in the distal colon and showed an additional increase in cell apoptosis. The development of an organoid model dedicated to the study of the distal colonic epithelium showed an imprinting of the changes in homeostatic functions induced by stress in epithelial cells. These changes in homeostatic functions were accompanied by modification in barrier functions as, in the distal colon, permeability was decreased by stress. Colonic microbiota diversity and composition were also found affected. In the distal colon the α-diversity was increased by stress, and we found the abundance of the ASV Lachnospiraceae NK4A136 g largely decreased in the epithelial-associated microbiota. Within the luminal microbiota of the distal colon, several genera's abundances were found modified. Finally, we were able to extract multi-omics associative signature including epithelial genes, epithelial-associated and luminal microbiota related to the increase in cell proliferation and cell death between control and stress individuals. To evaluate the capacity of the gut microbiota to affect epithelial homeostatic functions we measure the levels of SCFAs between control and stressed mice. Butyrate, Acetate, Propionate and total SCFAs were found decreased by stress. Furthermore, the exposition of HT-29 cells to fecal supernatant derived from stressed mice induced an increase in cell proliferation and total number of cells in culture compared to HT-29 cells subjected to fecal supernatant derived from control mice.

Altogether these results characterized the stress response in gut epithelium gene expression, homeostatic and barrier functions. We identified bacteria implicated in the remodeling of epithelial homeostatic functions induced by stress and hypothesized on how their products may influence cell proliferation.

The identification of multi-omics associative signatures related to the stress response should now be compared to data from human cohort to validate potential therapeutic target in stress related disorders. With personalized approaches combining probiotic, postbiotic and/or pharmaceutical target we could develop strategies to resolve defect of the host-microbiota interactome.

Annex

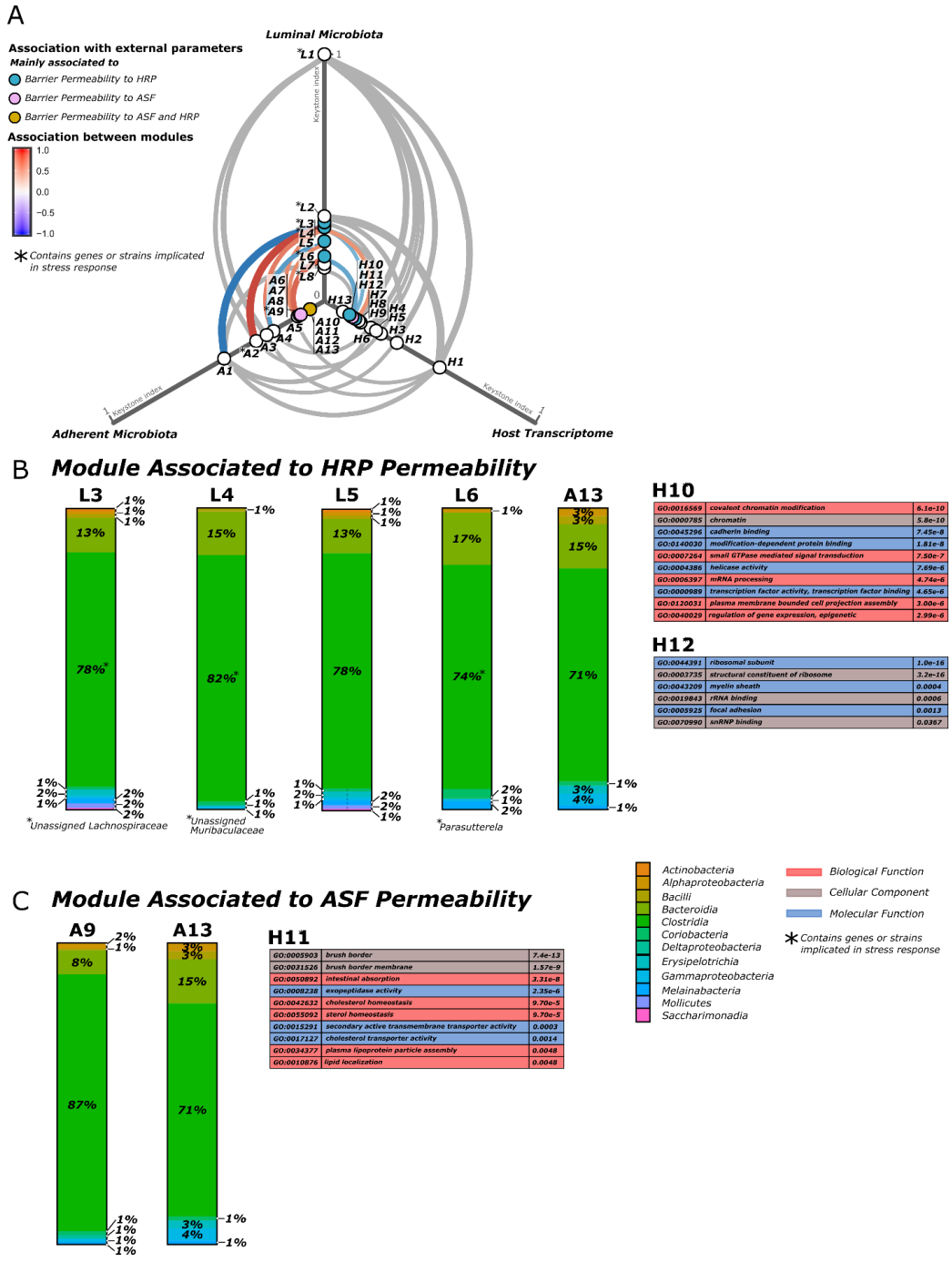

*Figure 27 Multi-WGCNA modules associated with changes in ASF and HRP permeability in luminal, epithelial-associated and host epithelial genes of the proximal colon. A Tri-partite hive plot describing the associations between multi-WGCNA modules. On each axis, the modules are ordered according to their keystone index (a measure of their interconnectivity in the network). They are colored according to their associations to permeability parameters. The size and color of the edges linking modules indicate the strength of correlation between these modules. B. Modules associated with HRP permeability changes. Relative order compositions of luminal and epithelial-associated modules are represented. * Indicates the presence of differentially expressed genes induced by repeated WAS in the module. Host epithelial modules are illustrated with their functional GO-term enrichment. C. Modules associated to ASF permeability changes. Relative order compositions of luminal and epithelial-associated modules are represented. * Indicates the presence of differentially expressed genes induced by repeated WAS in the module. Host epithelial modules are illustrated with their functional GO-term enrichment.*

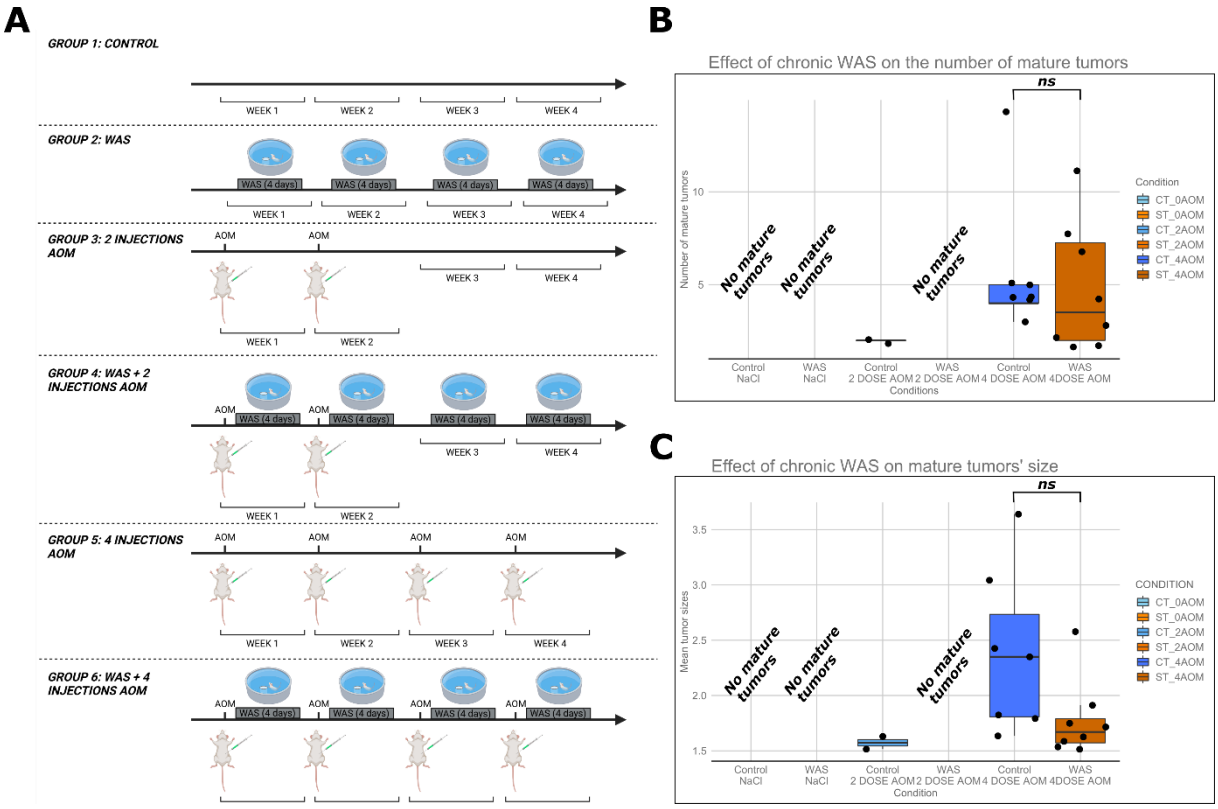

Figure 28 Macroscopic characterization of chronic WAS effects upon mature tumors' number and size. 6 experimental groups were used. Group 1 included control mice with intra-peritoneal NaCl injections. In group 2, mice were subjected to 4 cycles of WAS procedure (1h for 4 consecutive days) and intra-peritoneal NaCl injections. Group 3 included mice subjected to 2 intra-peritoneal AOM injections at week 1 and week 2. In group 4, mice were subjected to 4 cycles of WAS procedure (1h for 4 consecutive days) and 2 intra-peritoneal AOM injections. Group 5 mice had 4 intra-peritoneal AOM injections. Finally group 6 mice were subjected to 4 cycles of WAS procedure (1h for 4 consecutive days) and 4 intra-peritoneal AOM injections. B. Chronic WAS had no effects on the number of mature tumors. C. Chronic WAS had no effects on the mean size of mature tumors.

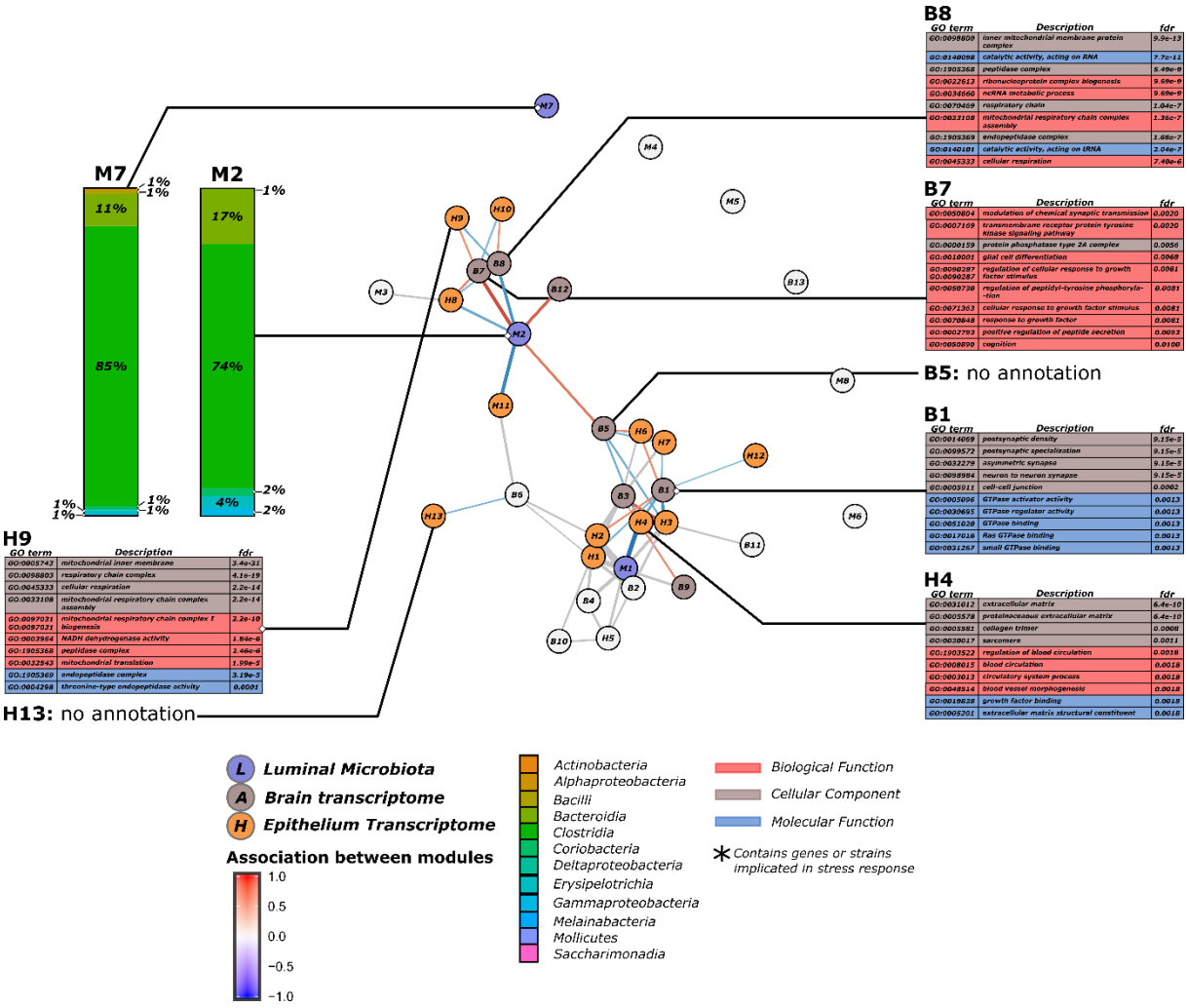

Figure 29 Multi-WGCNA modules associated with changes in corticosterone levels in epithelial genes of the proximal colon, genes of the hippocampus and proximal colon microbiota. Tri-partite network describing the associations between multi-WGCNA modules. Hippocampus genes' modules are colored in grey, proximal colonic epithelial genes' modules are in orange and proximal colonic microbiota's modules are colored in blue. Only modules associated to corticosterone and their neighbors are colored. The size and color of the edges linking modules indicate the strength of correlation between these modules. Modules associated with corticosterone concentration changes are described. Relative order compositions of luminal and epithelial-associated modules are represented.

Publications, oral presentation and posters

PUBLICATIONS PRESENTED IN THE CURRENT THESIS:

1) Zoppi J, Guillaume JF, Neunlist M, Chaffron S. MiBiOmics: an interactive web application for multi-omics data exploration and integration. BMC Bioinformatics. 2021;22:1–14. doi:10.1186/s12859-020-03921-8
2) Zoppi J, Marchix J, Bordron P, Durand T, Bessard A, Aubert P, Eveillard D, Parnet P, Mahe M, Chaffron S, Neunlist M. Multi-omics and functional characterization of psychological stress induced modulation of microbiota host-interactions in colonic epithelial cells. In preparation.

PUBLICATIONS NOT PRESENTED IN THE CURRENT THESIS:

1) Selber-Hnatiw S, Sultana T, Tse W, Abdollahi N, Abdullah S, Al Rahbani J, Zoppi J et al. Metabolic networks of the human gut microbiota. Microbiology (United Kingdom). 2020;166:96–119. (Contribution to the redaction of the *Microbial SCFAs and their effects on the gut microbiota and host metabolism*)
2) Fouesnard M, Zoppi J, Petera M, Le Gleau L, Migné C, Devime F, et al. Dietary switch to Western diet induces hypothalamic adaptation associated with gut microbiota dysbiosis in rats. International Journal of Obesity. 2021;45:1271–83. doi:10.1038/s41366-021-00796-4. (Contribution to this publication by performing multi-omics correlative analysis)
3) Gonzales J, Marchix J, Aymeric L, Le Berre-Scoul C, Zoppi J, Bordron P, et al. Fecal supernatant from adult with autism spectrum disorder alters digestive functions, intestinal epithelial barrier, and enteric nervous system. Microorganisms. 2021;9.

ORAL PRESENTATION:

1) Analyse Hôte-Microbiote, Journée Microbiote et Santé 2019, Nantes.
2) Development of a graph-based multi-omics data analysis framework for the characterization of host-microbiota interaction, NEM 2019, Nantes.
3) Effect of chronic stress on the spatial distribution of the host-microbiota interactome along mice intestine, GFNG 2019, Toulouse.
4) Environmentally induced neurodevelopmental diseases: Toward the characterization of the microbiome-gut-brain axis interactome, MiBiogate congress, 2019, Nantes.

5) Characterization of the host-microbiota interactome in mice reveals a regionalization of the stress response around the barrier, What's up Microbiote \& Santé, 2021, virtual congress.
6) Characterization of the host-microbiota interactome in mice reveals a regionalization of the stress response around the barrier, GFNF 2021, Rennes.

POSTERS:

1) MiBiOmics, a shiny application for graph-based multi-omics analysis, JOBIM 2019, Nantes.
2) Effect of chronic stress on the host-microbiota interaction in mice Proximal Colon, DHU 2019, Nantes.
3) The mice gut biogeography of the host-microbiota interactome, MiBiogate congress 2019, Nantes.
4) Characterization of the host-microbiota interactome in mice colon reveals a regionalization of the stress response around the barrier, IHMC 2021, virtual congress.

References:

1. Mescher A. Junqueira's Basic Histology. 13th edition. McGraw-Hill Education/Medical; 2013.

2. Simmons NS. Studies on the defense mechanisms of the mucous membranes with particular reference to the oral cavity. Oral Surgery, Oral Medecine and Oral Pathology. 1952;5:513–26.

3. Ganong W. Review of Medical Physiology. 15th edition. Connecticut: Appleton and Lange; 1991.

4. Mittal RK. Peristalsis in the Circular and Longitudinal Muscles of the Esophagus. In: Sciences. M& CL, editor. Motor Function of the Pharynx, Esophagus, and its Sphincters. 2011.

5. Kuo B, Urma D. Esophagus - anatomy and development. GI Motility online. 2006.

6. Barrett K. Gastrointestinal Physiology. McGraw-Hil. New York, NY; 2014.

7. Bornhorst GM. Gastric Mixing during Food Digestion: Mechanisms and Applications. Annual Review of Food Science and Technology. 2017;8 January:523–42.

8. Hoyle T. The digestive system: linking theory and practice. British journal of nursing (Mark Allen Publishing). 1997;6:1285–91.

9. Vanden Berghe P, Janssen P, Kindt S, Vos R, Tack J. Contribution of different triggers to the gastric accommodation reflex in humans. American Journal of Physiology - Gastrointestinal and Liver Physiology. 2009;297:902–6.

10. Agace WW, McCoy KD. Regionalized Development and Maintenance of the Intestinal Adaptive Immune Landscape. Immunity. 2017;46:532–48. doi:10.1016/j.immuni.2017.04.004.

11. Kooij IA, Sahami S, Meijer SL, Buskens CJ, te Velde AA. The immunology of the vermiform appendix: a review of the literature. Clinical and Experimental Immunology. 2016;186:1–9.

12. Enders G. Gut: The Inside Story of Our Body's Most Underrated Organ. Greystone. 2015.

13. Hortsch M. Small and Large Intestine | histology. 2021. https://histology.medicine.umich.edu/resources/small-large-intestine.

14. Salvo-Romero E, Alonso-Cotoner C, Pardo-Camacho C, Casado-Bedmar M, Vicario M. The intestinal barrier function and its involvement in digestive disease. Revista Espanola de Enfermedades Digestivas. 2015;107:686–96.

15. Hsu M, Safadi AO, Lui F. Physiology , Stomach. StatPearls Publishing; 2021.

16. Krause WJ. Brunner's glands: A structural, histochemical and pathological profile. Progress in Histochemistry and Cytochemistry. 2000;35:255–367. doi:10.1016/S0079-6336(00)80006-6.

17. Cornes JS. Number, size, and distribution of Peyer's patches in the human small intestine: Part I The development of Peyer's patches. Gut. 1965;6:225–9.

18. Schroeder BO. Fight them or feed them: How the intestinal mucus layer manages the gut microbiota. Gastroenterology Report. 2019;7:3–12.

19. Xiao S, Zhou L. Gastric Stem Cells: Physiological and Pathological Perspectives. Frontiers in Cell and Developmental Biology. 2020;8 September:1–13.

20. Santos J, Benjamin M, Yang PC, Prior T, Perdue MH. Chronic stress impairs rat growth and jejunal epithelial barrier function: role of mast cells. American journal of physiology Gastrointestinal and liver physiology. 2000;278:G847-54. doi:10.1152/ajpgi.2000.278.6.G847.

21. Karmakar S, Deng L, He XC, Li L. Intestinal epithelial regeneration: Active versus reserve stem cells and plasticity mechanisms. American Journal of Physiology - Gastrointestinal and Liver Physiology.

2020;318:G796–802.

22. Potten CS, Hume WJ, Reid P, Cairns J. The segregation of DNA in epithelial stem cells. Cell. 1978;15:899–906.

23. Bjerknes M, Cheng H. Gastrointestinal stem cells. II. Intestinal stem cells. American Journal of Physiology - Gastrointestinal and Liver Physiology. 2005;289 3 52-3:381–7.

24. Li L, Clevers H. Coexistence of Quiescent and Active Adult Stem Cells in Mammals. Science. 2010;327:542–5. doi:oi:10.1126/science.1180794.

25. Van Es JH, Sato T, Van De Wetering M, Lyubimova A, Yee Nee AN, Gregorieff A, et al. Dll1 + secretory progenitor cells revert to stem cells upon crypt damage. Nature Cell Biology. 2012;14:1099–104.

26. Schmitt M, Schewe M, Sacchetti A, Feijtel D, van de Geer WS, Teeuwssen M, et al. Paneth Cells Respond to Inflammation and Contribute to Tissue Regeneration by Acquiring Stem-like Features through SCF/c-Kit Signaling. Cell Reports. 2018;24:2312-2328.e7. doi:10.1016/j.celrep.2018.07.085.

27. Leushacke M, Tan SH, Wong A, Swathi Y, Hajamohideen A, Tan LT, et al. Lgr5-expressing chief cells drive epithelial regeneration and cancer in the oxyntic stomach. Nature Cell Biology. 2017;19:774–86.

28. Barker N, Van Es JH, Kuipers J, Kujala P, Van Den Born M, Cozijnsen M, et al. Identification of stem cells in small intestine and colon by marker gene Lgr5. Nature. 2007;449:1003–7.

29. Sangiorgi E, Capecchi MR, Genet Author manuscript N. Bmi1 is expressed in vivo in intestinal stem cells NIH Public Access Author Manuscript. Nat Genet. 2008;40:915–20. doi:10.1038/ng.165.Bmi1.

30. Muñoz J, Stange DE, Schepers AG, Van De Wetering M, Koo BK, Itzkovitz S, et al. The Lgr5 intestinal stem cell signature: Robust expression of proposed quiescent ' +4' cell markers. EMBO Journal. 2012;31:3079–91.

31. Sigal M, Logan CY, Kapalczynska M, Mollenkopf HJ, Berger H, Wiedenmann B, et al. Stromal R-spondin orchestrates gastric epithelial stem cells and gland homeostasis. Nature. 2017;548:451–5. doi:10.1038/nature23642.

32. Hayakawa Y, Jin G, Wang H, Chen X, Westphalen CB, Asfaha S, et al. CCK2R identifies and regulates gastric antral stem cell states and carcinogenesis. Gut. 2015;64:544–53.

33. Allaire JM, Crowley SM, Law HT, Chang SY, Ko HJ, Vallance BA. The Intestinal Epithelium: Central Coordinator of Mucosal Immunity. Trends in Immunology. 2018;39:677–96. doi:10.1016/j.it.2018.04.002.

34. Kong SE, Heel K, McCauley R, Hall J. The role of enterocytes in gut dysfunction. Pathology Research and Practice. 1998;194:741–51. doi:10.1016/S0344-0338(98)80063-0.

35. Pelaseyed T, Bergström J, Gustafsson JK, Ermund A, Birchenough GMH, Schütte A, et al. The mucus and mucins of the goblet cells and enterocytes provide the first defense line of the gastrointestinal tract and interact with the immune system. Immunology Review. 2014;260:8–20.

36. Teshima CW, Meddings JB. The measurement and clinical significance of intestinal permeability. Current Gastroenterology Reports. 2008;10:443–9.

37. Abreu MT, Vora P, Faure E, Thomas LS, Arnold ET, Arditi M. Decreased Expression of Toll-Like Receptor-4 and MD-2 Correlates with Intestinal Epithelial Cell Protection Against Dysregulated Proinflammatory Gene Expression in Response to Bacterial Lipopolysaccharide. The Journal of Immunology. 2001;167:1609–16.

38. Miron N, Cristea V. Enterocytes: Active cells in tolerance to food and microbial antigens in the gut. Clinical and Experimental Immunology. 2012;167:405–12.

39. Cheng H, Leblond C. Origin, differentiation and renewal of the four main epithelial cell types in the mouse small intestine. I. Columnar cell, II. mucous cell, III. entero-endocrine cells, IV. Paneth cells. American Journal of Anatomy. 1974;141:461–536.

40. Shields JM, Christy RJ, Yang VW. Identification and Characterization of a Gene Encoding a Gut-enriched Krüppel-like Factor Expressed during Growth Arrest. Journal of Biological Chemistry. 1996;271:20009–17.

41. Qin X, Caputo FJ, Xu DZ, Deitch EA. Hydrophobicity of mucosal surface and its relationship to gut barrier function. Shock. 2008;29:372–6.

42. Hansson GC, Johansson MEV. The inner of the two Muc2 mucin-dependent mucus layers in colon is devoid of bacteria. Gut Microbes. 2010;1:51–4.

43. Berry D, Stecher B, Schintlmeister A, Reichert J, Brugiroux S, Wild B, et al. Host-compound foraging by intestinal microbiota revealed by single-cell stable isotope probing. Proceedings of the National Academy of Sciences of the United States of America. 2013;110:4720–5.

44. McDole JR, Wheeler LW, McDonald KG, Wang B, Konjufca V, Knoop KA, et al. Goblet cells deliver luminal anrigen to CD103+ DCs in the small intestine. Nature. 2012;483:345–9.

45. McCauley HA, Guasch G. Three cheers for the goblet cell: Maintaining homeostasis in mucosal epithelia. Trends in Molecular Medicine. 2015;21:492–503.

46. Treveil A, Sudhakar P, Matthews ZJ, Wrzesinski T, Jones EJ, Brooks J, et al. Identification of master regulators in goblet cells and Paneth cells using transcriptomics profiling of gut organoids and multi-layered networks. bioRxiv. 2019;:575845. https://www.biorxiv.org/content/10.1101/575845v2.full.

47. Sei Y, Lu X, Liou A, Zhao X, Wank SA. A stem cell marker-expressing subset of enteroendocrine cells resides at the crypt base in the small intestine. American Journal of Physiology - Gastrointestinal and Liver Physiology. 2011;300.

48. Gribble FM, Reimann F. Enteroendocrine Cells: Chemosensors in the Intestinal Epithelium. Annual Review of Physiology. 2016;78:277–99.

49. Gribble FM, Reimann F. Function and mechanisms of enteroendocrine cells and gut hormones in metabolism. Nature Reviews Endocrinology. 2019;15:226–37. doi:10.1038/s41574-019-0168-8.

50. Worthington JJ, Reimann F, Gribble FM. Enteroendocrine cells-sensory sentinels of the intestinal environment and orchestrators of mucosal immunity. Mucosal Immunology. 2018;11:3–20. doi:10.1038/mi.2017.73.

51. Drucker DJ. Evolving concepts and translational relevance of enteroendocrine cell biology. Journal of Clinical Endocrinology and Metabolism. 2016;101:778–86.

52. Guo X, Lv J, Xi R. The specification and function of enteroendocrine cells in Drosophila and mammals: a comparative review. FEBS Journal. 2021;:1–24.

53. Grün D, Lyubimova A, Kester L, Wiebrands K, Basak O, Sasaki N, et al. Single-cell messenger RNA sequencing reveals rare intestinal cell types. Nature. 2015;525:251–5.

54. Nagatake T, Fujita H, Minato N, Hamazaki Y. Enteroendocrine cells are specifically marked by cell surface expression of claudin-4 in mouse small intestine. PLoS ONE. 2014;9.

55. Kucharzik T, Lügering N, Rautenberg K, Lügering A, Schmidt MA, Stoll R, et al. Role of M cells in intestinal barrier function. Annals of the New York Academy of Sciences. 2000;915:171–83.

56. Miller H, Zhang J, KuoLee R, Patel GB, Chen W. Intestinal M cells: The fallible sentinels? World Journal of Gastroenterology. 2007;13:1477–86.

57. Ohno H. Intestinal M cells. Journal of Biochemistry. 2015;159:151–60.

58. Schneider C, O'Leary CE, Locksley RM. Regulation of immune responses by tuft cells. Nature Reviews Immunology. 2019;19:584–93. doi:10.1038/s41577-019-0176-x.

59. Gerbe F, Sidot E, Smyth DJ, Ohmoto M, Matsumoto I, Dardalhon V, et al. Intestinal epithelial tuft cells initiate type 2 mucosal immunity to helminth parasites. Nature. 2016;529:226–30. doi:10.1038/nature16527.

60. Howitt MR, Lavoie S, Michaud M, Blum AM, Tran S V, Weinstock J V, et al. Tuft cells, taste-chemosensory cells, orchestrate parasite type 2 immunity in the gut. Science. 2016;351:1329–33.

61. Haber AL, Biton M, Rogel N, Herbst RH, Shekhar K, Smillie C, et al. A single-cell survey of the small intestinal epithelium. Nature. 2017;551:333–9.

62. Gerbe F, Legraverend C, Jay P. The intestinal epithelium tuft cells: Specification and function. Cellular and Molecular Life Sciences. 2012;69:2907–17.

63. Cunliffe RN, Rose FRAJ, Keyte J, Abberley L, Chan WC, Mahida YR. Human defensin 5 is stored in precursor form in normal Paneth cells and is expressed by some villous epithelial cells and by metaplastic Paneth cells in the colon in inflammatory bowel disease. Gut. 2001;48:176–85.

64. Bry L, Falk P, Huttner K, Ouellette A, Midtvedt T, Gordon JI. Paneth cell differentiation in the developing intestine of normal and transgenic mice. Proceedings of the National Academy of Sciences of the United States of America. 1994;91:10335–9.

65. Bevins CL, Salzman NH. Paneth cells, antimicrobial peptides and maintenance of intestinal homeostasis. Nature Reviews Microbiology. 2011;9:356–68.

66. Sato T, Van Es JH, Snippert HJ, Stange DE, Vries RG, Van Den Born M, et al. Paneth cells constitute the niche for Lgr5 stem cells in intestinal crypts. Nature. 2011;469:415–8.

67. Stappenbeck TS. Paneth Cell Development, Differentiation, and Function: New Molecular Cues. Gastroenterology. 2009;137:30–3.

68. Troughton WD, Trier JS. Paneth and goblet cell renewal in mouse duodenal crypts. The Journal of cell biology. 1969;41:251–68.

69. Mori-Akiyama Y, van den Born M, van Es JH, Hamilton SR, Adams HP, Zhang J, et al. SOX9 Is Required for the Differentiation of Paneth Cells in the Intestinal Epithelium. Gastroenterology. 2007;133:539–46.

70. Clevers HC, Bevins CL. Paneth cells: Maestros of the small intestinal crypts. Annual Review of Physiology. 2013;75:289–311.

71. Fre S, Huyghe M, Mourikis P, Robine S, Louvard D, Artavanis-Tsakonas S. Notch signals control the fate of immature progenitor cells in the intestine. Nature. 2005;435:964–8.

72. Beumer J, Clevers H. Cell fate specification and differentiation in the adult mammalian intestine. Nature Reviews Molecular Cell Biology. 2021;22:39–53. doi:10.1038/s41580-020-0278-0.

73. Jeon MK. Intestinal barrier: Molecular pathways and modifiers. World Journal of Gastrointestinal Pathophysiology. 2013;4:94.

74. Koch S. Extrinsic control of Wnt signaling in the intestine. Differentiation. 2017;97 June:1–8. doi:10.1016/j.diff.2017.08.003.

75. Niehrs C. Function and biological roles of the Dickkopf family of Wnt modulators. Oncogene. 2006;25:7469–81.

76. Van Der Flier LG, Clevers H. Stem cells, self-renewal, and differentiation in the intestinal epithelium. Annual Review of Physiology. 2009;71:241–60.

77. He TC, Sparks AB, Rago C, Hermeking H, Zawel L, Da Costa LT, et al. Identification of c-MYC as a

target of the APC pathway. Science. 1998;281:1509–12.

78. Kim AK, Kakitani M, Zhao J, Oshima T, Tang T, Binnerts M, et al. Mitogenic Influence of Human R-Spondin1 on the Intestinal Epithelium. American Association for the Advancement of Science. 2005;309:1256–9.

79. Wong MH, Huelsken J, Birchmeier W, Gordon JI. Selection of multipotent stem cells during morphogenesis of small intestinal crypts of Lieberkühn is perturbed by stimulation of Lef-1/β-catenin signaling. Journal of Biological Chemistry. 2002;277:15843–50. doi:10.1074/jbc.M200184200.

80. Valenta T, Degirmenci B, Moor AE, Herr P, Zimmerli D, Moor MB, et al. Wnt Ligands Secreted by Subepithelial Mesenchymal Cells Are Essential for the Survival of Intestinal Stem Cells and Gut Homeostasis. Cell Reports. 2016;15:911–8.

81. Perochon J, Carroll LR, Cordero JB. Wnt signalling in intestinal stem cells: Lessons from mice and flies. Genes. 2018;9:1–19.

82. Blobe GC, Schiemann WP, Lodish HF. Role of transforming growth factor beta in human disease. The New England Journal of Medecine. 2000;342:1350–8.

83. Fiocchi C. TGF-β/Smad signaling defects in inflammatory bowel disease: Mechanisms and possible novel therapies for chronic inflammation. Journal of Clinical Investigation. 2001;108:523–6.

84. Markowitz S, Wang J, Myeroff L, Parsons R, Sun L, Lutterbaugh J, et al. Inactivation of the type 11 TGF-f receptor in Colon Cancer Cells with Microsatellite Instability. Science. 1995;268 June:1336–8.

85. Haramis APG, Begthel H, Van Den Born M, Van Es J, Jonkheer S, Offerhaus GJA, et al. De Novo Crypt Formation and Juvenile Polyposis on BMP Inhibition in Mouse Intestine. Science. 2004;303:1684–6.

86. Cai J, Zhang N, Zheng Y, De Wilde RF, Maitra A, Pan D. The Hippo signaling pathway restricts the oncogenic potential of an intestinal regeneration program. Genes and Development. 2010;24:2383–8.

87. Chen L, Qin F, Deng X, Avruch J, Zhou D. Hippo pathway in intestinal homeostasis and tumorigenesis. Protein and Cell. 2012;3:305–10.

88. Lecarpentier Y, Schussler O, Hébert JL, Vallée A. Multiple Targets of the Canonical WNT/β-Catenin Signaling in Cancers. Frontiers in Oncology. 2019;9 November:1–17.

89. Massagué J. G1 cell-cycle control and cancer. Nature. 2004;432 November:298–306. www.nature.com/nature.

90. Daksis J, Lu R, Facchini L, Marhin W, Penn L. Myc induces cyclin D1 expression in the absence of de novo protein synthesis and links mitogen-stimulated signal transduction to the cell cycle. Oncogene. 1994;9:3635–45.

91. Van de Wetering M, Sancho E, Verweij C, De Lau W, Oving I, Hurlstone A, et al. The β-catenin/TCF-4 complex imposes a crypt progenitor phenotype on colorectal cancer cells. Cell. 2002;111:241–50.

92. Alao JP. The regulation of cyclin D1 degradation: Roles in cancer development and the potential for therapeutic invention. Molecular Cancer. 2007;6:1–16.

93. Niehrs C, Acebron SP. Mitotic and mitogenic Wnt signalling. EMBO Journal. 2012;31:2705–13. doi:10.1038/emboj.2012.124.

94. Matsumoto S, Fujii S, Sato A, Ibuka S, Kagawa Y, Ishii M, et al. A combination of Wnt and growth factor signaling induces Arl4c expression to form epithelial tubular structures. EMBO Journal. 2014;33:702–18.

95. Hu T, Weng S, Tang W, Xe R, Chen S, Cai G, et al. Overexpression of BIRC6 is a predictor of prognosis for colorectal cancer. PLoS ONE. 2015;10:1–18.

96. Xu W, Ying Y, Shan L, Feng J, Zhang S, Gao Y, et al. Enhanced expression of cohesin loading factor NIPBL confers poor prognosis and chemotherapy resistance in non-small cell lung cancer. Journal of Translational Medicine. 2015;13:1–12. doi:10.1186/s12967-015-0503-3.

97. Kim TH, Shivdasani RA. Genetic evidence that intestinal Notch functions vary regionally and operate through a common mechanism of math1 repression. Journal of Biological Chemistry. 2011;286:11427–33.

98. Kim TH, Li F, Ferreiro-Neira I, Ho L-L, Luyten A, Nalapareddy K, et al. Broadly permissive intestinal chromatin underlies lateral inhibition and cell plasticity. Nature. 2014;506:511–5.

99. Shroyer NF, Helmrath MA, Wang VYC, Antalffy B, Henning SJ, Zoghbi HY. Intestine-Specific Ablation of Mouse atonal homolog 1 (Math1) Reveals a Role in Cellular Homeostasis. Gastroenterology. 2007;132:2478–88.

100. Noah TH, Kazanjian A, Whitsett J, Shroyer NF. SAM Pointed Domain ETS Factor (SPDEF) regulates terminal differentiation and maturation of intestinal goblet cells. Experimental Cell Research. 2010;316:452–65. doi:doi:10.1016/j.yexcr.2009.09.020.

101. Roth S, Franken P, Sacchetti A, Kremer A, Anderson K, Sansom O, et al. Paneth cells in intestinal homeostasis and tissue injury. PLoS ONE. 2012;7.

102. Bastide P, Darido C, Pannequin J, Kist R, Robine S, Marty-Double C, et al. Sox9 regulates cell proliferation and is required for Paneth cell differentiation in the intestinal epithelium. Journal of Cell Biology. 2007;178:635–48.

103. Lee J.C. SSBWHLJSDWJMRGGMS, Lee JC, Smith SB, Watada H, Lin J, Scheel D, et al. Regulation of the pancreatic pro-endocrine gene neurogenin3. Diabetes. 2001;50:928–36. http://www.ncbi.nlm.nih.gov/pubmed/11334435.

104. Ghaleb AM, Aggarwal G, Bialkowska AB, Nandan MO, Yang VW. Notch inhibits expression of the Krüppel-like factor 4 tumor suppressor in the intestinal epithelium. Molecular Cancer Research. 2008;6:1920–7.

105. van der Sluis M, Vincent A, Bouma J, Male AK Van, van Goudoever JB, Renes IB, et al. Forkhead box transcription factors Foxa1 and Foxa2 are important regulators of Muc2 mucin expression in intestinal epithelial cells. Biochemical and Biophysical Research Communications. 2008;369:1108–13.

106. Schonhoff SE, Giel-Moloney M, Leiter AB. Minireview: Development and differentiation of gut endocrine cells. Endocrinology. 2004;145:2639–44.

107. Gehart H, van Es JH, Hamer K, Beumer J, Kretzschmar K, Dekkers JF, et al. Identification of Enteroendocrine Regulators by Real-Time Single-Cell Differentiation Mapping. Cell. 2019;176:1158-1173.e16. doi:10.1016/j.cell.2018.12.029.

108. Buczacki SJA, Zecchini HI, Nicholson AM, Russell R, Vermeulen L, Kemp R, et al. Intestinal label-retaining cells are secretory precursors expressing lgr5. Nature. 2013;495:65–9.

109. Krentz NAJ, van Hoof D, Li Z, Watanabe A, Tang M, Nian C, et al. Phosphorylation of NEUROG3 Links Endocrine Differentiation to the Cell Cycle in Pancreatic Progenitors. Developmental Cell. 2017;41:129-142.e6. doi:10.1016/j.devcel.2017.02.006.

110. Patankar J V., Becker C. Cell death in the gut epithelium and implications for chronic inflammation. Nature Reviews Gastroenterology and Hepatology. 2020;17:543–56. doi:10.1038/s41575-020-0326-4.

111. Shamas-Din A, Kale J, Leber B, Andrews DW. Mechanisms of action of Bcl-2 family proteins. Cold

Spring Harbor Perspectives in Biology. 2013;5:1–21.

112. Sträter J, Möller P. Expression and function of death receptors and their natural ligands in the intestine. Annals of the New York Academy of Sciences. 2000;915:162–70.

113. Segawa K, Nagata S. An Apoptotic "Eat Me" Signal: Phosphatidylserine Exposure. Trends in Cell Biology. 2015;25:639–50. doi:10.1016/j.tcb.2015.08.003.

114. Madara JL. Maintenance of the macromolecular barrier at cell extrusion sites in intestinal epithelium: Physiological rearrangement of tight junctions. The Journal of Membrane Biology. 1990;116:177–84.

115. Jorgensen I, Miao EA. Pyroptotic cell death defends against intracellular pathogens. Immunological Reviews. 2015;265:130–42.

116. Christofferson DE, Yuan J. Necroptosis as an alternative form of programmed cell death. Advances in Space Research. 2010;22:263–8.

117. Kayagaki N, Warming S, Lamkanfi M, Walle L Vande, Louie S, Dong J, et al. Non-canonical inflammasome activation targets caspase-11. Nature. 2011;479:117–21.

118. Demers MJ, Thibodeau S, Noël D, Fujita N, Tsuruo T, Gauthier R, et al. Intestinal epithelial cancer cell anoikis resistance: EGFR-mediated sustained activation of Src overrides Fak-dependent signaling to MEK/Erk and/or PI3-K/Akt-1. Journal of Cellular Biochemistry. 2009;107:639–54.

119. Poon IKH, Lucas CD, Rossi AG, Ravichandran KS. Apoptotic cell clearance: basic biology and therapeutic potential. Nature Reviews Immunology. 2014;14:166–80. doi:10.1038/nri3607.

120. Chaturvedi LS, Gayer CP, Marsh HM, Basson MD. Repetitive deformation activates Src-independent FAK-dependent ERK motogenic signals in human Caco-2 intestinal epithelial cells. American Journal of Physiology - Cell Physiology. 2008;294:1350–61.

121. Dignass AU, Baumgart DC, Sturm A. Review article: The aetiopathogenesis of inflammatory bowel disease - Immunology and repair mechanisms. Alimentary Pharmacology and Therapeutics, Supplement. 2004;20:9–17.

122. Iizuka M, Konno S. Wound healing of intestinal epithelial cells. World Journal of Gastroenterology. 2011;17:2161–71.

123. Beck PL, Rosenberg IM, Xavier RJ, Koh T, Wong F, Podolsky DK. Transforming Growth Factor-Beta Mediates Intestinal Healing and Susceptibility to Injury in Vitro and in Vivo Through Epithelial Cells. American Journal of Pathology. 2003;162:597–608.

124. Sommer K, Wiendl M, Müller TM, Heidbreder K, Voskens C, Neurath MF, et al. Intestinal Mucosal Wound Healing and Barrier Integrity in IBD–Crosstalk and Trafficking of Cellular Players. Frontiers in Medicine. 2021;8 March:1–12.

125. Zheng Z, Kang HY, Lee S, Kang SW, Goo B, Cho S Bin. Up-regulation of fibroblast growth factor (FGF) 9 expression and FGF-WNT/β-catenin signaling in laser-induced wound healing. Wound Repair and Regeneration. 2014;22:660–5.

126. Grotendorst GR, Soma Y, Takehara K, Charette M. EGF and TGF-alpha are potent chemoattractants for endothelial cells and EGF-like peptides are present at sites of tissue regeneration. Journal of Cellular Physiology. 1989;139:617–23.

127. Turner JR. Intestinal mucosal barrier function in health and disease. Nature Reviews Immunology. 2009;9:799–809.

128. Pratt C, Voet J. Fundamentals of Biochemistry upgrade. New York; 2002.

129. Shechter E. Transports actifs secondaires. Biochimie. 1986;68:357–65.

130. Reese JB, Urry LA, Cain ML, Wasserman SA, Minorsky P V, Jackson RB. Tenth Edition, Campbell's Biology. 10th edition. 2014.

131. Jones HF, Butler RN, Brooks DA. Intestinal fructose transport and malabsorption in humans. American Journal of Physiology - Gastrointestinal and Liver Physiology. 2011;300:202–6.

132. Heyman M, Ducroc R, Desjeux JF, Morgat JL. Horseradish peroxidase transport across adult rabbit jejunum in vitro. American Journal of Physiology - Gastrointestinal and Liver Physiology. 1982;5.

133. Terpend K, Boisgerault F, Blaton MA, Desjeux JF, Heyman M. Protein transport and processing by human HT29-19A intestinal cells: Effect of interferon γ. Gut. 1998;42:538–45.

134. Ménard S, Cerf-Bensussan N, Heyman M. Multiple facets of intestinal permeability and epithelial handling of dietary antigens. Mucosal Immunology. 2010;3:247–59.

135. Rao R. Occludin phosphorylation in regulation of epithelial tight junctions. Annals of the New York Academy of Sciences. 2009;1165:62–8. doi:doi:10.1111/j.1749-6632.2009.04054.x.

136. Kubota K, Furuse M, Sasaki H, Sonoda N, Fujita K, Nagafuchi A, et al. Ca2+-independent cell-adhesion activity of claudins, a family of integral membrane proteins localized at tight junctions. Current Biology. 1999;9:1035–8.

137. Tokunaga Y, Kojima T, Osanai M, Murata M, Chiba H, Tobioka H, et al. A novel monoclonal antibody against the second extracellular loop of occludin disrupts epithelial cell polarity. Journal of Histochemistry and Cytochemistry. 2007;55:735–44.

138. Dhawan P, Singh AB, Sharma A. Claudin family of proteins and cancer: An overview. Journal of Oncology. 2010;2010.

139. Hartsock A, Nelson WJ. Adherens and tight junctions: Structure, function and connections to the actin cytoskeleton. Biochimica et Biophysica Acta - Biomembranes. 2008;1778:660–9.

140. Escaffit F, Boudreau F, Beaulieu JF. Differential expression of claudin-2 along the human intestine: Implication of GATA-4 in the maintenance of claudin-2 in differentiating cells. Journal of Cellular Physiology. 2005;203:15–26.

141. Van Itallie CM, Anderson JM. Claudins and epithelial paracellular transport. Annual Review of Physiology. 2006;68:403–29.

142. Günzel D, Yu ASL. Claudins and the modulation of tight junction permeability. Physiological Reviews. 2013;93:525–69.

143. Mazaud-Guittot S, Meugnier E, Pesenti S, Wu X, Vidal H, Gow A, et al. Claudin 11 deficiency in mice results in loss of the sertoli cell epithelial phenotype in the testis. Biology of Reproduction. 2010;82:202–13.

144. Beeman N, Webb PG, Baumgartner HK. Occludin is required for apoptosiswhen claudin-claudin interactions are disrupted. Cell Death and Disease. 2012;3:1–7.

145. Liu Y, Nusrat A, Schnell FJ, Reaves TA, Walsh S, Pochet M, et al. Human junction adhesion molecule regulates tight junction resealing in epithelia. Journal of Cell Science. 2000;113:2363–74.

146. Otani T, Nguyen TP, Tokuda S, Sugihara K, Sugawara T, Furuse K, et al. Claudins and JAM-A coordinately regulate tight junction formation and epithelial polarity. Journal of Cell Biology. 2019;218:3372–96.

147. Luissint A-C, Nusrat A, Parkos CA. JAM related proteins in mucosal homeostasis and inflammation. Seminars in Immunology. 2014;36:211–26.

148. Nava P, Capaldo CT, Koch S, Kolegraff K, Rankin CR, Farkas AE, et al. JAM-A regulates epithelial

proliferation through Akt/β-catenin signalling. EMBO Reports. 2011;12:314–20. doi:10.1038/embor.2011.16.

149. Praetor A, McBride JM, Chiu H, Rangell L, Cabote L, Lee WP, et al. Genetic deletion of JAM-C reveals a role in myeloid progenitor generation. Blood. 2009;113:1919–28.

150. Witherden DA, Verdino P, Rieder SE, Garijo O, Robyn E, Teyton L, et al. The adhesion molecule JAML is a costimulatory receptor for epithelial gammadelta T cell activation. Science. 2010;329:1205–10.

151. Umeda K, Ikenouchi J, Katahira-Tayama S, Furuse K, Sasaki H, Nakayama M, et al. ZO-1 and ZO-2 Independently Determine Where Claudins Are Polymerized in Tight-Junction Strand Formation. Cell. 2006;126:741–54.

152. Fanning AS, Anderson JM. Zonula occludens-1 and -2 are cytosolic scaffolds that regulate the assembly of cellular junctions. Annals of the New York Academy of Sciences. 2009;1165:113–20.

153. Guan Y, Watson AJM, Marchiando AM, Bradford E, Shen L, Turner JR, et al. Redistribution of the tight junction protein ZO-1 during physiological shedding of mouse intestinal epithelial cells. American Journal of Physiology - Cell Physiology. 2011;300:1–19.

154. Raya-Sandino A, Castillo-Kauil A, Domínguez-Calderón A, Alarcón L, Flores-Benitez D, Cuellar-Perez F, et al. Zonula occludens-2 regulates Rho proteins activity and the development of epithelial cytoarchitecture and barrier function. Biochimica et Biophysica Acta - Molecular Cell Research. 2017;1864:1714–33. doi:10.1016/j.bbamcr.2017.05.016.

155. Gonzalez-Mariscal L, Bautista P, Lechuga S, Quiros M. ZO-2, a tight junction scaffold protein involved in the regulation of cell proliferation and apoptosis. Annals of the New York Academy of Sciences. 2012;1257:133–41.

156. Capaldo CT, Koch S, Kwon M, Laur O, Parkos CA, Nusrat A. Tight function zonula occludens-3 regulates cyclin D1-dependent cell proliferation. Molecular Biology of the Cell. 2011;22:1677–85.

157. Niessen CM, Gottardi CJ. Molecular Components of the Adherens Junction. Biochimica et Biophysica Acta. 2008;1778:562–71.

158. Garrod D, Chidgey M. Desmosome structure, composition and function. Biochimica et Biophysica Acta - Biomembranes. 2008;1778:572–87.

159. Kojima T, Murata M, Go M, Spray DC, Sawada N. Connexins induce and maintain tight junctions in epithelial cells. Journal of Membrane Biology. 2007;217:13–9.

160. Meşe G, Richard G, White TW. Gap junctions: Basic structure and function. Journal of Investigative Dermatology. 2007;127:2516–24.

161. Saez JC, Spray DC, Nairn AC, Hertzberg E, Greengard P, Bennett M V. cAMP increases junctional conductance and stimulates phosphorylation of the 27-kDa principal gap junction polypeptide. Proceedings of the National Academy of Sciences of the United States of America. 1986;83:2473–7.

162. Kumar NM, Gilula NB. The gap junction communication channel. Cell. 1996;84:381–8.

163. Qin J, Chang M, Wang S, Liu Z, Zhu W, Wang Y, et al. Connexin 32-mediated cell-cell communication is essential for hepatic differentiation from human embryonic stem cells. Scientific Reports. 2016;6 May:1–16.

164. Loewenstein WR. Junctional intercellular communication and the control of growth. BBA - Reviews on Cancer. 1979;560:1–65.

165. Gill N, Wlodarska M, Finlay BB. Roadblocks in the gut: Barriers to enteric infection. Cellular Microbiology. 2011;13:660–9.

166. Round JL, Lee SM, Li J, Tran G, Jabri B, A. Chatila T, et al. The Toll-like receptor pathway establishes commensal gut colonization. Science. 2011;332:974–7.

167. Okumura R, Takeda K. Maintenance of gut homeostasis by the mucosal immune system. Proceedings of the Japan Academy Series B: Physical and Biological Sciences. 2016;92:423–35.

168. Kuhn KA, Manieri NA, Liu TC, Stappenbeck TS. IL-6 stimulates intestinal epithelial proliferation and repair after injury. PLoS ONE. 2014;9:1–18.

169. Gieseck RL, Wilson MS, Wynn TA. Type 2 immunity in tissue repair and fibrosis. Nature Reviews Immunology. 2018;18:62–76. doi:10.1038/nri.2017.90.

170. Neunlist M, Toumi F, Oreschkova T, Denis M, Leborgne J, Laboisse CL, et al. Human ENS regulates the intestinal epithelial barrier permeability and a tight junction-associated protein ZO-1 via VIPergic pathways. American Journal of Physiology - Gastrointestinal and Liver Physiology. 2003;285 5 48-5:1028–36.

171. Savidge TC, Newman P, Pothoulakis C, Ruhl A, Neunlist M, Bourreille A, et al. Enteric Glia Regulate Intestinal Barrier Function and Inflammation Via Release of S-Nitrosoglutathione. Gastroenterology. 2007;132:1344–58.

172. Neunlist M, Rolli-Derkinderenn, Malvyne. Le Système Nerveux Entérique Et L ' Unité Neuro-Glio-Épithéliale Digestive the Enteric Nervous System and the Digestive. Bulletin de l'académie véterinaire de France. 2013;166:7–12.

173. Farack UM, Reiter J, Gross M, Moroder L, Wünsch E, Loeschke K. Influence of Vasoactive Intestinal Peptide, Secretin, and Ala4, Vals-Secretin. Scandinavian Journal of Gastroenterology. 1987;22:32–6.

174. Lahar N, Lei NY, Wang J, Jabaji Z, Tung SC, Joshi V, et al. Intestinal subepithelial myofibroblasts support in vitro and in vivo growth of human small intestinal epithelium. PLoS ONE. 2011;6:1–9.

175. Powell DW, Adegboyega PA, Di Mari JF, Mifflin RC. Epithelial cells and their neighbors: I. Role of intestinal myofibroblasts in development, repair, and cancer. American Journal of Physiology - Gastrointestinal and Liver Physiology. 2005;289 1 52-1:2–7.

176. Fernandes AD, Reid JNS, Macklaim JM, McMurrough TA, Edgell DR, Gloor GB. Unifying the analysis of high-throughput sequencing datasets: Characterizing RNA-seq, 16S rRNA gene sequencing and selective growth experiments by compositional data analysis. Microbiome. 2014;2:1–13.

177. Sender R, Fuchs S, Milo R. Revised Estimates for the Number of Human and Bacteria Cells in the Body. PLoS Biology. 2016;14:1–14.

178. Yang X, Xie L, Li Y, Wei C. More than 9,000,000 unique genes in human gut bacterial community: Estimating gene numbers inside a human body. PLoS ONE. 2009;4:0–7.

179. Lozupone CA, Stombaugh J, Gordon JI, Jansson JK, Knight R. Diversity, stability and resilience of the human gut microbiota Catherine. Nature. 2012;489:220–30.

180. Donaldson GP, Lee SM, Mazmanian SK. Gut biogeography of the bacterial microbiota. Nature Reviews Microbiology. 2015;14:20–32.

181. Caporaso JG, Lauber CL, Costello EK, Berg-Lyons D, Gonzalez A, Stombaugh J, et al. Moving pictures of the human microbiome. Genome Biology. 2011;12:R50. doi:10.1186/gb-2011-12-5-r50.

182. Ley RE, Turnbaugh PJ, Klein S, Gordon JI. Human gut microbes associated with obesity. Nature. 2006;444:1022_1023.

183. Mariat D, Firmesse O, Levenez F, Guimarăes VD, Sokol H, Doré J, et al. The firmicutes/bacteroidetes ratio of the human microbiota changes with age. BMC Microbiology. 2009;9:1–6.

184. Arumugam M, Raes J, Pelletier E, Le Paslier D, Yamada T, Mende DR, et al. Enterotypes of the human gut microbiome. Nature. 2011;473:174–80.

185. Gogarten JP, Townsend JP. Horizontal gene transfer, genome innovation and evolution. Nature Reviews Microbiology. 2005;3:679–87.

186. Spratt BG, Staley JT, Fisher MC. Introduction: species and speciation in micro-organisms. Philosophical Transactions of the Royal Society. 2006;365:1897–1898.

187. Ursell LK, Metcalf JL, Parfrey LW, Knight R. Defining the Human Microbiome Luke. Nutrition Reviews. 2012;299:38–44.

188. Bergström A, Skov TH, Bahl MI, Roager HM, Christensen LB, Ejlerskov KT, et al. Establishment of intestinal microbiota during early life: A longitudinal, explorative study of a large cohort of Danish infants. Applied and Environmental Microbiology. 2014;80:2889–900.

189. Tanaka M, Nakayama J. Development of the gut microbiota in infancy and its impact on health in later life. Allergology International. 2017;66:515–22. doi:10.1016/j.alit.2017.07.010.

190. Macpherson AJ, Harris NL. Interactions between commensal intestinal bacteria and the immune system. Nature Reviews Immunology. 2004;4 June:478–85.

191. Kabouridis PS, Lasrado R, McCallum S, Chng SH, Snippert HJ, Clevers H, et al. Microbiota controls the homeostasis of glial cells in the gut lamina propria. Neuron. 2015;85:289–95. doi:10.1016/j.neuron.2014.12.037.

192. Obata Y, Pachnis V. The Effect of Microbiota and the Immune System on the Development and Organization of the Enteric Nervous System. Gastroenterology. 2016;151:836–44. doi:10.1053/j.gastro.2016.07.044.

193. Kundu P, Blacher E, Elinav E, Pettersson S. Our Gut Microbiome: The Evolving Inner Self. Cell. 2017;171:1481–93. doi:10.1016/j.cell.2017.11.024.

194. Markle JGM, Frank DN, Mortin-Toth S, Robertson CE, Feazel LM, Rolle-Kampczyk U, et al. Sex differences in the gut microbiome drive hormone-dependent regulation of autoimmunity. Science. 2013;339:1084–8.

195. Koren O, Goodrich JK, Cullender TC, Spor A, Laitinen K, Kling Bäckhed H, et al. Host remodeling of the gut microbiome and metabolic changes during pregnancy. Cell. 2012;150:470–80.

196. Kostic AD, Howitt MR, Garrett WS. Exploring host-microbiota interactions in animal models and humans. Genes and Development. 2013;27:701–18.

197. Maltby R, Leatham-Jensen MP, Gibson T, Cohen PS, Conway T. Nutritional Basis for Colonization Resistance by Human Commensal Escherichia coli Strains HS and Nissle 1917 against E. coli O157:H7 in the Mouse Intestine. PLoS ONE. 2013;8:1–10.

198. Donaldson GP. Colonization of the intestinal surface by indigenous microbiota. 2018.

199. Martinez-Guryn K, Leone V, Chang EB. Regional Diversity of the Gastrointestinal Microbiome. Cell Host and Microbe. 2019;26:314–24. doi:10.1016/j.chom.2019.08.011.

200. Welch JLM, Rossetti BJ, Rieken CW, Dewhirst FE, Borisy GG. Biogeography of a human oral microbiome at the micron scale. Proceedings of the National Academy of Sciences of the United States of America. 2016;113:E791–800.

201. Shang L, Deng D, Buskermolen JK, Janus MM, Krom BP, Roffel S, et al. Multi-species oral biofilm promotes reconstructed human gingiva epithelial barrier function. Scientific Reports. 2018;8:1–12.

202. Schmidt TS, Hayward MR, Coelho LP, Li SS, Costea PI, Voigt AY, et al. Extensive transmission of microbes along the gastrointestinal tract. eLife. 2019;8.

203. Dong L, Yin J, Zhao J, Ma S rui, Wang H rui, Wang M, et al. Microbial similarity and preference for specific sites in healthy oral cavity and esophagus. Frontiers in Microbiology. 2018;9 JUL:1–10.

204. May M, Abrams JA. Emerging Insights into the Esophageal Microbiome. Current Treatment Options in Gastroenterology. 2018;16:72–85.

205. Nardone G, Compare D. The human gastric microbiota: Is it time to rethink the pathogenesis of stomach diseases? United European Gastroenterology Journal. 2015;3:255–60.

206. Slade E, Williams L, Gagnon J. Hydrogen sulfide suppresses ghrelin secretion in vitro and delays postprandial ghrelin secretion while reducing appetite in mice. Physiological Reports. 2018;6.

207. O'Hara AM, Shanahan F. The gut flora as a forgotten organ. EMBO Reports. 2006;7:688–93.

208. Angelakis E, Armougom F, Carrière F, Bachar D, Laugier R, Lagier JC, et al. A metagenomic investigation of the duodenal microbiota reveals links with obesity. PLoS ONE. 2015;10:1–15.

209. Li D, Chen H, Mao B, Yang Q, Zhao J, Gu Z, et al. Microbial Biogeography and Core Microbiota of the Rat Digestive Tract. Scientific Reports. 2017;8 November 2016:1–16.

210. Ivanov II, Atarashi K, Manel N, Brodie EL, Shima T, Karaoz U, et al. Induction of Intestinal Th17 Cells by Segmented Filamentous Bacteria. Cell. 2009;139:485–98. doi:10.1016/j.cell.2009.09.033.

211. Atarashi K, Tanoue T, Ando M, Kamada N, Nagano Y, Narushima S, et al. Th17 Cell Induction by Adhesion of Microbes to Intestinal Epithelial Cells. Cell. 2015;163:367–80.

212. Pédron T, Mulet C, Dauga C, Frangeul L, Chervaux C, Grompone G, et al. A crypt-specific core microbiota resides in the mouse colon. mBio. 2012;3:1–7.

213. Vaga S, Lee S, Ji B, Andreasson A, Talley NJ, Agréus L, et al. Compositional and functional differences of the mucosal microbiota along the intestine of healthy individuals. Scientific Reports. 2020;10:1–12. doi:10.1038/s41598-020-71939-2.

214. Gu S, Chen D, Zhang JN, Lv X, Wang K, Duan LP, et al. Bacterial Community Mapping of the Mouse Gastrointestinal Tract. PLoS ONE. 2013;8.

215. Koh A, De Vadder F, Kovatcheva-Datchary P, Bäckhed F. From dietary fiber to host physiology: Short-chain fatty acids as key bacterial metabolites. Cell. 2016;165:1332–45.

216. Sommer F, Bäckhed F. Know your neighbor: Microbiota and host epithelial cells interact locally to control intestinal function and physiology. BioEssays. 2016;38:455–64.

217. Nava GM, Friedrichsen HJ, Stappenbeck TS. Spatial organization of intestinal microbiota in the mouse ascending colon. ISME Journal. 2011;5:627–38. doi:10.1038/ismej.2010.161.

218. Albenberg L, Esipova T V., Judge CP, Bittinger K, Chen J, Laughlin A, et al. Correlation between intraluminal oxygen gradient and radial partitioning of intestinal microbiota. Gastroenterology. 2014;147:1055-1063.e8. doi:10.1053/j.gastro.2014.07.020.

219. Johansson MEV, Phillipson M, Petersson J, Velcich A, Holm L, Hansson GC. The inner of the two Muc2 mucin-dependent mucus layers in colon is devoid of bacteria. Proceedings of the National Academy of Sciences of the United States of America. 2008;105:15064–9.

220. Wexler HM. Bacteroides: The good, the bad, and the nitty-gritty. Clinical Microbiology Reviews. 2007;20:593–621.

221. Chang YC, Ching YH, Chiu CC, Liu JY, Hung SW, Huang WC, et al. TLR2 and interleukin-10 are involved in Bacteroides fragilis-mediated prevention of DSS-induced colitis in gnotobiotic mice. PLoS ONE. 2017;12:1–16.

222. Lyu Y, Wu L, Wang F, Shen X, Lin D. Carotenoid supplementation and retinoic acid in immunoglobulin A regulation of the gut microbiota dysbiosis. Experimental Biology and Medicine.

2018;243:613–20.

223. Siavoshian S, Segain JP, Kornprobst M, Bonnet C, Cherbut C, Galmiche JP, et al. Butyrate and trichostatin a effects on the proliferation/differentiation of human intestinal epithelial cells: Induction of cyclin D3 and p21 expression. Gut. 2000;46:507–14.

224. Martens EC, Koropatkin NM, Smith TJ, Gordon JI. Complex glycan catabolism by the human gut microbiota: The bacteroidetes sus-like paradigm. Journal of Biological Chemistry. 2009;284:24673–7.

225. Lee SM, Donaldson GP, Mikulski Z, Boyajian S, Ley K, Mazmanian SK. Bacterial colonization factors control specificity and stability of the gut microbiota. Nature. 2013;501:426–9.

226. Png CW, Lindén SK, Gilshenan KS, Zoetendal EG, McSweeney CS, Sly LI, et al. Mucolytic bacteria with increased prevalence in IBD mucosa augment in vitro utilization of mucin by other bacteria. American Journal of Gastroenterology. 2010;105:2420–8.

227. Natividad JMM, Hayes CL, Motta JP, Jury J, Galipeau HJ, Philip V, et al. Differential induction of antimicrobial REGIII by the intestinal microbiota and Bifidobacterium breve NCC2950. Applied and Environmental Microbiology. 2013;79:7745–54.

228. Cash HL, Whitham C V., Behrendt CL, Hooper L V. Symbiotic bacteria direct expression of an intestinal bactericidal lectin. Science. 2006;313:1126–30.

229. Ouellette AJ. Paneth cell α-defensins in enteric innate immunity. Cellular and Molecular Life Sciences. 2011;68:2215–29.

230. Lehrer RI, Barton A, Daher KA, Harwig SSL, Ganz T, Selsted ME. Interaction of human defensins with Escherichia coli. Mechanism of bactericidal activity. Journal of Clinical Investigation. 1989;84:553–61.

231. Lambert PA, Hammond SM. Potassium fluxes, first indications of membrane damage in micro-organisms. Biochemical and Biophysical Research Communications. 1973;54:796–9.

232. Mantis NJ, Forbes SJ. Secretory IgA: Arresting Microbial Pathogens at Epithelial Borders. Immunological Investigations. 2010;39:383–406.

233. Sekirov I, Russell SL, Caetano M Antunes L, Finlay BB. Gut microbiota in health and disease. Physiological Reviews. 2010;90:859–904.

234. Randal Bollinger R, Everett M Lou, Palestrant D, Love SD, Lin SS, Parker W. Human secretory immunoglobulin A may contribute to biofilm formation in the gut. Immunology. 2003;109:580–7.

235. Favre L, Spertini F, Corthésy B. Secretory IgA Possesses Intrinsic Modulatory Properties Stimulating Mucosal and Systemic Immune Responses. The Journal of Immunology. 2005;175:2793–800.

236. Mantis NJ, Rol N, Corthésy B. Secretory IgA's complex roles in immunity and mucosal homeostasis in the gut. Mucosal Immunology. 2011;4:603–11.

237. Ridlon JM, Kang DJ, Hylemon PB, Bajaj JS. Bile Acids and the Gut Microbiome. Current Opinion in Gastroenterology. 2014;30:332–8.

238. Percy-Robb IW. Bile Acids: A pH Dependent Antibacterial System in the Gut? British Medical Journal. 1972;3:813–5.

239. van Best N, Rolle-Kampczyk U, Schaap FG, Basic M, Olde Damink SWM, Bleich A, et al. Bile acids drive the newborn's gut microbiota maturation. Nature Communications. 2020;11. doi:10.1038/s41467-020-17183-8.

240. Falony G, Joossens M, Vieira-Silva S, Wang J, Darzi Y, Faust K, et al. Population-level analysis of gut microbiome variation. Science. 2016;352:560–4.

241. Wang F, Meng J, Zhang L, Johnson T, Chen C, Roy S. Morphine induces changes in the gut microbiome and metabolome in a morphine dependence model. Scientific Reports. 2018;8:1–15. doi:10.1038/s41598-018-21915-8.

242. Bueno L, Fioramonti J. Action of opiates on gastrointestinal function. Bailliere's Clinical Gastroenterology. 1988;2:123–39.

243. Crespo-Piazuelo D, Estellé J, Revilla M, Criado-Mesas L, Ramayo-Caldas Y, Óvilo C, et al. Characterization of bacterial microbiota compositions along the intestinal tract in pigs and their interactions and functions. Scientific Reports. 2018;8:1–12.

244. Waliullah S, Harris M, Zaki H. Microbial DNA regulates intestinal homeostasis via the AIM2 inflammasome. Receptors & Clinical Investigation. 2016;:4–7.

245. Soderholm AT, Pedicord VA. Intestinal epithelial cells: at the interface of the microbiota and mucosal immunity. Immunology. 2019;158:267–80.

246. Wells JM, Rossi O, Meijerink M, van Baarlen P. Epithelial crosstalk at the microbiota-mucosal interface. Proceedings of the National Academy of Sciences. 2011;108 Supplement_1:4607–14. doi:10.1073/pnas.1000092107.

247. Thomas JP, Parker A, Divekar D, Pin C, Watson A. The gut microbiota influences intestinal proliferative potential. Gut. 2018;67 Suppl 1:A204.

248. Abrams GD, Bauer H, Sprinz H. Influence of the Normal Flora on Mucosal Morphology and Cellular Renewal in the Ileum. Lab Invest. 1963;12:355–64.

249. Hayes CL, Dong J, Galipeau HJ, Jury J, McCarville J, Huang X, et al. Commensal microbiota induces colonic barrier structure and functions that contribute to homeostasis. Scientific Reports. 2018;8:1–14. doi:10.1038/s41598-018-32366-6.

250. Geirnaert A, Calatayud M, Grootaert C, Laukens D, Devriese S, Smagghe G, et al. Butyrate-producing bacteria supplemented in vitro to Crohn's disease patient microbiota increased butyrate production and enhanced intestinal epithelial barrier integrity. Scientific Reports. 2017;7:1–14. doi:10.1038/s41598-017-11734-8.

251. Mathewson ND, Jenq R, Mathew A V., Koenigsknecht M, Hanash A, Toubai T, et al. Gut microbiome-derived metabolites modulate intestinal epithelial cell damage and mitigate graft-versus-host disease. Nature Immunology. 2016;17:505–13.

252. Pascale A, Marchesi N, Marelli C, Coppola A, Luzi L, Govoni S, et al. Microbiota and metabolic diseases. Endocrine. 2018;61:357–71. doi:10.1007/s12020-018-1605-5.

253. Venegas DP, De La Fuente MK, Landskron G, González MJ, Quera R, Dijkstra G, et al. Short chain fatty acids (SCFAs)mediated gut epithelial and immune regulation and its relevance for inflammatory bowel diseases. Frontiers in Immunology. 2019;10 MAR.

254. Duncan SH, Holtrop G, Lobley GE, Calder AG, Stewart CS, Flint HJ. Contribution of acetate to butyrate formation by human faecal bacteria. British Journal of Nutrition. 2004;91:915–23.

255. Donohoe DR, Garge N, Zhang X, Sun W, O'Connell TM, Bunger MK, et al. The microbiome and butyrate regulate energy metabolism and autophagy in the mammalian colon. Cell Metabolism. 2011;13:517–26. doi:10.1016/j.cmet.2011.02.018.

256. Louis P, Flint HJ. Formation of propionate and butyrate by the human colonic microbiota. Environmental Microbiology. 2017;19:29–41.

257. Chang SC, Shen MH, Liu CY, Pu CM, Hu JM, Huang CJ. A gut butyrate-producing bacterium Butyricicoccus pullicaecorum regulates short-chain fatty acid transporter and receptor to reduce the progression of 1,2-dimethylhydrazine-associated colorectal cancer. Oncology Letters. 2020;20:1–9.

258. Zhang J, Song L, Wang Y, Liu C, Zhang L, Zhu S, et al. Beneficial effect of butyrate-producing Lachnospiraceae on stress-induced visceral hypersensitivity in rats. Journal of Gastroenterology and Hepatology (Australia). 2019;34:1368–76.

259. Orchel A, Dzierzewicz Z, Parfiniewicz B, Weǵlarz L, Wilczok T. Butyrate-induced differentiation of colon cancer cells is PKC and JNK dependent. Digestive Diseases and Sciences. 2005;50:490–8.

260. Sengupta S, Muir JG, Gibson PR. Does butyrate protect from colorectal cancer? Journal of Gastroenterology and Hepatology (Australia). 2006;21 1 PART2:209–18.

261. Singh B, Halestrap AP, Paraskeva C. Butyrate can act as a stimulator of growth or inducer of apoptosis in human colonic epithelial cell lines depending on the presence of alternative energy sources. Carcinogenesis. 1997;18:1265–70.

262. Peng L, Li Z-R, Green RS, Holzman IR, Lin J. Butyrate Enhances the Intestinal Barrier by Facilitating Tight Junction Assembly via Activation of AMP-Activated Protein Kinase in Caco-2 Cell Monolayers. The Journal of Nutrition. 2009;139:1619–25. doi:10.3945/jn.109.104638.1619.

263. Lewis K, Lutgendorff F, Phan V, Söderholm JD, Sherman PM, McKay DM. Enhanced translocation of bacteria across metabolically stressed epithelia is reduced by butyrate. Inflammatory Bowel Diseases. 2010;16:1138–48.

264. Peng L, He Z, Chen W, Holzman IR, Lin J. Effects of butyrate on intestinal barrier function in a caco-2 cell monolayer model of intestinal barrier. Pediatric Research. 2007;61:37–41.

265. Gaudier E, Rival M, Buisine MP, Robineau I, Hoebler C. Butyrate enemas Upregulate Muc genes expression but decrease adherent mucus thickness in mice colon. Physiological Research. 2009;58:111–9.

266. Bilotta AJ, Ma C, Yang W, Yu Y, Yu Y, Zhao X, et al. Propionate Enhances Cell Speed and Persistence to Promote Intestinal Epithelial Turnover and Repair. Cellular and Molecular Gastroenterology and Hepatology. 2021;11.

267. Silva YP, Bernardi A, Frozza RL. The Role of Short-Chain Fatty Acids From Gut Microbiota in Gut-Brain Communication. Frontiers in Endocrinology. 2020;11 January:1–14.

268. Thomas C, Pellicciari R, Pruzanski M, Auwerx J, Schoonjans K. Targeting bile-acid signalling for metabolic diseases. Nature Reviews Drug Discovery. 2008;7:678–93.

269. Merlen G, Kahale N, Ursic-Bedoya J, Bidault-Jourdainne V, Simerabet H, Doignon I, et al. TGR5-dependent hepatoprotection through the regulation of biliary epithelium barrier function. Gut. 2020;69:146–57.

270. Ji CG, Xie XL, Yin J, Qi W, Chen L, Bai Y, et al. Bile acid receptor TGR5 overexpression is associated with decreased intestinal mucosal injury and epithelial cell proliferation in obstructive jaundice. Translational Research. 2017;182:88–102. doi:10.1016/j.trsl.2016.12.001.

271. Dossa AY, Escobar O, Golden J, Frey MR, Ford HR, Gayer CP. Bile acids regulate intestinal cell proliferation by modulating EGFR and FXR signaling. American Journal of Physiology - Gastrointestinal and Liver Physiology. 2016;310:G81–92.

272. Bernard C. La constitution physico-chimique du milieu intérieur [The physicochemical constitution of the environment within]. Revue Scientifique. 1872;2:670–2.

273. Cannon WB. Organization for physiological homeostasis. Physiological Reviews. 1929;IX:399–431. https://doi.org/10.1152/physrev.1929.9.3.399.

274. Billman GE. Homeostasis: The Underappreciated and Far Too Often Ignored Central Organizing Principle of Physiology. Frontiers in Physiology. 2020;11 March:1–12.

275. Cannon WB. Bodily changes in pain, hunger, fear and rage. 2nd edition. New York, NY; 1929.

276. Hinkle LEJ. The concept of “stress” in the biological and social sciences. Science, Medecine, and Man. 1973;1:31–48.

277. Seyle H. The physiology and pathology of exposure to stress: A treatise based on the concepts of the general adaptation syndrome and the disease of adaptation. Montreal, Quebec Canada; 1950.

278. Robinson AM. Let’s talk about stress: History of stress research. Review of General Psychology. 2018;22:334–42.

279. Szabo S, Tache Y, Somogyi A. The legacy of Hans Selye and the origins of stress research: A retrospective 75 years after his landmark brief “letter” to the Editor of Nature. Stress. 2012;15:472–8.

280. Levi L. Society, Stress and disease, Vol 1, The psychological environment and psychosomatic disease. London; 1971.

281. Seyle H. Stress without distress. Philadelphia PA; 1974.

282. Lazarus RS. A cognitively oriented psychologist looks at biofeedback. The American psychologist. 1975;30:553–61.

283. Folkman S, Lazarus RS. An Analysis of Coping in a Middle-Aged Community Sample. Journal of Health and Social Behavior. 1980;21:219–39.

284. Labanski A, Langhorst J, Engler H, Elsenbruch S. Stress and the brain-gut axis in functional and chronic-inflammatory gastrointestinal diseases: A transdisciplinary challenge. Psychoneuroendocrinology. 2020;111 April 2019.

285. Smoller JW. The Genetics of Stress-Related Disorders: PTSD, Depression, and Anxiety Disorders. Neuropsychopharmacology. 2016;41:297–319.

286. Mayer EA. The neurobiology of stress and gastrointestinal disease. Gut. 2000;47:861–9. http://gut.bmj.com/content/47/6/861.full.

287. MacEwen BS. The physiologic response to stress. New England Journal of Medicine. 1998;338:171–9.

288. Gold PW, Goodwin FK, Chrousos GP. Clinical and Biochemical Manifestations of Depression. New England Journal of Medicine. 1988;319:348–53.

289. Albeck DS, McKittrick CR, Caroline Blanchard D, Blanchard RJ, Nikulina J, McEwen BS, et al. Chronic social stress alters levels of corticotropin-releasing factor and arginine vasopressin mRNA in rat brain. Journal of Neuroscience. 1997;17:4895–903.

290. Jacobson L, Sapolsky R. The role of the hippocampus in feedback regulation of the hypothalamic-pituitary-adrenocortical axis. Endocrine Reviews. 1991;12:118–34.

291. Ladd CO, Huot RL, Thrivikraman K V, Nemeroff CB, Meaney MJ, Plotsky PM. Long-term behavioral and neuroendocrine adaptations to adverse early experience. Progress in Brain Research. 2000;122:81–101.

292. Muller JE, Tofler GH, Stone PH. Circadian variation and triggers of onset of acute cardiovascular disease. Circulation. 1989;79:733–43.

293. Kirschbaum C, Prussner JC, Stone AA. Persistent High Cortisol Responses to Repeated Psychological Stress in a Subpopulation of Healthy Men In humans and subhuman primates , repeated ex- result in rapid habituation of cortisol responses . showed that monkeys subjected to 72-hour shock avoidan. 1995;474:468–74.

294. Gerin W, Pickering TG. Association between delayed recovery of blood pressure after acute mental stress and parental history of hypertension. Journal of Hypertension. 1995;13:603–10.

295. Munckt A, Guyre PM, Holbrooke NJ. Physiological Functions of Glucocorticoids in Stress and Their Relation to Pharmacological Actions. Endocrine Reviews. 1984;5:25–44. http://press.endocrine.org/doi/pdf/10.1210/edrv-5-1-25.

296. Godoy LD, Rossignoli MT, Delfino-Pereira P, Garcia-Cairasco N, Umeoka EH de L. A comprehensive overview on stress neurobiology: Basic concepts and clinical implications. Frontiers in Behavioral Neuroscience. 2018;12 July:1–23.

297. De Kloet ER, Joëls M, Holsboer F. Stress and the brain: From adaptation to disease. Nature Reviews Neuroscience. 2005;6:463–75.

298. Oakley RH, Cidlowski JA. The Biology of the Glucocorticoid Receptor: New Signaling Mechanisms in Health and Disease. Journal of Allergy and Clinical Immunology. 2013;135:1033–44.

299. Tank AW, Wong DL. Peripheral and central effects of circulating catecholamines. Comprehensive Physiology. 2015;5:1–15.

300. Dünser MW, Hasibeder WR. Sympathetic overstimulation during critical illness: Adverse effects of adrenergic stress. Journal of Intensive Care Medicine. 2009;24:293–316.

301. Hauger R, Risbrough V, Brauns O, Dautzenberg F. Corticotropin Releasing Factor (CRF) Receptor Signaling in the Central Nervous System: New Molecular Targets. CNS & Neurological Disorders - Drug Targets. 2008;5:453–79.

302. Bonfiglio JJ, Inda C, Refojo D, Holsboer F, Arzt E, Silberstein S. The corticotropin-releasing hormone network and the hypothalamic-pituitary- adrenal axis: Molecular and cellular mechanisms involved. Neuroendocrinology. 2011;94:12–20.

303. Benjannet S, Rondeau N, Day R, Chrétien M, Seidah NG. PC1 and PC2 are proprotein convertases capable of cleaving proopiomelanocortin at distinct pairs of basic residues. Proceedings of the National Academy of Sciences of the United States of America. 1991;88:3564–8.

304. Myers B, Mcklveen JM, Herman JP. Neural regulation of the stress response: The many faces of feedback. Cellular and Molecular Neurobiology. 2014;February:1–20.

305. Spencer RL, Deak T. A users guide to HPA axis research. Physiology & behavior. 2017;178:43–65.

306. Beato M. Gene regulation by steroid hormones. Cell. 1989;56:335–44.

307. Galon J, Franchimont D, Hiroi N, Frey G, Boettner A, Ehrhart-Bornstein M, et al. Gene profiling reveals unknown enhancing and suppressive actions of glucocorticoids on immune cells. The FASEB Journal. 2002;16:61–71.

308. John S, Sabo PJ, Thurman RE, Sung M-H, Biddie SC, Johnson TA, et al. Chromatin accessibility pre-determines glucocorticoid receptor binding patterns HHS. Nat Genet. 2011;43:264–8. doi:10.1038/ng.759.Chromatin.

309. Reddy TE, Gertz J, Crawford GE, Garabedian MJ, Myers RM. The Hypersensitive Glucocorticoid Response Specifically Regulates Period 1 and Expression of Circadian Genes. Molecular and Cellular Biology. 2012;32:3756–67.

310. Sperber AD, Drossman DA. Irritable bowel syndrome: A multidimensional disorder cannot be understood or treated from a unidimensional perspective. Therapeutic Advances in Gastroenterology. 2012;5:387–93.

311. Murray CDR, Flynn J, Ratcliffe L, Jacyna MR, Kamm MA, Emmanuel A V. Effect of acute physical and psychological stress on gut autonomic innervation in irritable bowel syndrome. Gastroenterology. 2004;127:1695–703.

312. Mawdsley JE, Rampton DS. Psychological stress in IBD: New insights into pathogenic and therapeutic implications. Gut. 2005;54:1481–91.

313. Targan SR, Karp LC. Defects in mucosal immunity leading to ulcerative colitis. Immunological Reviews. 2005;206:296–305.

314. Greene BR, Blanchard EB, Wan CK. Long-term monitoring of psychosocial stress and symptomatology in inflammatory bowel disease. Behaviour Research and Therapy. 1994;32:217–26.

315. Lloyd-Price J, Arze C, Ananthakrishnan AN, Schirmer M, Avila-Pacheco J, Poon TW, et al. Multi-omics of the gut microbial ecosystem in inflammatory bowel diseases. Nature. 2019;569:655–62.

316. Machiels K, Joossens M, Sabino J, De Preter V, Arijs I, Eeckhaut V, et al. A decrease of the butyrate-producing species roseburia hominis and faecalibacterium prausnitzii defines dysbiosis in patients with ulcerative colitis. Gut. 2014;63:1275–83.

317. Carroll IM, Ringel-Kulka T, Siddle JP, Ringel Y. Alterations in composition and diversity of the intestinal microbiota in patients with diarrhea-predominant irritable bowel syndrome. Neurogastroenterology and Motility. 2012;24.

318. Frank DN, St. Amand AL, Feldman RA, Boedeker EC, Harpaz N, Pace NR. Molecular-phylogenetic characterization of microbial community imbalances in human inflammatory bowel diseases. Proceedings of the National Academy of Sciences of the United States of America. 2007;104:13780–5.

319. Li B, Wang Y, Yin L, Huang G, Xu Y, Su J, et al. Glucocorticoids promote the development of azoxymethane and dextran sulfate sodium-induced colorectal carcinoma in mice. BMC Cancer. 2019;19:1–10.

320. Baritaki S, de Bree E, Chatzaki E, Pothoulakis C. Chronic Stress, Inflammation, and Colon Cancer: A CRH System-Driven Molecular Crosstalk. Journal of Clinical Medicine. 2019;8:1669.

321. Rodriguez JA, Huerta-Yepez S, Law IKM, Baay-Guzman GJ, Tirado-Rodriguez B, Hoffman JM, et al. Diminished Expression of Corticotropin-Releasing Hormone Receptor 2 in Human Colon Cancer Promotes Tumor Growth and Epithelial-to-Mesenchymal Transition via Persistent Interleukin-6/Stat3 Signaling. Cmgh. 2015;1:610–30. doi:10.1016/j.jcmgh.2015.08.001.

322. Yang L, Zhao Y, Wang Y, Liu L, Zhang X, Li B, et al. The Effects of Psychological Stress on Depression. Current Neuropharmacology. 2015;13:494–504.

323. Dinan TG, Scott L V. Anatomy of melancholia: Focus on hypothalamic-pituitary-adrenal axis overactivity and the role of vasopressin. Journal of Anatomy. 2005;207:259–64.

324. Sotiropoulos I, Catania C, Pinto LG, Silva R, Pollerberg GE, Takashima A, et al. Stress acts cumulatively to precipitate Alzheimer's disease-like tau pathology and cognitive deficits. Journal of Neuroscience. 2011;31:7840–7.

325. Green KN, Billings LM, Roozendaal B, McGaugh JL, LaFerla FM. Glucocorticoids increase amyloid-β and tau pathology in a mouse model of Alzheimer's disease. Journal of Neuroscience. 2006;26:9047–56.

326. Ennis GE, An Y, Resnick SM, Ferrucci L, O'Brien RJ, Moffat SD. Long-term cortisol measures predict Alzheimer disease risk. Neurology. 2017;88:371–8.

327. Fournier AP, Baudron E, Wagnon I, Aubert P, Vivien D, Neunlist M, et al. Environmental enrichment alleviates the deleterious effects of stress in experimental autoimmune encephalomyelitis. Multiple Sclerosis Journal - Experimental, Translational and Clinical. 2020;6.

328. Tsigos C, Kyrou I, Kassi E, Chrousos GP. Stress, Endocrine Physiology and Pathophysiology. Endotext. 2000;:1–52. http://www.ncbi.nlm.nih.gov/pubmed/25905226.

329. Spencer SJ, Tilbrook A. The glucocorticoid contribution to obesity. Stress. 2011;14:233–46.

330. van der Valk ES, Savas M, van Rossum EFC. Stress and Obesity: Are There More Susceptible

Individuals? Current obesity reports. 2018;7:193–203.

331. Wester VL, Staufenbiel SM, Veldhorst MAB, Visser JA, Manenschijn L, Koper JW, et al. Long-term cortisol levels measured in scalp hair of obese patients. Obesity. 2014;22:1956–8.

332. Barclay JL, Agada H, Jang C, Ward M, Wetzig N, Ho KKY. Effects of glucocorticoids on human brown adipocytes. Journal of Endocrinology. 2015;224:139–47.

333. Patchev VK, Patchev A V. Experimental models of stress. Dialogues in Clinical Neuroscience. 2006;8:417–32.

334. O'Mahony SM, Hyland NP, Dinan TG, Cryan JF. Maternal separation as a model of brain-gut axis dysfunction. Psychopharmacology. 2011;214:71–88.

335. Barreau F, Ferrier L, Fioramonti J, Bueno L. New insights in the etiology and pathophysiology of irritable bowel syndrome: Contribution of neonatal stress models. Pediatric Research. 2007;62:240–5.

336. Plotsky PM, Meaney MJ. Early, postnatal experience alters hypothalamic corticotropin-releasing factor (CRF) mRNA, median eminence CRF content and stress-induced release in adult rats. Molecular Brain Research. 1993;18:195–200.

337. Lowman BC, Drossman DA, Cramer EM, McKee DC. Recollection of childhood events in adults with irritable bowel syndrome. Journal of Clinical Gastroenterology. 1987;9:324–30.

338. Hill OW, Price JS. Chilhood Bereavement and Adult Depression. The British Journal of Psychiatry. 1967;113:743–51.

339. Larauche M, Mulak A, Taché Y. Stress-related alterations of visceral sensation: Animal models for irritable bowel syndrome study. Journal of Neurogastroenterology and Motility. 2011;17:213–34.

340. Rau V, DeCola JP, Fanselow MS. Stress-induced enhancement of fear learning: An animal model of posttraumatic stress disorder. Neuroscience and Biobehavioral Reviews. 2005;29:1207–23.

341. Bailey MT, Engler H, Powell ND, Padgett DA, Sheridan JF. Repeated social defeat increases the bactericidal activity of splenic macrophages through a Toll-like receptor-dependent pathway. American Journal of Physiology - Regulatory Integrative and Comparative Physiology. 2007;293:1180–90.

342. Galley JD, Nelson MC, Yu Z, Dowd SE, Walter J, Kumar PS, et al. Exposure to a social stressor disrupts the community structure of the colonic mucosa-associated microbiota. BMC Microbiology. 2014;14:1–13.

343. Avitsur R, Stark JL, Sheridan JF. Social stress induces glucocorticoid resistance in subordinate animals. Hormones and Behavior. 2001;39:247–57.

344. Moloney RD, O'Mahony SM, Dinan TG, Cryan JF. Stress-induced visceral pain: Toward animal models of irritable-bowel syndrome and associated comorbidities. Frontiers in Psychiatry. 2015;6 FEB:1–30.

345. Nukina H, Sudo N, Komaki G, Yu XN, Mine K, Kubo C. The restraint stress-induced elevation in plasma interleukin-6 negatively regulates the plasma TNF-α level. NeuroImmunoModulation. 1998;5:323–7.

346. Gué M, Del Rio-Lacheze C, Eutamene H, Théodorou V, Fioramonti J, Buéno L. Stress-induced visceral hypersensitivity to rectal distension in rats: Role of CRF and mast cells. Neurogastroenterology and Motility. 1997;9:271–9.

347. Schwetz I, Bradesi S, McRoberts JA, Sablad M, Miller JC, Zhou H, et al. Delayed stress-induced colonic hypersensitivity in male Wistar rats: Role of neurokinin-1 and corticotropin-releasing factor-1 receptors. American Journal of Physiology - Gastrointestinal and Liver Physiology. 2004;286 4 49-

4:683–91.

348. Goswami S, Rodríguez-Sierra O, Cascardi M, Paré D. Animal models of post-traumatic stress disorder: Face validity. Frontiers in Neuroscience. 2013;7 7 MAY:1–14.

349. Enck P, Merlin V, Erckenbrecht JF, Wienbeck M. Stress effects on gastrointestinal transit in the rat. Gut. 1989;30:455–9.

350. Bonaz B, Taché Y. Water-avoidance stress-induced c-fos expression in the rat brain and stimulation of fecal output: role of corticotropin-releasing factor. Brain Research. 1994;641:21–8.

351. Bradesi S, Schwetz I, Ennes HS, Lamy CMR, Ohning G, Fanselow M, et al. Repeated exposure to water avoidance stress in rats: A new model for sustained visceral hyperalgesia. American Journal of Physiology - Gastrointestinal and Liver Physiology. 2005;289 1 52-1:42–53.

352. Boudry G, Jury J, Ping CY, Perdue MH. Chronic psychological stress alters epithelial cell turn-over in rat ileum. American Journal of Physiology - Gastrointestinal and Liver Physiology. 2007;292:1228–32.

353. Patel S, Hillard CJ. Adaptations in Endocannabinoid Signaling in Response to Repeated Homotypic Stress: A Novel Mechanism for Stress Habituation. European Journal of Neuroscience. 2008;27:2821–9.

354. Zheng J, Babygirija R, Bülbül M, Cerjak D, Ludwig K, Takahashi T. Hypothalamic oxytocin mediates adaptation mechanism against chronic stress in rats. American Journal of Physiology - Gastrointestinal and Liver Physiology. 2010;299:946–53.

355. Sherwin E, Rea K, Dinan TG, Cryan JF. A gut (microbiome) feeling about the brain. Current Opinion in Gastroenterology. 2016;32:96–102.

356. Fasano A. All disease begins in the (leaky) gut : role of zonulin-mediated gut permeability in the pathogenesis of some chronic inflammatory diseases. F1000Research. 2020;9:1–12.

357. Greant P, Delvaux G, Willems G. Influence of stress on epithelial cell proliferation in the gut mucosa of rats. Digestion. 1988;40:212–8.

358. Tutton PJ, D HR. Stress induced inhibition of jejunal crypt cell proliferation. Virchows Archiv B Cell Pathology. 1973;15:23–34.

359. Räsänen T. Fluctuations in the Mitotic Frequency of the Glandular Stomach and Intestine of Rat under the Influence of ACTH, Glucocorticoids, Stress and Heparin. Acta Physiologica Scandinavica. 1963;58:201–10.

360. Verburg M, Renes IB, Einerhand AWC, Büller HA, Dekker J. Isolation-stress increases small intestinal sensitivity to chemotherapy in rats. Gastroenterology. 2003;124:660–71.

361. Yeh KY, Yeh M, Holt PR. Induction of intestinal differentiation by systemic and not by luminal corticosterone in adrenalectomized rat pups. Endocrinology. 1989;124:1898–904.

362. Zulian JG, Hosoya LYM, Figueiredo PM, Ogias D, Osaki LH, Gama P. Corticosterone activity during early weaning reprograms molecular markers in rat gastric secretory cells. Scientific Reports. 2017;7 March:1–13.

363. Quaroni A, Tian JQ, Göke M, Podolsky DK. Glucocorticoids have pleiotropic effects on small intestinal crypt cells. American Journal of Physiology - Gastrointestinal and Liver Physiology. 1999;277 5 40-5.

364. Bagchi D, Carryl OR, Tran MX, Bagchi M, Garg A, Milnes MM, et al. Acute and chronic stress-induced oxidative gastrointestinal mucosal injury in rats and protection by bismuth subsalicylate. Molecular and Cellular Biochemistry. 1999;196:109–16.

365. Vanuytsel T, Van Wanrooy S, Vanheel H, Vanormelingen C, Verschueren S, Houben E, et al. Psychological stress and corticotropin-releasing hormone increase intestinal permeability in humans by a mast cell-dependent mechanism. Gut. 2014;63:1293–9.

366. Da Silva S, Robbe-Masselot C, Ait-Belgnaoui A, Mancuso A, Mercade-Loubière M, Salvador-Cartier C, et al. Stress disrupts intestinal mucus barrier in rats via mucin O-glycosylation shift: Prevention by a probiotic treatment. American Journal of Physiology - Gastrointestinal and Liver Physiology. 2014;307:420–9.

367. De Punder K, Pruimboom L. Stress induces endotoxemia and low-grade inflammation by increasing barrier permeability. Frontiers in Immunology. 2015;6 MAY:1–12.

368. Kelly JR, Kennedy PJ, Cryan JF, Dinan TG, Clarke G, Hyland NP. Breaking down the barriers: the gut microbiome, intestinal permeability and stress-related psychiatric disorders. Frontiers in cellular neuroscience. 2015;9 October:392. doi:10.3389/fncel.2015.00392.

369. Chakaroun RM, Massier L, Kovacs P. Bacteria in Metabolic Disease : Perpetrators or Bystanders ? Nutrients. 2020.

370. Kiliaan AJ, Saunders PR, Bijlsma PB, Cecilia Berin M, Taminiau JA, Groot JA, et al. Stress stimulates transepithelial macromolecular uptake in rat jejunum. American Journal of Physiology - Gastrointestinal and Liver Physiology. 1998;275 5 38-5:1037–44.

371. Ait-Belgnaoui A, Han W, Lamine F, Eutamene H, Fioramonti J, Bueno L, et al. Lactobacillus farciminis treatment suppresses stress induced visceral hypersensitivity: A possible action through interaction with epithelial cell cytoskeleton contraction. Gut. 2006;55:1090–4.

372. Vanhaecke T, Aubert P, Grohard PA, Durand T, Hulin P, Paul-Gilloteaux P, et al. L. fermentum CECT 5716 prevents stress-induced intestinal barrier dysfunction in newborn rats. Neurogastroenterology and Motility. 2017;29:1–12.

373. Zheng G, Wu SP, Hu Y, Smith DE, Wiley JW, Hong S. Corticosterone mediates stress-related increased intestinal permeability in a region-specific manner. Neurogastroenterology and Motility. 2013;25:1–21.

374. Song Y, Zhu S, Zhang S, Zheng G, Wiley JW, Hong S. Chronic Stress and Intestinal Permeability: Lubiprostone Regulates Glucocorticoid Receptor-mediated Changes in Colon Epithelial Tight Junction Proteins, Barrier Function and Visceral Pain. Neurogastroenterology and Motility. 2019;31.

375. Bharwani A, Mian MF, Foster JA, Surette MG, Bienenstock J, Forsythe P. Structural and functional consequences of chronic psychosocial stress on the microbiome and host. Psychoneuroendocrinology. 2016;63:217–27.

376. Enqi W, Jingzhu S, Lingpeng P, Yaqin L. Comparison of the Gut Microbiota Disturbance in Rat Models of Irritable Bowel Syndrome Induced by Maternal Separation and Multiple Early-Life Adversity. Frontiers in Cellular and Infection Microbiology. 2021;10 January:1–12.

377. Bailey MT, Dowd SE, Parry NMA, Galley JD, Schauer DB, Lyte M. Stressor exposure disrupts commensal microbial populations in the intestines and leads to increased colonization by Citrobacter rodentium. Infection and Immunity. 2010;78:1509–19.

378. Bailey MT, Dowd SE, Galley JD, Hufnagle AR, Rebecca G, Lyte M. Exposure to social stressors alters the structure of the intestinal microbiota. Brain Behav Immun 2011 March ; 25(3): 397–407 doi:101016/j.bbi201010023. 2011;25:397–407.

379. Bangsgaard Bendtsen KM, Krych L, Sørensen DB, Pang W, Nielsen DS, Josefsen K, et al. Gut Microbiota Composition Is Correlated to Grid Floor Induced Stress and Behavior in the BALB/c Mouse. PLoS ONE. 2012;7.

380. Watanabe Y, Arase S, Nagaoka N, Kawai M, Matsumoto S. Chronic psychological stress disrupted

the composition of the murine colonic microbiota and accelerated a murine model of inflammatory bowel disease. PLoS ONE. 2016;11:1–18.

381. Li S, Wang Z, Yang Y, Yang S, Yao C, Liu K, et al. Lachnospiraceae shift in the microbial community of mice faecal sample effects on water immersion restraint stress. AMB Express. 2017;7.

382. Zhang J, Song L, Wang Y, Liu C, Zhang L, Zhu S, et al. Beneficial effect of butyrate-producing Lachnospiraceae on stress-induced visceral hypersensitivity in rats. Journal of Gastroenterology and Hepatology (Australia). 2019;34:1368–76.

383. Brooks JP, Edwards DJ, Harwich MD, Rivera MC, Fettweis JM, Serrano MG, et al. The truth about metagenomics: Quantifying and counteracting bias in 16S rRNA studies Ecological and evolutionary microbiology. BMC Microbiology. 2015;15:1–14.

384. Durazzi F, Sala C, Castellani G, Manfreda G, Remondini D, De Cesare A. Comparison between 16S rRNA and shotgun sequencing data for the taxonomic characterization of the gut microbiota. Scientific Reports. 2021;11:1–10. doi:10.1038/s41598-021-82726-y.

385. Yuan F, Tan W, Ren H, Yan L, Wang Y, Luo H. The effects of short-chain fatty acids on rat colonic hypermotility induced by water avoidance stress. Drug Design, Development and Therapy. 2020;14:4671–84.

386. Kukurba KR, Montgomery SB. RNA sequencing and analysis. Cold Spring Harbor Laboratory Press. 2016;2015:951–69.

387. Bruning O, Rodenburg W, Wackers PFK, Van Oostrom C, Jonker MJ, Dekker RJ, et al. Confounding factors in the transcriptome analysis of an in-vivo exposure experiment. PLoS ONE. 2016;11:1–23.

388. Xiong Y, Soumillon M, Wu J, Hansen J, Hu B, Van Hasselt JGC, et al. A Comparison of mRNA Sequencing with Random Primed and 3'-Directed Libraries. Scientific Reports. 2017;7:1–12.

389. Clark DP, Pazdernik NJ, McGehee MR. Molecular Biology. 3rd edition. London; 2018.

390. Best K, Oakes T, Heather JM, Shawe-Taylor J, Chain B. Computational analysis of stochastic heterogeneity in PCR amplification efficiency revealed by single molecule barcoding. Scientific Reports. 2015;5 November 2014:1–13. doi:10.1038/srep14629.

391. Parekh S, Ziegenhain C, Vieth B, Enard W, Hellmann I. The impact of amplification on differential expression analyses by RNA-seq. Scientific Reports. 2016;6 January:1–11.

392. Ma F, Fuqua BK, Hasin Y, Yukhtman C, Vulpe CD, Lusis AJ, et al. A comparison between whole transcript and 3' RNA sequencing methods using Kapa and Lexogen library preparation methods 06 Biological Sciences 0604 Genetics. BMC Genomics. 2019;20:1–12.

393. Cock PJA, Fields CJ, Goto N, Heuer ML, Rice PM. The Sanger FASTQ file format for sequences with quality scores, and the Solexa/Illumina FASTQ variants. Nucleic Acids Research. 2009;38:1767–71.

394. Ewels P, Magnusson M, Lundin S, Käller M. MultiQC: Summarize analysis results for multiple tools and samples in a single report. Bioinformatics. 2016;32:3047–8.

395. Conesa A, Madrigal P, Tarazona S, Gomez-Cabrero D, Cervera A, McPherson A, et al. A survey of best practices for RNA-seq data analysis. Genome Biology. 2016;17:1–19.

396. Carrara M, Beccuti M, Lazzarato F, Cavallo F, Cordero F, Donatelli S, et al. State-of-the-art fusion-finder algorithms sensitivity and specificity. BioMed Research International. 2013;2013.

397. Langmead B. Aligning short sequencing reads with Bowtie. Current Protocols in Bioinformatics. 2010; SUPP.32:1–24.

398. Leek JT, Scharpf RB, Bravo HC, Simcha D, Landmead D, Johnson WE, et al. Tackling the widespread and critical impact of batch effects in high-throughput data. Nature Reviews Genetics. 2010;11:1–7. doi:10.1038/nrg2825.

399. Goh WW Bin, Wang W, Wong L. Why Batch Effects Matter in Omics Data, and How to Avoid Them. Trends in Biotechnology. 2017;35:498–507. doi:10.1016/j.tibtech.2017.02.012.

400. Bourgon R, Gentleman R, Huber W. Independent filtering increases detection power for high-throughput experiments. Proceedings of the National Academy of Sciences of the United States of America. 2010;107:9546–51.

401. Evans C, Hardin J, Stoebel DM. Selecting between-sample RNA-Seq normalization methods from the perspective of their assumptions. Briefings in bioinformatics. 2018;19:776–92.

402. Love MI, Huber W, Anders S. Moderated estimation of fold change and dispersion for RNA-seq data with DESeq2. Genome Biology. 2014;15:1–21.

403. Maza E. In papyro comparison of TMM (edgeR), RLE (DESeq2), and MRN normalization methods for a simple two-conditions-without-replicates RNA-seq experimental design. Frontiers in Genetics. 2016;7 SEP:1–8.

404. Box GEP, Cox DR. An Analysis of Transformations. Journal, Source Statistical, Royal Series, Society. 1964;26:211–52.

405. Abrams ZB, Johnson TS, Huang K, Payne PRO, Coombes K. A protocol to evaluate RNA sequencing normalization methods. BMC Bioinformatics. 2019;20 Suppl 24:1–7. doi:10.1186/s12859-019-3247-x.

406. Zyprych-Walczak J, Szabelska A, Handschuh L, Górczak K, Klamecka K, Figlerowicz M, et al. The Impact of Normalization Methods on RNA-Seq Data Analysis. BioMed Research International. 2015;2015.

407. Ramette A. Multivariate analyses in microbial ecology. FEMS Microbiology Ecology. 2007;62:142–60.

408. Legendre P, Legendre L. Numerical Ecology. 2nd edition. Amsterdam; 1998.

409. Song L, Langfelder P, Horvath S. Comparison of co-expression measures: Mutual information, correlation, and model based indices. BMC Bioinformatics. 2012;13.

410. Butte AJ, Kohane IS. Unsupervised knowledge discovery in medical databases using relevance networks. Proceedings / AMIA . Annual Symposium AMIA Symposium. 1999; November 1998:711–5.

411. Bonferroni CE. Teoria statistica delle classi e calcolo delle probabilità. Firenze; 1936.

412. Benjamini Y, Hochberg Y. Controlling the False Discovery Rate: A Practical and Powerful Approach to Multiple Testing. Journal of the Royal Statistical Society. Serie B (Methological). 1995;57:289–300.

413. The gene ontology consortium. Gene Ontology : tool for the unification of biology. Nature America. 2000;25 may:25–9. doi:10.1038/75556.

414. Kanehisa M, Goto S, Furumichi M, Tanabe M, Hirakawa M. KEGG for representation and analysis of molecular networks involving diseases and drugs. Nucleic Acids Research. 2009;38 SUPPL.1:355–60.

415. Reimand J, Isserlin R, Voisin V, Kucera M, Tannus-Lopes C, Rostamianfar A, et al. Pathway enrichment analysis and visualization of omics data using g:Profiler, GSEA, Cytoscape and EnrichmentMap. Nature Protocols. 2019;14:482–517. doi:10.1038/s41596-018-0103-9.

416. Noller H. Carl woese (1928—2012). Nature. 2013;493:610.

417. Rosselló-Mora R, Amann R. The species concept for prokaryotes. FEMS Microbiology Reviews. 2001;25:39–67.

418. Sunagawa S, Coelho LP, Chaffron S, Kultima JR, Labadie K, Salazar G, et al. Structure and function of the global ocean microbiome. Science. 2015;348:1261359. doi:10.1126/science.1261359.

419. Bordenstein SR, Theis KR. Host biology in light of the microbiome: Ten principles of holobionts and hologenomes. PLoS Biology. 2015;13:1–23.

420. Pereira F, Carneiro J, Matthiesen R, Van Asch B, Pinto N, Gusmão L, et al. Identification of species by multiplex analysis of variable-length sequences. Nucleic Acids Research. 2010;38.

421. Head IM, Saunders JR, Pickup RW. Microbial evolution, diversity, and ecology: A decade of ribosomal RNA analysis of uncultivated microorganisms. Microbial Ecology. 1998;35:1–21.

422. Gloor GB, Macklaim JM, Pawlowsky-Glahn V, Egozcue JJ. Microbiome datasets are compositional: And this is not optional. Frontiers in Microbiology. 2017;8 NOV:1–6.

423. Bolyen E, Rideout JR, Dillon MR, Bokulich NA, Abnet CC, Al-Ghalith GA, et al. Reproducible, interactive, scalable and extensible microbiome data science using QIIME 2. Nature Biotechnology. 2019;37:852–7.

424. Martin M. Cutadapt removes adapter sequences from high-throughput sequencing reads. EMBnet Journal. 2011;17.

425. Amir A, McDonald D, Navas-Molina JA, Kopylova E, Morton JT, Xu ZZ, et al. Deblur Rapidly Resolves Single-Nucleotide Community Sequence Patterns. American Society for Microbiology. 2016;2:1–7.

426. Callahan BJ, Mcmurdie PJ, Rosen MJ, Han AW, A AJ. DADA2: High resolution sample inference from Illumina amplicon data. 2016;13:581–3.

427. Sokal RR, Sneath PHA. Principles of Numerical Taxonomy. W. H. Free. San Francisco and London; 1963.

428. Escudié F, Auer L, Bernard M, Mariadassou M, Cauquil L, Vidal K, et al. FROGS: Find, Rapidly, OTUs with Galaxy Solution. Bioinformatics. 2018;34:1287–94.

429. Yilmaz P, Parfrey LW, Yarza P, Gerken J, Pruesse E, Quast C, et al. The SILVA and "all-species Living Tree Project (LTP)" taxonomic frameworks. Nucleic Acids Research. 2014;42:643–8.

430. McDonald D, Price MN, Goodrich J, Nawrocki EP, Desantis TZ, Probst A, et al. An improved Greengenes taxonomy with explicit ranks for ecological and evolutionary analyses of bacteria and archaea. ISME Journal. 2012;6:610–8.

431. Price MN, Dehal PS, Arkin AP. FastTree 2 - Approximately maximum-likelihood trees for large alignments. PLoS ONE. 2010;5.

432. Katoh K, Misawa K, Kuma K, Miyata T. MAFFT: a novel method for rapid multiple sequence alignment based on fast Fourier transform. Nucleic acids research. 2002;30:3059–66.

433. Lozupone C, Lladser ME, Knights D, Stombaugh J, Knight R. UniFrac: An effective distance metric for microbial community comparison. ISME Journal. 2011;5:169–72. doi:10.1038/ismej.2010.133.

434. Faith DP, Minchin PR, Belbin L. Compositional dissimilarity as a robust measure of ecological distance. Vegetatio. 1987;69:57–68.

435. Aitchison J. The Statistical Analysis of Compositional Data. Journal of the Royal Statistical Society: Series B (Methodological). 1982;44:139–60.

436. Lin H, Peddada S Das. Analysis of compositions of microbiomes with bias correction. Nature Communications. 2020;11:1–11. doi:10.1038/s41467-020-17041-7.

437. Callahan BJ, Sankaran K, Fukuyama JA, McMurdie PJ, Holmes SP. Bioconductor Workflow for Microbiome Data Analysis: from raw reads to community analyses. F1000Research. 2016;5:1492. doi:10.12688/f1000research.8986.2.

438. Schloss PD. Removal of rare amplicon sequence variants from 16S rRNA gene sequence surveys biases the interpretation of community structure data. bioRxiv. 2020;:2020.12.11.422279. https://doi.org/10.1101/2020.12.11.422279.

439. Selber-Hnativ S, Rukundo B, Ahmadi M, Akoubi H, Al-Bizri H, Aliu AF, et al. Human gut microbiota: Toward an ecology of disease. Frontiers in Microbiology. 2017;8 JUL.

440. Krassowski M, Das V, Sahu SK, Misra BB. State of the Field in Multi-Omics Research: From Computational Needs to Data Mining and Sharing. Frontiers in Genetics. 2020;11 December:1–17.

441. Picard M, Scott-Boyer M-P, Bodein A, Périn O, Droit A. Integration strategies of multi-omics data for machine learning analysis. Computational and Structural Biotechnology Journal. 2021;19:3735–46. doi:10.1016/j.csbj.2021.06.030.

442. Duan R, Gao L, Gao Y, Hu Y, Xu H, Huang M, et al. Evaluation and comparison of multi-omics data integration methods for cancer subtyping. 2021. doi:10.1371/journal.pcbi.1009224.

443. Rohart F, Gautier B, Singh A, Lê Cao KA. mixOmics: An R package for 'omics feature selection and multiple data integration. PLoS Computational Biology. 2017;13:1–19.

444. Paliy O, Shankar V. Application of multivariate statistical techniques in microbial ecology. Molecular Biology and Evolution. 2017;25:1032–57.

445. Dolédec S, Chessel D. Co-inertia analysis: an alternative method for studying species–environment relationships. Freshwater Biology. 1994;31:277–94.

446. Hurley JR, Cattell RB. The Procrustes Program: Producing Direct Rotation to Test a Hypothesized Factor Structure. Computers in Behavioral Science. 1962;7:258–62.

447. Gower JC. Generalized procrustes analysis. Psychometrika. 1975;40:33–51.

448. Wang B, Mezlini AM, Demir F, Fiume M, Tu Z, Brudno M, et al. Similarity network fusion for aggregating data types on a genomic scale. Nature Methods. 2014;11:333–7.

449. Dugourd A, Kuppe C, Sciacovelli M, Gjerga E, Gabor A, Emdal KB, et al. Causal integration of multi-omics data with prior knowledge to generate mechanistic hypotheses. Molecular Systems Biology. 2021;17:1–17.

450. Langfelder P, Horvath S. WGCNA: An R package for weighted correlation network analysis. BMC Bioinformatics. 2008.

451. Hasin Y, Seldin M, Lusis A. Multi-omics approaches to disease. Genome Biology. 2017;18:1–15.

452. Heintz-Buschart A, May P, Laczny CC, Lebrun LA, Bellora C, Krishna A, et al. Integrated multi-omics of the human gut microbiome in a case study of familial type 1 diabetes. Nature Microbiology. 2016;2:1–12. doi:10.1038/nmicrobiol.2016.180.

453. Zhang B, Gaiteri C, Bodea LG, Wang Z, McElwee J, Podtelezhnikov AA, et al. Integrated systems approach identifies genetic nodes and networks in late-onset Alzheimer's disease. Cell. 2013;153:707–20. doi:10.1016/j.cell.2013.03.030.

454. Chen R, Mias GI, Li-Pook-Than J, Jiang L, Lam HYK, Chen R, et al. Personal omics profiling reveals dynamic molecular and medical phenotypes. Cell. 2012;148:1293–307. doi:10.1016/j.cell.2012.02.009.

455. Subramanian I, Verma S, Kumar S, Jere A, Anamika K. Multi-omics Data Integration, Interpretation, and Its Application. Bioinformatics and Biology Insights. 2020;14:7–9.

456. Chong J, Soufan O, Li C, Caraus I, Li S, Bourque G, et al. MetaboAnalyst 4.0: Towards more transparent and integrative metabolomics analysis. Nucleic Acids Research. 2018;46:W486–94.

457. Jang Y, Yu N, Seo J, Kim S, Lee S. MONGKIE: An integrated tool for network analysis and visualization for multi-omics data. Biology Direct. 2016;11:1–9. doi:10.1186/s13062-016-0112-y.

458. Krisenko MO, Geahlen RL. Calling in SYK : SYK ' s dual role as a tumor promoter and tumor suppressor in cancer. BBA - Molecular Cell Research. 2015;1853:254–63. doi:10.1016/j.bbamcr.2014.10.022.

459. Minoo P, Zlobec I, Peterson M, Terracciano L, Lugli A. Characterization of rectal, proximal and distal colon cancers based on clinicopathological, molecular and protein profiles. International Journal of Oncology. 2010;37:707–18.

460. Glebov OK, Rodriguez LM, Nakahara K, Jenkins J, Cliatt J, Humbyrd CJ, et al. Distinguishing right from left colon by the pattern of gene expression. Cancer Epidemiology Biomarkers and Prevention. 2003;12:755–62.

461. Xu P, Elizalde M, Masclee A, Pierik M, Jonkers D. Corticosteroid enhances epithelial barrier function in intestinal organoids derived from patients with Crohn's disease. Journal of Molecular Medicine. 2021;99:805–15.

462. Boivin MA, Ye D, Kennedy JC, Al-Sadi R, Shepela C, Ma TY. Mechanism of glucocorticoid regulation of the intestinal tight junction barrier. American Journal of Physiology - Gastrointestinal and Liver Physiology. 2007;292:590–8.

463. Moisan MP, Le Moal M. Overview of acute and chronic stress responses. Medecine/Sciences. 2012;28:612–7.

464. Weaver ICG, Korgan AC, Lee K, Wheeler R V., Hundert AS, Goguen D. Stress and the emerging roles of chromatin remodeling in signal integration and stable transmission of reversible phenotypes. Frontiers in Behavioral Neuroscience. 2017;11 March:1–19.

465. Rispal J, Escaffit F, Trouche D. Chromatin Dynamics in Intestinal Epithelial Homeostasis: A Paradigm of Cell Fate Determination versus Cell Plasticity. Stem Cell Reviews and Reports. 2020;16:1062–80.

466. Roopra A. MAgIC: A tool for predicting transcription factors and cofactors driving gene sets using ENCODE data. PLoS Computational Biology. 2020;16:1–20. doi:10.1371/journal.pcbi.1007800.

467. Serra D, Mayr U, Boni A, Lukonin I, Rempfler M, Challet Meylan L, et al. Self-organization and symmetry breaking in intestinal organoid development. Nature. 2019;569:66–72.

468. Lukonin I, Serra D, Challet Meylan L, Volkmann K, Baaten J, Zhao R, et al. Phenotypic landscape of intestinal organoid regeneration. Nature. 2020;586:275–80. doi:10.1038/s41586-020-2776-9.

469. Min S, Kim S, Cho SW. Gastrointestinal tract modeling using organoids engineered with cellular and microbiota niches. Experimental and Molecular Medicine. 2020;52:227–37. doi:10.1038/s12276-020-0386-0.

470. Poletti M, Arnauts K, Ferrante M, Korcsmaros T. Organoid-based Models to Study the Role of Host-microbiota Interactions in IBD. Journal of Crohn's and Colitis. 2021;15:1222–35.

471. Co JY, Margalef-Català M, Li X, Mah AT, Kuo CJ, Monack DM, et al. Controlling Epithelial Polarity: A Human Enteroid Model for Host-Pathogen Interactions. Cell Reports. 2019;26:2509-2520.e4.

472. Huang EY, Inoue T, Leone VA, Dalal S, Touw K, Wang Y, et al. Using corticosteroids to reshape the gut microbiome: Implications for inflammatory bowel diseases. Inflammatory Bowel Diseases. 2015;21:963–72.

473. Pereira FC, Berry D. Microbial nutrient niches in the gut. Environmental Microbiology.

2017;19:1366–78.

474. Deines P, Hammerschmidt K, Bosch TCG. Exploring the Niche Concept in a Simple Metaorganism. Frontiers in Microbiology. 2020;11 August:1–11.

475. Meehan CJ, Beiko RG. A phylogenomic view of ecological specialization in the lachnospiraceae, a family of digestive tract-associated bacteria. Genome Biology and Evolution. 2014;6:703–13.

476. Li J, Wu T, Li N, Wang X, Chen G, Lyu X. Bilberry anthocyanin extract promotes intestinal barrier function and inhibits digestive enzyme activity by regulating the gut microbiota in aging rats. Food and Function. 2019;10:333–43.

477. Zoppi J, Guillaume JF, Neunlist M, Chaffron S. MiBiOmics: an interactive web application for multi-omics data exploration and integration. BMC Bioinformatics. 2021;22:1–14. doi:10.1186/s12859-020-03921-8.

478. Fouesnard M, Zoppi J, Petera M, Le Gleau L, Migné C, Devime F, et al. Dietary switch to Western diet induces hypothalamic adaptation associated with gut microbiota dysbiosis in rats. International Journal of Obesity. 2021;45:1271–83. doi:10.1038/s41366-021-00796-4.

479. Chowdhury SR, King DE, Willing BP, Band MR, Beever JE, Lane AB, et al. Transcriptome profiling of the small intestinal epithelium in germfree versus conventional piglets. BMC Genomics. 2007;8.

480. Slowicka K, Petta I, Blancke G, Hoste E, Dumas E, Sze M, et al. Zeb2 drives invasive and microbiota-dependent colon carcinoma. Nature Cancer. 2020;1:620–34. doi:10.1038/s43018-020-0070-2.

DOCTORAT BIOLOGIE BRETAGNE SANTE LOIRE

UNIVERSITÉ DE NANTES

Titre : Impact du stress psychologique sur le remodelage de l'interactome hôte-microbiote

Mots clés : Analyse Multi-Omics, Stress Psychologique, Holobiont

Résumé : A la frontière entre notre milieu interne et l'environnement, le tube digestif constitue une succession d'organe spécialisé qui permet la récolte d'énergie nécessaire au fonctionnement du corps et qui assure une fonction de barrière biologique contre les pathogènes et toxines de l'environnement. Il est en relation avec le microbiome qu'il abrite, et qui complète ses fonctions grâce à son vaste métagénome.
Dans les phases pré-symptologiques des maladies chroniques, une rupture de l'homéostasie est observée et reflète des défauts de cet interactome hôte-microbiote. L'étude de ces phases dynamiques qui marquent le passage de l'équilibre au déséquilibre est complexe et requiert le développement de méthodes systémiques.
Dans ce travail de thèse, nous avons employé un modèle de stress psychologique (SP) pour étudier ces phases précoces des physiopathologies intestinales. Les microenvironnements intestinaux de souris soumises à un stress d'évitement de l'eau ont été caractérisé macroscopiquement et à l'échelle moléculaire pour déterminer les changements de composition du microbiote adhérent et luminal, ainsi que les modifications de l'expression des gènes de l'épithélium.
Nous avons pu mettre en évidence un effet régional pro-prolifératif et pro-apoptotique du SP sur la partie distale du colon, ainsi que des changements de diversité et composition du microbiote intestinal adhérent et luminal. Enfin le développement de nouvelles analyses multi-omiques a permis l'extraction de signatures intégratives et l'identification de biomarqueurs transcriptomiques de l'épithélium intestinal et bactériens adhérents et luminaux associés à des changements d'états des barrières d'organes.

Title: Impact of psychological stress on the remodeling of the host-microbiota interactome

Keywords: Multi-Omics Analysis, Psychological Stress, Holobiont.

Abstract: At the frontier between our internal and external milieu, the digestive tract constitutes a succession of specialized organs which harvest energy from diet to fulfill our body needs and ensures a biological barrier function against pathogens and toxins from the environment. It is associated to the microbiome, which completes its functions through its vast metagenome.
In the pre-symptological phases of chronic diseases, a disruption of homeostasis is observed and reflects defects in this host-microbiota interactome. The study of these dynamic phases that mark the transition from equilibrium to disequilibrium and remain complex to capture; it requires the development of systemic methods.
In this thesis work, we employed a psychological stress (PS) model to study these early phases of gut pathophysiology. The gut microenvironments of mice subjected to water avoidance stress were characterized macroscopically and at the molecular level to determine changes in the composition of the adherent and luminal microbiota, as well as changes in epithelial gene expression.
We were able to demonstrate a regional pro-proliferative and pro-apoptotic effect of SP on the distal part of the colon, as well as changes in the diversity and composition of the adherent and luminal intestinal microbiota. Finally, the development of new multi-omics analyses allowed the extraction of integrative signatures and the identification of transcriptomic biomarkers of the intestinal epithelium and adherent and luminal bacteria associated with changes in organ barrier states.